SYNTHESIS AND PHOTOLYSIS

OF

AROMATIC NITRATE ESTERS

by

IMRE G. CSIZMADIA

Dipl. Chem. Eng.,

Polytechnical University of Budapest, 1956.

M.Sc.,

University of British Columbia, 1959.

A Thesis Submitted in Partial Fulfilment of the

Requirements for the Degree of

DOCTOR OF PHILOSOPHY

in the Department

of

CHEMISTRY

We accept this thesis as conforming to the

required standard

THE UNIVERSITY OF BRITISH COLUMBIA

SEPTEMBER, 1962.

In presenting this thesis in partial fulfilment of the requirements for an advanced degree at the University of British Columbia, I agree that the Library shall make it freely available for reference and study. I further agree that permission for extensive copying of this thesis for scholarly purposes may be granted by the Head of my Department or by his representatives. It is understood that copying or publication of this thesis for financial gain shall not be allowed without my written permission.

Department of Chemistry

The University of British Columbia,
Vancouver 8, Canada.

Date September 28, 1962

PUBLICATION

1. I.G. Csizmadia and L.D. Hayward, Steric Effects in Nitrate Esters I. The Synthesis and Spectra of 1, 2-Acenaphthenediol Derivatives and the Steric Interaction of Contiguous Nitroxy Groups. Tetrahedron, submitted for publication.

The University of British Columbia

FACULTY OF GRADUATE STUDIES

PROGRAMME OF THE

FINAL ORAL EXAMINATION

FOR THE DEGREE OF

DOCTOR OF PHILOSOPHY

of

IMRE G. CSIZMADIA

Dipl. Chem. Eng. Polytechnical University of Budapest, 1956
M.Sc., University of British Columbia, 1959

FRIDAY, SEPTEMBER 28, 1962, AT 2:30 P.M.
IN ROOM 261, CHEMISTRY BUILDING

COMMITTEE IN CHARGE

Chairman: F.H. SOWARD

J.E. BLOOR	J.P. KUTNEY
W.A. BRYCE	C A. McDOWELL
J.B. FARMER	D.E. McGREER
L.D. HAYWARD	C. REID

External Examiner: P. de MAYO
University of Western Ontario

SYNTHESIS AND PHOTOLYSIS OF

AROMATIC NITRATE ESTERS

ABSTRACT

Nitrate esters of aromatic alcohols were synthesized by esterification which involved competition between O-nitration and aromatic C-nitration. TLC analysis gave a pattern of adsorption affinities for the nitroxy group and other substituents consistent with the molecular conformations. The NMR frequency of the α-protons showed a linear correlation with the accepted group electronegativities of the substituents in molecules with rigid carbon skeletons and gave a value of 4.18 kcal/mole for the nitroxy group. The symmetric and asymmetric IR stretching frequencies of nitroxy groups in dilute cyclohexane solution were shifted to higher values by steric interaction between contiguous groups when the C-ONO_2 bonds were constrained to coplanarity. The UV spectra showed benzenoid, $\pi \rightarrow \pi^*$, and $n \rightarrow \pi^*$ bands and a solvent perturbation effect assigned to a solvent $\rightarrow$ solute charge-transfer interaction.

The nitrate esters reacted with the solvent when irradiated in solution in the wavelength range of the $n \rightarrow \pi^*$ excitation. Product analysis indicated that C-C bond cleavage occurred via intermediate alkoxyl radicals. Rate studies showed the following order of reactivity: benzyl nitrate $<$ dl-hydrobenzoin dinitrate $<$ meso-hydrobenzoin dinitrate, $<$ trans-1, 2-acenaphthenediol nitrate $<$ cis-1, 2-acenaphthenediol dinitrate. The rate measurements and ESR spectra gave evidence of intra-molecular energy transfer from the naphthalene moiety to the nitroxy groups in the 1, 2-acenaphthenediol dinitrates assigned as a singlet $\rightarrow$ singlet transfer. Calculations from the apparent first-order rate constants and spectra showed that benzyl nitrate, and meso- and dl-hydrobenzoin dinitrates photolysed with a quantum yield of about 2 in benzene solution. A solvent effect caused $k_{Et_2O} > k_{EtOH} > k_{PhH}$.

On the basis of product analysis, rate measurements, estimated quantum yields and ESR spectra a mechanism for the nitrate ester photolysis was proposed.

GRADUATE STUDIES

Field of Study: Organic Chemistry

Quantum Chemistry.....J.A.R. Coope

Statistical Mechanics.....R.F. Snider

Crystal Structures.....K.B. Harvey
L.W. Reeves

Physical Organic Chemistry.....R. Stewart
R.E. Pincock

Molecular Rearrangements.....A. Rosenthal

Recent Synthetic Methods.....R.A. Bonnett
D.E. McGreer

Chemistry of Polysaccharides.....G.G.S. Dutton

Related Studies:

Biochemistry.....M. Darrach
J. Polglase
S.H. Zbarsky

Differential Equations.....J. Abramowich

Computer Programming.....H. Dempster

Analogue Computers.....E.V. Bohn

ABSTRACT

Nitrate esters of aromatic alcohols have been synthesized successfully by direct esterification which involved competition between O-nitration and aromatic C-nitration. The physical properties of the fully characterised nitrate esters have been studied by TLC and by NMR, IR, and UV spectroscopy.

TLC results gave a consistent pattern of adsorption affinities for the nitroxy group and other substituents and also revealed stereochemical features of the nitrate esters.

The NMR frequency of the α-protons in substituted carbinols, R'R"CHOX, showed correlation with the accepted group electronegativities of X if the system had a rigid carbon skeleton. The correlation failed however when free rotation was possible on the common bond in substituted diols. The correlation also showed the nitroxy group electronegativity to be higher (ca. 4.18 kcal/mole) than hitherto reported.

The characteristic infrared frequencies of nitroxy groups were measured in dilute cyclohexane solutions of the nitrate esters and showed shifts to higher frequencies due to steric interaction between contiguous nitrate ester groups when the C-ONO_2 bonds were constrained to coplanarity.

The UV spectra of the aromatic nitrate esters showed benzenoid, $\pi \rightarrow \pi^*$ and $n \rightarrow \pi^*$ - bands and a solvent perturbation effect which was tentatively assigned to a solvent $\rightarrow$ solute charge-transfer interaction similar to that previously reported for aliphatic nitro compounds.

Photolytic experiments revealed that nitrate esters underwent photochemical reaction when irradiated in the wavelength range of the $n \rightarrow \pi^*$ excitation. Product analysis indicated that C-C bond cleavage occurred

which was explained in terms of intermediate alkoxyl radical formation.

Rate studies of the photolysis showed the following order of reactivity: Benzyl Nitrate < dl-Hydrobenzoin Dinitrate < meso-Hydrobenzoin Dinitrate, < trans-1,2-Acenaphthenediol Dinitrate < cis-1,2-Acenaphthenediol Dinitrate. Both rate measurements and ESR spectra gave evidence of extensive intramolecular energy transfer from the naphthalene moiety to the nitroxy groups in the 1,2-acenaphthenediol dinitrates which was assigned as a singlet $\longrightarrow$ singlet transfer. Calculations from the kinetic data and spectra showed that benzyl nitrate, and meso- and dl-hydrobenzoin dinitrates photolysed with a quantum yield of about 2 in benzene solution. A solvent effect caused the following rate enhancement:

$$k_{Et_2O} > k_{EtOH} > k_{PhH}$$

On the basis of product analysis, rate and quantum yield measurements and ESR spectra a mechanism for the nitrate ester photolysis was proposed.

A D D E N D A

Pages 63-66. The 1,2-acenaphthenediol dinitrates were fully characterised by the author in a previous research (68). The nitrogen analyses (Table XII) and IR spectra (Figure 9) of the crude by-products (B_{cis}, B_{trans}, C_{cis} and C_{trans}) were examined in an attempt to establish the occurrence of ring-nitration and complete characterisation was not undertaken.

Pages 101 and 103. The identities of substances E, E' and E'' given on page 101 are not correct. The bands at 2900 and 1726 cm^{-1} (Figure 24) pointed to the presence of aldehyde groups in conjugated bond systems.

Pages 120 and 121. The energy transfer process suggested in paragraph 3 would only be probable if the (undetermined) energy levels were related as shown in Figure 30. The observed spectra (68) implied this would be an "uphill" energy transfer. This is a rarely observed phenomenon, but cannot be entirely excluded. Very efficient utilisation of $n \rightarrow \pi^*$ energy in the photodecomposition might shift the equilibrium toward this form. Alternatively, and more probably, there may be transfer to some state of lower energy than the $\pi \rightarrow \pi^*$ state. This might be a charge-transfer state, from which direct decomposition is possible.

Page 142. Other factors including the presence of the relatively heavy atoms O and N and the altered symmetry of the molecule could also be expected to reduce the lifetime of the triplet state sufficiently to make the ESR signal undetectable.

Pages 152 and 153. The identities of Fractions A, B, and C were not satisfactorily established since the elementary analyses were either lacking or did not agree with the calculated values.

ACKNOWLEDGMENTS

I wish to express my very sincere thanks and appreciation to Dr. L. D. Hayward for his help and encouragement throughout the course of the research and the preparation of this thesis.

I wish also to express sincere gratitude to the Head of the Department, Dr. C. A. McDowell for his continuing interest in the work and for making available the ESR facilities of his laboratory.

My thanks are also due to Dr. J. B. Farmer of this Department for help with the analysis of the ESR spectra, to Dr. D. Hollis of Varian Associates, Palo Alto, who at my request, kindly recorded the first exploratory ESR spectrum of an irradiated nitrate ester, and to the students and staff of the Department ESR laboratory for their valuable technical assistance.

For helpful discussion on theoretical and spectroscopic questions I am indebted to Dr. J. Bloor of the B.C. Research Council and to Drs. D. McGreer and L. W. Reeves of this Department. For mass-spectral analysis I wish to thank Dr. D. C. Frost.

Finally, I wish to express my appreciation to the National Research Council of Canada for a studentship for the period 1960-62.

TABLE OF CONTENTS

LIST OF FIGURES

LIST OF TABLES

GENERAL INTRODUCTION

Synthetic photochemistry utilizes light energy to bring about specific chemical reactions. Classical examples are the hydrogen chloride synthesis in the gas phase and the vitamin D_2 synthesis in the liquid phase. There are, in addition, numerous other photosynthetic reactions which may be used for the preparation of a variety of compounds in excellent yields whose syntheses by conventional chemical techniques would involve lengthy and tedious routes from available starting materials (1).

During the irradiation of a chemical system particles of matter suffer "collisions" with the photons of light and in the annihilation of the photons the molecules absorb the energy of the light quanta ($\epsilon = h\nu$) and go into ~~the~~ an excited state (2). The ~~normal maximum~~ usual lifetime of ~~an~~ singlet excited state is of the order of 10^{-8} to 10^{-7} sec. Deactivation of an excited state by one or more of several processes must occur within this period. If the process is physical the energy absorbed is either degraded to heat or the primary absorption process is reversed and the energy is radiated as fluorescence or phosphorescence. If, however, the molecule becomes unstable when excited it breaks up into fragments almost instantaneously (10^{-13} -- 10^{-10} sec.), photochemical reactions take place and the deactivation process can be classified as chemical.

In many photochemical reactions the primary fragments of the decomposition are free radicals. Most of the free radical intermediates possess very short lifetimes and their structure and reactivity determine the further steps in the reactions.

The properties of the electronically excited molecule usually differ from those of the same molecule in the ground state and thus the excited molecule may undergo reactions with chemical reagents to which

it would be resistant in the ground state. Therefore detailed study of the nature of photochemical reactions gives information not only about the nature of the free radicals formed in the primary reaction but also furnishes valuable information about the chemical bond.

Photosynthetic processes occur daily in every green living organism in the presence of light and raw materials. Much effort has been directed toward achieving understanding of these processes which occur in the green chloroplasts of plants (3). Recently an Italian school reported investigations (4) (5) of the in vitro photosynthesis of amino acids based on the photolysis of nitrate (NO_3^-) and nitrite (NO_2^-) ions in aqueous solutions of relatively simple organic molecules e.g. glucose. Consequently there is a demand for a better understanding of the photolytic processes of nitrogen-oxygen compounds from both theoretical and practical points of view.

This thesis is concerned with the synthesis and photolysis of a certain type of aromatic nitrate esters. The aim of this research work was twofold. Firstly it was hoped that radicals liberated by the photolysis of the aromatic nitrate esters in solution might have lifetimes sufficiently long that their characteristic properties could be studied. Secondly it was hoped that the fragmentation pattern of the nitroxy group during photodecomposition might be determined which in turn would throw light on the chemical and physiological properties of the several classes of organic compounds which contain oxygen-nitrogen bonds.

HISTORICAL INTRODUCTION

The Chemistry of the Nitrate Esters

I. $(R^1)_nXNO_2$ Compounds.

The NO_2 group as a substituent plays a particularly important role in chemistry. The compounds in which it occurs (II) may be considered as derivatives of hydrides (I) in which a hydrogen attached to a particular atom (X), has been substituted by NO_2 (1).

$$\underset{\text{I}}{(R^1)_nXH} \longrightarrow \underset{\text{II}}{(R^1)_nXNO_2} \qquad (1)$$

where ^{1} = I, II, III, ... represents the type of the substituents

and n = 0, 1, 2, or 3 represents the number of the substituents. Thus, most conveniently, compound II may be termed an X-nitro derivative. This classification may be extended in principle to the whole periodic system. As examples the alkyl hydrides and the corresponding X-nitro derivatives for the second period elements are as follows:

$\overset{\delta+}{Li}\overset{\delta-}{H}$	RBeH	$R'R''BH$	$R'R''R'''CH$	$R'R''NH$	ROH	$\overset{\delta-}{F}\overset{\delta+}{H}$
$\overset{\delta+}{Li}\overset{\delta-}{NO_2}$	$RBeNO_2$	$R'R''BNO_2$	$R'R''R'''CNO_2$	$R'R''NNO_2$	$RONO_2$	$\overset{\delta-}{F}\overset{\delta+}{NO_2}$

It is interesting to note that at the beginning of the period NO_2^- bears a negative charge while at the end the positive charge is on the NO_2 group and that there are intermediate distributions of charge over the X - N bond within the period. The formation of the X - N bond may be considered as a combination of free radicals which may proceed by one of three different routes:

$$(R^1)_nX^{\circ}\!\overset{\curvearrowright}{+}\!{:}NO_2 \longrightarrow (R^1)_nX^+ + {:}NO_2^- \qquad (2)$$

$$(R^1)_nX\cdot + \cdot NO_2 \longrightarrow (R^1)_nX{:}NO_2 \qquad (3)$$

$$(R^1)_nX\cdot\!\overset{\curvearrowleft}{+}\!\cdot NO_2 \longrightarrow (R^1)_nX^- + NO_2^+ \qquad (4)$$

Although one may distinguish these three reactions it should be

emphasized that 3 is the general case resulting in a covalent bond. The bond formed, however, may still possess a certain degree of ionic character. The extreme cases are 2 and 4.

The amount of ionic character in a given bond may be estimated (6) from Pauling's equation (5) for the reaction

$$A\cdot + \cdot B \longrightarrow A\text{-}B$$

$$\text{Amount of ionic character} = 1-e^{-\frac{1}{4}(\chi_A - \chi_B)^2} \qquad (5)$$

where $\chi_A - \chi_B$ is the difference between the electronegativities of the radicals A· and B· expressed in the units of Pauling's scale (kcal/mole).

The amount of ionic character of the X-N bonds in $(R^1)_nXNO_2$ compounds may be estimated if one takes in the first approximation χ_X as the electronegativity of X· rather than of $(R^1)_nX\cdot$. The electronegativity of the NO_2 radical in Mulliken's scale (ev/particle) is the sum of the ionization potential and electronaffinity of NO_2 and its equivalent in Pauling's scale (kcal/mole) may be calculated (7) from equation 6: (6)

$$\chi_P = 0.168\ (\chi_M - 1.23) \qquad (6)$$

where the subscripts P and M refer to Pauling's and Mulliken's scales respectively.

Difficulty arises however in the selection of the value of the ionization potential of nitrogen dioxide among the several which have been reported so far. Each value corresponds to the ionization of an electron in a particular molecular orbital (8). The first ionization potential has been re-determined recently (9) as 9.80 ± 0.05 ev while the published second ionization potentials range between 11 and 12.3 ev; thus the reported value of 11.62 ev (10) may be accepted as reasonable. In the calculation of the electronegativity of NO_2 the first ionization potential should be used since it has been assigned as the ionization of the unpaired electron. For some

unknown reason, however, the second ionization potential provides more reasonable values for the estimated partial ionic character of X-N bonds (Table II). For example, the first ionization potential gives about 80% ionic character for the $F-NO_2$ bond whereas the second ionization potential gives the value of 60% which is in better agreement with the chemical properties of the compound. The selected constants for NO_2 are given in Table I.

Table I

Second Ionization Potential, Electron Affinity and Electronegativity of NO_2

		Experimental (10) (11)	Theoretical (12)	Theoretical after zero adjustment
I_p	(ev)	11.62	12.89	11.62
E_a	(ev)	-	4.12	2.85
$\chi_M = I_p + E_a$	(ev)	-	-	14.47
χ_P	(kcal/mole)	-	-	2.23

The corresponding χ_X values in Pauling's scale (13) and the values of $\chi_X - \chi NO_2$ together with the estimated ionic character of the X-N bonds are given in Table II.

Table II

Estimated Ionic Character of X-N Bonds in $(R^1)_n XNO_2$

Atomic Number	X	χ_X^* (kcal/mole)	$\chi_X - \chi_{NO_2}$ (kcal/mole)	Ionic Character of $X-NO_2$
3	Li	0.55	-1.68	0.50
4	Be	1.10	-1.13	0.27
5	B	1.85	-0.38	0.04
6	C	2.50	+0.27	0.01
7	N	3.15	+0.92	0.19
8	O	3.60	+1.37	0.37
9	F	4.15	+1.92	0.60

* From Reference (13).

If Pauling's theoretical curve for ionic character (5) is extended over the negative side of the scale, one may estimate the magnitude of the positive or negative charge existing on the nitrogen atom in the $(R^1)_nXNO_2$ compounds as shown in Figure 1.

The two extremes are singular cases i.e. there is only one lithium nitrite and only one nitryl fluoride, however as the middle of the period is approached the number of possibilities are increased. At the geometrical mid-point the C-nitro derivatives usually called "nitro compounds" have the smallest amount of ionic character in the $C-NO_2$ bond and are the most thoroughly studied NO_2 derivatives. Because of the possible variation of the substituents R', R", R"' the number of possible C-nitro compounds is virtually unlimited.

On the left hand side of the period only $LiNO_2$ is known so far, which is a simple inorganic compound. The beryllium and boron compounds have not been reported as yet but there seems to be no obvious reason why they should not exist.

It might be possible that the known mixed alkyl or aryl beryllium (14) (15) and boron halides (16) (17) would undergo a metathetical reaction with silver nitrite as in 7 and 8:

$$R\text{-}BeHal + AgNO_2 \longrightarrow R\text{-}\overset{\delta+}{Be}\text{-}\overset{\delta-}{NO_2} + AgHal \qquad (7)$$

$$R'R''BHal + AgNO_2 \longrightarrow R'R''\overset{\delta+}{B}\text{-}\overset{\delta-}{NO_2} + AgHal \qquad (8)$$

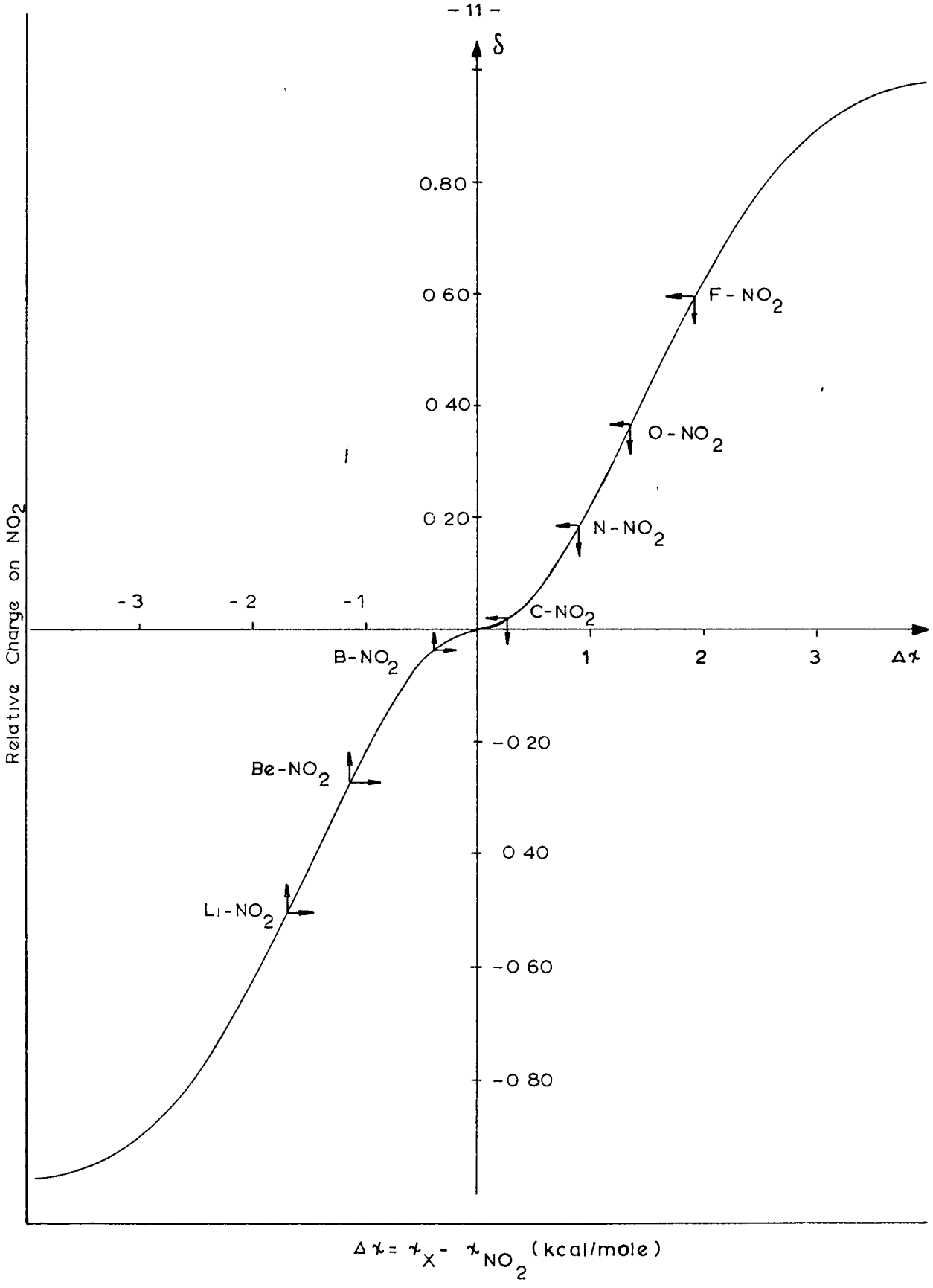

FIGURE 1. Calculated Ionic Character of $X-NO_2$ Bonds

The NO_2^- in $AgNO_2$ would be a nucleophilic reagent so that the reactions may be considered as nucleophilic substitutions on Be or B (18).

These compounds containing elements from the left side of the periodic system probably would constitute "chemical mirror images" of their counterparts from the right hand side. In other words the stability of the above hypothetical beryllium and boron nitro compounds would be expected to depend on the successful creation of a partial positive charge on the metalloid element (especially in the case of beryllium) and this would be a function of the nature of the R^i groups. From this reasoning it follows that groups with higher electron withdrawing power (such as aryl or perfluoroalkyl) would tend to stabilize these compounds. Two pieces of indirect evidence seem to support this idea.

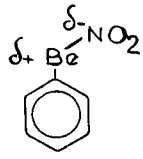

III

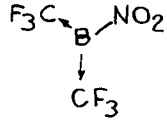

IV

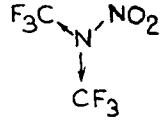

V

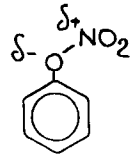

VI

Firstly phenyl nitrate (VI) does not exist (19) very likely because the electron withdrawing phenyl group decreases the necessary negative charge of the oxygen atom and creates positions with higher electron density in the aromatic ring. For this very reason an aryl group probably would maintain a sufficient positive charge on the corresponding beryllium compound (III).

Secondly the electron withdrawing effect of the CF_3 group is well demonstrated by the lowering of the basicity of an amine in which it is substituted. The change of pK_b from 3.25 for $CH_3CH_2NH_2$ to 5.7 for $CF_3CH_2NH_2$ illustrates this effect (20). N - Nitrodimethylamine has an N-N

bond with a certain amount of ionic character: $(CH_3)_2 \overset{\delta-}{N} - \overset{\delta+}{NO_2}$. Replacing the methyl groups by perfluoromethyls would cause a decrease in the ionic character, that is, the compound would be covalent because of the electron withdrawing effect of the CF_3-substituents. The N-nitro bis-trifluoromethylamine (bp 17°) has been reported (21) and the very much lower boiling point compared (20) to that of N-nitrodimethylamine (bp. 187°) suggests that this is indeed the case and that the corresponding boron compound (IV) should also be sufficiently stable for isolation.

On the right hand side of the period FNO_2 is a well-known, relatively stable, inorganic compound. The remaining two types, N-nitro and O-nitro compounds, are stable although highly reactive and are usually classified as organic compounds even if the rest of the molecule contains elements other than carbon as in Me_3SONO_2 and Et_3SONO_2 (22) or in Me_3SiONO_2 and $Me_2Si(ONO_2)_2$ (23).

Compounds bearing the $O-NO_2$ group (nitroxy or O-nitro group, less frequently nitrate group) are occasionally termed "O-nitro" derivatives but are more frequently given the name "nitrate esters" because of the common method of synthesis from nitric acid and the corresponding alcohols.

II. Properties of the Nitrate Esters.

Nitrate esters (VII) are important from the chemical, technical and physiological points of view. In synthetic organic chemistry (24) the NO_2 group is used (especially in the carbohydrate field) for blocking free hydroxyl groups as nitrate esters until manipulations may be carried out on other parts of the molecule. The blocking covalent nitrate is conveniently removable by hydrogenolysis or by other reductions. The technical importance (25) of the nitrate esters is based on their explosive nature.

"Nitroglycerine" (glycerol trinitrate), ethylene glycol dinitrate and "nitrocellulose" (cellulose nitrate) are well known explosives and large quantities are manufactured both for military and industrial purposes. The medical application (26) (27) of nitrate esters as successful drugs in the therapy of hypertension and angina is of long standing and great importance. The symptoms of angina are "dramatic and terrorizing pain in the chest radiating from the region of the heart to the left shoulder and down the arm. It may last for a period of several seconds terminating in death or it may return repetitiously over a period of several decades" (27). Nitrate esters relieve these attacks extremely rapidly although the mechanism of their action is not known. Immunity to a given nitrate compound is built up over a period of time and new ones must be prescribed frequently.

In spite of the importance of nitrate esters our knowledge about their physical and chemical behaviour is still limited in comparison to that of other families of organic compounds. This may be due to the fact that their chemical reactions are numerous and complex and mechanisms vary not only with reagent, reaction conditions and substituent groups,

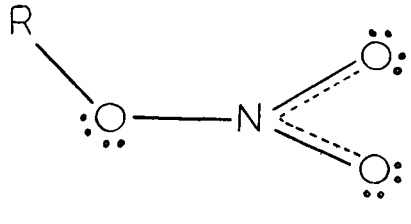

VII

but are also multiplied within the nitroxy group itself. This means in

practice that in contrast to the chemistry of other functional groups in a particular set of reaction conditions one cannot at present predict with confidence how a new nitrate ester will behave, that is, what type of reaction is to be expected.

III. The Structure of Nitrate Esters.

The structure of the nitroxy group (Figure 2) is more or less accepted as planar (28) (29) (30) in spite of some evidence for a pyramidal arrangement (31). This planar arrangement is considered to be general, although the electron diffraction (28) (30) and X-ray crystallographic (29) evidence was obtained from only two simple molecules, methyl nitrate and pentaerythritol tetranitrate (Table III). Raman and infrared spectra agree for the structure shown in Figure 2 and NMR indicates only two types of oxygen atoms in the ratio 1:2 in ^{17}O labelled ethyl nitrate (32).

Table III

Molecular Parameters of the ONO_2 Group.

	References		
Location	(31)	(28)	(29)
$C - O_1$	1.44 Å	1.43 Å	1.37 Å
$O_1 - N$	1.37 Å	1.36 Å	1.36 Å
$N - O_{2,3}$	1.22 Å	1.26 Å	1.272 Å
$\angle CO_1N$	109° 28'	105 ± 5°	——
$\angle O_2NO_3$	131 ± 5°	125° 16'	123°

This geometrical arrangement seems to be general for $(R^i)_nXNO_2$ compounds and may be considered as a function of the NO_2 group.*

*) There are 4π electrons in the group $-NO_2$ and thus it does not fit Huckel's 4n-2 rule. However it is planar and therefore similar to other 4π electron systems (33) such as trimethylenemethane.

It was proposed by Chedin (34) from Raman spectra and was confirmed by Booth and Llewellyn (29) by X-ray analysis that the carbon atom lies in a plane perpendicular to that of the ONO_2 group. A set of resonance structures for the group was suggested (19) similar to those of the C-nitro group (Figure 3).

IV. Syntheses of Nitrate Esters.

Among the several possible synthetic methods there are three most frequently used for the preparation of nitrate esters:

(i) The metathesis of organic halides with silver nitrate in organic solvents

$$RBr + AgNO_3 \longrightarrow RONO_2 + AgBr \qquad (9)$$

(ii) The double decomposition of chloroformate esters with silver nitrate (Boschan's method)

$$ROCOCl + AgNO_3 \longrightarrow RONO_2 + AgCl + CO_2 \qquad (10)$$

(iii) The direct esterification (O-nitration) of the corresponding alcohol

$$ROH + NO_2Y \longrightarrow RONO_2 + HY \qquad (11)$$

Method (i) is a favoured technique because the corresponding halogen compounds are readily available (35) in many cases and the by-product silver bromide can be separated easily. The reaction may be carried out in either homogeneous (in glacial acetic acid or acetonitrile) or in heterogeneous (in ether, benzene, nitrobenzene or nitromethane) medium. In the case of synthesis of dinitrates, difficulties arise in the exchange of the second vicinal halogen atom which was indicated clearly by Fishbein (36) in a study of the reaction of racemic- and meso-dibromobutane (VIII) with silver

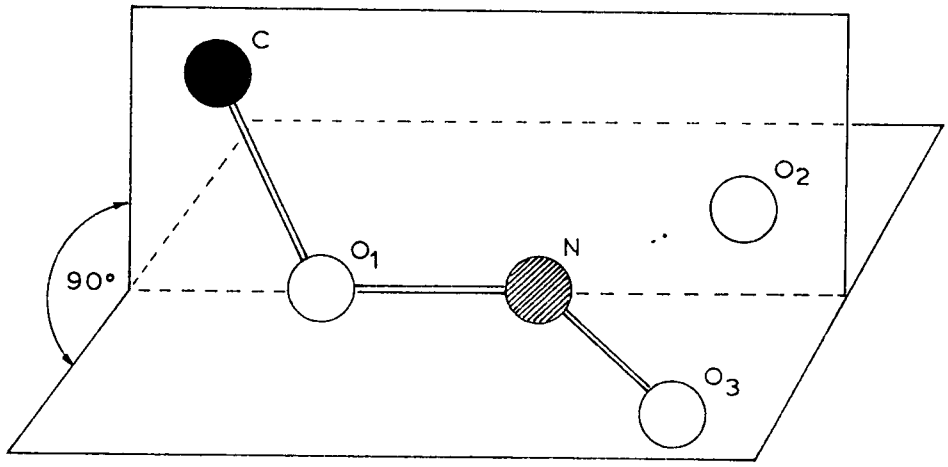

FIGURE 2 The Structure of the Organic Nitrate Group

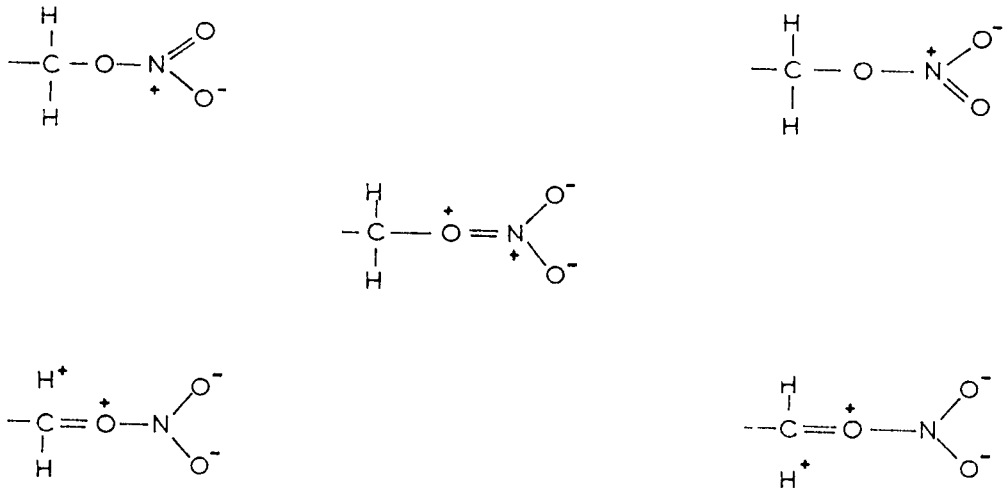

FIGURE 3. Resonance Structures of the Nitroxy Group

nitrate in acetonitrile.

The reaction occurred in a stepwise manner and the exchange of the first bromine atom for nitroxy group was considerably faster than that of the second one. Furthermore the first step proceeded with retention of configuration and the second with inversion. The first step was explained by a push-pull mechanism where "the neighbouring bromine atom participates in a back side internal displacing action while the C-Br bond of the carbon undergoing substitution is being weakened by an electrophilic attack on halogen by silver" (IX) (12). The cyclic bromonium ion (X) is attacked by the nitrate ion and with overall retention of configuration produces threo-2-bromo-3-nitroxy butane (XI) (13). Since the nitrate ester group does not participate in the elimination of the second bromine atom via a cyclic ester therefore the next step proceeds by simple S_N2 mechanism with practically complete inversion of configuration (14).

Method (ii) was introduced first by Boschan (32) in 1959. This technique has the advantage that it "does not involve rupture of the bond on the carbon atom adjacent to the nitrate ester group" therefore the nitrate ester obtained retains the configuration of the parent alcohol. The reaction is considered to proceed via an intermediate which readily decomposes to the final product (15). Further development of this reaction is now in progress (38).

The chloroformate starting material is usually prepared from the corresponding alcohol and phosgene. For this reason dinitrates may not be prepared where the geometrical location of the two hydroxyl groups favors the formation of cyclic carbonates.

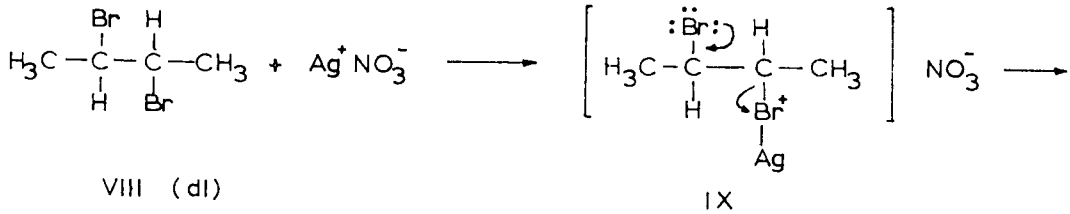

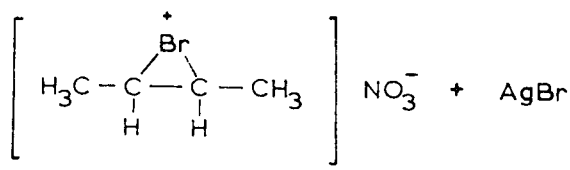

(12)

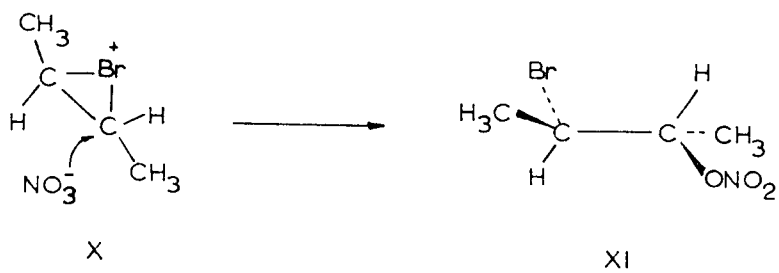

(13)

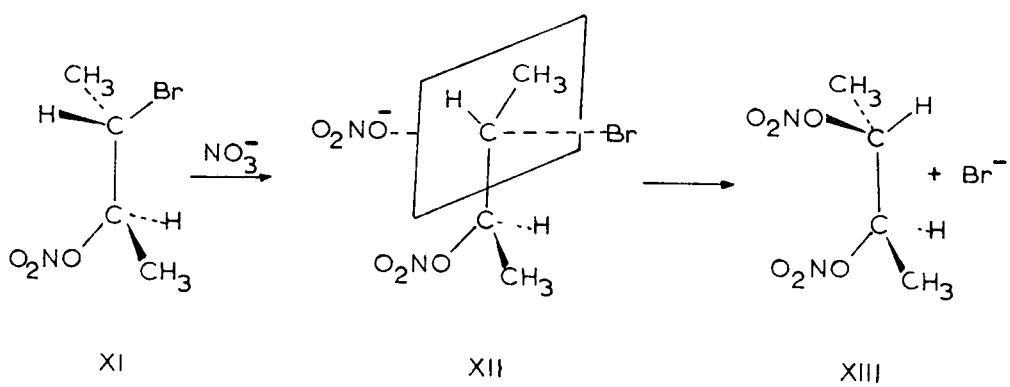

(14)

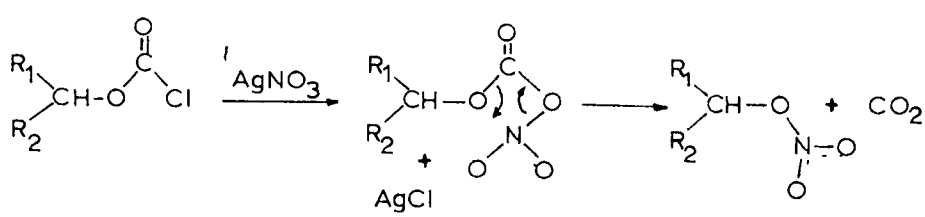

(15)

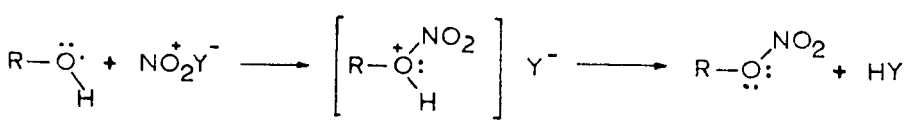

(16)

Method (iii) is the most widely used to synthesize organic nitrate esters. The reacting species is NO_2^+ as in aromatic nitration (C-nitration) "where the attack by the substituting agent is on the unsaturation electrons, i.e. conjugated carbon 2p electrons. Since non-bonding electrons of nitrogen and oxygen can participate deeply in such conjugation we should expect them to share many properties with the unsaturation 2p electrons of carbon including general vulnerability to electrophilic substituting agents" (39). Since the mechanism (16) is closely related to that of C-nitration the originally suggested (40) O-nitration term is retained (41).

There are a number of reagents which possess the structure $NO_2^+ Y^-$ required for O-nitration and consequently a great diversity of preparative procedures. The reaction is usually carried out at or below 0^oC with one of the following reagents (a) HNO_3; (b) $HNO_3/HCCl_3$; (c) HNO_3/H_2SO_4; (d) HNO_3/Ac_2O; (e) HNO_3/Ac_2O + AcOH; (f) $N_2O_5/HCCl_3$; (g) gaseous N_2O_5; (h) NO_2Cl (with or without catalyst); (i) NO_2F (with or without catalyst). These and other special synthetic routes were extensively reviewed recently (27) (24) (42). A more detailed examination of the various nitration mechanisms is made in the chapter on "Results and Discussion."

V. Reactions of Nitrate Esters.

Since the reactions of organic nitrates depend on the structure of the nitrate ester as well as on the reagent and reaction conditions and often two or more types of reaction take place simultaneously only a few mechanistic studies have so far been reported (43). It has been pointed out recently (44) that all of the chemical transformations on

record may be considered as involving one or more of five possible modes of scission of the ester group. Reactions which cause such bond cleavages range from solvolysis and hydrolysis through catalytic hydrogenolysis to photochemical decomposition and explosions.

The first three of the five modes of scission (Figure 4) are heterolytic while the last two are claimed to be homolytic. In other words all reactions which proceed via an ionic mechanism seem to cause bond cleavage in the nitrate moiety by one of modes 1, 2 or 3, while reactions occurring by free radical mechanism seem to involve mode 4 or 5. The first four modes are well established, while mode 5 is tentative as yet and is based on indirect evidence.

Reagents causing ionic decomposition (modes 1, 2 and 3) may be either electrophilic or nucleophilic and the reactions which occur may be substitutions or eliminations. The substitution may be electrophilic (S_E) or nucleophilic (S_N) according to the nature of the reagent. The elimination reactions may be classified as carbonyl elimination ($E_{C=O}$) and olefinic elimination ($E_{C=C}$) depending on whether carbonyl or olefinic compounds are the final products (43). Ionic reactions of the above types are summarized in Table IV.

It is interesting to note that electrophilic reagents in substitution (A, which may be charged e.g. H^+ or uncharged e.g. Lewis acids) always attack the electron rich oxygen atom while nucleophilic reagents in substitution (B: , which may be charged e.g. HO^- or EtO^- or uncharged e.g. pyridine) always attack the carbon neighbouring to the NO_2 or the nitrogen of the nitroxy group which indicates that they must be more electron deficient than oxygen.

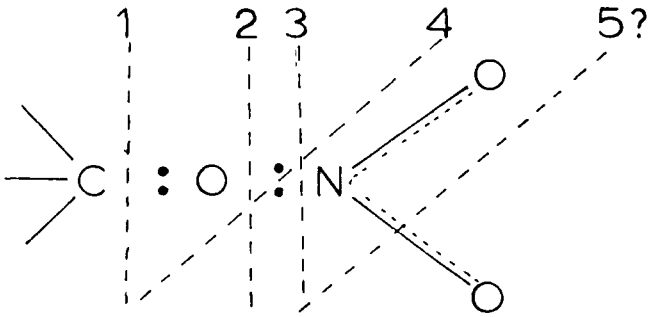

FIGURE 4 Modes of Scission of the Nitroxy Group

TABLE IV Reaction Mechanisms

	Reaction Mechanisms	Mode of Scission
1 Electrophilic substitution on oxygen : 	S_{EO}	3
2 Nucleophilic substitution on carbon: 	S_{NC}	1
3 Nucleophilic substitution on nitrogen: 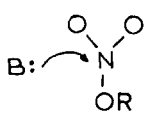 $\longrightarrow$ $B:NO_2^+ + RO^-$	S_{NN}	3
4 β-Hydrogen elimination $B: + H-C-C-ONO_2 \longrightarrow B:H^+ + >C=C< + NO_3^-$	$E_{C=C}$	1
5 α-Hydrogen elimination: $B: + H-C-ONO_2 \longrightarrow B:H^+ + >C=O + NO_2^-$	$E_{C=O}$	2

A. Electrophilic Substitution on Oxygen (S_{EO})

Electrophilic substitution by proton (protonation) of nitrate esters may be considered as the reverse reaction of O-nitration (17). The reaction occurs when a nitrate ester is dissolved in concentrated sulfuric acid and the equilibrium is very likely shifted far to the right (the alcohol may react further with the concentrated acid) since the original nitrate ester may not be recovered by addition of water. Furthermore ultraviolet spectroscopy indicated the presence of NO_2^+ and the absence of the original ester in the aqueous solution (42).

Because of this phenomenon nitrate esters may be used as nitrating agents (45) which is an obvious extension of the principle of nitration by NO_2Y since the more frequently used nitric acid may be considered as the zero member of the nitrate ester family. It is worthy of mention that certain nitrate esters with high mobility of NO_2^+ can exhibit mild nitrating activity through self ionization. Among these compounds are the nitrate esters of cyanohydrins (XIV, XV, XVI) which can be used for nitration of sensitive compounds as was discussed recently in a review by Topchiev (46).

Nitrate esters also undergo electrophilic substitution on oxygen (S_{EO}) by other agents (18). A number of Lewis acids may be used as effective nitration catalyst with nitrate esters. Thus benzene and toluene are nitrated by ethyl nitrate in the presence of aluminium chloride (47).

Just as protonation or other electrophilic substitution occurred on the oxygen atom of a nitrate ester it should also occur on the element (X) of every $(R^1)_nXNO_2$ compound in which the element X possesses the necessary electron density. In other words this should be true for

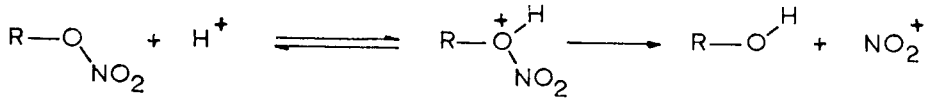

(17)

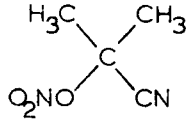

XIV

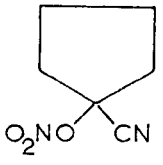

XV

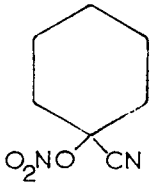

XVI

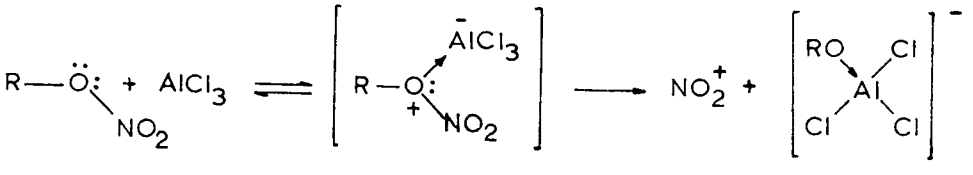

(18)

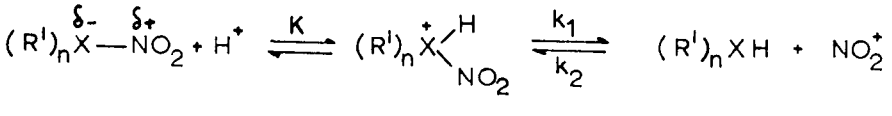

(19)

elements other than oxygen from the right hand side of the period (N, O, F). Consequently the originally introduced S_{EO} (electrophilic substitution on oxygen) is a special form of S_{EX} (electrophilic substitution on element X, i.e.: E_{SN}; E_{SO}; E_{SF}) (19). Since the NO_2^+ formed in this reaction is the nitrating species in every nitration therefore the availability of NO_2^+ determines the nitrating power of $(R^1)_nXNO_2$ or more precisely that of the corresponding conjugate acid, $(R^1)_nX^+<^{NO_2}_{H}$

It has been known since 1905 that nitryl fluoride (FNO_2) is a powerful nitrating agent (48) (49). This fact was confirmed in a more recent publication (50) and the efficiency of nitryl fluoride as an O-nitrating agent was compared (51) with that of nitryl chloride ($ClNO_2$) (52). It was pointed out that "generally there is a greater yield of nitrated material with nitryl fluoride than with the chloride, even when the latter is used with a catalyst. This suggests that nitryl fluoride stands higher than nitryl chloride in the series of nitrating agents of the type XNO_2 in which the nitrating power increases with the electron accepting quality of X." (51).

On this basis one may assemble a preliminary series of nitrating agents from the electronegativity estimations in Figure 1 as shown in equation 20.

$$\begin{array}{lllll} \ldots & R_3C\text{-}NO_2 < & R_2N\text{-}NO_2 < & RO\text{-}NO_2 < & F\text{-}NO_2 \\ & & & & \vee \\ & \ldots\ldots\ldots\ldots & \ldots\ldots\ldots\ldots & \ldots\ldots\ldots\ldots & < Cl\text{-}NO_2 \end{array} \qquad (20)$$

Evidently each member of this series except FNO_2 and $ClNO_2$ represents a class of compounds and the actual nitrating power largely depends on the chemical nature of R. Consequently for those members of the series there are subdivisions which may fill the gap between two neighbouring elements

or they may even overlap each other. We may consider the series previously compiled by Gillespie and Millen (31) as a portion of the subdivision for O-nitro compounds (53):

$$EtONO_2 < HO\text{-}NO_2 < AcO\text{-}NO_2 < O_2NO\text{-}NO_2 < H_2\overset{+}{O}\text{-}NO_2 \quad (21)$$

B. Nucleophilic Substitution on Carbon (S_{NC}) and Nitrogen (S_{NN})

Nucleophilic substitution in nitrate esters may take place on the two neighbouring atoms of the electron rich oxygen namely on carbon and nitrogen.

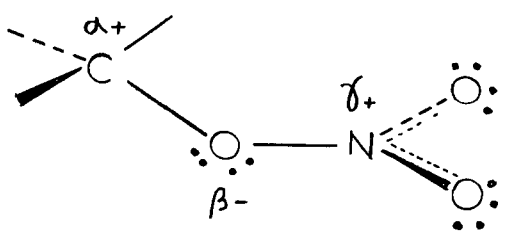

XVII

It is rational to assume that nucleophilic reagents (B:) with high electron density (Table IV) would attack the more positive site in the nitrate esters. In such a simple electrostatic model (XVII) taking no account of steric effects, if $\alpha > \gamma$ then S_{NC} would predominate and if $\gamma > \alpha$ an S_{NN} reaction should take place. Under special circumstances ($\alpha \simeq \gamma$) both reactions may occur simultaneously. In practice, however, the number of reported S_{NN} reactions is much larger than the number of S_{NC} reactions, indicating that the polarization of the O-N bond is much larger than that of the C-O bond.

"Alkylation with nitrate esters" i.e. the S_{NC} reaction, has been recently reviewed in detail by Boschan and co-workers (42). One of the

classical examples (54) of the S_{NC} reaction is the decomposition of benzhydryl nitrate ester with primary or secondary amines such as piperidine. On the basis of the reaction products isolated one may interpret the reaction according to equation 22. However this is not the only reaction which occurs under these conditions, the carbonyl elimination proceeds simultaneously with the formation of benzophenone but to considerably smaller extent (3:1). Weaker bases (aniline, benzylamine) on the other hand gave almost exclusively the corresponding product with N-C bond formation according to 22.

In certain reactions such as basic and neutral hydrolyses and solvolyses of nitrate esters (55) (56) it is not obvious whether the S_{NC} or S_{NN} mechanism is operative since the products would be the same in either case (23, 24).

For this reason Yoffe and co-workers (57) studied the mechanism of hydrolysis of several nitrate esters by means of the ^{18}O isotope technique. According to their findings the mechanism of hydrolytic cleavage may proceed by either mechanism 25 or 26 depending on the structure of the nitrate ester in question.

A change in the hydrocarbon portion may cause a change in the order of the reaction ($S_N2 \longrightarrow S_N1$) and furthermore such a change may also alter the point of attack in the alkaline hydrolysis of nitrate esters from $S_{NC} \longrightarrow S_{NN}$. These changes are summarized in the series 27:

Ph- , n-alkyl, sec. alkyl, tert. alkyl, Ph_3C-, H- ,

$$S_{NN}1 \longrightarrow S_{NN}2 \longrightarrow S_{NC}2 \longrightarrow S_{NC}1 \qquad (27)$$

Extensive investigation has been made of sugar and related polynitrates by treating them with nitrogen bases (such as pyridine, piperdine,

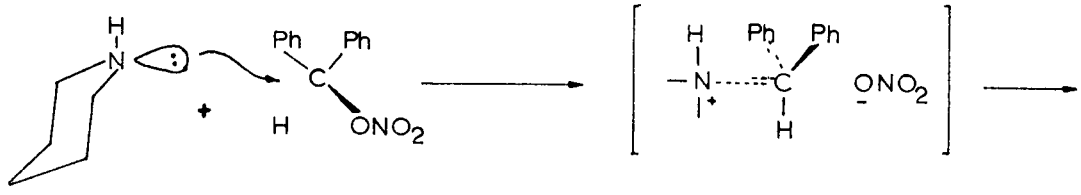

(22)

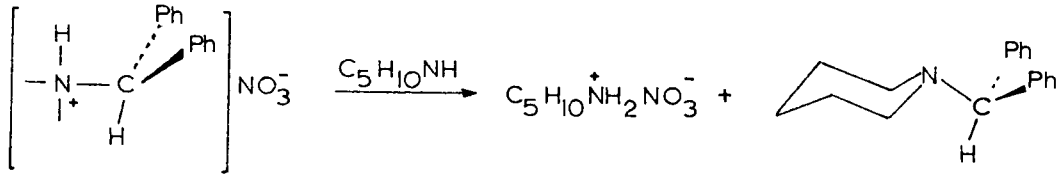

$$PhCH_2ONO_2 + OH^- \longrightarrow PhCH_2OH + NO_3^- \qquad (23)$$

$$t\text{-}BuONO_2 + 2\ H_2O \longrightarrow t\text{-}BuOH + H_3O^+ + NO_3^- \qquad (24)$$

$$^{18}OH + \text{-}\overset{|}{C}\text{-}O\text{-}NO_2 \longrightarrow H^{18}O\text{-}\overset{|}{C}\text{-} + NO_3^- \qquad (S_{NC}) \qquad (25)$$

$$\text{-}\overset{|}{C}\text{-}O\text{-}NO_2 + {}^{18}OH^- \longrightarrow \text{-}\overset{|}{C}\text{-}O^- + H^{18}ONO_2 \qquad (S_{NN}) \qquad (26)$$

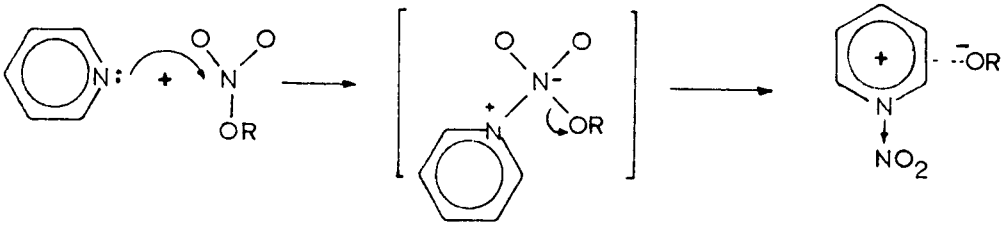

(28)

hydroxylamine, etc.) (24) (62). In all cases full or partial denitration produced the parent alcohol with retention of configuration. This proved that the C-O bond was not ruptured and therefore the nucleophilic substitution took place on the nitrogen (S_{NN}). In general such a reaction involves the formation of the alcoholate anion as an intermediate (28) while the other component of the ion pair contains the N-nitro base cation. During the customary working up procedure in aqueous solution the alcoholate anion produced the corresponding alcohol.

In certain cases special stereoselective denitration took place. Pyridine denitrated mannitol hexanitrate (58) selectively at C_3 or its equivalent C_4, at 25° (29). Dulcitol hexanitrate gave the pentanitrate by selective denitration (59) on C_3 and equivalent C_4 with pyridine at 50° (30). Cellulose 2, 3, 6-trinitrate denitrated at C_2 selectively (60) with hydroxylamine in pyridine (31). Similar results were obtained with methyl β-D-glucoside tetranitrate and hydroxylamine in pyridine (61). In this case (32) the 4-O-nitro group, not present in cellulose, was also replaced by the hydroxyl group and to a greater extent than the 2-O-nitro group.

Isohexide (i.e. isoidide: 1, 4;3,6-di-O-anhydro-L-iditol (XVIII); isosorbide: 1,4;3,6-di-O-anhydro-D-glucitol (XIX); and isomannide: 1,4;3,6-di-O-anhydro-D-mannitol (XX)) dinitrates (62) and 1,2- cyclohexanediol dinitrates (XXI) (XXII) (63) reacted with boiling anhydrous pyridine. Kinetic evidence (62) excluded the possibility of an S_{NC} mechanism and instead of the parent diols, as might be expected for S_{NN} reactions, polymeric material was obtained as the chief carbon-containing reaction product.

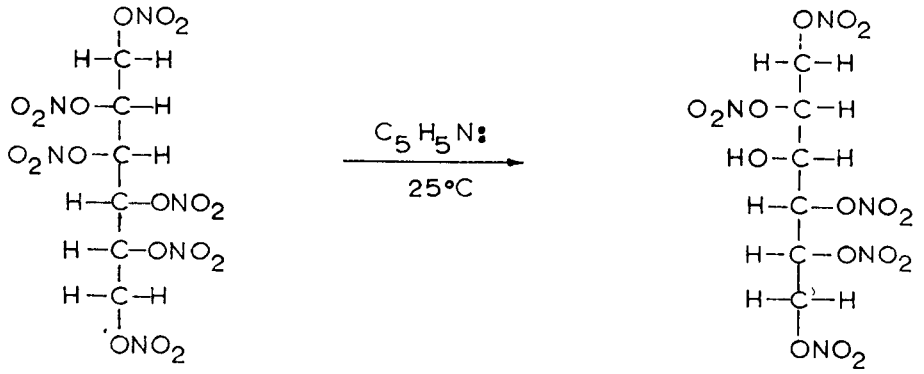

(29)

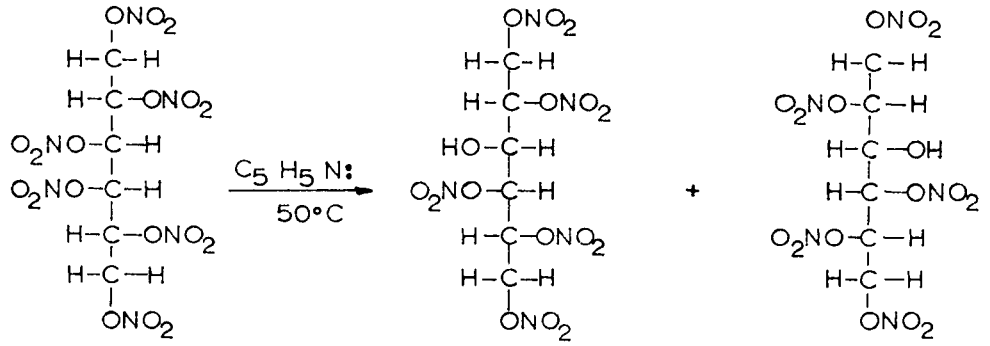

(30)

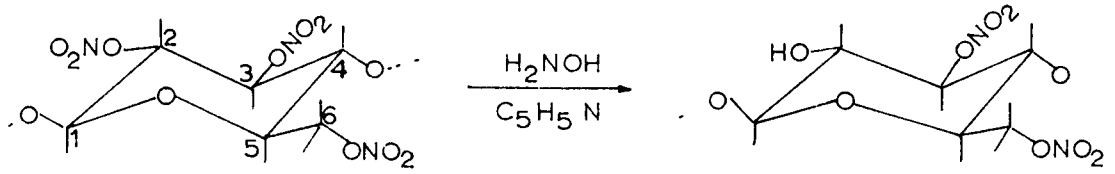

(31)

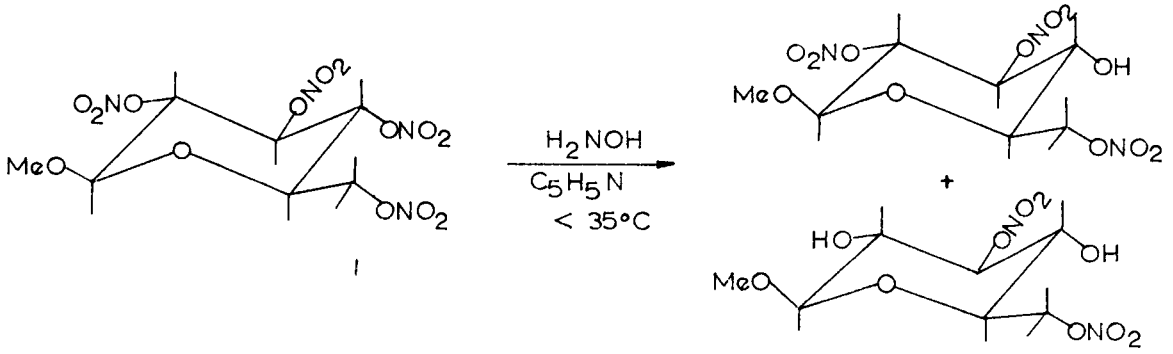

(32)

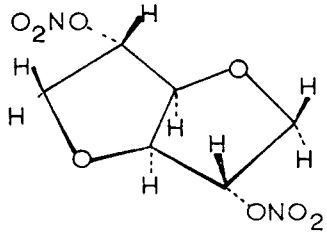

XVIII

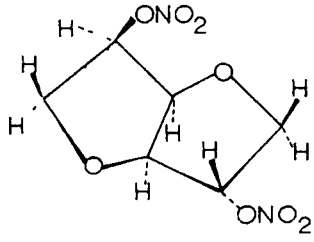

XIX

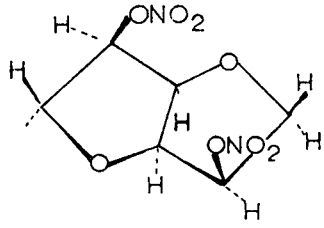

XX

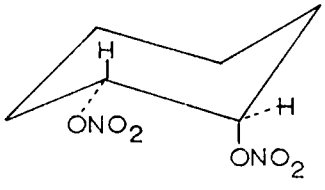

XXI

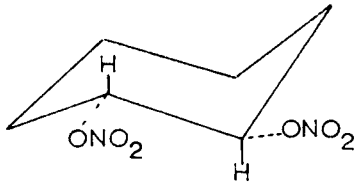

XXII

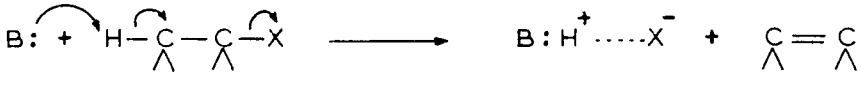

(33)

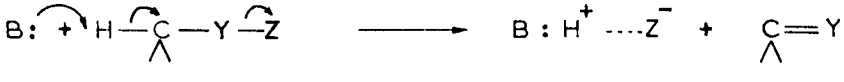

(34)

C. Olefin ($E_{C=C}$) and Carbonyl ($E_{C=O}$) Elimination Reactions.

The difference between these elimination reactions 33 and 34, is that the double bond formed is between carbon atoms in one case, and between carbon and oxygen atoms in the other. This variation in product formation reflects a difference in the detailed mechanism. In the case of olefin elimination the hydrogen atom at the β-position to the nitroxy group is attacked by the nucleophile (33) and the reaction is thus frequently called "β-elimination" (64). Carbonyl elimination represents a nucleophilic attack (34) on the hydrogen atom at the α-position to the nitroxy group and consequently is called "α-elimination".

These elimination reactions may occur as side reactions to nucleophilic substitution on nitrogen (S_{NN}) and on carbon (S_{NC}), thus they caused considerable confusion in the older literature. Nucleophilic reagents (like HO^-) attack the partially positive nitrogen or α-carbon in nitrate esters. If, however, by any means hydrogen atoms elsewhere in the molecule become acidic to such an extent that their electrophilicity becomes comparable to that of the nitrogen or α-carbon atom then in addition to nucleophilic substitution elimination reactions also will take place.

In the aliphatic series the percentage of olefinic elimination increases with the branching of the chain; i.e. with the stability of the intermediate carbonium ion. Both second and first order reactions (cf. 33) may take place in olefin elimination while carbonyl elimination (34) seems to be always bimolecular. Comparable figures for the two reactions are given in Table V from the data of Baker and coworkers (65) (66).

Table V.

Elimination Reactions with Nucleophilic Reagent OH^- in 90% Aqueous Ethanol Solution

	$E_{C=C}2$				$E_{C=O}2$			
	%		k x 10^5		%		k x 10^5	
Nitrate Ester	20°	60°	20°	60°	20°	60°	20°	60°
$CH_3CH_2ONO_2$		2		0.08		4.8		0.21
$(CH_3)_2CHONO_2$		14.5		0.09		13.7		0.09
$(CH_3)_3CONO_2$	23		1.54**	260*	-	-	-	-
$PhCH_2ONO_2$	-	-	-	-	87	-	9.24	847
$PhCH_2CH_2ONO_2$		90		8.1		5		0.33
$PhCH(CH_3)ONO_2$		1		0.016	3.0		0.127	
$(Ph)_2CHONO_2$	-	-	-	-	1.0		31.7	

*) Extrapolated from values observed at 0°, 20° and 30°; $kx10^5$ = 0.06; 1.54 and 5.5 respectively. Because of deviations the true value may lie between 130 and 460.

**) First order reaction: $E_{C=C}1$.

Nucleophilic reagents other than OH^- also cause carbonyl elimination reactions. Aralkyl nitrate esters yielded almost exclusively the corresponding carbonyl compounds with anhydrous pyridine (35) (67) (36) (68).

A detailed study of the elimination mechanism in benzyl nitrate has been carried out recently by means of kinetic isotope techniques (69). Both the 5.04 deuterium isotope effect and the 1.02 nitrogen-15 isotope effect ("which is one of the largest observed for nitrogen in a rate process") favoured a concerted mechanism (37) over a two step carbanion mechanism (38) for carbonyl elimination (Table VI). A value of 1.16 for the secondary deuterium isotope was indicated in the nucleophilic substitution. No significance, however, was attached to the difference between this value and unity because of the rather large percentage error in the determination of the small amount of nitrate ion.

Table VI.

Isotope Effects in the Reaction of Benzylnitrate with Sodium Ethoxide in Absolute Ethanol at 60.2°.

	$PhCH_2ONO_2$	$PhCD_2ONO_2$
% $E_{CO}2$	88.7	64.4
% S_N2	11.3	35.6
$k_{total} \times 10^3$	13.9	3.79
$k_{E_{CO}2} \times 10^3$	12.3	2.44
$k_{S_N2} \times 10^3$	1.57	1.35
$(k_H/k_D)E_{CO}2$	5.04 ± 0.25	
$(k_H/k_D)_{S_N2}$	1.16	
$(k^{14}/k^{15})E_{CO}2$	1.0196 ± 0.0007	

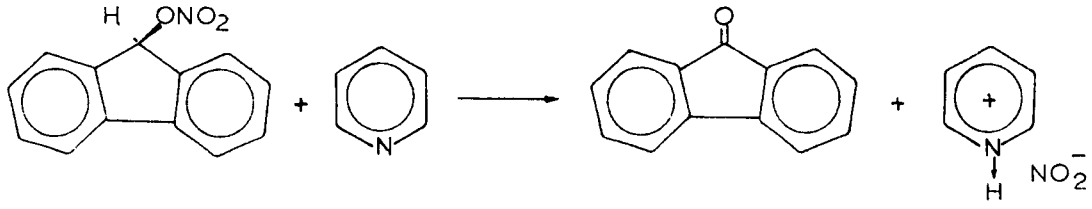
H
ONO2
N
O
N
H
NO2

(35)

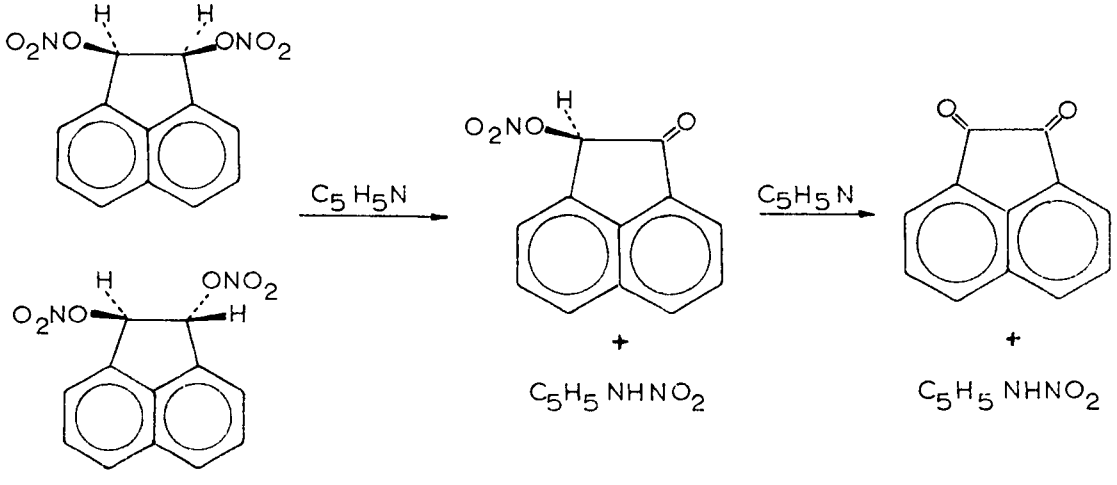
O2NO
ONO2
H
H
C5H5N
O2NO
O
C5H5N
O
O
C5H5NHNO2
C5H5NHNO2

(36)

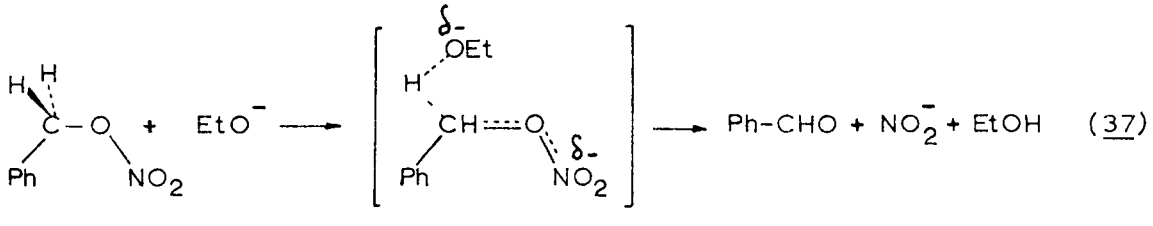
H
H
C
O
Ph
NO2
EtO⁻
δ-
OEt
H
CH
O
δ-
Ph
NO2
Ph-CHO + NO2⁻ + EtOH

(37)

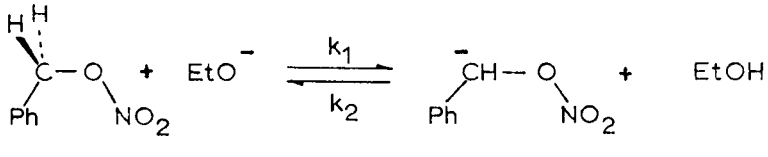
H
H
C
O
Ph
NO2
EtO⁻
k1
k2
CH
O
Ph
NO2
EtOH

(38)

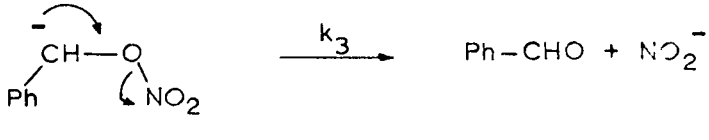
CH
O
Ph
NO2
k3
Ph-CHO + NO2⁻

D. Homolytic Decomposition of Nitrate Esters

Presumably both thermal decomposition (70) and explosion (~~71~~ 25) of nitrate esters proceed via a free radical mechanism. The principal cleavage occurs between the ester oxygen and nitrogen atoms with the formation of alkoxyl radicals (39).

$$RONO_2 \longrightarrow RO\cdot + NO_2 \qquad (39)$$

This conclusion was confirmed by several authors working either on slow thermolysis with the aid of reaction kinetics or on flames (combustion) utilizing infrared technique. Equation 39 thus indicates that homolytic cleavage takes place according to mode of scission 4 (Figure 4).

A number of simple primary aliphatic nitrate esters have been studied by both of the above techniques and the results from the thermolysis of n-propyl nitrate (72) support a degradation scheme essentially similar to that postulated for ethyl nitrate (40).

$$CH_3CH_2CH_2ONO_2 \longrightarrow NO_2+CH_3CH_2CH_2O\cdot \longrightarrow CH_3CH_2\cdot+CH_2O \qquad (40)$$

However, it is not certain whether the initiation proceeds according to 40 or by intramolecular rearrangement of the biradical formed in 41.

$$CH_3CH_2CH_2ONO_2 \longrightarrow HONO+(\cdot CH_2CH_2CH_2O\cdot) \longrightarrow CH_2{=}CH_2+CH_2O \qquad (41)$$

Further reaction may occur via attack of the original ester by NO_2 or HONO (but not $C_3H_7O\cdot$), in agreement with a "chain thermal" process suggested by Gray and Yoffe (73) for the ignitions of methyl and ethyl nitrates (42 and 43).

$$NO_2+CH_3CH_2CH_2ONO_2 \longrightarrow HONO+(\dot{C}H_2CH_2CH_2ONO_2) \longrightarrow CH_2{=}CH_2+H_2CO+NO_2 \qquad (42)$$

$$NO_2+CH_3CH_2CH_2ONO_2 \longrightarrow HONO+(\dot{C}H_3\dot{C}HCH_2ONO_2) \longrightarrow CH_3CHO+H_2CO+NO \qquad (43)$$

The decomposition of the secondary isopropyl nitrate ester showed close analogy to the pattern observed in the case of the normal isomer (44).

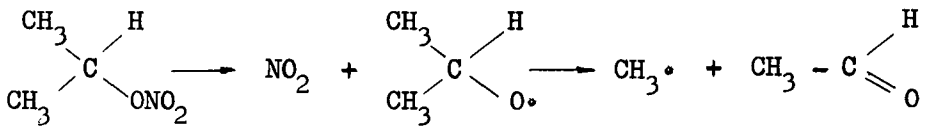

(44)

It was suggested furthermore (72) that the NO_2 attacks the nitrate esters as in 45 and 46. A remarkable difference has been observed (74), however, in the flame decomposition of butanediol dinitrates with respect to that of monoesters. "The results indicate that these esters (2, 3-butanediol dinitrate and 1, 4-butanediol dinitrate) in contrast to those of mononitrates so far studied, break down in a unimolecular fashion" according to 47 and 48. Only traces of the suspected intermediates acetoin (XXIII) and diacetyl (XXIV) were found among the products.

Nitrate esters with more complex structure were also investigated. Glycerol trinitrate (75) showed a close analogy to the decomposition of vicinal dinitrates (47). The first step in the thermal decomposition is probably the scission of an O-N bond (49). There are, however, two possibilities since nitroglycerine has both primary and secondary nitroxy groups. Both of these alkoxyl radicals (49) will yield essentially the same products according to (50).

Recent publications of Wolfrom and co-workers (76) (77) (78) provide some interpretation of the cellulose nitrate thermal decomposition. Interesting results were obtained by means of ^{14}C - labelled cellulose (mostly at position 2 and 5) which gave an initial pattern for the thermal degradation of cellulose nitrate as shown in 51.

In spite of the early (1901) pioneering work of Will (79) on nitrate stability, kinetic studies of thermal decomposition have been carried out in a

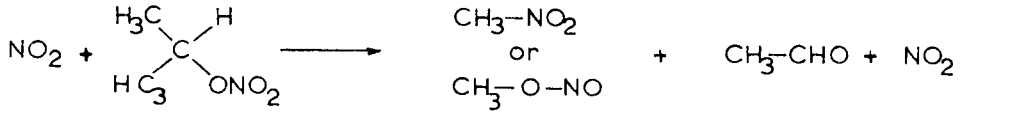

(45)

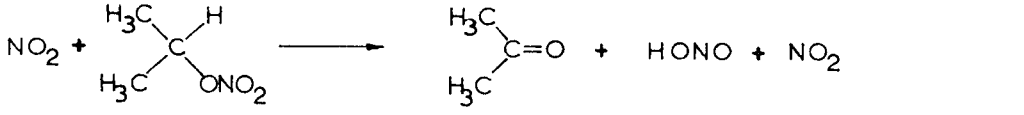

(46)

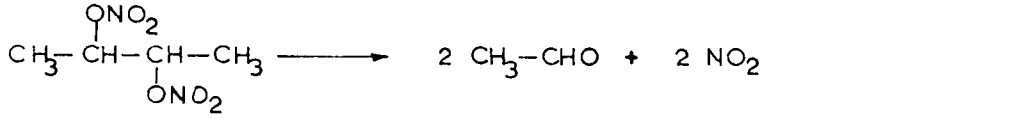

(47)

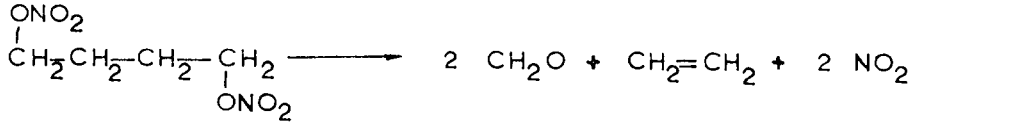

(48)

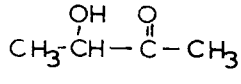

XXIII

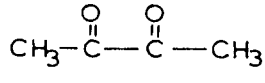

XXIV

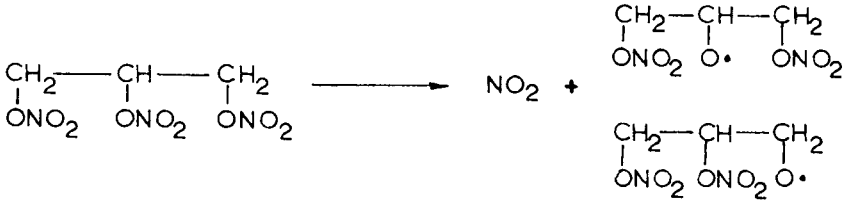

(49)

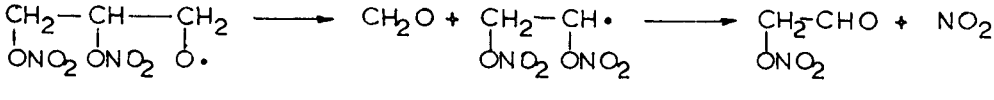

(50)

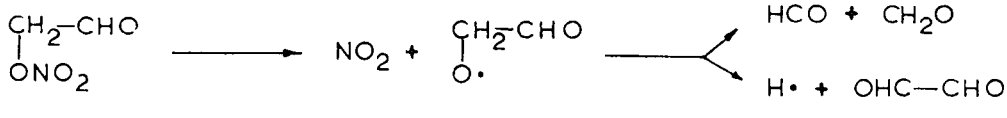

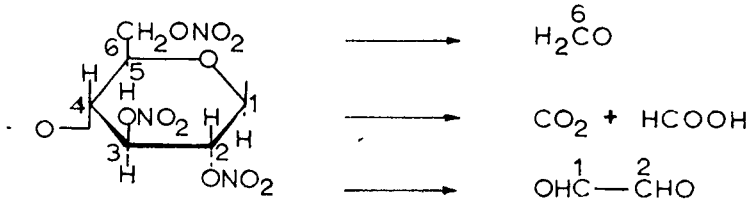

(51)

Table VII.

Log Frequency Factors and Activation Energies for Thermal Decomposition of Nitrate Esters.

	log A(sec^{-1})	E_a (kcal/mol)	Year	Ref.
$CH_3CH_2ONO_2$	16.85	41.23	1954	81
$CH_3CH_2CH_2ONO_2$	14.7	36.86	1949	82 cf42
$O_2NOCH_2CH_2ONO_2$	15.9	39.0	1947	83
$O_2NOCH_2CH(ONO_2)CH_2ONO_2$	13.6	35.0	1959	84
	17.1	40.3	1947	83
Nitrocellulose	18.95	43.7	1955	85
	-	32.8-35.8	1961	86
Isosorbide dinitrate	15	37	1960	62
$ClONO_2$	14.18	30.0	1961	62
$FONO_2$	13.76	29.7	1958	88

more elaborate way only in the last 15 or 20 years. The unimolecular decomposition of nitrate esters followed Arrhenius' rate equation (52).

$$k = A.e^{-\frac{Ea}{RT}} \qquad (52)$$

The apparent activation energies, E_a (kcal/mol), and log frequency factors, log A (sec^{-1}), for representative esters are summarized in Table VII.

Although one would expect some sort of correlation between structure and reactivity, one should treat these rate constants cautiously because two or more types of decomposition may take place simultaneously. Furthermore, the measurements were carried out by different experimental techniques in different laboratories and because of the large variations in the values no generalization seems permissable.

Steinberg and co-workers (80) reported differences in the burning rates, k (cm/sec), of ordinary and deuterated nitrate esters. As the degree of deuteration increased the burning rates were decreased extensively. For example, perdeutero-isopropyl nitrate did not even burn under the experimental conditions. The isotope effects obtained are summarized in Table VIII. It has not been determined as yet whether these effects are comparable with those kinetic isotope effects which might have been observed in slow thermal decomposition.

Table VIII

The Effect of Deuterium Substitution on Burning Rates of Nitrate Esters (80).

Compound	k_H/k_D
$CD_3CD_2ONO_2$	1.4
$(CH_3)_2CDONO_2$	1.26
$(CD_3)_2CHONO_2$	1.54
$(CD_3)_2CDONO_2$	∞

The Photochemistry of the Nitrate Esters

and

Related Compounds.

Photolysis of the $\geq$C–O–X group where X may be halogen, –OR, –NO, or $-NO_2$ is of current interest (89)(90). Photochemical reactions are considered in general as transformations via free radical intermediates and thus photolysis provides an alternative route to thermolysis for the decomposition of nitrite and nitrate esters by free radical mechanisms.

A recent review (91) on the photolysis of nitrite esters, RONO, summarized the synthetic potential of the technique. The photolytic decomposition is considered to proceed via a homolytic O–NO bond cleavage which provides nitric oxide and alkoxyl radical. The alkoxyl radical thus formed has a relatively short lifetime and may undergo further transformation by one of several possible routes. The products isolated thus entirely depend on the route "selected" by the radical and the "selected" mechanism is a function of the intra-and intermolecular chemical environment.

Alkyl nitrites (XXV) exhibit a number of possibilities for electronic excitation (92). The lowest energy (longest wavelength) transition (~3600 Å) seems to be (93) an $n_N \longrightarrow \pi^*$ excitation since the non-bonded electrons of

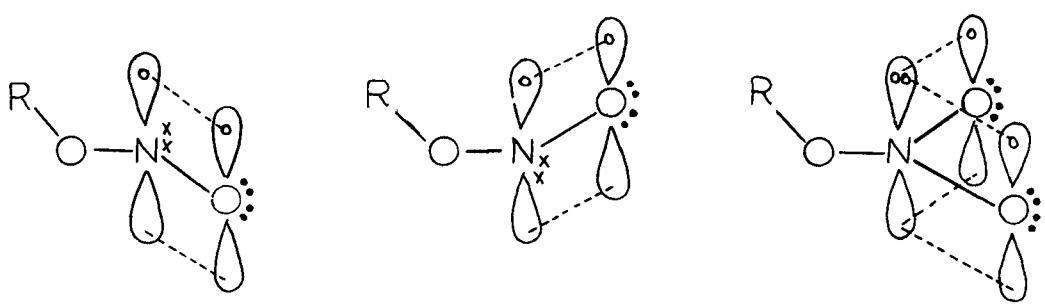

trans- cis-

XXV XXVI

nitrogen (x) are the most loosely bound and in this excitation one nonbonding electron of nitrogen is transferred to the lowest empty antibonding π (i.e. π^*) orbital. The nonbonded electrons of oxygen (•) are more tightly bound because of the greater electronegativity of oxygen and thus their electronic

excitation $n_O \longrightarrow \pi^*$ requires higher energy (i.e. shorter wavelengths) seemingly around 2700 Å (Figure 5). At even shorter wavelengths is the very intense $\pi \longrightarrow \pi^*$ band representing the excitation from a low energy level π orbital (o) to the antibonding π orbital (π^*).

Apparently it has not been conclusively determined as yet which one of these excitations brings about the suggested O-NO bond cleavage in solution photolysis. It is possible that one of the two low energy excitations, $n_N \longrightarrow \pi^*$ or $n_O \longrightarrow \pi^*$, or both of them are responsible for the photolysis since the $n_N \longrightarrow \pi^*$ excited nitrite ester readily decomposed in the gaseous phase (94).

In nitrate esters, however, the nitrogen atom does not possess non-bonding electrons, therefore, the corresponding long wavelength absorption is absent from the spectrum (Fig. 6 B). On the other hand there are twice as many π and n_O electrons in the nitroxy group (XXVI) as in the oxynitroso group (XXV).

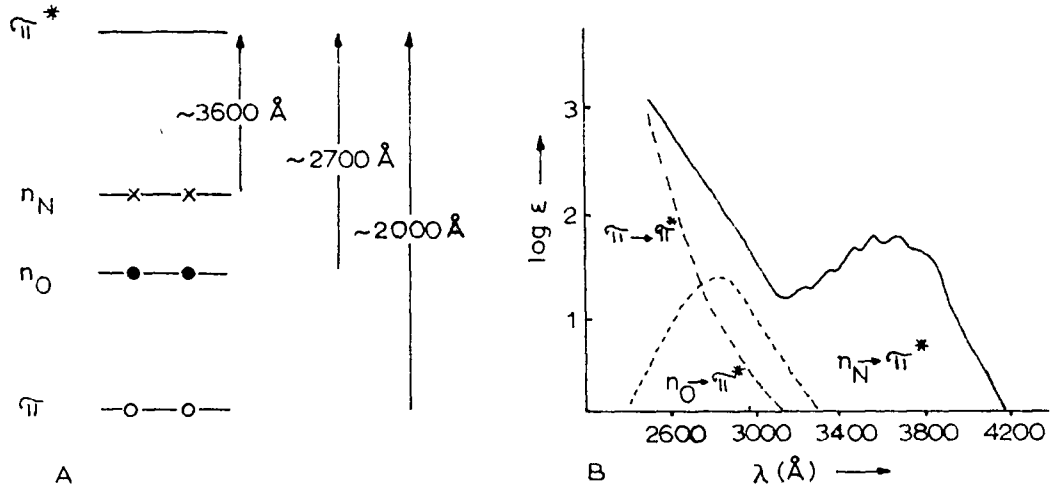

Figure 5.

A: Energy Levels of Molecular Orbitals and Possible Electronic Transitions for Nitrite Esters.

B: Typical Electronic Spectrum of a Nitrite Ester (2-butyl nitrite in ether (95)). The dotted lines represent the estimated separation of the various transitions.

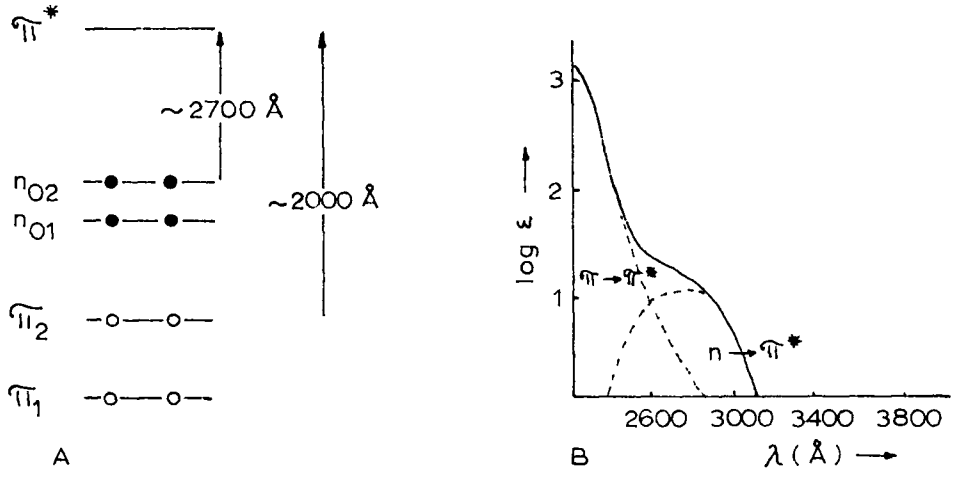

Figure 6.

A: Energy Levels of Molecular Orbitals and Possible Electronic Transitions for Nitrate Esters.

B: Typical Electronic spectrum of a Nitrate Ester (2-butyl nitrate in ethanol (95)). The dotted lines represent the estimated separation of the various transitions.

No systematic study of the electronic spectra of nitrate esters has been published as yet but Rao (96) suggested that the shoulder at 2700 Å is really due to an n $\longrightarrow \pi^*$ transition, while the high intensity band at the shorter wavelength would represent the $\pi \longrightarrow \pi^*$ excitation. A typical nitrate ester spectrum together with an illustrative energy level diagram* is shown in Figure 6.

Very little is known about the photochemical behaviour of nitrate esters. Photolysis of ethyl nitrate in the gas phase with the 2537 Å lines and 2650 Å of the mercury arc led to the conclusion that the oxy-nitro bond scission is the predominant reaction of the excited nitrate ester molecule. Equations 53 to 58 seemed to explain the observations (99):

$$(1.00)\quad C_2H_5ONO_2 + h\nu \longrightarrow C_2H_5O\bullet + NO_2 \qquad (53)$$

$$(0.53)\quad C_2H_5O\bullet \longrightarrow CH_3\bullet + CH_2O \qquad (54)$$

$$(0.47)\quad C_2H_5O\bullet \longrightarrow H\bullet + CH_3\text{-}CHO \qquad (55)$$

$$(0.485)\quad CH_3\bullet + NO_2 \longrightarrow CH_3NO_2 \qquad (56)$$

$$(0.045)\quad CH_3\bullet + C_2H_5ONO_2 \longrightarrow C_2H_5OCH_3 + NO_2 \qquad (57)$$

$$(0.37)\quad H\bullet + C_2H_5ONO_2 \longrightarrow C_2H_5OH + NO_2 \qquad (58)$$

The gaseous phase photolysis of nitrite and nitrate esters by sunlight is also a current problem of air pollution (100).

A recent Japanese patent (101) seemed to confirm the free radical nature of the photo-decomposition fragments of nitrate esters in solution since the esters (generated *in situ* from alcohol, inorganic nitrate, and acid) were claimed to function as polymerization accelerators when irradiated during the preparation of crystalline polymers. A detailed study some years ago (102)

---

*) These energy level diagrams (Figure 5 A and 6 A) were constructed by analogy to those of NO_2 (11), NO_2^- (97) and $Na^+\,^-CH_2NO_2$ (98).

proved that thermolysis of alkylnitrate also accelerated additional polymerization of methyl methacrylate via a free radical mechanism. The efficiency of alkylnitrates as "anti-knock" additives in gasolines points to a similar mechanism.

The photo-decomposition of cellulose nitrate has been recently studied by Claesson and co-workers (103) (104). Fully and partially nitrated cellulose samples (13.87 and 12.12% N respectively) were photolysed with 99.5% monochromatic light of 2537 Å. The extent of depolymerization was followed viscometrically. It was found that the quantum yields for the depolymerization did not differ greatly for the two samples being 0.02 for the partially nitrated cellulose and 0.01 for the fully nitrated polymer. This might indicate that the presence of an active group (-OH) in the molecule aided the depolymerization. On the other hand the possible occurrence of reactions other than depolymerization was not excluded and the low quantum yield of depolymerization might mean that most of the light quanta were utilized for other processes.

A wavelength dependence study (104) indicated that while the effectiveness of the light quanta was roughly the same at 2537 and 3020 Å, monochromatic light at 3340 and 3650 Å was practically inactive. On the other hand the utilization of β-naphthylamine as photosensitizer caused photo-depolymerization even at the lower energy wavelengths (3340 and 3650 Å). The quantum yield obtained, however, was lower by about an order of magnitude (0.0006) indicating that the efficiency for energy transfer from naphthylamine to nitroxy group is less than 10%.

The effective spectral region for the photolysis of nitrate esters has been determined recently in this laboratory (105) to be 2650-3340 Å, at the tail-end of the characteristic UV -absorption (Figure 6 B) where the suggested $n \longrightarrow \pi^*$ band is located. In the same study the photolysis of

25 different nitrate esters in both ethanol and benzene solutions in the presence of diphenylamine was reported. The experiments were carried out at 15°C with the unfiltered mercury arc spectrum and an approximately 1:1 molar ratio of nitrate ester and diphenylamine. For the detailed study isosorbide dinitrate (1,4;3,6-dianhydro-D-glucitol-2,5-dinitrate) (XIX) was used in $2\text{-}4 \times 10^{-2}$ molar solutions and nitro- and nitroso- diphenylamines were identified among the products (59).

There were two possible mechanisms for the photodecomposition which would rationalize the experimental results. In the first, the excited nitrate ester was thought to break up to alkoxyl radical and nitrogen dioxide in a manner similar to that proposed for the gas phase photolysis of ethyl nitrate (53). The alkoxyl radical would then react further either by decomposition to fragments or by attack on other molecules. The nitrogen dioxide would be scavenged by the diphenylamine. In this model the origin of the small amount of nitroso-compounds formed remained unexplained since an intermediate photolysis of NO_2 to NO and O would be less likely because NO is not very reactive toward organic compounds as a nitrosating agent.

The second alternative was that the excited nitrate ester had a relatively long lifetime and could undergo reactions with the neighboring molecules. This would provide an explanation for the origin of the nitroso-compounds by assuming that excited nitrate esters would be reduced to nitrite esters by simultaneous oxidation of the surrounding compounds. Similar photoreduction of the $-NO_2$ group has been reported in the photolysis of inorganic nitrates (4) and in the photoisomerization (106) (107) (108) of o-nitrobenzaldehyde to o-nitrosobenzoic acid (60).

If the fifth mode of cleavage for the excited nitroxy group (Figure 4) was accepted then both the excited nitrate and nitrite esters might react with

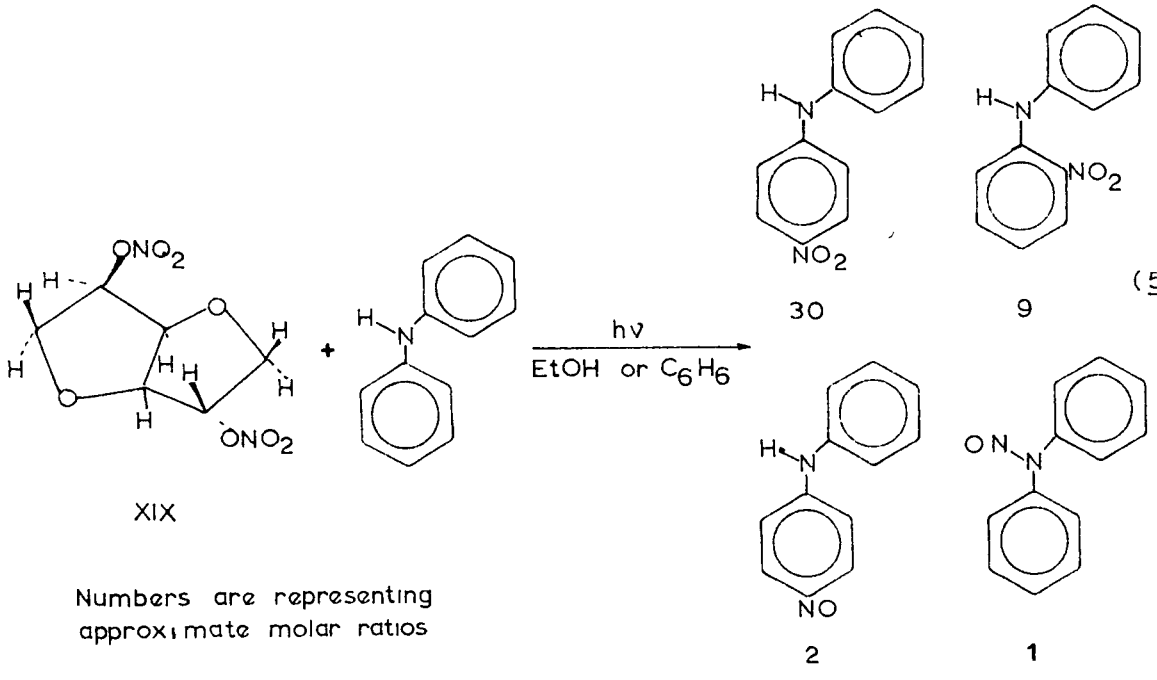

Numbers are representing approximate molar ratios

(59)

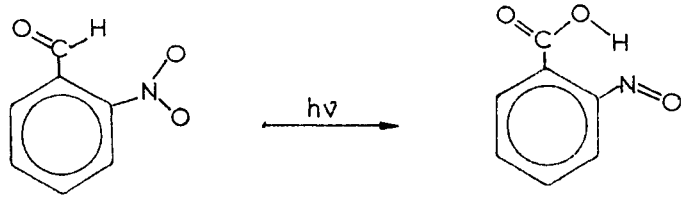

(60)

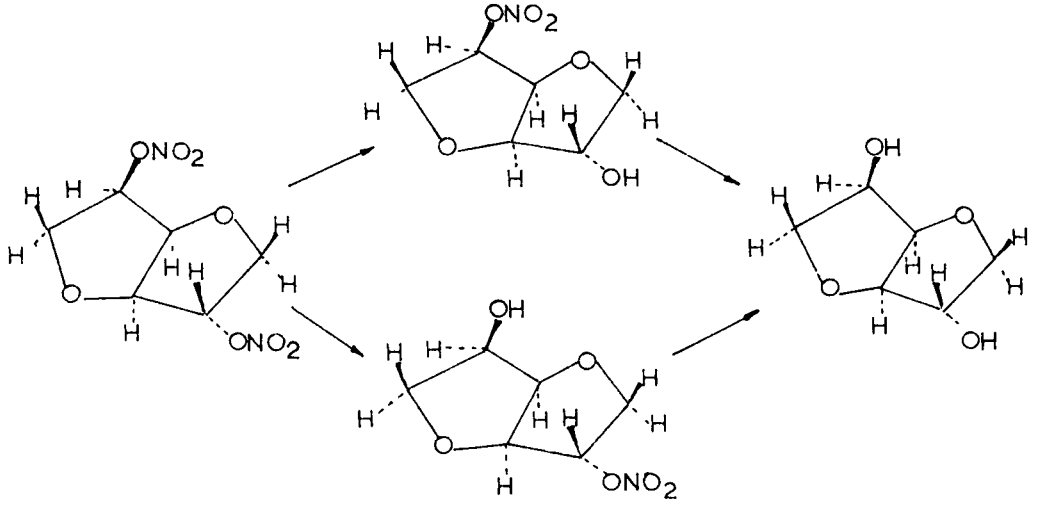

(61)

diphenylamine providing an exchange of $-NO_2$ and -NO groups with the amine hydrogen and the N-nitro and N-nitroso compounds thus formed would undergo intramolecular rearrangement.

The recent discovery (109) that both of the isomeric mononitrates as well as the parent diol were present among the photo-products in appreciable quantities indicated that in the predominant course the reaction proceeded via mononitrates to the parent diol and that $O-NO_2$ groups were replaced by O-H without inversion at the asymmetric carbons (61). This result would seem to favour the second proposed mechanism.

Since the amount of information concerning the photochemistry of the nitrate esters was limited it was considered useful to make comparisons with the photochemistry of related nitrogen-oxygen compounds (Table IX). This idea was based on the assumption that there is a correlation between the UV-absorption of $X-NO_2$ compounds and the structure of X. No report of such an analysis was available but a similar correlation between the UV -spectra (the $n_N \longrightarrow \pi^*$ band) of $(R^1)_nXNO$ compounds and the nature of X has been pointed out (93) (Table X). The regular change observable in the infrared absorption (110) (Table XI) and in molecular geometry (Figure 7) of the $(R^1)_nXNO_2$ molecules (111) as X was varied seemed to justify this analogy.

TABLE IX Structural Properties* of Nitrogen-Oxygen Compounds

Valence electrons N—O			N≡O 11 1150 Å		
Valence electrons ∠ ONO N—O	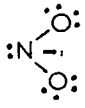 18 115.4° 1 236 Å		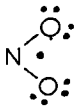 17 134 1° 1.188 Å		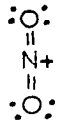 16 180 0° 1.154 Å
Valence electrons ∠ ONO N—O X—N		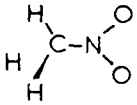 24 127° 1 22 Å 1.48 Å	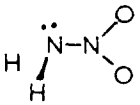 24	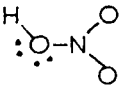 24 130° 1 206 Å 1 405 Å	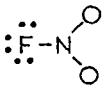 24 125° 1 23 Å 1 35 Å
Valence electrons ∠ ONO N—O X—N		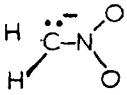 24 ---- ---- ----	—	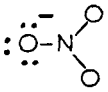 24 120.5° 1.24 Å 1 25 Å	—
Valence electrons ∠ ONO N—O X—N		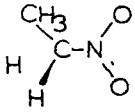 30 --- --- ---	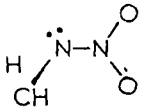 30 --- --- ---	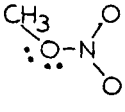 30 125 3° 1 26 Å 1.36 Å	—

* Values taken from (133)

Table X

$n_N \longrightarrow \pi^*$ Transitions of $(R^1)_nXNO$ Compounds

X	χ_X * (kcal/mole)	$(R^1)_nXNO$	λ (Å) $n_N \longrightarrow \pi^*$
C	2.50	$(CH_3)_3C-NO$	6650
S	2.45	$(CH_3)_3CS-NO$	5988
Cl	3.10	Cl-NO	4600
N	3.15	$(CH_3)_2N-NO$	3610
O	3.60	$CH_3(CH_2)_3O-NO$	3560
F	4.15	F-NO	3110

*) Values taken from (13).

Table XI

Fundamental Infrared Frequencies (cm^{-1}) of $(R^1)_nXNO_2$ Compounds

Type of Vibration	CH_3-NO_2	H_2N-NO_2	$HO-NO_2$	$F-NO_2$
$\nu^{stret.}_{as}$ (NO_2)	1562	1540	1675	1779
$\nu^{stret.}_{sym}$ (NO_2)	1377	1379	1300	1306
δdeform (ONO)	657	709	680	466
$\nu^{stret.}$ $(X-NO_2)$	919	1043	925	821
$\nu_{NO} \equiv \frac{\nu_{as} + \nu_{sym}}{2}$	1470 *	1460	1490	1552

Photolysis of NO

Mercury photosensitized decomposition of nitric oxide in the gaseous phase has been studied by Strausz and Gunning (112) and N_2, N_2O, and higher

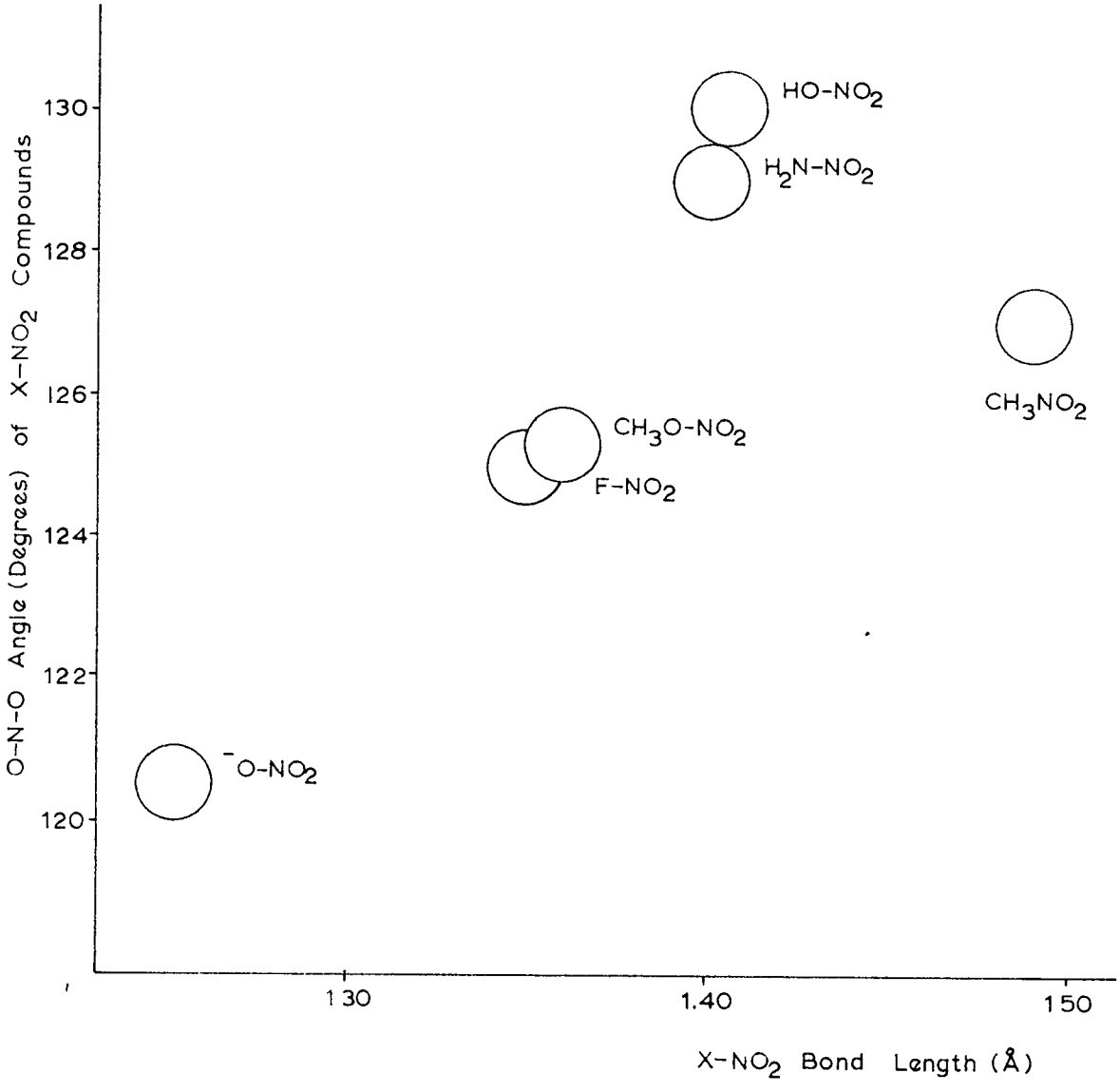

FIGURE 7 Correlation of ∠ ONO and X–NO_2 Bond Length in $(R^1)_n XNO_2$ Compounds

oxides of nitrogen were found to be major products. The rate of photolysis was linearly proportional to the intensity of the 2537 Å band.

According to the proposed mechanism excited NO molecules form an energy-rich dimer, $(NO)_2^*$, which underwent a stepwise decomposition process illustrated in 65 and 66:

$$Hg + h\nu \longrightarrow Hg^* \quad (62)$$

$$Hg^* + NO \longrightarrow NO^* + Hg \quad (63)$$

$$NO^* + NO \longrightarrow (NO)_2^* \quad (64)$$

$$(NO)_2^* \longrightarrow N_2 + \text{oxygen} \quad (65)$$

$$(NO)_2^* + NO \longrightarrow N_2O + NO_2 \quad (66)$$

Photolysis of NO in benzene solution produced unexpected products as recently reported by Kemula and Grabowska (113). The formation of o-nitrophenol and 2,4-dinitrophenol and the absence (or questionable presence) of p- or m- nitrophenol could not be explained by a simple reaction mechanism.

The primary process was explained in terms of the forbidden singlet-triplet ($T \longleftarrow S_0$) excitation* of benzene since the mixture was irradiated with a wavelength range of 2900-3600 Å and from previous experiments (117) it was clear that the regularly forbidden singlet-triplet absorption would appear in this range of wavelengths in the presence of paramagnetic species like NO or O_2.

It was proposed that the excited triplet state of benzene (which acts as a biradical), being in contact with the paramagmetic NO molecule, produced the nitrophenols in some unknown manner (67). Control experiments were carried out with oxygen (118) and in addition to minor amounts of o-quinone, phenol was isolated as the major product (68).

---

*) This electronic transition is forbidden by the "spin momentum conservation" rule of quantum mechanics (114) (115) (116).

Photolysis of NO_2

The gas phase photolysis of nitrogen dioxide was investigated by Norrish (119) (120) as early as 1929. Recent reviews (121) (122) proposed seven distinctive mechansims (depending on the reaction conditions) in terms of fifteen equations. "It now appears that below 3700 Å atomic oxygen is an important product of the primary photochemical process" (120) according to 69.

$$NO_2 \xrightarrow{h\nu} \overset{*}{N}O_2 \longrightarrow NO + O \qquad (69)$$

The reaction of nitrogen dioxide with aromatic compounds was reviewed by Riebsomer (123). "Reaction may be brought about by heating to 80° in sealed tubes, by the action of light (4000-7000 Å) at 55-60°, or by a glow discharge in a Siemens tube" (124).

Photolysis of HNO_3

The decomposition of nitric acid by light was described in the last century by Berthelot (125). A more detailed study of the reaction as reported by Reynolds and Taylor (126) is summarized by equation 70.

$$4\ HNO_3 \underset{\text{dark (slow)}}{\overset{\text{light (fast)}}{\rightleftharpoons}} 2H_2O + 2N_2O_4 + O_2 \qquad (70)$$

According to the authors "the decomposition may possibly take place in stages, the first product being nitrous acid and oxygen, the former and the excess nitric acid then producing water and nitrogen peroxide" as represented in equation 71, 72, 73.

$$HO\text{-}NO_2 + h\nu \longrightarrow HO\text{-}NO + O \qquad (71)$$

$$HO\text{-}NO_2 + O \longrightarrow HO\text{-}NO + O_2 \qquad (72)$$

$$HONO_2 + HONO \longrightarrow H_2O + N_2O_4 \qquad (73)$$

This reaction would thus support the suggested fifth mode of scission of nitrate esters (Figure 4).

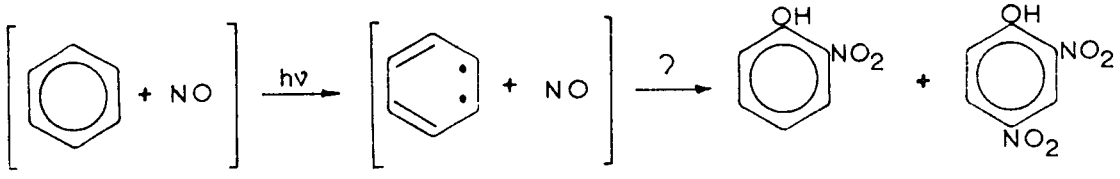

(67)

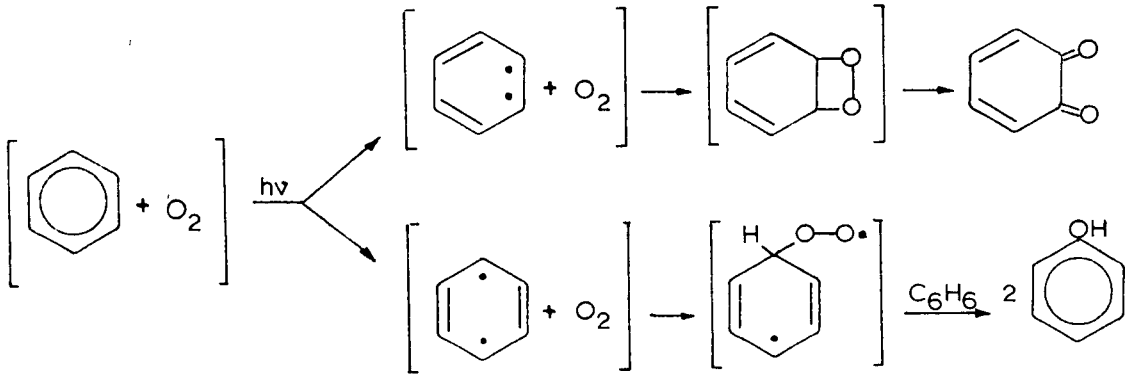

(68)

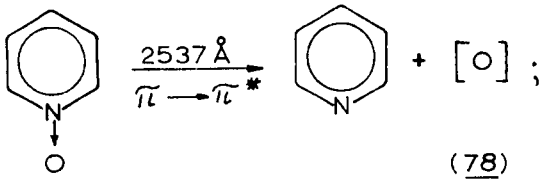

(78)

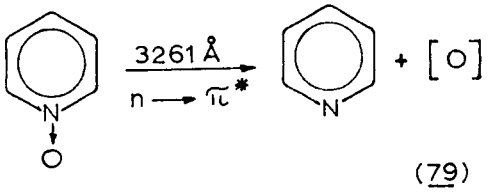

(79)

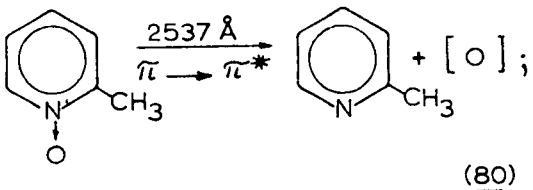

(80)

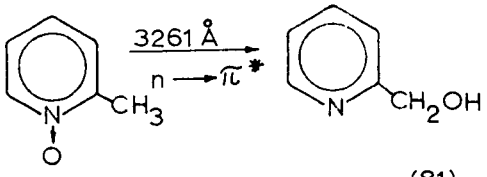

(81)

The results of Co^{60} γ-radiolysis of HNO_3 suggested (127) that both the fourth and fifth modes of scission occurred simultaneously under high energy irradiation (74) (75).

$$HONO_2 \longrightarrow HO\overset{*}{N}O_2 \longrightarrow HO\cdot + NO_2 \qquad (74)$$

$$HONO_2 \longrightarrow HO\overset{*}{N}O_2 \longrightarrow HNO_2 + \tfrac{1}{2}O_2 \qquad (75)$$

Photolysis of NO_3^-

Nitrate ions undergo photochemical reduction in aqueous solution to NO_2^- which in turn is transformed to hydroxylamine. The photoreduction occurs readily in the presence of simple organic substances at the cost of their simultaneous oxidation (4).

Inorganic nitrates were photolysed in the presence of diphenylamine by Coldwell and McLean (128) (129). Nitrodiphenylamines were isolated as in the case of the photolysis of covalent nitrates (59)(105) but no evidence of nitroso derivatives was found.

Photolysis of CH_3NO_2

Nitromethane in argon matrix at 20°K has been photolysed and the nature of the products studied by infrared spectroscopy (130). The homolytic cleavage according to equation 76 has been ruled out by the absence of NO_2, CH_4 and C_2H_6.

$$CH_3\text{-}NO_2 \not\longrightarrow CH_3\cdot + NO_2 \qquad (76)$$

The photolysis was performed on solid CH_3NO_2 and CD_3NO_2 with the aid of a high pressure (A-H6) (Figure 45) or medium pressure (A-H4) mercury arc spectrum. The stepwise transformation is described by 77 where the major products were CH_2O, CO, CO_2, N_2O, NO, H_2O, HOCN, and HNO.

$$CH_3\text{-}NO_2 \xrightarrow{h\nu_1} CH_3O\text{-}NO \xrightarrow{h\nu_2} \text{products.} \qquad (77)$$

The fact that methyl nitrite was formed exclusively as the trans-isomer at 20°K provided interesting evidence for the mechanism. Although more

than one tentative mechanism has been suggested, it seems rational that the methyl group participated in a stereo-specific manner in the rearrangement by association with one of the oxygen atoms of the excited NO_2 group.

Photolysis of Pyridine N-oxides

Pyridine N-oxides are somewhat analogous to $-NO_2$ groups since one doubly bonded oxygen of $-NO_2$ may be considered as replaced by the aromatic double bond. No $n_N \longrightarrow \pi^*$ excitation is possible but the group exhibits both $n_o \longrightarrow \pi^*$ and $\pi \longrightarrow \pi^*$ transitions (131).

Irradiating pyridine N-oxide at two different wavelengths (132) produced in both cases (78, 79) pyridine and atomic oxygen (which in turn caused some destructive oxidation) in spite of the fact that 3261 Å (pyrex Cd resonance lamp) caused an $n \longrightarrow \pi^*$ transition while the line at 2537 Å (quartz Hg resonance lamp) produced a $\pi \longrightarrow \pi^*$ excitation.

On the other hand when the α- picoline N-oxide was irradiated at the same two wavelengths, the products of the photolysis varied according to the wavelength applied. In the $\pi \longrightarrow \pi^*$ case the α-methyl group did not effect the course of decomposition (80), while in the $n \longrightarrow \pi^*$ excited state the α-methyl group acted as an oxygen acceptor (81)analogous to the formyl group in the o-nitrobenzaldehyde photorearrangement (60).

These results were clear demonstrations of the chemical differences of the two types of excited states ($\pi \longrightarrow \pi^*$ and $n \longrightarrow \pi^*$), even so, this distinction was not always reflected in the product formation.

RESULTS AND DISCUSSION

I. Synthesis of Aromatic Nitrate Esters.

It has long been known (53) that in nitric acid-sulfuric acid nitration nitronium ion, NO_2^+, is actually the nitrating species. Although this mixed acid is a powerful and widely used nitrating agent it has been established that for the nitration of sensitive polyols nitric acid-acetic anhydride mixture is more desirable (24). The question of the identity of the nitrating agent in the latter mixture, however, remained unsettled until recently. Both N_2O_5 (134) and CH_3COONO_2 (135) were proposed as the nitrating agent in agreement with Raman spectroscopic evidence (136), however, NO_2^+ also has been detected by infrared spectroscopy (137) in concentrated solutions of nitric acid in acetic anhydride.

Recent kinetic investigations confirmed nitronium ion as the nitrating entity. Equations 82, 83, 84 were proposed (138) to fit the experimental results.

$$HONO_2 + H^+ \xrightleftharpoons{\text{equil.}} H_2\overset{+}{O}-NO_2 \qquad (82)$$

$$H_2\overset{+}{O}-NO_2 + Ac_2O \xrightleftharpoons{\text{equil.}} 2AcOH + NO_2^+ \qquad (83)$$

$$C_6H_6 + NO_2^+ \xrightarrow{\text{slow}} C_6H_5(H^+)(NO_2) \qquad (84)$$

Under the experimental conditions the rate of nitration was first-order with respect to the nitrating substance (84), but was second-order with respect to nitric acid concentration in agreement with the self-ionization shown in 82 and 85.

$$HNO_3 + HNO_3 \xrightleftharpoons{\text{equil.}} H_2\overset{+}{O}-NO_2 + NO_3^- \qquad (85)$$

The fact that the addition of 0.001 M $NaNO_3$ slowed the rate of nitration confirmed that the self-ionization (85) was an important component of the experimentally observed rate constant. On the other hand the addition

of 0.01 M sulfuric acid introduced a large amount of protons into the system which dismissed the rate determining character of the selfionization (85) and the observed rate then became first-order with respect to nitric acid concentration (82).

The observation (139) that acetoxylation occurred as a side reaction in aromatic nitration (86), (87), (88) could also be taken as chemical evidence for the nitronium ion mechanism.

Brown has pointed out (140) that all electrophilic substitutions (including nitration) on aromatic nuclei proceed by the same general mechanism *via* the formation of charge-transfer complexes. According to this model when the electrophile NO_2^+ approaches the aromatic nucleus, negative charge is transferred from the aromatic " π-electron cloud" to the positive nitronium ion (XXVII). Consequently, the classical intermediate or transition state (84) (XXVIII) has to be replaced by a series of equilibria as shown in 90, 91 and 92.

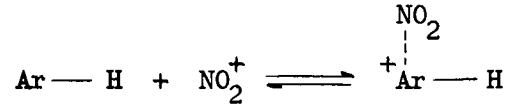

(90)

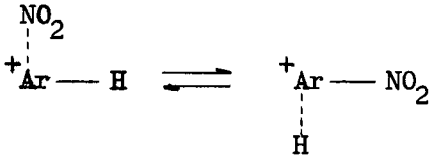

(91)

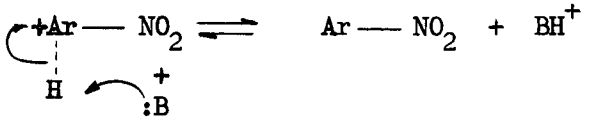

(92)

In nitrations with nitric acid-acetic anhydride mixture the base, :B, corresponds to NO_3^- generated in the self-ionization (85) and BH^+ would be the recovered nitric acid.

The discovery that aromatic C-nitration does not differ in principle from O- and N-nitration (39) permitted extension of the theory of charge-transfer

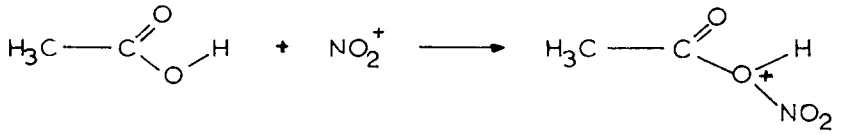

(86)

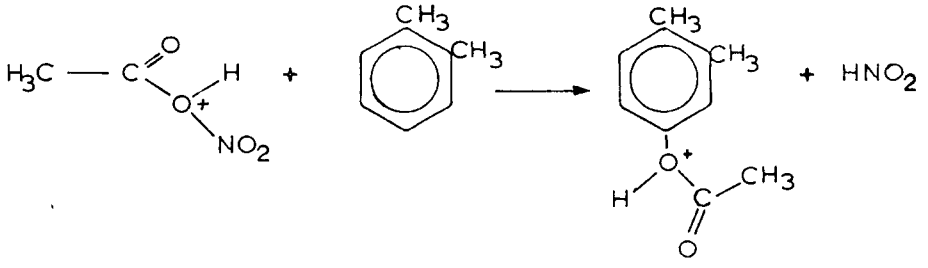

(87)

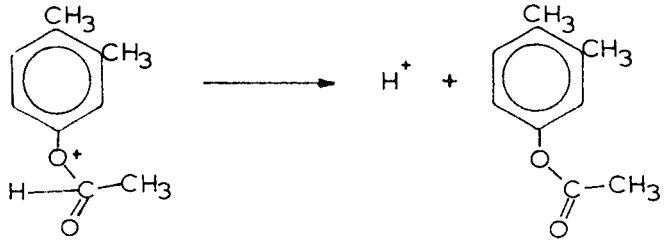

(88)

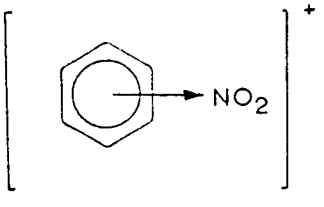

XXVII

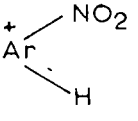

XXVIII

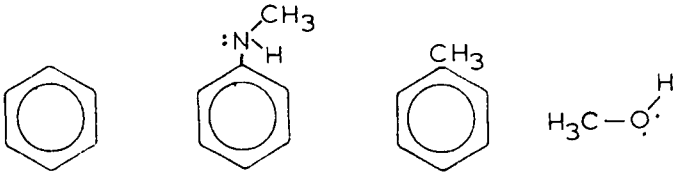

Molecule				
Relative reactivity toward NO_2^+	10	14	24	30

(89)

complex intermediates to the formation of nitrate esters. In the latter case the oxygen of the alcohol, with loosely held unshared electrons, played the role of electron donor in the place of the aromatic nucleus in formation of the charge-transfer complex.

Hughes (141) created reaction conditions (high substrate concentration with respect to NO_2^+ concentration by dilution with water) in which the rates observed were measures of the relative reactivities of C, N and O atoms located in various chemical environments. In this manner a scale of relative reactivities (89) was established.

In this research aromatic nitrate esters were required for photochemical study and for several reasons (as discussed in the introduction) direct esterification of the corresponding alcohols seemed to be the most desirable synthetic route. The structures of the selected aromatic alcohols were such that the relative location of the OH group with respect to the aromatic nucleus was analogous to that in benzyl alcohol. The synthesis seemed to be feasible since Hughes' figures (89) indicated the higher efficiency of O-nitration compared to ring nitration of benzene. On the other hand the increased rate of nitration on an activated aromatic nucleus, as in toluene, pointed toward a close competition between C- and O-nitration in the case of the aromatic alcohols.

The experimental results showed higher yields of nitrate esters than would be predicted from the foregoing. In the case of meso-hydrobenzoin (XXIX) and dl-hydrobenzoin (XXXI) the amounts of aromatic nitro by-products were relatively small and did not cause any difficulty in the isolation of the pure dinitrates (yield: 57%). In the nitration of benzoin (XXXIII), under similar conditions, the formation of yellow C-nitro compounds was somewhat more pronounced and small amounts of benzil were also isolated as the result of unwanted oxidation; however, the pure nitrate was still isolated in reasonably good yield (35%).

In the case of the 1,2-acenaphthenediols (XXXV) (XXXIX) the reactivity of the naphthalene portions of the molecules was much higher than that of the benzene moiety of the hydrobenzoins as predicted from the lower ionization potentials* and chemical reactivities of the corresponding hydrocarbons. Consequently, a number of ring nitro by-products could be expected to originated from both the cis- and trans-diols (96, 97).

Three different compounds (A, B, and C) were isolated by chromatography from the crude nitration mixtures from both isomers. Compounds A_{cis} and A_{trans} were the pure dinitrates, while B_{cis}, B_{trans}, C_{cis} and C_{trans} were suspected to be ring nitro by-products. According to TLC analysis (Figure 8) the compounds isolated were chromatographically pure with the exception of B_{trans} which contained minor amounts of a second substance.

~~Elementary~~ Nitrogen analyses indicated that ring mononitro dinitrate esters (Table XII) (XXXVII)(XLI) were among the products and this was confirmed by the infrared spectra (Figure 9).

The nature of the C fractions remained undetermined although the slow running (low R_f) isomer which originated from the trans-diol (C_{trans}) was suspected to be nitroacenaphthoin (XLII) from the elementary analysis and infrared spectrum.

Since acenaphthene is readily substitutable by electrophilic reagents almost exclusively at the peri-positions (143), there could be little doubt about the position of the ring-substituted NO_2 group.

A systematic literature survey (27) indicated that the present research (144) was the first attempted synthesis of aromatic nitrate esters by direct esterification.

---

* The ionization potential for benzene is 9.25 ev and for naphthalene 8.12 ev (142).

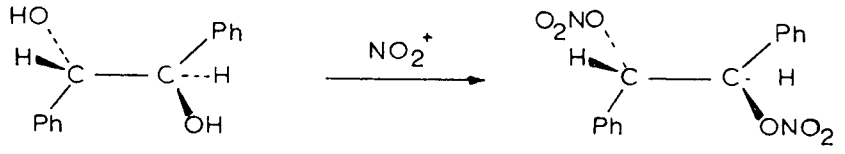

XXIX XXX (93)

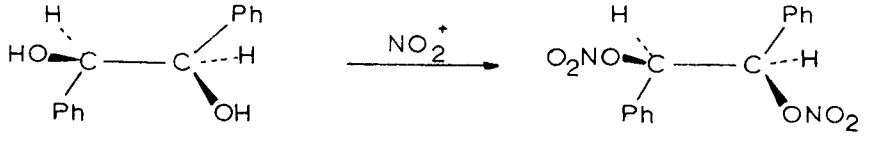

XXXI XXXII (94)

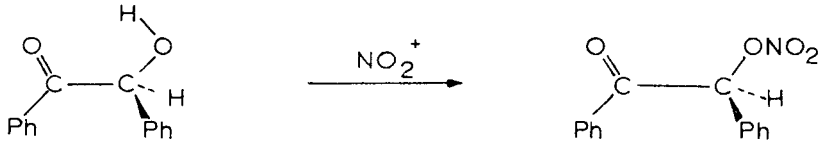

XXXIII XXXIV (95)

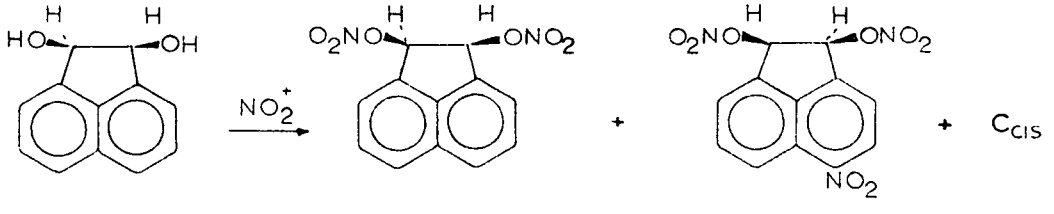

XXXV XXXVI (A_{cis}) XXXVII (B_{cis}) XXXVIII (96)

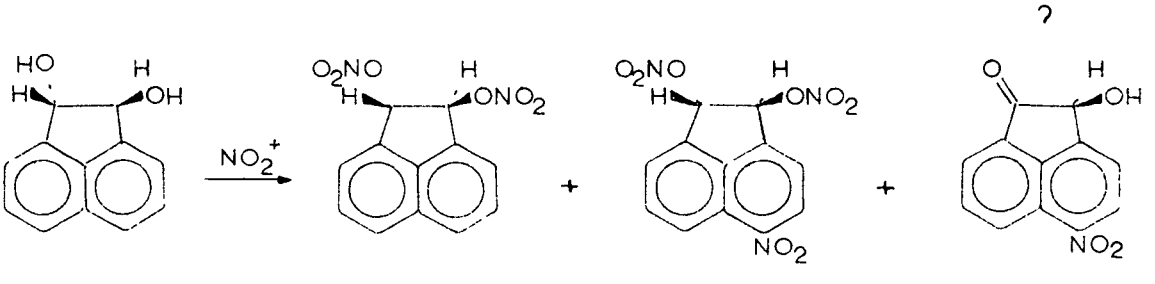

XXXIX XL (A_{trans}) XLI (B_{trans}) XLII (C_{trans})

(97)

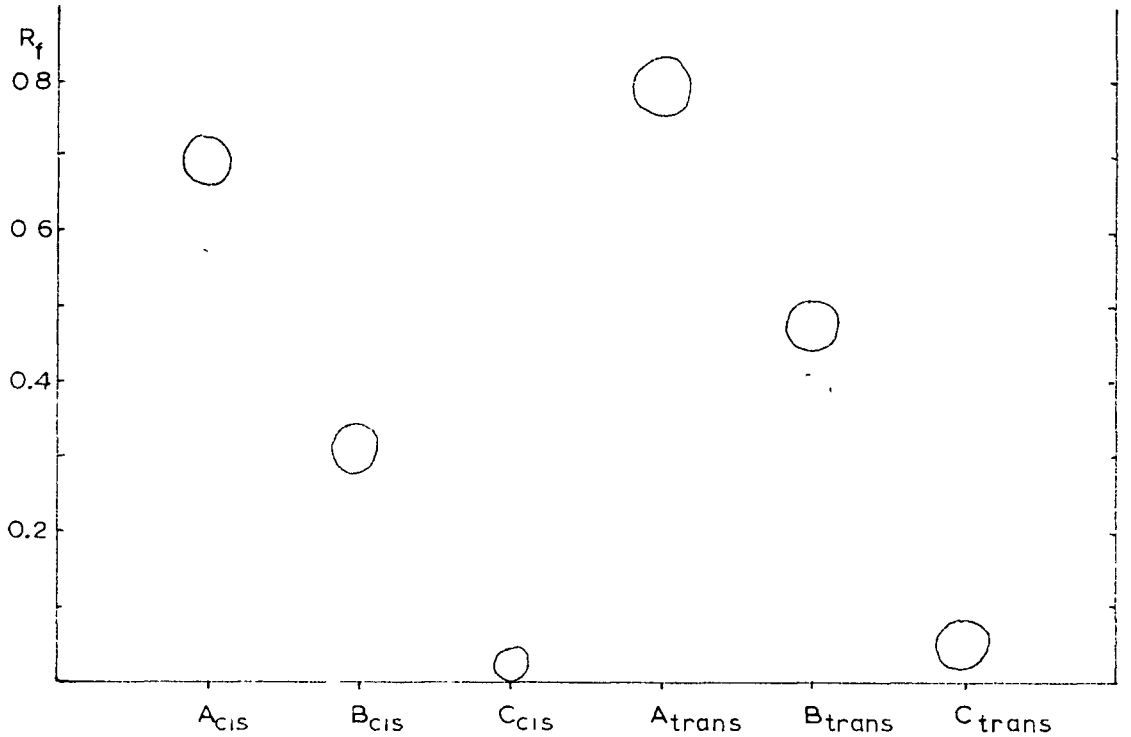

FIGURE 8 Thin-layer Chromatography of Nitration Products from cis- and trans-1,2-Acenaphthenediols (M-3 , S-1 , R-1)

TABLE XII Nitration Products from cis-and trans-1,2-Acenaphthenediols.

Product		Formula		R_f (M-3 S-1 R-1)	MP (°C)	N °/o	
Symbol	Isomer	Number	Empirical			Obt	Calc
A	cis-	XXXVI	$C_{12}H_8O_6N_2$	0 69	129 5–132 5	10 03	10.15
	trans-	XL		0.79	98–100	10.07	
B	cis-	XXXVII	$C_{12}H_7O_8N_3$	0 32	95 - 98	12.50	13.10
	trans-	XLI		0.47	oil	11 81	
C	cis-	XXXVIII	$C_{12}H_7O_4N$	0 02	----	8 89	6.10
	trans-	XLII		0.05	210 - 215	6.36	

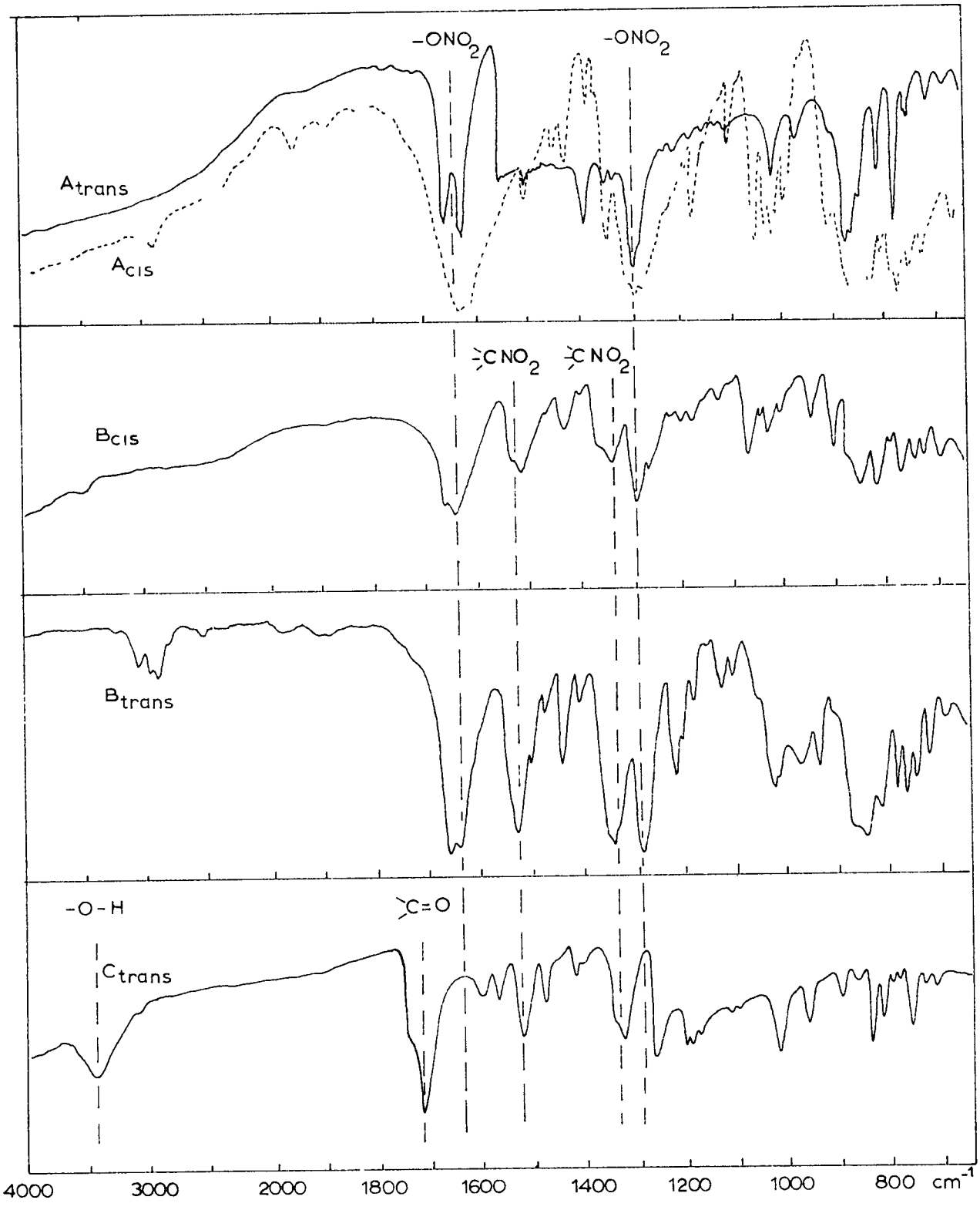

FIGURE 9 Infrared Spectra of Nitration Products of cis- and trans-1,2-Acenaphthenediol.

II. Chromatography of Nitrate Esters.

It has been recognized for more than a decade (145)(146) that hydrogen bonding plays an important role in adsorption on silicic acid and that the adsorption sites (147) are the weakly acidic hydroxyl groups of the adsorbent. Recently it was shown (148)(149)(150)(151) that the infrared absorption band of the surface silanol group is shifted toward lower frequencies upon interaction with absorbate molecules. This frequency shift ($\Delta\nu$) in the adsorption of diethylamine was as large as 73 cm^{-1} (from 3743 to 3670 cm^{-1}) (152). Hydrogen bonding is a special case of charge-transfer interactions, and it has been found that the strength of hydrogen bonding (i.e. $\Delta\nu$ cm^{-1}), which is in fact a measure of adsorption, varies with the ionization potential of the adsorbate (152). This was experimental evidence that the adsorbate molecule is the electron donor (i.e. proton acceptor) and the hydrogen atom of the silanol group acts as a hydrogen bridge between adsorbent and adsorbate.

It has been calculated by Sporer and Trueblood (153) that the O.....O distances of hydroxyl groups on adjacent silicon atoms lie between 4.3 and 5.8 Å. It was found experimentally by the same authors that the most favorable "inter-adsorbing atom distance" (O...O or O....N) in an adsorbed molecule was about 6.1 - 6.2 Å (or a multiple of that value) which was close to the 5.8 Å calculated value. This favoured inter-nuclear distance was shown to be available in meta- and para- substituted benzene derivatives.

The equilibrium constant K for the adsorption process (98) of the chromatographed substrate (S) was determined experimentally (99) and was termed the "adsorption affinity" of the substrate.

$$S_{solution} \rightleftharpoons S_{adsorbed} \qquad (98)$$

$$K = \frac{[S_a]}{[S_s]} \qquad (99)$$

From equation (100) the standard free-energy change for the adsorption process was calculated and shown to be dependent on the structure of the chromatographed substrate.

$$\Delta F^{o} = -RT\ln K \qquad (100)$$

Furthermore it was pointed out (153) that there was a characteristic "adsorption affinity" not only for molecules (K) but also for substituent groups (K_i). Thus the value of K for a particular molecule which carried i different substituents was the product of the separate K_i values (101).

$$K = \prod_i K_i \qquad (101)$$

and the resultant standard free energy change for a molecule (ΔF^{o}) was the sum of the values of the individual substituting groups (ΔF_i^{o}) according to equation (102).

$$\Delta F^{o} = \sum_i F_i^{o} \qquad (102)$$

A sequence of group adsorption affinities (K_i) was compiled for individual substituents on aromatic nuclei in decreasing order of adsorption affinities (103).

$-CH_2NH_2$,	$-COOH$,	$-CH_2OH$,	$-NH_2$,	$-COCH_3$,	$-OH$,	$-CHO$,	$-NO_2$,	$-OCH_3$,	H	(103)
7000	370	260	80	70	27	23	3.1	-	-	

This sequence explained why the ring nitro by-products of 1,2-Acenaphthenediol dinitrates possessed lower R_f values than the unsubstituted dinitrates (Figure 8, Table XII).

"In chromatography the experimentally measurable quantities are the distances that the zone of solute and the front of solvent have travelled in the same period of time" (153). The ratio of these distances, the "development rate", designated R^{o}, may be determined in column chromatography when the

concentration is low enough that the process is in the linear region of the Langmuir adsorption isotherm. In this case K may be calculated from the experimental R^o values according to (104).

$$K = \frac{1 - R^o}{R^o} \qquad (104)$$

In the more recently developed microadsorption thin-layer chromatography (TLC) the value R^o would be replaced by R_f and K in equation 105 may be taken as a measure of the adsorption affinity.

$$K = \frac{1 - R_f}{R_f} = \left(\frac{1}{R_f} - 1\right) \qquad (105)$$

Similarly the value R_M (106) which is also used in paper chromatography (154) would be proportional to the standard free energy change of adsorption according to equation 107.

$$R_M = \log \left(\frac{1}{R_f} - 1\right) \qquad (106)$$

$$\Delta F^o = -2.303\ RTR_M \qquad (107)$$

On this basis the TLC technique should be capable of distinguishing compounds according to their functional groups.* It was suggested some time ago in this laboratory (155) that elucidation of the molecular structure of unknown compounds (particularly that of nitrate esters) might be aided by TLC through a comparison of R_M values determined under standarized conditions and this principle has been successfully applied in a qualitative manner (105), (144).

In a quantitative study a number of carbohydrate nitrates and their parent alcohols were chromatographed on chromatoplates (M-3, S-10, R-2) and the experimental R_f values together with the calculated R_M and $R_M(-NO_2)$

* Phenol protons may contribute slightly to the total hydrogen bonding process (153).

values for representative compounds are summarized in Table XIII.

Table XIII

Relationship of R_f Values and Structure in Polynitroxy Compounds

Compound	Δn a)	R_f (b)	$\frac{1}{R_f} - 1$	R_M c)	ΔR_M d)	ΔR_M e)
mannitol hexanitrate		0.747	0.339	-0.469		
	1				-1.031	-1.031
mannitol pentanitrate		0.215	3.647	0.562		
dulcitol hexanitrate		0.706	0.417	-0.380		
	1				-1.011	-1.011
dulcitol pentanitrate		0.190	4.272	0.631		
methyl-β-D-glucoside tetranitrate		0.775	0.291	-0.536		
	2				-1.873	-0.936
methyl-β-D-glucoside-2,4-dinitrate		0.044	21.727	1.337		
average ΔR_M per nitroxy group						-0.993

a) Difference in number of nitroxy groups between corresponding pair of compounds.

b) Average of four determinations.

c) from (106).

d) Difference of R_M values between corresponding compounds.

e) ΔR_M per nitroxy group.

The nearly constant value of ΔR_M (variation about $\pm$ 5%) for the O-NO_2 group over the range of compounds with varied structures indicated an independent contribution to the adsorption by each nitrate ester group in thin-layer chromatography. The order of group "adsorption affinities" calculated according to equation 108 from ΔR_M values.

$$K_1 = 10^{-\Delta R_M} \qquad (108)$$

for O-substituted (ROX) polyhydroxy compounds (where -X may be NO_2 or other substituent) determined for a series of compounds (155) are given in 109, where the numerical figures for K_1 apply for TLC (M-3, S-10, R-2) at 300°K.

$$\begin{array}{ccccc} -COCH_3 & > & -NO_2 & > & -CH_3 \\ 0.121 & & 0.102 & & 0.076 \end{array} \qquad (109)$$

The remarkable fact that in changing from column chromatography to TLC, and from aromatic C-substitution to aliphatic O-substitution the sequence of adsorption affinities of the substituents was virtually unchanged (103) from those determined by Sporer and Trueblood (153) made it evident that TLC results would be just as important in structural elucidations. ~~as those from other classical methods~~.

Figure 10 shows a typical chromatographic pattern (TLC, M-3, S-1, R-2) of aromatic and representative non-aromatic nitrate esters and Table XIV summarizes the observed R_f values (300°K) together with the calculated constants: R_M, ΔF^o (the standard free energy change for adsorption) and K (the adsorption affinity).

It was clear from these data that if other active substituents were also present in the molecule, such as the two cyclic ether oxygen atoms in (A) or the ketone oxygen in benzoin nitrate (B) the compounds showed increased affinity toward the adsorbent (K = 5.54 and 1.98 respectively). A similar effect resulted from an accumulated number of nitroxy groups in a molecule as illustrated by mannitol hexanitrate (K = 9.00) (C). In contrast, cholesteryl nitrate (D) having practically no other group to adsorb with other than the one O-NO_2 group had the lowest adsorption affinity: K = 0.258. Benzylnitrate (E), also a mononitrate, with the benzene ring as a second functional group for hydrogen bonding, showed an affinity more than twice as large (K = 0.647)

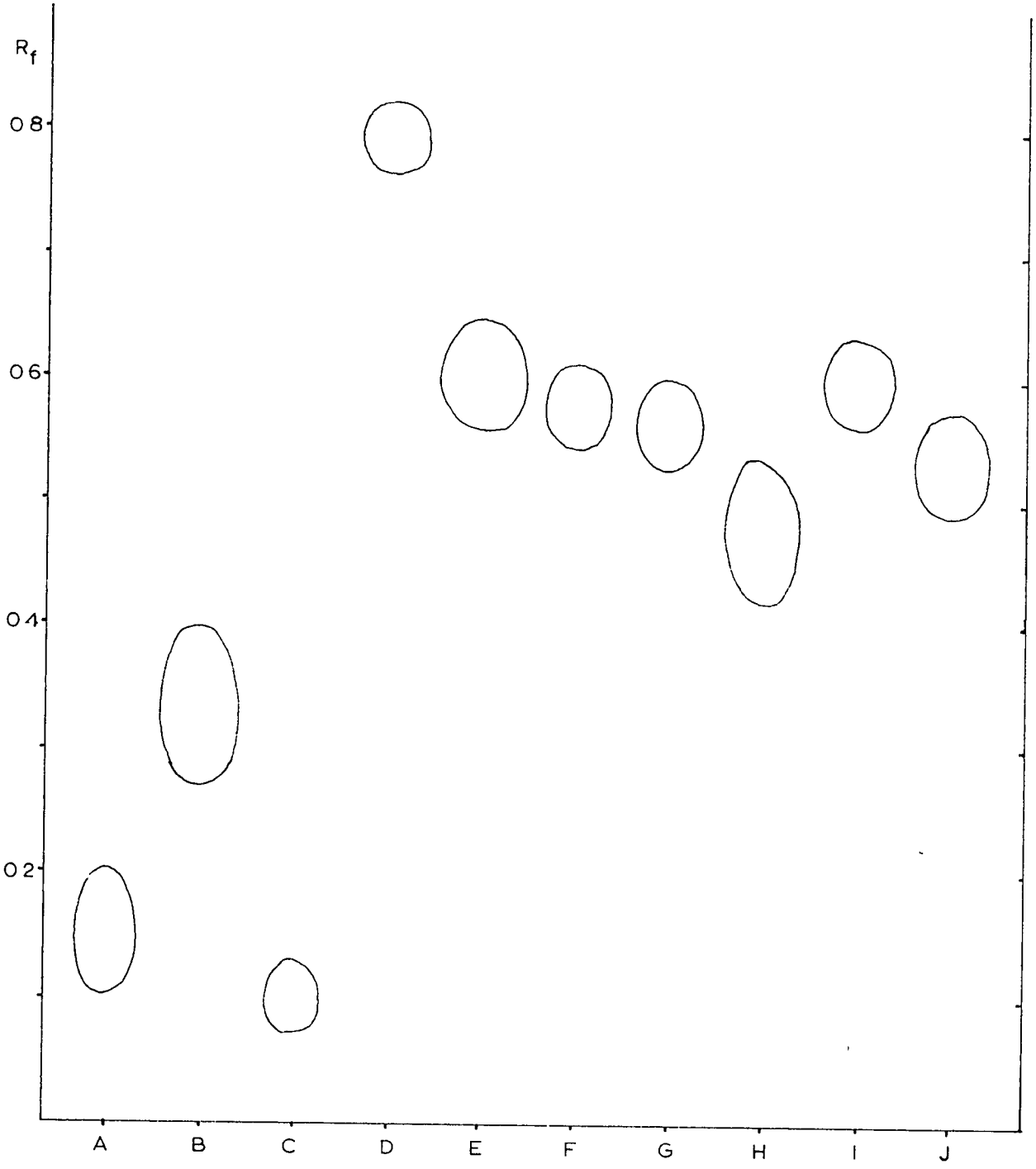

FIGURE 10 Chromatographic Pattern of Representative Nitrate Esters TLC, M-3, S-1, R-2. The compounds and calculated R_M, $\Delta F°$, and K values are listed in Table XIV

Table XIV

Chromatographic Constants for Nitrate Esters

	Compound Name	Formula	R_f *	R_M	ΔF^o cal/mole	K
A	Isosorbide Dinitrate	XIX	0.151	0.743	-1020	5.54
B	Benzoin Nitrate	XXXIV	0.336	0.296	-463	1.92
C	Mannitol Hexanitrate		0.100	0.954	-1310	9.00
D	Cholesteryl Nitrate		0.258	-0.588	-807	0.258
E	Benzyl Nitrate		0.607	-0.189	+259	0.647
F	meso-Hydrobenzoin Dinitrate	XXX	0.578	-0.137	+188	0.730
G	dl-Hydrobenzoin Dinitrate	XXXII	0.560	-0.105	+144	0.786
H	cis-1,2-Acenaphthene-diol Dinitrate	XXXVI	0.477	0.040	-55	1.10
I	trans-1,2-Acenaphthene-diol Dinitrate	XL	0.596	-0.169	+232	0.678
J	trans-1,2-Cyclohexane-diol Dinitrate	XXII	0.536	-0.062	+85	0.866

* See Figure 10.

as that of cholesteryl nitrate.

meso- and dl-Hydrobenzoin dinitrates (F)(G) although dimers of benzylnitrate did not exhibit doubled adsorption affinities (Table XIV) indicating that rotation on the C_1-C_2 bond, statistically did not on the average bring much more than one nitroxy group per molecule into contact with the adsorbent.

The trans-isomer of 1,2-acenaphthenediol dinitrate (I), having a fixed conformation, apparently could be adsorbed by one nitrate ester per molecule, thus the value of K (0.678) was very close to that of benzyl nitrate (E). In contrast the cis-isomer had almost twice as large adsorption affinity (K = 1.096) since both of the nitroxy groups were situated on the same side of the acenaphthene moiety.

It was of interest also that the trans-1,2-cyclohexandiol dinitrate (J)(K = 0.866) fell in between trans- and cis-1,2-acenaphthenediol dinitrates, which indicated that the two equatorial nitroxy groups were stereochemically not as favourably oriented for adsorption as were those of the cis-dinitrate. This probably meant that the separation of the two nitroxy groups in the trans-1,2-cyclohexandiol dinitrate was larger than that of the two neighbouring active sites (5.8 Å) in the silicic acid. They were, however, more suitably oriented for absorption than those of the trans-1,2-Acenaphthenediol dinitrates.

In addition to providing structural information on the pure substances TLC was used in the analysis of nitration and other reaction mixtures and as a guide for developing appropriate column chromatographic techniques (156) for the purification of crude products. Furthermore TLC was also invaluable as a technique (157) for preparative isolation of compounds on a micro scale.

III. Analysis of Aromatic Nitrate Esters.

Elementary analysis carried out by the conventional combustion techniques does not provide satisfactory results with aliphatic nitrate esters (158, 159) due to insufficient combustion and too rapid gas evolution. The difficult has been largely overcome in Dumas nitrogen analyses by diluting the sample with glucose to aid combustion and decrease the rate of gas formation.

Table XV

Combustion Analyses of Polynitrates

Element	Content (%)		Reproducibility		Calcd. - Obs.	
	Calcd.	Obsd.	Abs.	Per.	Abs.	Per.
			meso-Hydrobenzoin Dinitrate			
C	55.26	55.43	-0.03	-0.05%	-0.17	-0.4%
H	3.28	3.87	-0.06	-1.5%	-0.59	-19.7%
N	9.21	9.11	-0.39	-4.3%	-0.10	-1.1%
			Mannitol Hexanitrate			
N	18.59	18.06	-0.46	-2.6	-0.53	-2.9%

In the present work experiments were carried out to assess the accuracy of combustion analyses of the crystalline aromatic nitrate esters since these had not previously been studied. A chromatographically pure sample of *meso*-hydrobenzoin dinitrate was selected as model compound and three parallel micro Liebig-Pregl combustions and six parallel micro Dumas analyses were carried out without added glucose. The average values from these analyses and the calculated reproducibility as well as the differences between the

analytical values and the theoretical values are summarized in Table XV. For comparison the nitrogen content of mannitol hexanitrate, obtained as an average from twelve analyses (160) is also given.

It was apparent from these results that the C% obtained was very consistant and also close to the calculated value, while there was a noticeable discrepancy in the H% values. For the N analysis the absolute values of both reproducibility and difference seemed to be better for the aromatic nitrate ester than for mannitol hexanitrate. Although the percentage reproducibility was somewhat worse for the aromatic nitrate (because of low N content), the percentage difference between the average of the analyses and the calculated value was almost three times larger for mannitol hexanitrate. These results were consistent with the high carbon content of the hydrobenzoin nitrate in which the aromatic moiety acted as a "built in carbon diluent" for the Dumas nitrogen combustion.

IV. Spectra of Aromatic Nitrate Esters.

A. Nuclear Magnetic Resonances Spectra (NMR).

Methyl nitrate (161) and ethyl nitrate (162) were the only nitrate esters which had previously been investigated by proton magnetic resonance spectroscopy. In aromatic nitrate esters, if the aromatic nucleus can rotate freely in the molecule the resonance of the aromatic hydrogens average out resulting in a single "benzene peak". This was found to be the case for benzyl nitrate. On the other hand if the aromatic portion constitutes a rigid system the coupling between ring protons may be observable. This was the situation in the case of the 1,2-acenaphthenediol dinitrates. The analysis of these and related ring proton spectra as ABC systems by the use of ABX approximation (163) is still in progress (144) (164) and is not included here.

From the spectra the greatest effect of the nitroxy substituents was revealed in the resonance of the protons in the α-positions.

Table XVI

Group Electronegativities and τ Values for α-Hydrogens in Nitrate Esters and Related Compounds.

Substituent Group		-H	-OH	-OAc	$-ONO_2$
Group Electronegativity		2.21[a]	3.51[b]	3.83[b]	3.81[c], 3.91[b] 4.18[d]
Hydrocarbon Group	Isomer		τ_{α_H}[e]		
	cis-		4.47[f]	3.87	3.27
1,2-Acenaphthenyl-		6.71			
	trans-		4.60	4.00	3.46
	m-		6.04	4.02	3.97
1,2-Diphenylethyl-		7.60			
	dl-		5.87	3.93	4.05
Benzyl-	...	7.70	5.35	4.90	4.45
1,2-Cyclohexanyl-	trans-	8.57	6.17	5.27	4.77

[a] Ref. (7), [b] Ref. (162), [c] Ref. (161), [d] This work

[e] In acetone solution 0.2 to 1.0 M, tetramethylsilane = 10.00.

[f] In glacial acetic acid.

Changing the substituents in the order -H , -OH , -OAc , $-ONO_2$ caused ~~an~~ a ~~increase of the acidities (lower~~ decrease in the τ values~~)~~ of the α-hydrogens (Table XVI). A plot of the τ-values of the α-hydrogens against the reported group

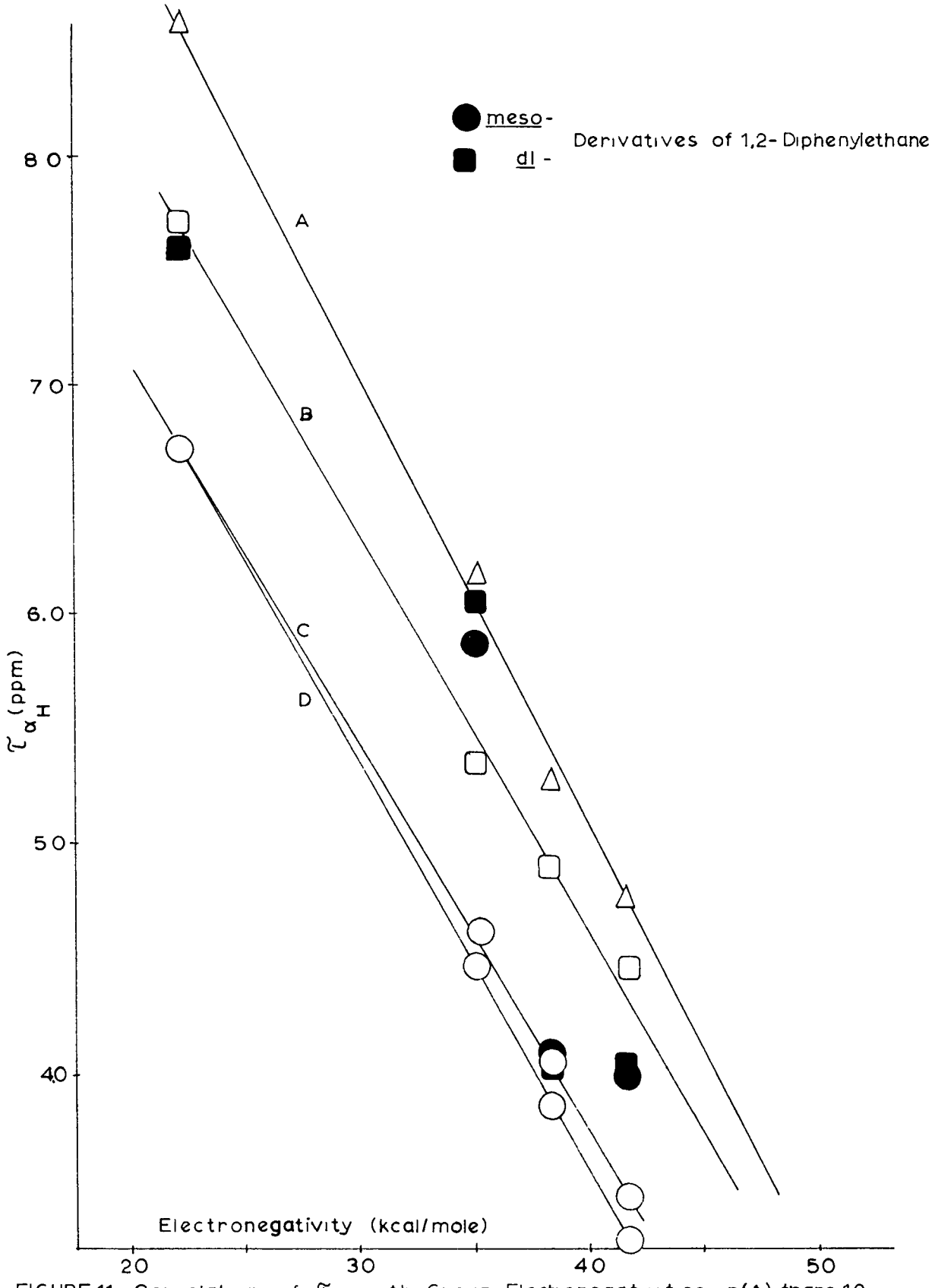

FIGURE 11 Correlation of τ_{α_H} with Group Electronegativities in (A) trans-1,2-Cyclohexane-, (B) Benzyl-, (C) trans- and (D) cis-1,2-Acenaphthenyl-Derivatives

electronegativities (7)(162)(Figure 11) revealed that the nitroxy group was apparently much more electronegative than was hitherto reported (161)(162) and it appeared to be even more electronegative than fluorine (3.93 kcal/mole).

From the straight line plots (Figure 11) of the values for the hydrocarbons, alcohols and acetates the extrapolated value of the electronegativity of the nitroxy group was 4.18 kcal/mole (Table XVII).

The meso- and dl-hydrobenzoin derivatives did not give a linear correlation and this was attributed to the flexibility of the molecular conformations which could therefore be different for each type of derivative.

The relative contribution to the shielding of the α-protons by the hydrocarbon portion of the molecule ~~was assessed from the intercepts on the axes of the plot and~~ was in the order cyclohexyl > benzyl > acenaphthenyl which corresponded exactly to the known order of the positive inductive effect of these groups. The ~~acidity~~ shielding of the α-protons in a given nitrate ester was ~~therefore~~ determined by both the nitroxy group and the structure of the parent hydrocarbon and it was therefore probable that there should be a correlation between τ values of the α-protons and the reactivity of the nitrate ester with basic reagents.

Unfortunately, the available data was rather limited but a plot of the pseudo first-order rate constants for the pyridine reaction of nitrate esters at 25°(62)(63)(144) against the τ values of the α protons (Figure 12) seemed to confirm the predicted result.

Obviously more data would be required to test the proposed correlation but some predictions were suggested at this preliminary stage. It seemed that compounds which undergo carbonyl elimination with bases were located at the top left of the plot. Benzyl nitrate which reacted via both $E_{C=O}$ and S_{NN} mechanisms (69) would be located somewhere near the first point

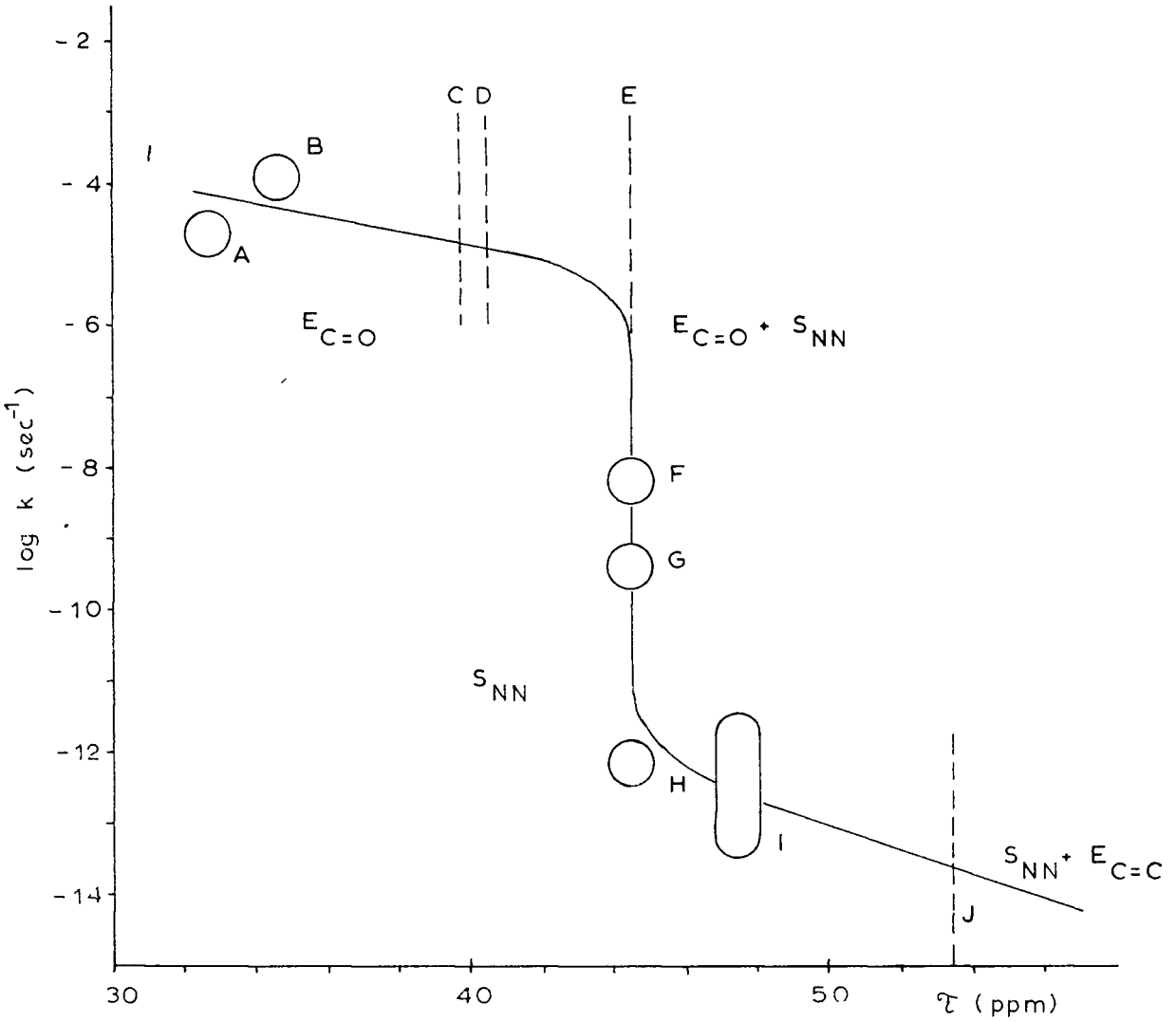

FIGURE 13 Tentative Correlation of $\tau_{\alpha H}$ and Mechanism in the Reaction of Nitrate Esters with Pyridine at 25°

A: cis-1,2-Acenaphthenediol Dinitrate (XXXVI)
B trans-1,2-Acenaphthenediol Dinitrate (XL)
C meso-Hydrobenzoin Dinitrate (XXIX)
D dl-Hydrobenzoin Dinitrate (XXXI)
E: Benzyl Nitrate
F Isoidide Dinitrate (XVIII) (165)
G Isosorbide Dinitrate (XIX) (165)
H: Isomannide Dinitrate (XX) (165)
I. trans-1,2-Cyclohexanediol Dinitrate (XXII)
J: Ethyl Nitrate

of inflexion. Compounds F, G, H, and I in the middle and at the lower inflexion in the curve showed S_{NN} decomposition (62) (63) and finally ethyl nitrate (J) which reacted with bases by both S_{NN} and $E_{C=C}$ mechanisms (55) (56) probably would occupy a position on the lower slope at the right.

It is hoped that this correlation in a refined form will serve in the future as a "diagnostic diagram" for predicting ionic mechanisms of new nitrate esters.

B. Infrared Spectra (IR).

Infrared spectra have been reported (166) (167) (168) (169) for more than one hundred nitrate esters in the condensed (solid or liquid) state.

Table XVII

Infrared Frequencies of Nitroxy Groups from Condensed State Spectra

Band	I	II	III	IV	V
Range (cm^{-1})	1665-1613	1285-1267	871-833	759-738	716-685
Assignment:	$\nu_a(NO_2)$	$\nu_s(NO_2)$	$\nu(ON)$	$\gamma_w(NO_2)$	$\delta(NO_2)$
Benzyl Nitrate	1626	1278	860	756	697
meso-Hydrobenzoin Dinitrate	1625 1645 1652	1279 1295 1310	842 860	770	(697)* 709
dl-Hydrobenzoin Dinitrate	1636 1660	1271	852 867	761	(696)
Benzoin Nitrate	1643 1672	1265 1285	840 844	 745	(675) (690) (705)
trans-1,2-Acenaphthenediol Dinitrate	1649 1621	1283	860	754	708
cis-1,2-Acenaphthenediol Dinitrate	1648 1627	1294 1278 1269	868	758	(728)

* Values in parentheses represent bands overlapped by others in the spectra of the parent alcohols.

Five principal infrared absorption bands were defined for the nitroxy group by Guthrie and Spedding (166) as shown in Table XVII. The infrared spectra of the aromatic nitrate esters synthesized in the present work were recorded in the condensed state,

Table XVIII

Infrared Frequencies of Nitroxy Groups from Solution Spectra**

Band	I	II	III	IV	V
Assignment	$\nu_a(NO_2)$	$\nu_s(NO_2)$	$\nu(ON)$	$\gamma_w(NO_2)$	$\delta(NO_2)$
Benzyl Nitrate	1637	1276	842	750	694
trans-1,2-Acenaphthenediol Dinitrate	1646	1276	843	750	705
cis-1,2-Acenaphthenediol Dinitrate	1655	1285	844	(779)*	(726)*

** 10^{-2}M in cyclohexane.

as neat liquids, or as potassium bromide windows (Table XVII) and also for some of them in 10^{-2}M cyclohexane solutions (Table XVIII).

It was clear from the tabulated data that the multiplicity of bands in the solid state was a function of the crystal structure rather than of intramolecular interaction of vicinal nitroxy groups since only singlet absorptions were observed in the solution spectra.

The significantly higher frequencies (9 to 18 cm^{-1}) of the asymmetric and symmetric stretching frequencies in the solution spectrum of cis-1,2-acenaphthenediol dinitrate compared to those of the trans-isomer and benzyl nitrate has been attributed to steric interaction of the contiguous nitroxy groups in the cis-dinitrate (144).

C. Ultraviolet Spectra (UV)

The UV- spectrum of iso-amylnitrate in ethanol solution was similar to that of other aliphatic mononitrates (95). It was suspected from the spectrum that the tail on the high wavelength side hid weak band(s) of unknown origin as shown in Figure 13.

It was reported recently (105) that the shoulder at 2700 Å was not observable in dinitroxy compounds such as isosorbide dinitrate (XIX) indicating that upon disubstitution the $\pi \rightarrow \pi^*$ band became twice as intense as in the mononitrates and overshadowed the weak $n \rightarrow \pi^*$ band. For this reason mononitrates were more suitable for spectral study than di- or poly-nitrates. This absence of fine structure was also observed in the case of the aromatic dinitrates (e.g. meso-hydrobenzoin dinitrate) and therefore an aromatic mononitrate, benzyl nitrate (23) was also examined (Figure 14 and 15).

Since aromatic nitrate esters in addition to the $n \rightarrow \pi^*$ and $\pi \rightarrow \pi^*$ bands of the nitroxy group contain the benzenoid absorption as well it was not surprising that the shoulder representing the $n \rightarrow \pi^*$ transition was not as clear as in the aliphatic mononitrates.

It was known from the work of von Halban and Eisenbrand (170) that the $n \rightarrow \pi^*$ band in ethylnitrate was not subject to as large a solvent effect as the $n \rightarrow \pi^*$ bands of pyridine N-oxides (171) or even of carbonyl groups (172) (173).

An attempt to reveal the $n \rightarrow \pi^*$ band by the differential absorption technique (taking the spectrum of benzyl nitrate while benzyl alcohol was in the blank cell in the same molar concentration ($2x10^{-3}$M/l)) failed because the electronegative NO_2 changed the intensity of the benzenoid absorption band with respect to that in benzyl alcohol (Figure 14). On the other hand the differential spectrum in higher concentration ($2x10^{-2}$M/l)

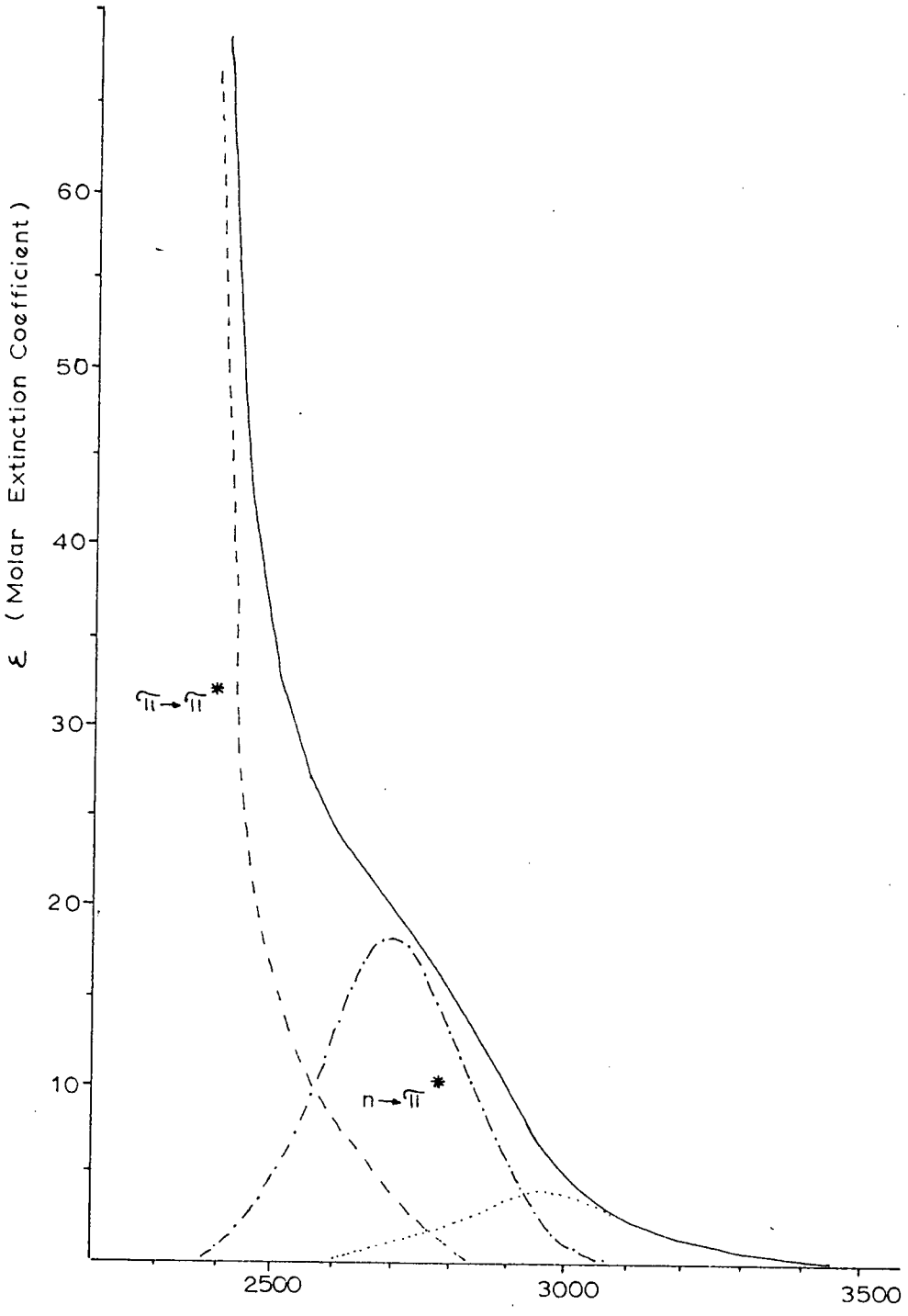

FIGURE 13. Ultraviolet Spectrum of iso-Amylnitrate in Methanol.

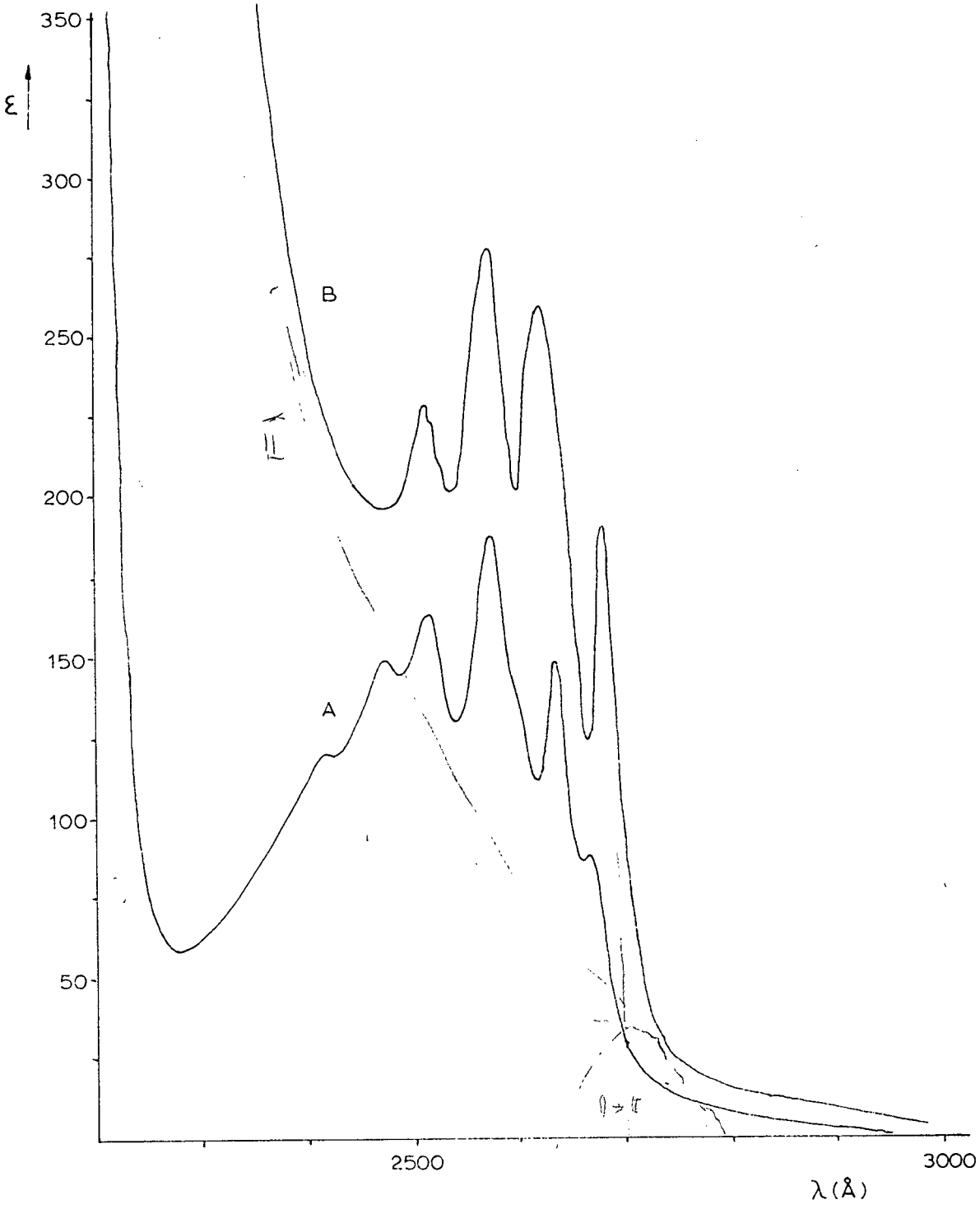

FIGURE 14. Benzenoid Absorption of Benzylalcohol (A), Benzylnitrate (B) in Hexane Solution.

revealed new weak bands at 200-300 Å longer wavelengths which could not be due to the difference in intensity of the benzenoid absorption (Figure 15). Similar solvent perturbation effects have been reported for carbonyl compounds (173) which were assigned to hydrogen bonding. In aliphatic nitro compounds the tailing portion of the spectrum was found to be a charge-transfer band due to a weak charge-transfer complex $RCH_2NO_2^- \ldots\ldots\ldots {}^+$Solvent (174). Plotting the frequency $\tilde{\nu}$ (cm^{-1}) of the two weak bands in four different solvents (Table XIX) versus the ionization potential of the solvents revealed interesting features of these transitions (Figure 16 and 17).

Band I showed a fair correlation with the solvent ionization potential indicating that at least to some extent, this band ~~was~~ may have been due to a solvent-solute charge-transfer interaction. This might explain the nature of the third weak band in <u>iso</u>-amylnitrate (Figure 13).

On the other hand band II did not correlate linearly with the ionization potential of the solvents but rather it leveled off after an initial increase. No firm assignment for this band was made but it seemed probable that this weak absorption was really due to the molecule itself and might be due to an intramolecular interaction of groups. A vapour spectrum of benzylnitrate confirmed the existence of another band at longer wavelength than the $n \rightarrow \pi^*$ transition but further work would be required on this line to settle the questions of assignment.

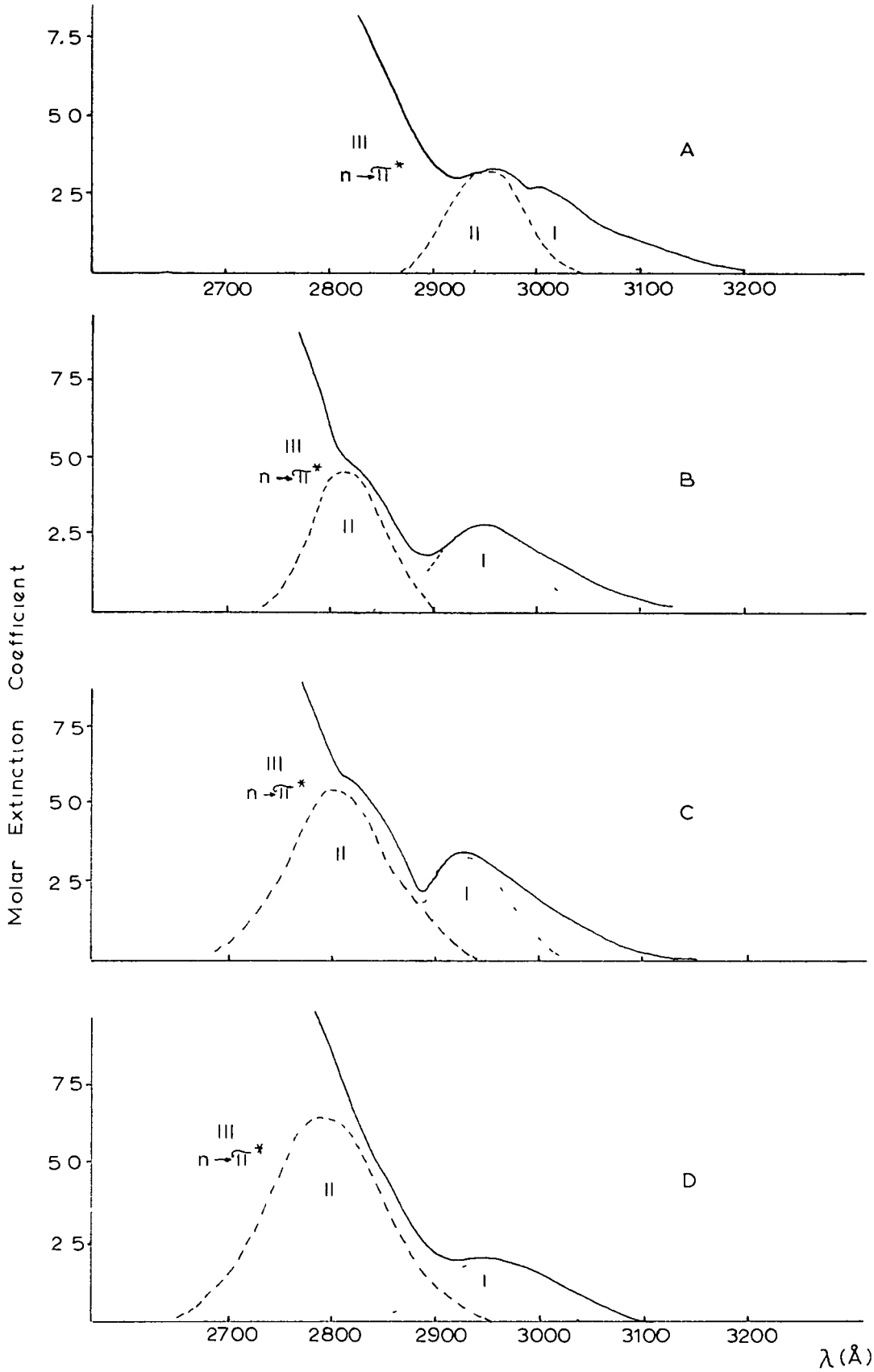

FIGURE 15. Difference Spectrum of Benzyl Nitrate and Benzyl Alcohol in Various Solvents A benzene, B ether, C hexane, D alcohol

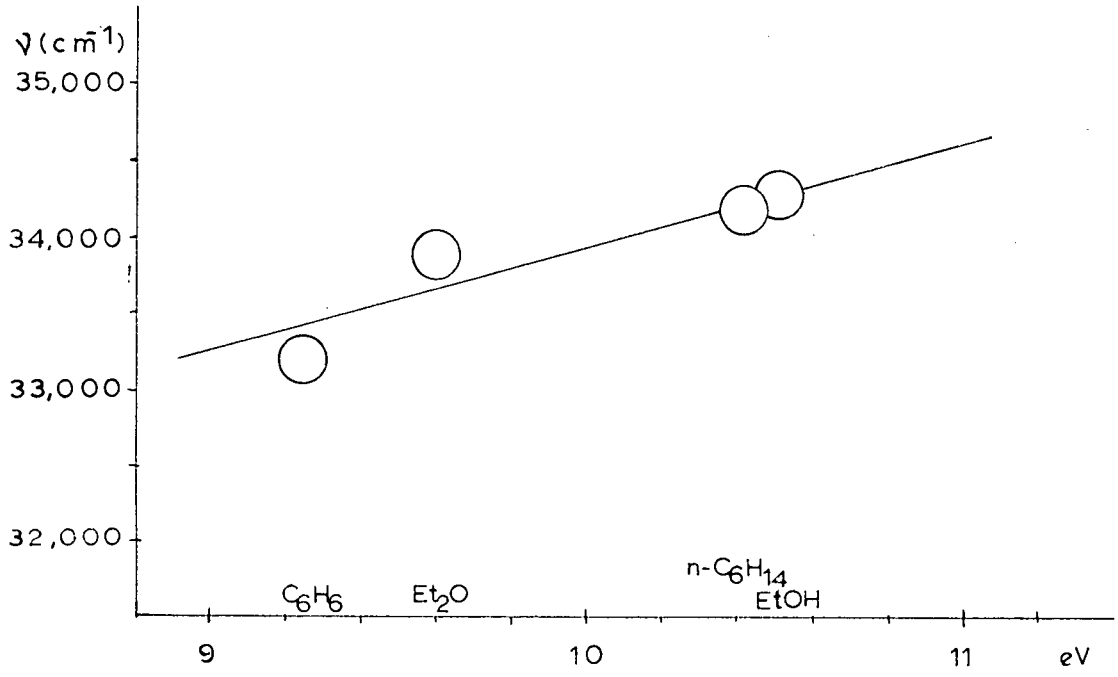

FIGURE 16. Correlation of the Frequency of Band I with the Solvent Ionization Potential

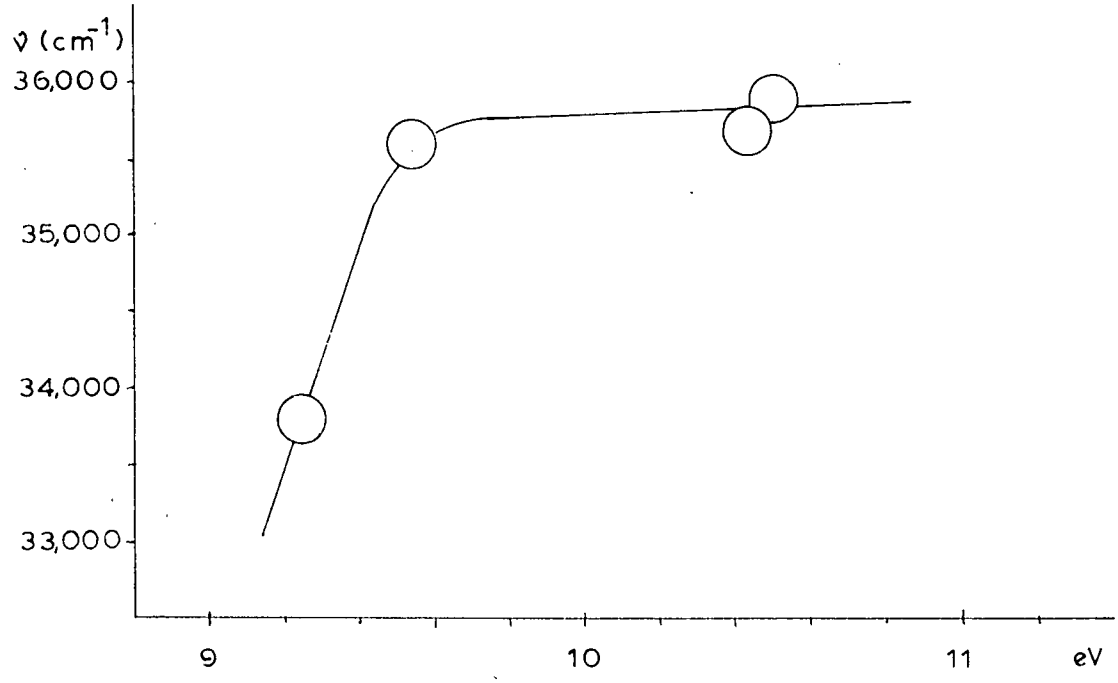

FIGURE 17. Correlation of the Frequency of Band II with the Solvent Ionization Potential.

Table XIX

Solvent Effects in Differential Spectra of Benzyl Nitrate and Benzyl Alcohol

Symb	Solvent	Ionization Pot. of Solvent[a)]	Band I		Band II		Band III $n \rightarrow \pi^*$	
			λ(Å)	$\tilde{\nu}$(cm^{-1})	λ(Å)	$\tilde{\nu}$(cm^{-1})	λ(Å)	$\tilde{\nu}$(cm^{-1})
A	Benzene	9.25[b)]	3010	33,223	2960	33,784		
B	Ether	9.53[b)]	2950	33,898	2815	35,524	2700	37,037
C	Hexane	10.43[c)]	2930	34,130	2800	35,714		
D	Alcohol	10.50[b)]	2920	34,247	2790	35,842		

a) in eV.

b) from Ref. (142)

c) from Ref. (13)

V. Photolysis of Aromatic Nitrate Esters.

A. Preliminary Experiments

In general it was found, that all of the aromatic nitrate esters, synthesized for this study, underwent photochemical decomposition upon irradiation with the full mercury arc spectrum. In a typical experiment a benzene solution of trans-1,2-acenaphthenediol dinitrate decomposed readily producing a number of unknown compounds which were separated by TLC and detected as fluorescent spots (Figure 48).

It seemed to be quite well established from earlier studies (104) (105) that photoreaction resulted from the $n \rightarrow \pi^*$ excitation of the nitroxy group and experiments carried out in quartz and Corex cells under a nitrogen

atmosphere (Figure 51) and in a degassed and sealed quartz tube (Figure 49) confirmed this result. Although the chromatographic pattern was somewhat simpler for the sample irradiated in the Corex cell, the products were generally the same for the three samples indicating that the longer wavelengths passed by Corex were chiefly responsible for the photolysis. It was also concluded from these results that the unfiltered mercury arc could be safely used for an ESR study of the photolysis of the nitroxy groups since these were the most light-sensitive of the chromophores present.

Benzene solutions (1.0 ml., 0.01 M) of four secondary aromatic dinitrates, one primary aromatic mononitrate , and one secondary alicyclic nitrate (Table XX) were photolysed with the Corex filtered mercury arc (Figure 46.Exp.) and aliquots were examined at intervals. In each case there was a gradual decrease of the original nitrate ester concentration and a gradual accumulation of the photolysis products as indicated by TLC. At the end of 9 hours irradiation only the solutions from meso- and dl-hydrobenzoin and isosorbide dinitrates showed the presence of the original nitrate esters in agreement with the relative rates of colour development (Table XX). Chromatographic analysis showed (Figure 18 and Figure 19) that neither of the 1,2-diketo compounds, acenaphthenequinone and benzil, were among the yellow products from the acenaphthene and hydrobenzoin nitrates.

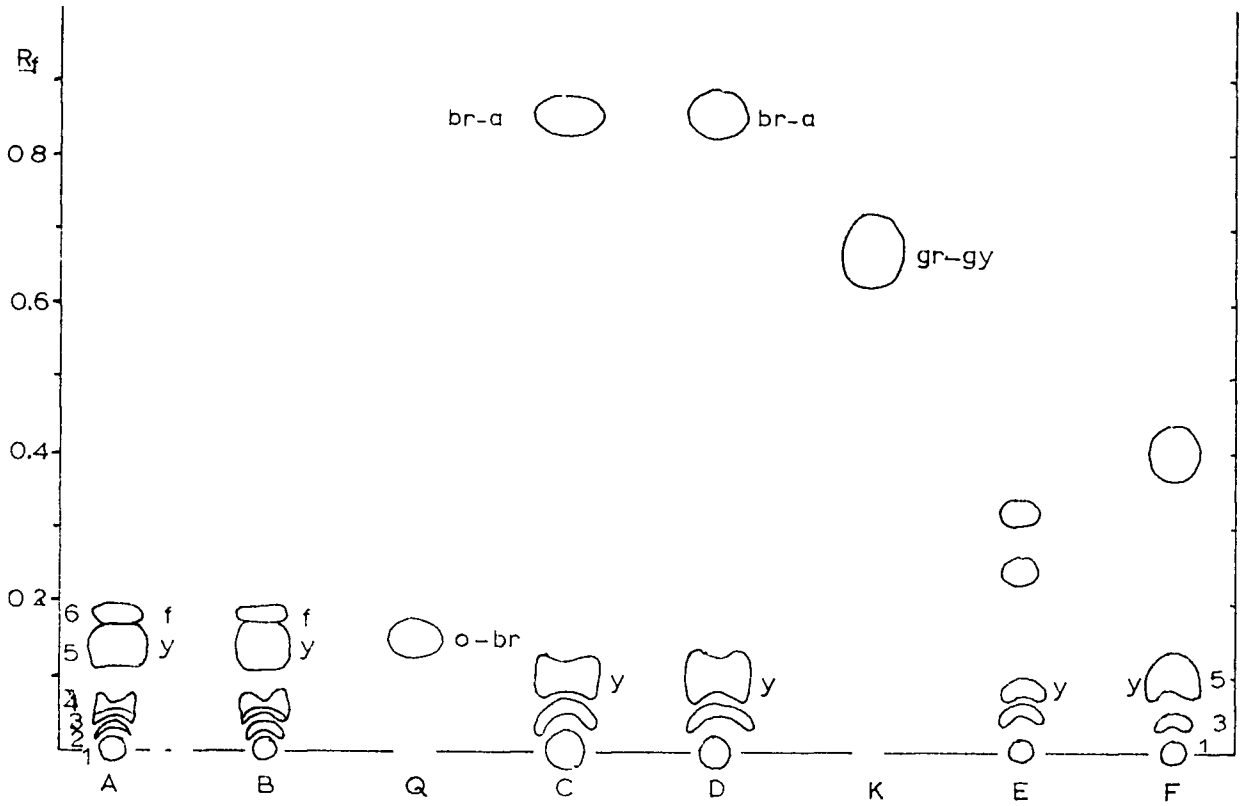

Figure 18. Chromatographic Separation of Photolysis Products of Nitrate Esters (TLC; M-3, S-6).

A.	cis-1,2-Acenaphthenediol Dinitrate	f:	fluorescence (UV)
B.	trans-1,2-Acenaphthenediol Dinitrate	y:	yellow
Q.	Acenaphthenequinone	o:	orange
C.	meso-Hydrobenzoin Dinitrate	r:	red
D.	dl-Hydrobenzoin Dinitrate	br:	brown
K.	Benzil (1,2-Diketo-1,2-diphenylethane)	br-a:	brown absorption (UV)
E.	Benzoin nitrate	gr-gy:	green-gray
F.	Isosorbide Dinitrate		

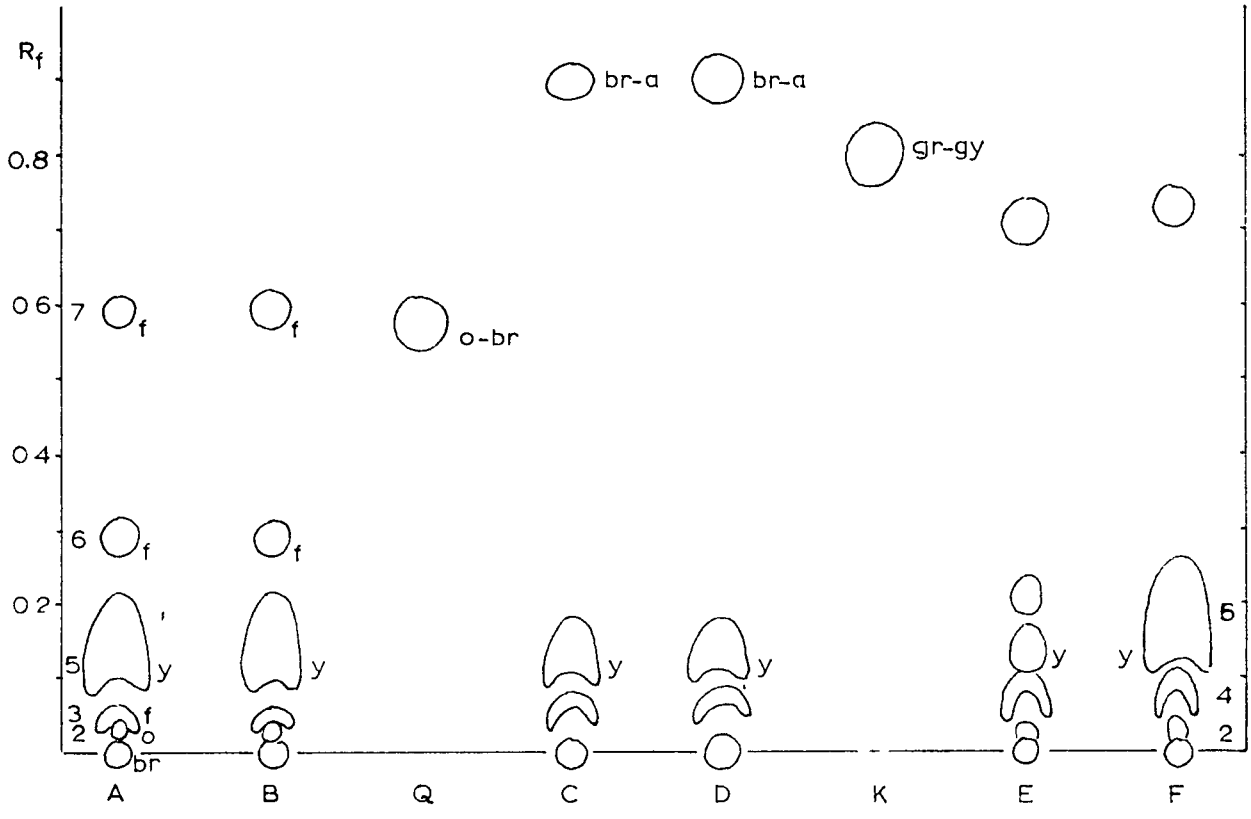

Figure 19. Chromatographic Separation of Photolysis Products of Nitrate Esters (TLC; M-3, S-10).

A. cis-1,2-Acenaphthenediol Dinitrate
B. trans-1,2-Acenaphthenediol Dinitrate
Q. Acenaphthenequinone
C. meso-Hydrobenzoin Dinitrate
D. dl-Hydrobenzoin Dinitrate
K. Benzil (1,2-Diketo-1,2-diphenylethane)
E. Benzoin nitrate
F. Isosorbide Dinitrate

f: fluorescence (UV)
y: yellow
o: orange
r: red
br: brown
br-a: brown absorption
gr-gy: green-gray

Table XX

Photolysis of Nitrate Esters in Benzene Solutions:
Preliminary Experiments

		Initial Concentration		Relative Intensity of Yellow Colour After Irradiation		
		Comp'd.	ONO_2 grps.			
	Original Nitrate Ester	mg/ml	mM/lit.	0.5hr.	1.5hr.	9.0hr
A	cis-1,2-Acenaphthene-diol Dinitrate	2.7	19.6	++	+++	++++
B	trans-1,2-Acenaphthene-diol Dinitrate	2.9	21.0	++	+++	++++
C	meso-Hydrobenzoin Dinitrate	3.1	20.4	—	+	+++
D	dl-Hydrobenzoin Dinitrate	3.1	20.4	—	+	+++
E	Benzoin nitrate	2.5	9.7	+	++	++++
F	Isosorbide Dinitrate*	2.5	21.2	—	+	+++

* 1,4;3,6-dianhydro-D-glucitol-2,5-dinitrate.

The alicylic secondary nitrate ester (F) showed much the same pattern of products as was obtained with the four aromatic vicinal dinitrates, indicating that the nature of the R- group in the esters $RONO_2$ was not critical in determining the course of the reaction.

Although care was taken in these experiments to exclude atmospheric oxygen, in order to prove that the yellow products formed during the photolysis in benzene did not originate from oxidation due to the presence of dissolved oxygen or water, a similar experiment was conducted in degassed and sealed quartz tubes in carefully purified benzene. The quartz tubes were opened and in the moment when the tube was cracked, the colourless gas in the tubes

became yellow-brown indicating that a gaseous product of photolysis was NO which immediately oxidized to NO_2 on the admission of oxygen. Qualitative observations for the reactions are summarized in Table XXI.

The pattern obtained by TLC agreed with the results of the previous experiment. The use of alkaline permanganate spray reagent (R-3) showed that the pronounced yellow spots resembled phenols in ease of oxidation and the presence of ortho-nitrophenol was confirmed by comparison with a reference sample on the chromatogram (Figure 20), by the similar response to spray reagent R-3 and also by the fact that the yellow colour faded at the same rate on the chromato-plates upon standing while other coloured spots were permanent for several weeks.

Table XXI

Photolysis of Nitrate Esters in Oxygen-free Absolute Benzene Solutions

Symbol	Name	Initial Conc.		After Irradiation for 22 hrs.		
		Comp'd	ONO_2 grps.	Relative Colour of Solution	Relative Amount of Pre-cipitate	Relative Amount of NO gas
	Original Nitrate Ester	mg/ml	mM/lit			
A	cis-1,2-Acenaphthene-diol Dinitrate	26.9	195	++	+++	+++
B	trans-1,2-Acenaphthene-diol Dinitrate	27.7	200	++	+++	+++
C	meso-Hydrobenzoin Dinitrate	30.0	197	++	++	++
D	dl-Hydrobenzoin Dinitrate	30.4	200	++	++	++
E	Benzoin Nitrate	25.8	101	+++	—	—
F	Isosorbide Dinitrate*	23.4	198	+	+	+

* 1,4;3,6-dianhydro-D-glucitol-2,5-dinitrate

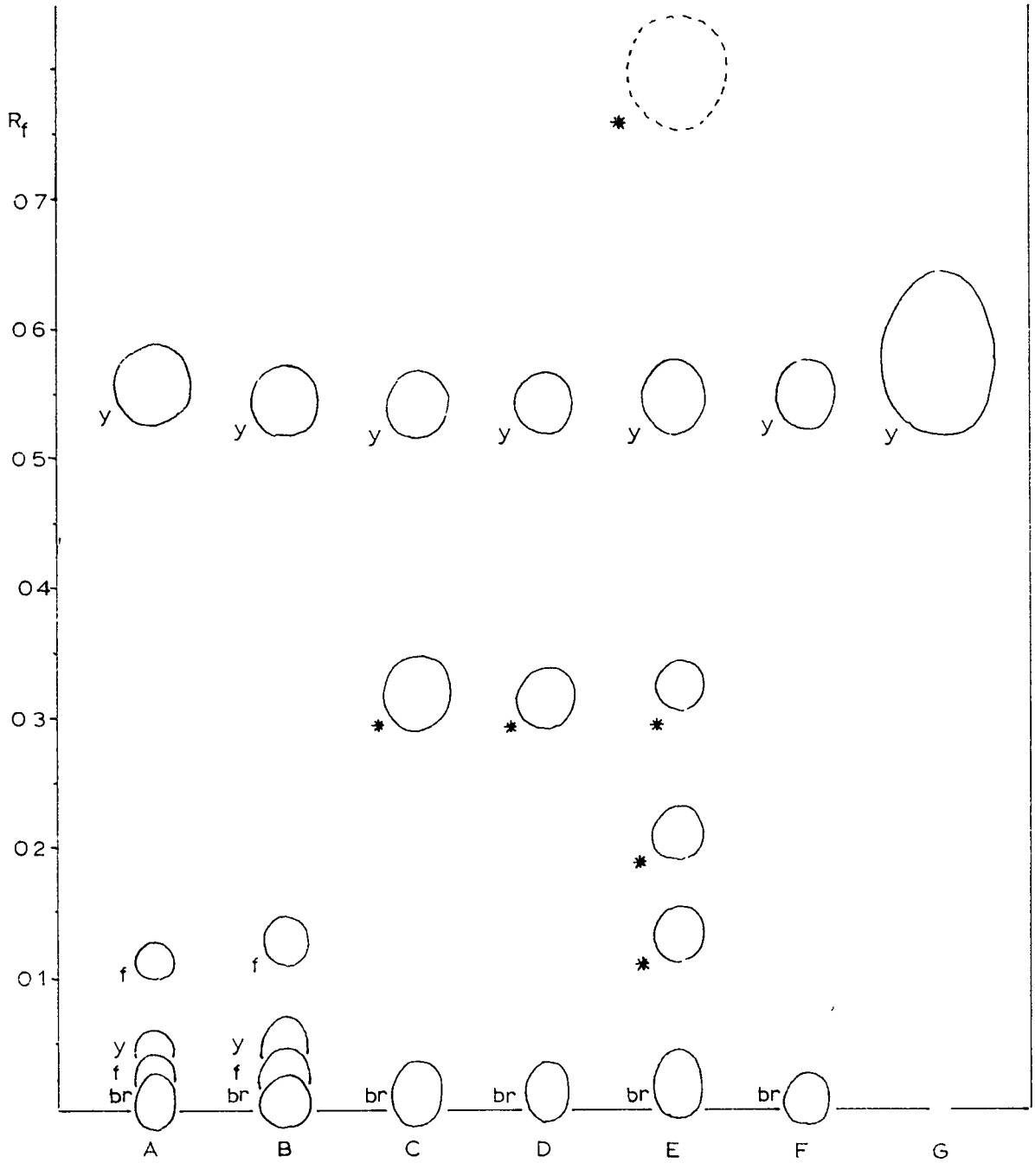

FIGURE 20 Chromatographic Separation (M–3, S–1, R–3) of Photolysis Products of Nitrate Esters

A cis-1,2-Acenaphthenediol Dinitrate; B trans-1,2-Acenaphthenediol Dinitrate, C meso–, D dl-Hydrobenzoin Dinitrate, E Benzoin Nitrate, F Isosorbidedinitrate, G ortho-Nitrophenol; f: fluorescence (UV), y yellow, b· brown, ✱: colourless before spraying, white spot on pink background after spraying with R–3

The same yellow photo-products were detected in the case of benzoin nitrate but in addition other colourless spots, not present among the products originating from the other nitrate esters showed up after spraying with reagent R-3. Other differences in the products from benzoin nitrate (an α-keto nitrate ester) and the other nitrate esters are shown in Table XXI.

B. Identification of Photolysis Products.

The preliminary experiments showed that o-nitrophenol and probably other nitrophenols were formed from the solvent benzene. This consecutive (or simultaneous) oxidation and nitration of the benzene ring could have taken place only at the expense of the nitrate esters since no other oxygen and nitrogen source was available in the system. This observation made it evident that care had to be taken to distinguish between products originating from the solvent and those originating from the nitrate ester in the photolysis.

meso-Hydrobenzoin dinitrate was therefore irradiated in thirteen different solvents* on a micro scale to obtain preliminary information and then in three solvents; benzene, ether, and alcohol for more detailed investigation.

(i) Products from Solvents

Irradiation in Benzene Solutions

Benzene solutions of meso-hydrobenzoin dinitrate (0.01 M) ~~was~~ were irradiated in the photoreactor (Figure 47) with Corex filter (Figure 46) for various lengths of time. o-Nitrophenol was isolated from the irradiation mixtures by vacuum and steam distillations and its identity was confirmed

---

* Diethylamine, ethanol, ethylmercaptan, dioxane, cyclohexane, cyclohexene, benzene, carbon disulfide, acetic acid, ethyl acetate, diethyl ether, acetal, and phenol.

by its nitrogen content and by thin layer chromatography. For isolation and identification of the other yellow photolysis products, the unreacted nitrate ester and the o-nitrophenol were removed by column chromatography and the resulting mixture was analyzed by TLC as shown in Figure 21 (A-P) for various times of irradiation.

It was evident that not all of the coloured spots originated from the primary interaction of nitrate esters and benzene since the pattern changed with the time of irradiation. Certain spots (G and J) appeared early (0.5 hrs.) and their concentration after reaching a maximum value gradually decreased with time. Other spots (D, H, L, M, and O) were not detectable in the early stages of the irradiation and some of them started to appear after 5 or even 10 hours, indicating that they either accumulated by a very slow process which did not dominate over the main course of the reaction or that they were secondary products originating from the nitro compounds formed in the primary process.

Because of the similarities in R_f values, column chromatographic separation under similar conditions failed completely (156) and thick-layer microadsorption chromatography (105) (208) also did not provide satisfactory results. Repeated TLC was used successfully for separating these products but because of the micro scale of the method and the large number of components, only the compounds which occurred in relatively high concentration were isolated on a milligram scale.

Figure 22 shows a chromatogram of ten pure compounds isolated from the photoreaction products. Comparison with known compounds indicated that E might be 2,4-dinitrophenol, while G agreed very well with 2,6-dinitrophenol and F was similar to 2,6-dinitro-4-phenylphenol. The infrared spectra of C and D (Figure 23) indicated the presence of nitroxy groups as well as aromatic nitro groups in a structure similar to that of meso-hydrobenzoin dinitrate.

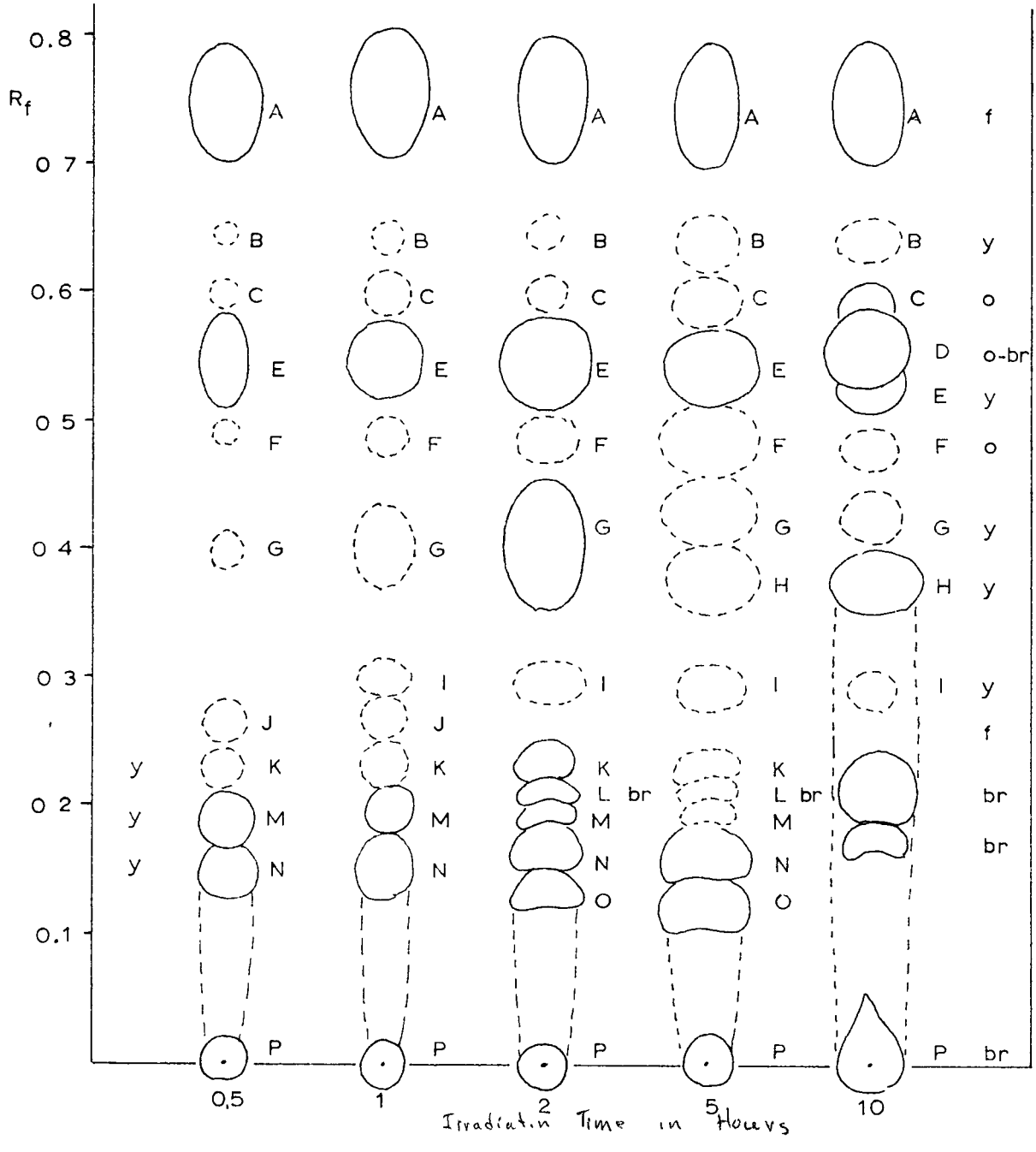

FIGURE 21 Chromatographic Separation of Products from Photolysis of <u>meso</u>-Hydrobenzoin Dinitrate in Benzene Solution (M-3, S-5)

f. fluorescence (UV), y yellow, o orange, o-br orange brown; brown = br.

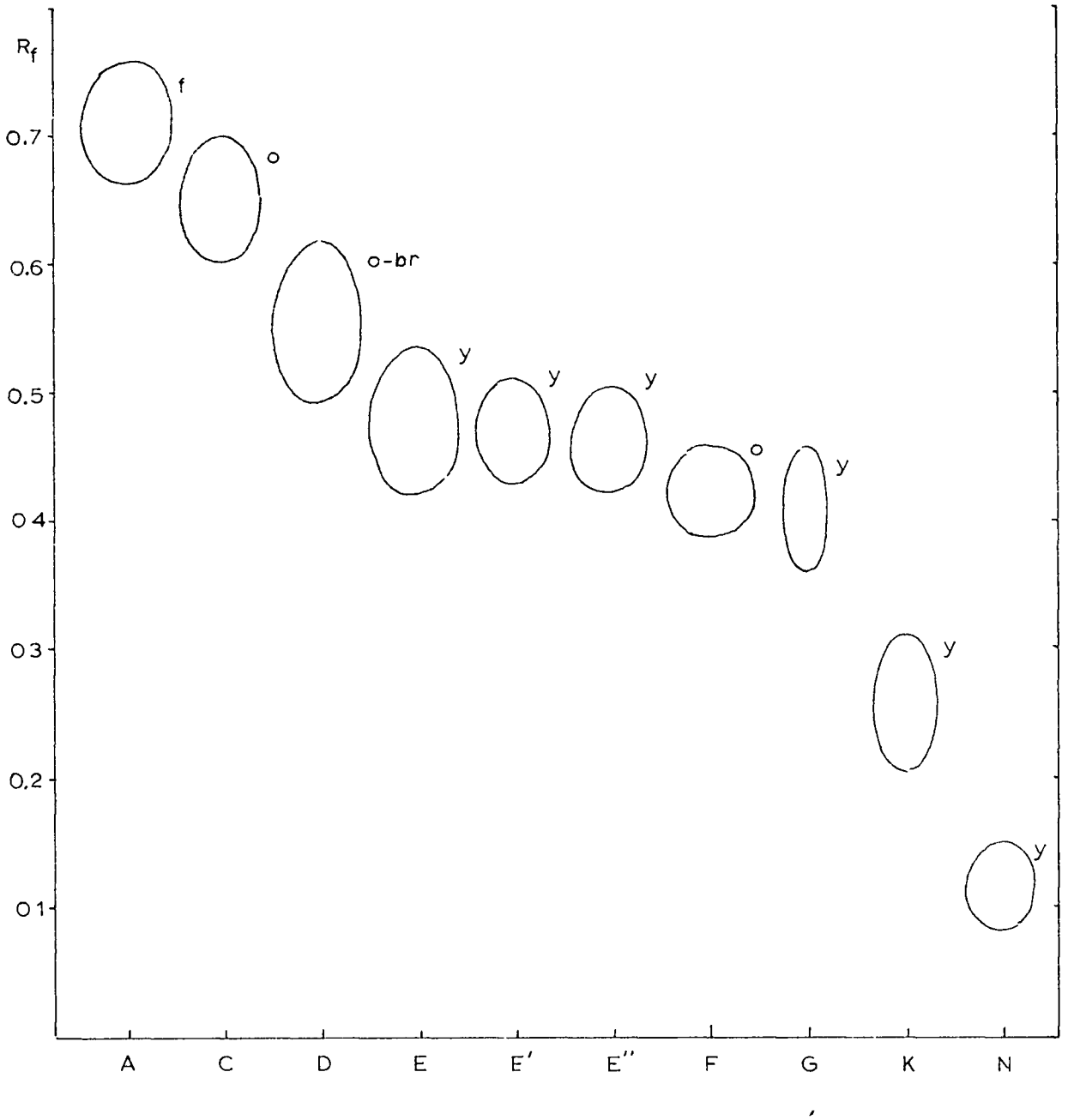

FIGURE 22 Phenolic Products Isolated from Photolyzed (in C_6H_6) <u>meso</u> – Hydrobenzoin Dinitrate

f fluorescence (UV); y yellow; o orange, o-br orange brown, b brown

Since no unreacted meso-hydrobenzoin dinitrate was present, these compounds were identified as ring-nitrated meso-hydrobenzoin derivatives (Figure 23). Although C showed a broad OH band at 3400 cm^{-1} this was possibly due to moisture since the parent meso-hydrobenzoin exhibited a sharp OH peak. On the basis that $R_f(C) > R_f(D)$ and that D showed up later than C in the photoreaction (Figure 21) it was suspected that C was the 4-mononitro- and D the 4,4' -dinitro meso-hydrobenzoin dinitrate. These compounds would be the products of intermolecular nitration rather than of intramolecular re-arrangement.

The infrared spectrum of E, the petroleum ether soluble portion of E', (Figure 24) matched that of 2,4-dinitrophenol even in the fingerprint region so that there was no doubt that E was 2,4-dinitrophenol in agreement with TLC results, however, there were two additional peaks in the spectrum of E at 2900 and 1726 cm^{-1} indicating that some E' contaminated the sample. E' and E" gave distinctive although quite similar spectra (Figure 24) and were probably isomeric dinitrophenols.

The infrared spectra of F, K, and N were compared to that of 2,6-dinitro-4-phenylphenol (Figure 25) but no firm identification was possible in these cases. However, the fact that orange spots similar to F occurred also among the photolysis products from dl-hydrobenzoin dinitrate and from benzyl nitrate but were completely absent in the irradiation mixtures from cis- and trans-1,2-acenaphthenediol dinitrates suggested that this compound originated in the nitrate esters rather than in the solvent. On the other hand if F were really 2,6-dinitro-4-phenylphenol that would mean that phenyl radicals were generated with three out of five nitrate esters and attacked the simultaneously formed nitrophenols as represented in equation 110. The suspected reaction would be somewhat analogous to one (111) reported by Price and Convery (175) for meta-dinitrobenzene.

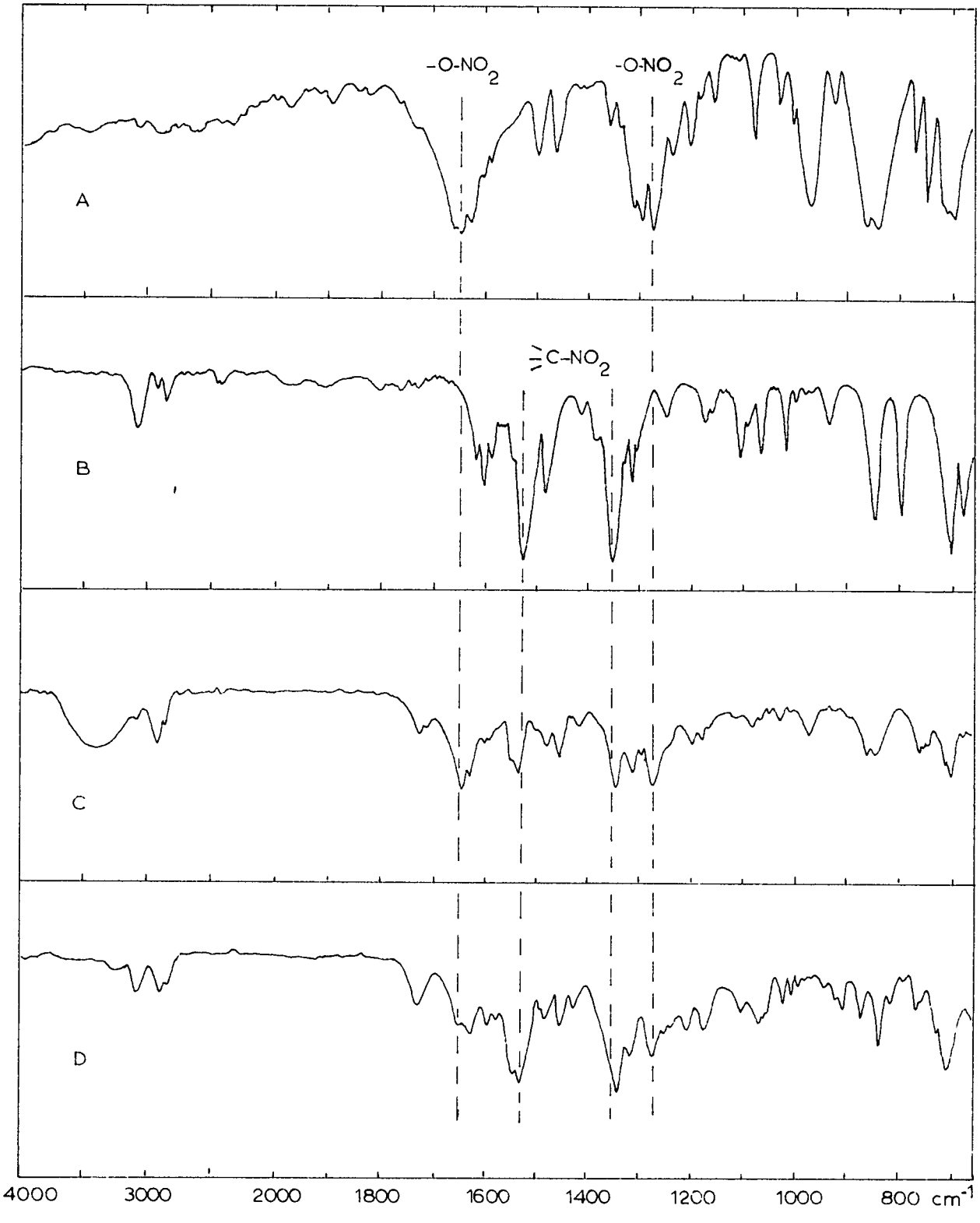

FIGURE 23 Infrared Spectra of meso-Hydrobenzoin Dinitrate (A), Nitrobenzene (B) and Photolysis Products of A (C and D)

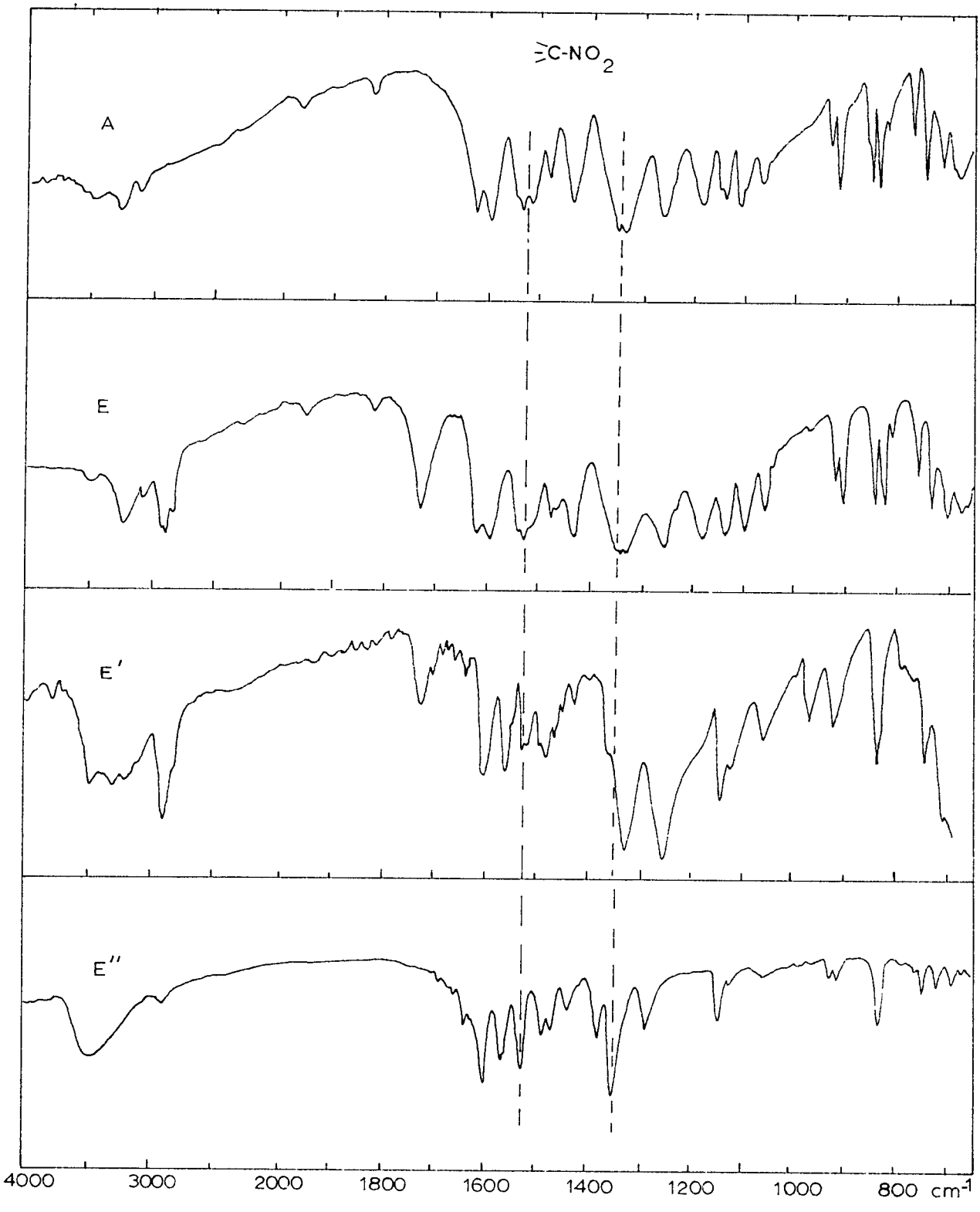

FIGURE 24 Spectra (IR) of 2,4-Dinitrophenol (A) and Photolysis Products from <u>meso</u>-Hydrobenzoin Dinitrate (E, E' and E'')

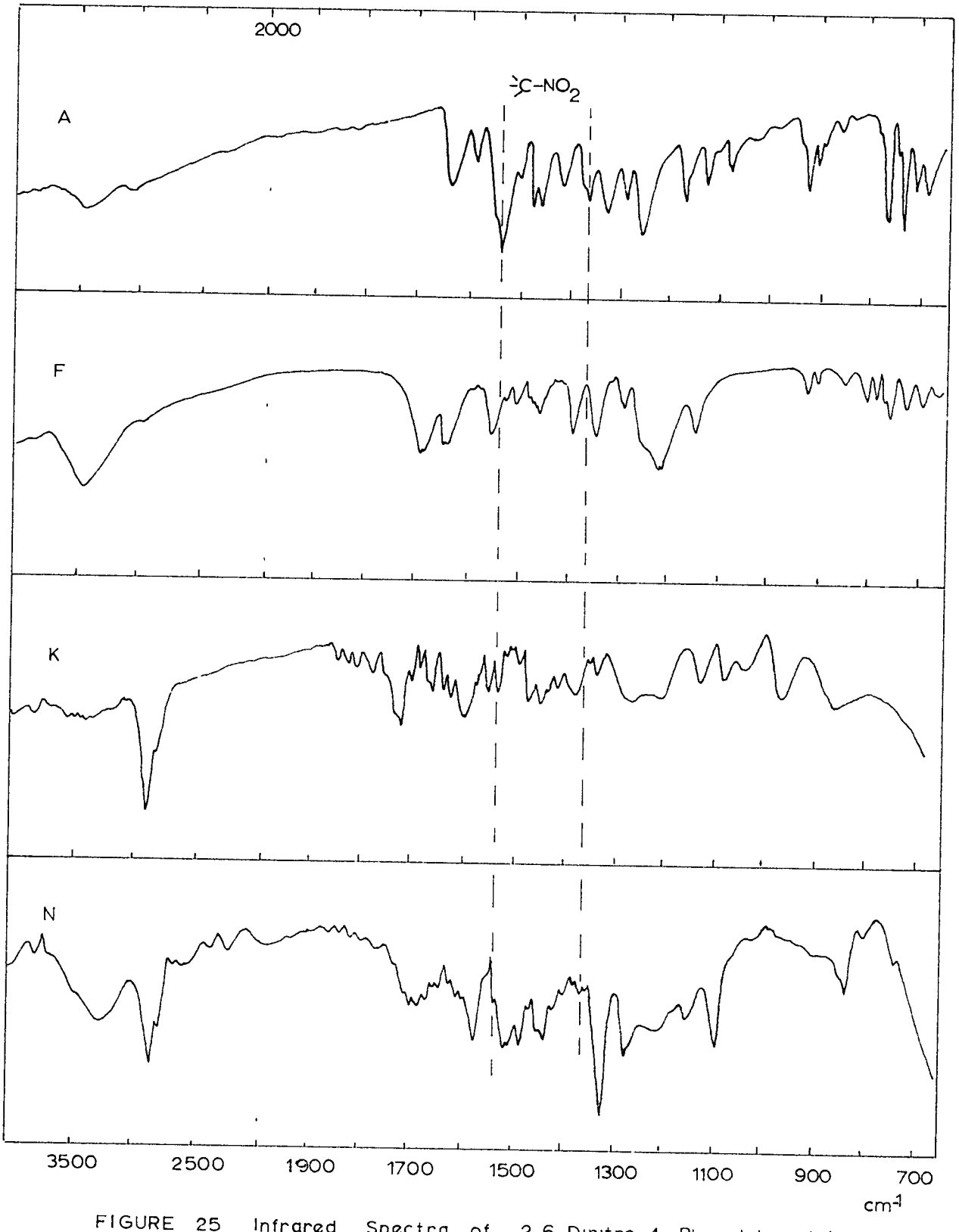

FIGURE 25 Infrared Spectra of 2,6-Dinitro-4-Phenylphenol (A) and Photolytic Products from meso-Hydrobenzoin Dinitrate (F, K and N)

Irradiation in Ether Solution.

No product which originated solely from the solvent was isolated in the irradiation of meso-hydrobenzoin dinitrate in ether solution. A major spot in the chromatogram was located above the unreacted nitrate ester which was quite unusual since in most cases the nitrate ester possessed a higher R_f value than any of the photolysis products. The characteristic feature of this compound was its bright fluorescence under ultraviolet light and upon spraying the chromatogram with concentrated nitric acid-sulfuric acid mixture (R-1) the spot turned green immediately. Only solvents which possessed the structure X-O-Y, i.e. diethylether, ethyl acetate, acetal, and dioxane, produced this or similar compound. From the high R_f value the compound was suspected to be the ketal of the corresponding diketone (benzil), however, acid catalysed hydrolysis of the isolated crystalline compound (m.p. 95-98°) failed to yield benzil. The NMR spectrum of the sample was recorded and there seemed to be little doubt that some sort of alkylation had taken place on the parent molecule (Figure 26), in other words the solvent molecule was incorporated (in part or in full) into the meso-hydrobenzoin moiety, however, further work would be required to elucidate the structure of this unknown product.

Irradiation in Alcohol Solutions

Acetaldehyde was isolated as the 2,4-dinitrophenylhydrazone from irradiation of ethanol solutions of the nitrates. The same product was obtained by irradiating either meso-hydrobenzoin dinitrate or benzyl nitrate under similar conditions. The 2,4-dinitrophenylhydrazone was identified by its melting point, elementary analysis, than layer chromatography and nuclear magnetic resonance spectrum.

This oxidation of alcohol to aldehyde during the photo-reduction

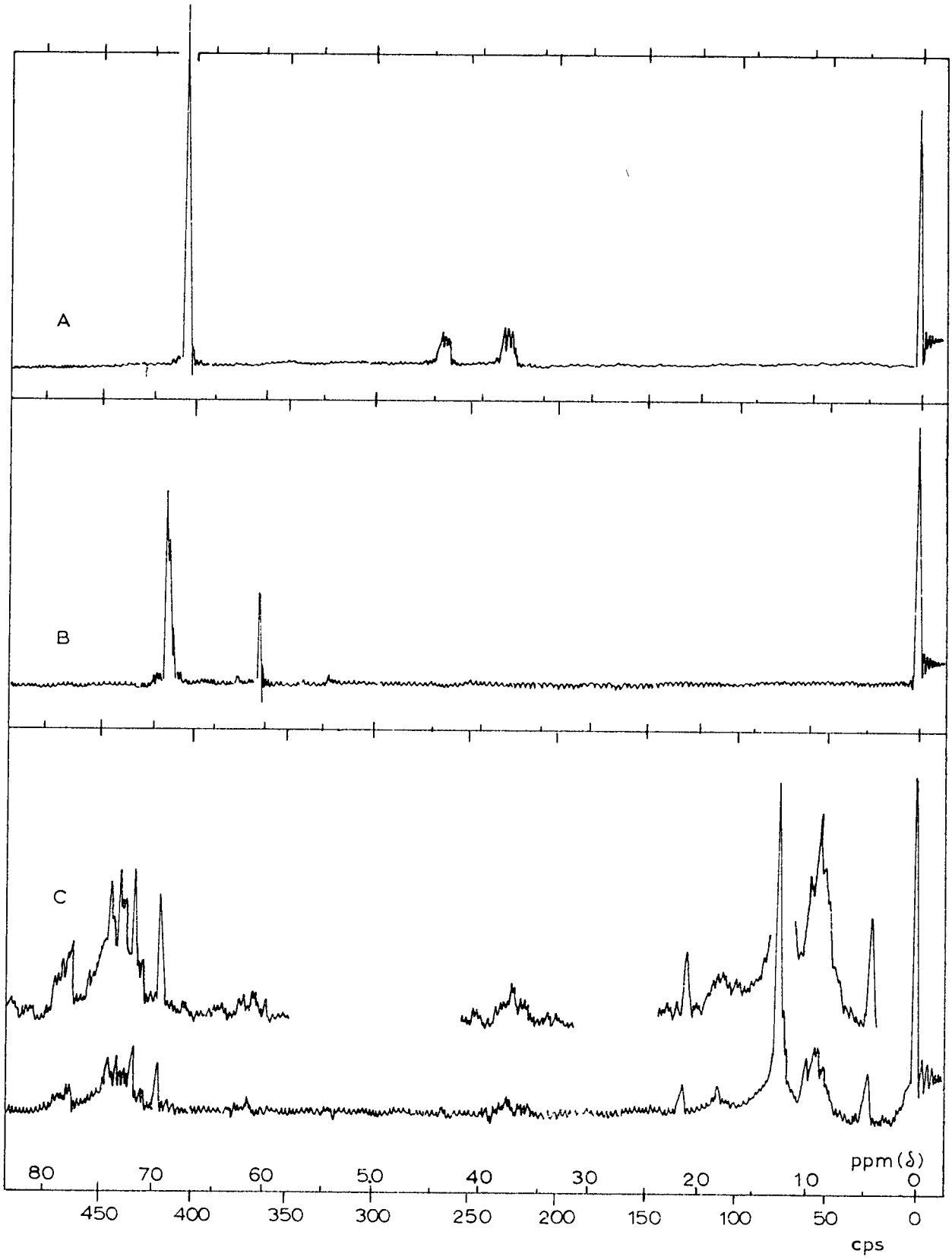

FIGURE 26 NMR Spectra of 1,2-Diphenylethane Derivatives

A meso-Hydrobenzoin, B meso-Hydrobenzoin Dinitrate, C Product from B Irradiated in Ether Solution

of nitrate esters seemed to be analogous to the oxidation of benzene to phenol.

(ii) Products from Irradiated Nitrate Esters.

The nitrate esters during photolysis split up to fragments, the nitrogen-oxygen portion reacted with the solvent or active solute but gaseous nitrogen oxides were also detected. Semi-quantitative mass spectral analysis indicated a ratio of 40:1 for $NO:NO_2$ in a gas mixture which was a blue solid when trapped at $77^{o}K$.

Skeletal fragments of the nitrate esters were also isolated and identified in most cases.

Irradiation of 1,2-Acenaphthenediol Dinitrates.

Both cis- and trans-1,2-acenaphthenediol dinitrates irradiated in benzene solution yielded, in addition to some unidentified fluorescent spots of low R_f values, naphthalene-1,8-dialdehyde which was isolated and identified both as the 4-nitrophenylhydrazone and in the oxidized form as naphthalene-1, 8-dicarboxylic acid. Thus the main course of the photolysis seemed to proceed to equations 112 and 113.

On the other hand it was likely that o-nitrophenol was not formed in one simple step but that the nitration was preceded by the oxidation of the aromatic ring. This production of the intermediate phenol occurred at the cost of the simultaneous reduction of nitrate ester to nitrite ester which in turn photolysed to alkoxyl radical and NO at the longer wavelengths.

The splitting of the carbon-carbon bond between adjacent nitrate ester groups (112 and 113) has also been observed (74) in the thermolysis of 2,3-dinitroxy-butane (47) as discussed in the introduction. The similarity of the reaction in the photolysis of vicinal dinitrates was experimental evidence that in the solution photolysis of nitrate esters just as

(110)

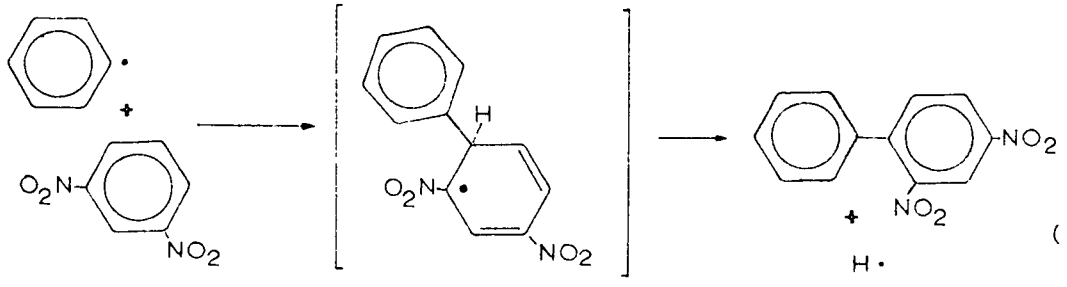

(111)

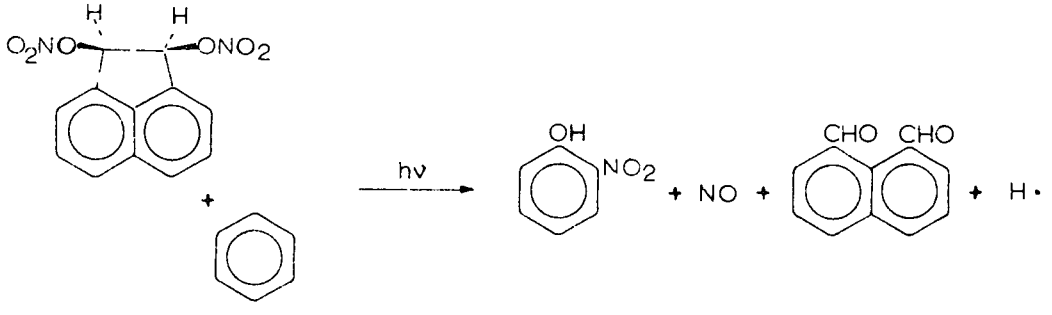

(112)

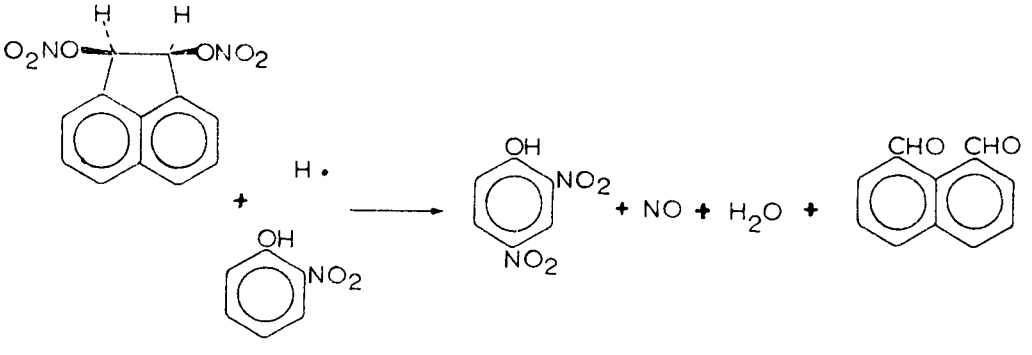

(113)

in thermolytic reactions alkoxyl radicals play a vital role as intermediates.

Irradiation of Benzyl Nitrate

Photolysis of benzyl nitrate in both benzene and alcohol solutions gave rise to the same products originating from the solvents, namely nitrophenols from benzene and acetaldehyde from alcohol, as were found with the hydrobenzoin dinitrates. Consequently, there can be no doubt that the fragmentation pattern of the nitroxy group was the same for this primary mononitrate as for the secondary dinitrates, in other words it was a function of the nitroxy group and independent of the structure of the rest of the molecule. The intermediate alkoxyl radical probably underwent one or more of the following reactions as described in recent reviews (91) (70):

1. Intermolecular hydrogen abstraction (114)

2. Disproportionation (115)

3. Radical elimination, which could have occurred in two different ways.

(a) The elimination of the α-hydrogen (116) (energetically unfavourable) (70) (176).

(b) Carbon-carbon scission (117)

The carbon-carbon cleavage in benzyloxyl radical has not been previously reported (70) (177), however, tertiary alkoxyl radical transformation with simultaneous generation of phenyl radical and the corresponding ketone (118) has been established (70). The generation of phenyl radicals would also be consistent with the formation of biphenyl derivatives (110).

Irradiation of meso-Hydrobenzoin Dinitrate.

The two isomeric hydrobenzoin dinitrates behaved similarly to the acenaphthenediol dinitrates in that C-C bond scission occurred between the

(114)

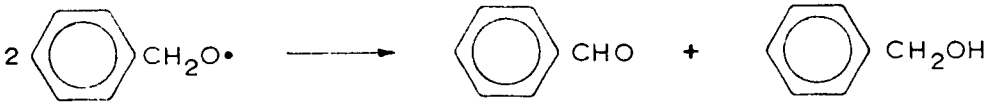

(115)

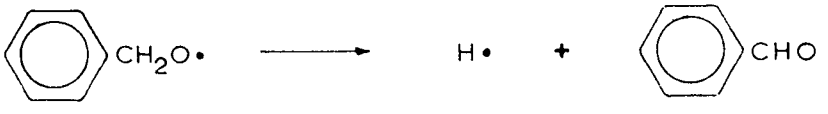

(116)

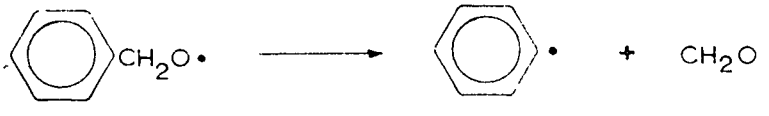

(117)

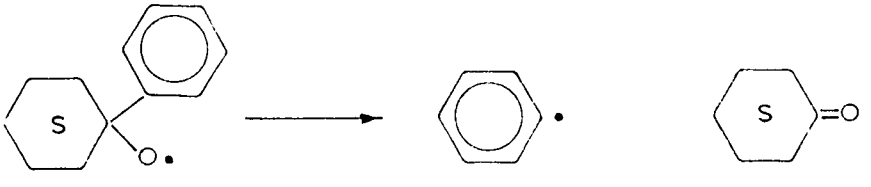

(118)

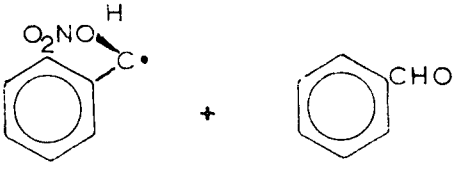

(119)

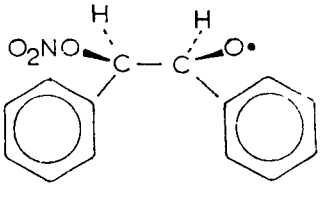

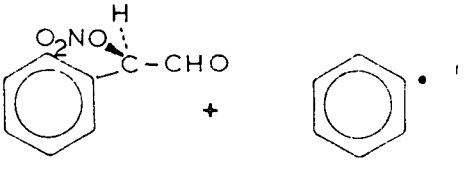

(120)

two vicinal nitroxy groups to produce aldehydes. Since in this case the original molecule was split into halves it gave rise to two moles of benzaldehyde per mole of nitrate ester. This reaction (119) seemed to be preferred over aralkyl C-C bond scission (120), however, both could have taken place simultaneously.

The benzaldehyde originated from meso-hydrobenzoin dinitrate upon irradiation in both benzene and ethanol solutions and was isolated and characterized as the 2,4-dinitrophenylhydrazone. A possible mechanism for the photo-decomposition of meso-hydrobenzoin dinitrate is given in Figure 27.

Since in the preliminary investigation of solvent effects, phenol was found to be very reactive with excited nitrate esters (upon irradiation the sample turned brown within minutes) it was not surprising that the steady state concentration of phenol could not be detected. On the other hand it was also possible that the phenol remained tied up to the decomposing nitrate ester molecule in a complex until it was substituted by the NO_2 group in its ortho-position.

In the generation of dinitrophenols from o-nitrophenol by the consumption of a second mole of nitrate ester, the preferential substitution for the entering NO_2 group was likely to be on carbon 4, however, substitution on position 6 also occurred but seemed to be somewhat less extensive as judged from the chromatograms. Other activated benzene rings in unreacted meso-hydrobenzoin dinitrate may also have acted as NO_2 acceptors as was discussed above.

By comparison with previous work on the photonitration of diphenylamine (105) it seemed that ring photonitration occurred when the aromatic system was activated by appropriate substituents, but with only non-activated benzene rings present oxidation seemed to be the preferred reaction.

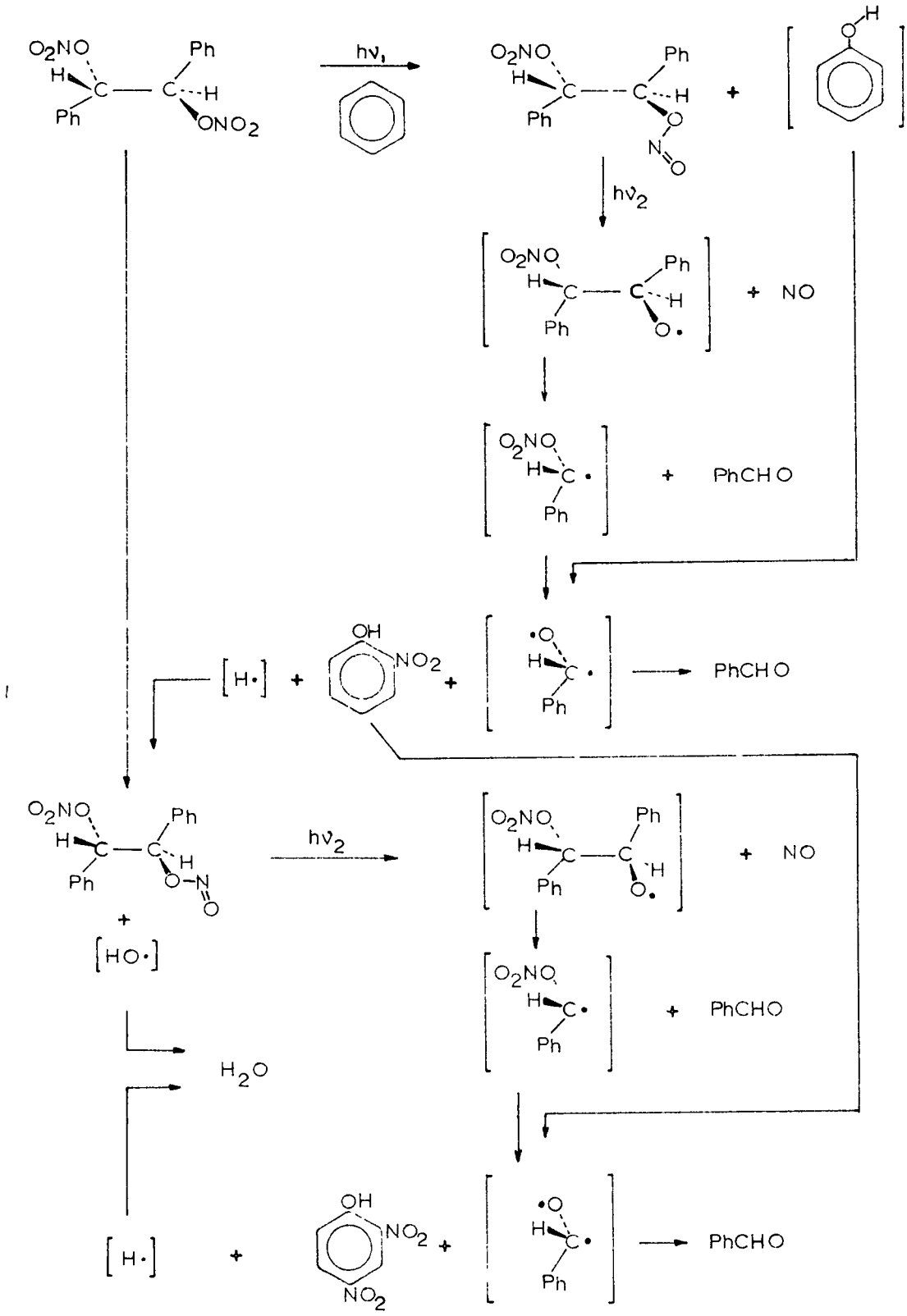

FIGURE 27 Possible Mechanism of Photolysis of meso-Hydrobenzoin Dinitrate

The fact that in the Kemula-Grabowska reaction (67) (113) the photonitration of benzene by means of NO also produced o-nitrophenol and 2,4-dinitrophenol provided a clue for the elucidation of the mechanism of the present reaction which will be discussed in a later section.

C. Kinetic Study of the Photolysis.

Five aromatic nitrate esters were subjected to kinetic measurements. Three of the five (benzyl nitrate, meso- and dl-hydrobenzoin dinitrates) contained benzene rings while the remaining two (cis- and trans-1,2-acenaphthenediol dinitrate) had naphthalene nuclei in their molecules.

A Corex filter was used in all kinetic experiments in order to eliminate the short wavelength lines of the mercury arc. In these conditions only the tail of the nitrate ester spectrum was involved providing $n \rightarrow \pi^*$ excitation of the NO_2 group and only negligible numbers of quanta were supplied to the $\pi \rightarrow \pi^*$ bands of both nitrate ester and benzene nuclei. This practically selective excitation gave a reasonably clear picture of the photodecomposition of these nitrate esters bearing benzene rings in their molecules.

In the case of the dinitrates of cis- and trans-1,2-acenaphthenediol this selective excitation was not possible because the naphthalene portion of the molecule has an extinction coefficient about 100 times larger than that of the two nitroxy substituents at the same wavelengths and it over powered the weak ($\varepsilon \approx 25$/nitroxy group) $n \rightarrow \pi^*$ absorption. On this basis it was expected that acenaphthene derivatives would photolyse considerably more slowly than the benzene derivatives.

The rate measurements were based on the rate of disappearance of nitrate esters. Since not all of the nitrate ester molecules which reached the excited state decomposed (because a certain fraction of them became deactivated) the rate of decomposition should be slower than the rate of

light absorption.

It is generally accepted that triplet states are involved in photochemical processes, and that triplet excited states always have longer lifetimes than singlet excited states because of their ~~lower energies~~ multiplicity. Figure 28 illustrates these principles of primary photoreactions (178) applied to the nitrate esters (NE). Whether the radiative deactivation processes (fluorescence and phosphorescence) labelled k_{-11} and k_{-13}, would be actually observable experimentally in the case of nitrate esters was not known but it seemed reasonable to assume that they also occurred here as they do in many other reactions.

Reaction k_1 was responsible for excitation and assuming 100% efficiency, the same number of molecules became excited as the number of photons absorbed by the nitroxy group. The total energy absorbed was then dissipated by three routes, two of which (K_{-11} and k_{-13}) were deactivations and thus represented loss of energy as far as photolysis was concerned, only the third route (k_2) led to the decomposition of nitrate ester molecules forming the reaction products. The quantum yield (121)related the decomposition (k_2) to the total excitation (k_1) assuming that one photon excited one molecule.

$$\phi = \frac{\Delta [NE] \text{decomposed}}{\Delta [NE] \text{excited}} \qquad (121)$$

If there was no chain reaction and only one photon was required for causing the photoreaction of one molecule, ϕ would have a value between 0 and 1. If the deactivation process was negligible with respect to decomposition then $\phi \longrightarrow 1$, if the rate of decomposition (k_2) was exceeded by the rate of the deactivation process, $\phi \longrightarrow 0$.

It was found that at initial concentrations of less than 0.1 mole of nitroxy group per liter the early part of the photoreaction followed a

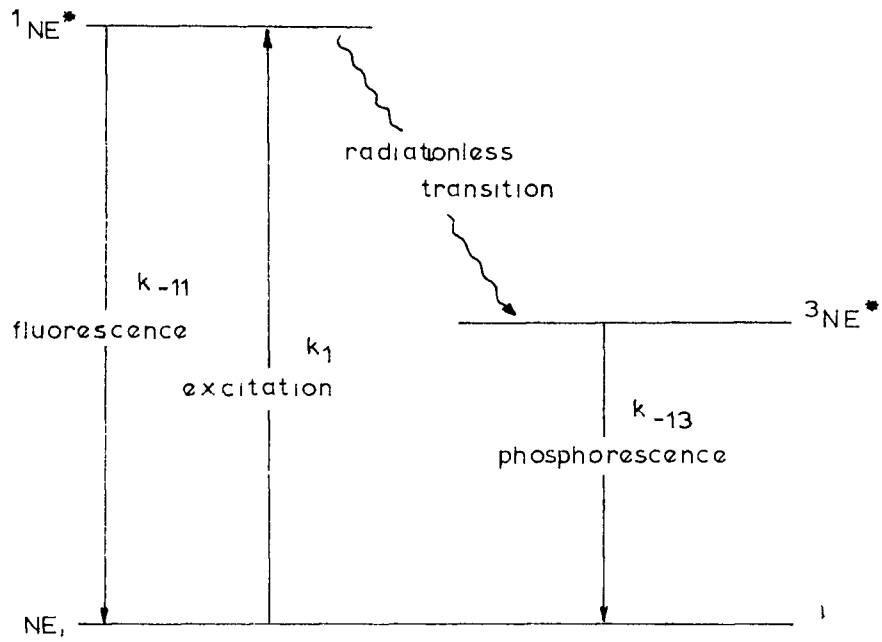

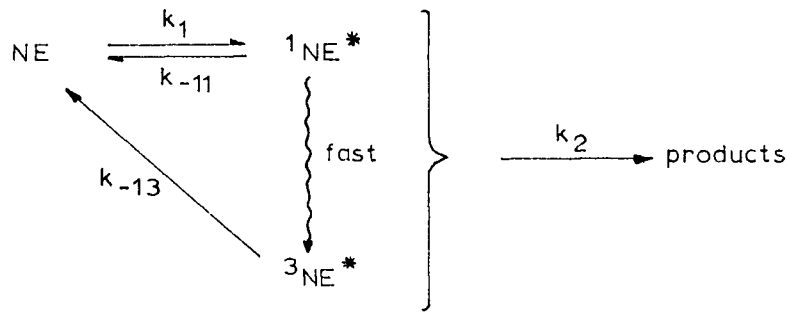

FIGURE 28 Primary Photochemical Reactions of Nitrate Esters (NE)

first-order rate law as shown in Figures 29 and 31. Since the products (nitrophenols, etc.) also absorbed in the effective wavelength region, on more extended irradiation even with low initial concentrations (0.02 M), the reaction slowed down as observed in the rate plot (log concentration versus time) by the departure from the straight line (Figure 29). This effect was particularly pronounced with the acenaphthene nitrates because the products containing the naphthalene nucleus absorbed strongly in the active region.

Equation 122 described the amount of light absorbed (I_A) with respect to the incident intensity (I_o) as a function of the optical density (O.D.).

$$I_A = I_o \ (1-e^{-O.D.}) \qquad (122)$$

If O.D. $\gg 1$ then the exponential term would be negligible and $I_A \rightarrow I_o$, if, however, O.D. $\ll 1$ then $I_A \rightarrow I_o \times$ O.D. since the exponential term would be approximated by the first two members of a Taylor series. This second condition was satisfied by the low initial concentration of the nitrate ester. On the other hand at the low concentration the Lambert-Beer law was also valid and O.D. could be replaced by $\varepsilon \ell [NE]$ to give equation 123.

$$I_A \simeq I_o \varepsilon \ell [NE] \qquad (123)$$

Since the total O.D. or total ε was the sum of the values for the several components of the system, equation 123 could be used to calculate the light absorption for a particular mode of excitation. Substituting for the $n \longrightarrow \pi^*$ band of the nitrate ester, the calculated I_A (einstein/sec) represented the number of excitations, which in turn was a measure of the number of $n \rightarrow \pi^*$ excited states (moles/sec) generated during the irradiation. Since the rate of decomposition was proportional to the number of quanta absorbed per unit time, I_A, according to 123, the rate of decomposition was also proportional to the concentration of the nitrate ester and this was the

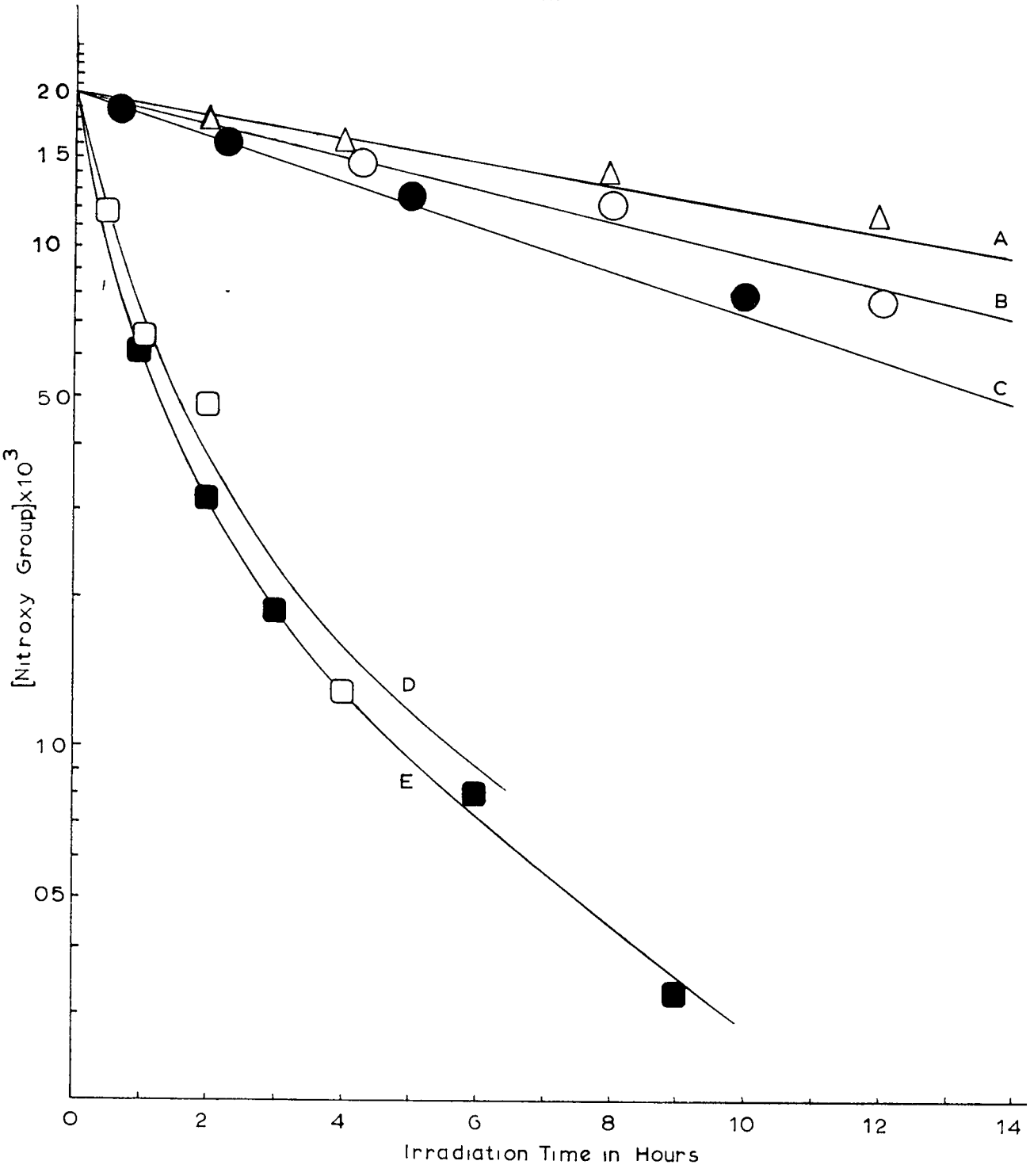

FIGURE 29 Rates of Photoreaction of (A) Benzyl Nitrate, (B) dl- and (C) meso-Hydrobenzoin Dinitrates, (D) trans- and (E) cis-1,2-Acenaphthenediol Dinitrates in Benzene Solution at 25°

origin of the observed first-order rate law.

In the photoreactor, the solution thickness was 0.665 cm., therefore I_A for one particular wavelength (λ) was given by 124.

$$I_A^{\lambda} = 0.665\ I_o^{\lambda}\ \varepsilon\ [NE] \qquad (124)$$

In this investigation not monochromatic light but a portion of the spectrum of the mercury arc (Figure 33) was employed and therefore the above equation was used for each of the active wavelengths and the values of I_A were summed up for estimating the total number of quanta/sec absorbed (125).

$$I_A^{Total} = 0.665 \times (\sum_{\lambda} I_o^{\lambda}\ \varepsilon^{\lambda}) \times [NE] \qquad (125)$$

The first-order rate constants were calculated from the rate plots (Figure 29) for benzyl nitrate (A) and meso-, and dl-hydrobenzoin dinitrates (B and C respectively). For cis- and trans-1,2-acenaphthenediol dinitrates, the constants were calculated by extrapolation to zero time. These data are summarized in Table XXII.

Table XXII

Apparent First-order Rate Constants for the Photolysis of Aromatic Nitrate Esters at 24.20°C.

	Compound	In Benzene Solution[a]			In Ethanol Solution[a]			
		$t_{\frac{1}{2}}$(hrs)	$k \times 10^4$ (sec^{-1})	k/k_A[b]	$t_{\frac{1}{2}}$(hrs)	$k \times 10^4$ (sec^{-1})	k/k_A[b]	k_{EtOH}/k_{PhH}
A	Benzyl nitrate	13.0	0.148±0.032	1.0	6.21	0.310±0.053	1.0	2.1
B	dl-Hydrobenzoin dinitrate	9.53	0.202±0.023	1.4	....	.....	...	...
C[c]	meso-Hydrobenzoin dinitrate	6.88	0.280±0.059	1.9	3.11	0.619±0.061	2.0	2.2
D	trans-1,2-Acenaphthenediol dinitrate	0.54	3.6 ±0.4[d]	24	....	.....	...	...
E	cis-1,2-Acenaphthenediol dinitrate	0.46	4.2 ±0.2[d]	28	....	.....	...	...

a Initial concentration 0.02 mole nitroxy group per liter.

b For benzyl nitrate.

c In 0.02 M ether solution, $t_{\frac{1}{2}}$ = 0.79 hours, $k = 2.42 \pm 0.37 \times 10^{-4} sec^{-1}$.

d Extrapolated to zero time.

Instead of the expected slower decomposition of the acenaphthene nitrates because of competitive light absorption, the results showed that they photolysed 15-30 times faster than those containing phenyl groups and indicated that photosensitization took part in these reactions (Figure 29, D and E). A possible explanation was that the naphthalene portion of the molecule absorbed most of the incident light, but the excited aromatic moeity did not deactivate by the usual processes (fluorescence, phosphorescence, etc.) but rather released its excitation energy via energy transfer to the unexcited nitroxy groups. In other words the naphthalene portion of the acenaphthene molecule acted as a "built in" photosensitizer.

A somewhat similar energy transfer but in the opposite sense has been reported for a mixture of benzophenone and naphthalene. Benzophenone was selectively excited through the $n \rightarrow \pi^*$ transition and after the molecules had passed from the first excited singlet state to the first excited triplet state, energy was transferred to the unexcited naphthalene and brought it to the triplet state (triplet $\rightarrow$ triplet energy transfer) (Figure 30). The mechanism of this process has been confirmed by phosphorescence spectroscopy (179), flash photolysis (180) reaction kinetic measurements (181) and ESR spectroscopy (182).

In the present case energy may have been transferred intramolecularly from the naphthalene portion to the nitroxy group. Energetically (Figure 30) this process seemed to be a singlet $\rightarrow$ singlet transition similar to those observed in other intermolecular (183) (naphthalene $\rightarrow$ alkyliodide) and intramolecular (184) (naphthalene $\rightarrow$ anthracene XLIII, XLIV and XLV) processes.

The rates of photolysis of benzyl nitrate (k_A) and of meso-hydrobenzoin (k_C) dinitrate were also determined in ethanol solutions (Figure 31 and Table XXII). The fact that the ratio k_C/k_A was about 2 in both benzene and ethanol solutions indicated that the same type of reaction

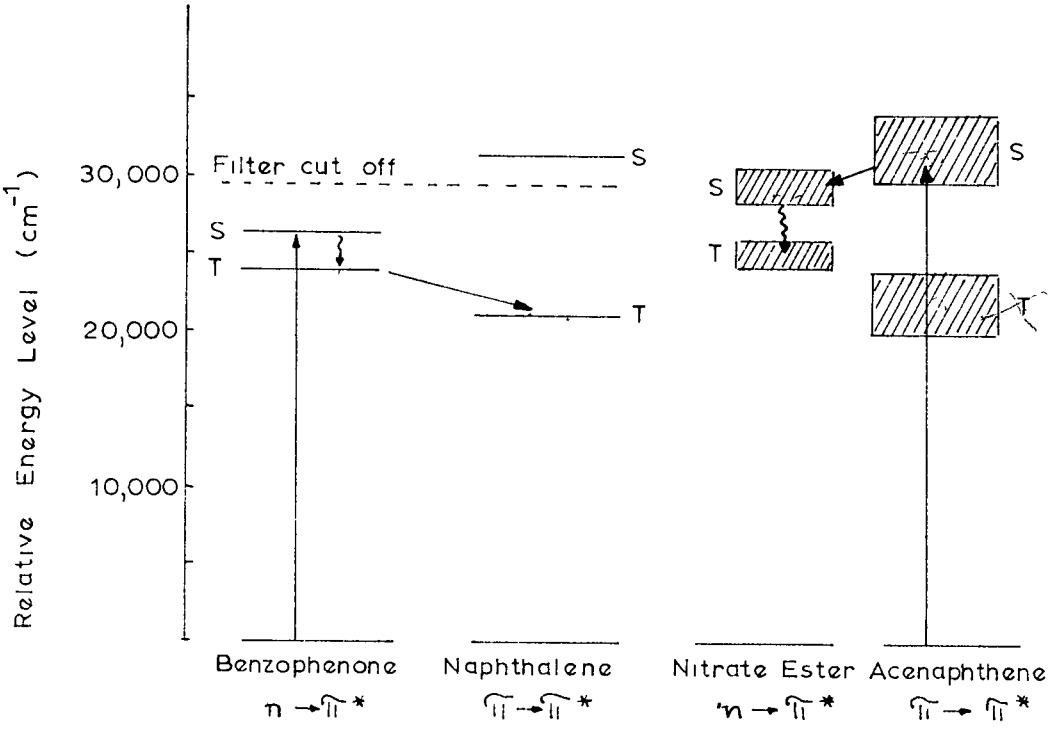

FIGURE 30 Triplet–Triplet Energy Transfer Between Benzophenone and Naphthalene (180) and Singlet–Singlet Energy Transfer within 1,2 Acenaphthenediol Dinitrates

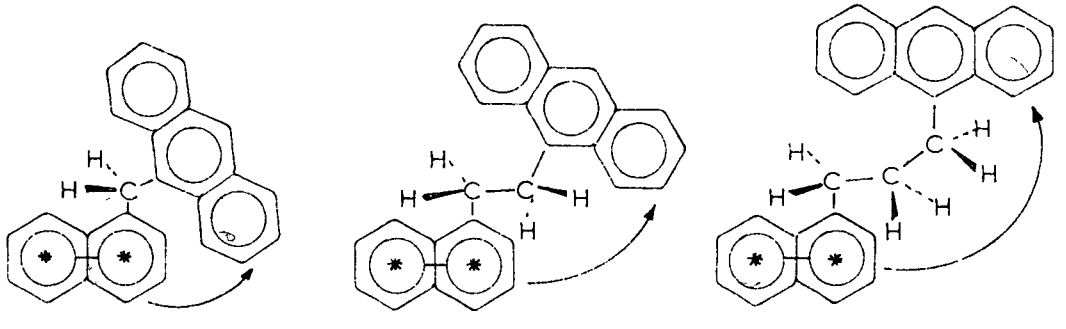

XLIII XLIV XLV

occurred with the two nitrate esters even in different solvents. On the other hand the observation that the rates of decomposition of the same nitrate ester, meso-hydrobenzoin dinitrate, was different in three different solvents: $k_{Et_2O} : k_{EtOH} : k_{PhH} = 8.6 : 2.2 : 1$ (Figures 29 and 31 and Table XXII) ~~and~~ indicated that the solvent in which the photodecomposition took place participated in the reaction. This agreed with the evidence of solvent participation gained from the preliminary experiments and product analyses.

Weller (185) summarized the characteristics of fast reactions of excited molecules into four classes:

(a) Quenching of fluorescence (probably electron transfer)

$$A^* + B \rightarrow \left[A^{(\mp)} \cdot B^{(\pm)}\right] \rightarrow A + B \qquad (126)$$

(b) Complex formation

$$A^* + A \rightarrow A^*A \qquad (127)$$

Or $$A^* + B \rightarrow A^*B \qquad (128)$$

(c) Acid-base reaction

$$A^*H + B \rightarrow A^{*\mp} + HB^+ \qquad (129)$$

$$A^* + HB \rightarrow A^{*\pm}H \quad B^- \qquad (130)$$

(d) Isomerization

$$A^* \rightarrow A^{\dagger} \qquad (131)$$

Furthermore, it was shown that the probable occurrence of any of these reactions in the excited state could be estimated on the basis of the UV spectra if the reaction occurred, even to a minor extent, in the ground state. A recent report (186) showed that the acidities of weak acids were enhanced in their excited states with respect to their ground states. For example, phenol became some 20,000 times more acidic upon UV-irradiation (i.e. $pK_a = 10.02$, $pK_a^* = 5.7$) according to reactions 129 and 132.

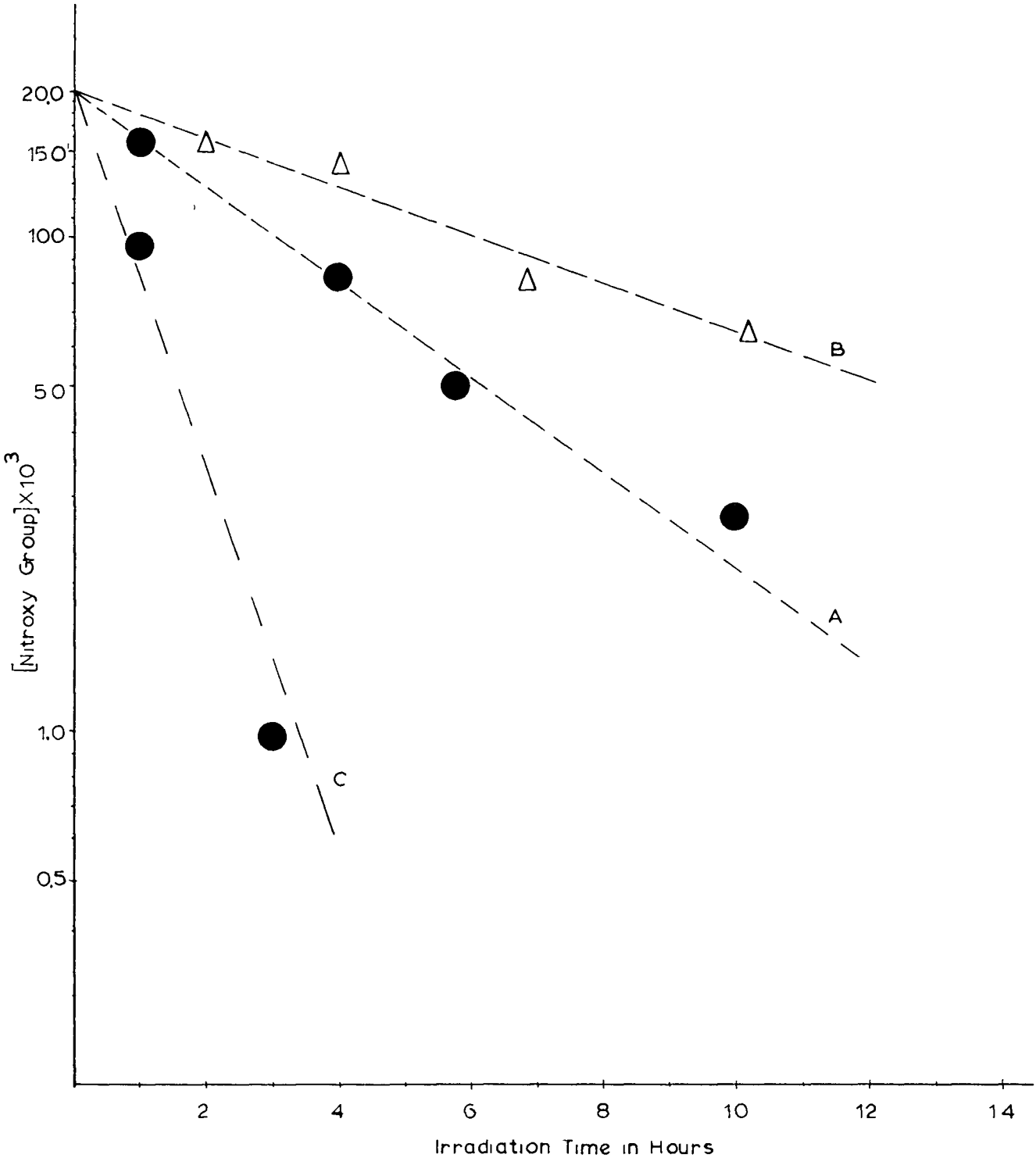

FIGURE 31 Rates of Photoreactions of meso-Hydrobenzoin Dinitrate (A) and Benzyl Nitrate (B) in Ethanol and of meso-Hydrobenzoin Dinitrate in Ether (C) at 24.2°C

$$\overset{*}{PhOH} + H_2O \rightarrow \overset{*}{PhO}^- + H_3O^+ \qquad (132)$$

If one considered compounds A and B reacting with each other in the ground state according to equation 133 and

$$A \ (+B) \underset{}{\overset{K^o}{\rightleftharpoons}} A' \ (+B') \qquad (133)$$

excited A (i.e. A^*) also reacting with B (134); K^o and K^* would represent the corresponding equilibrium constants.

$$A^* \ (+B) \overset{K^*}{\rightleftharpoons} A^{*\prime} \ (+B') \qquad (134)$$

According to Weller (185) equation 135 would give the ratio of the two equilibrium constants.

$$\ln \frac{K^*}{K^o} = \frac{\Delta E - \Delta E'}{RT} = \frac{hc}{kT} \Delta\tilde{\nu} \qquad (135)$$

where "$\Delta\tilde{\nu}$ is the frequency interval between the long wavelength absorption bands of A and A'. Equation [135] holds with the assumption of equal reaction entropies in the fluorescent and ground states" (i.e. $\Delta H - \Delta H^* = \Delta E - \Delta E'$).

In the present case Weller's reaction (b) (128) could be considered as the formation of a charge-transfer complex and applied to the previously discussed (Figure 15) charge-transfer interaction between nitrate ester and solvent according to equation 136, and the energy level diagram in Figure 32. The K^*/K^o ratios were calculated from $n \rightarrow \pi^*$ band (2700 Å) and the charge transfer bands (2900-3000Å) for benzyl nitrate (Figure 16 Table XIX) according to equation 135 and provided a sequence of values

$$\begin{array}{ccc} NE + Solvent & \overset{K^o}{\rightleftharpoons} & NE^- \ \ldots\ldots\ {}^+Solvent \\ \downarrow h\nu_{n\rightarrow\pi^*} & & \downarrow h\nu_{c.T.} \\ NE^* + Solvent & \overset{K^*}{\rightleftharpoons} & \overset{*}{NE}^- \ \ldots\ldots\ {}^+Solvent \end{array} \qquad (136)$$

(Table XXIII) which was consistent with the order of the ionization potentials of the solvents. The order of the individual calculated values

(137) did not agree with the order of experimental rate constants (139), however, the ratio K^*/K^o

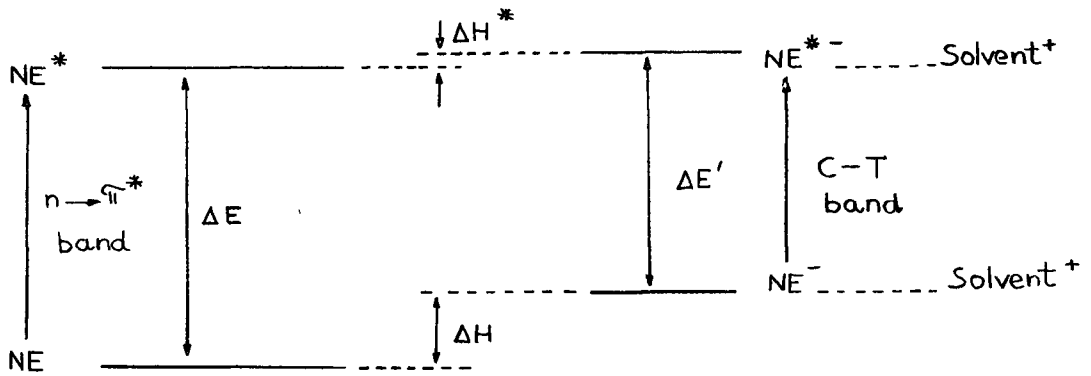

Figure 32. Energy Level Diagram for Nitrate Ester -Solvent Complex Excitation.

(Table XXIII) definitely showed that charge-transfer interaction between excited nitrate ester and solvent was much more pronounced than the same interaction in the ground state.

Table XXIII

Calculated Ratios of Charge-Transfer Equilibrium Constants for Benzyl Nitrate in Solution

Solvent	I_P^a (ev)	$\tilde{\nu}_{n\to\pi^*}$ (cm^{-1})	$\tilde{\nu}_{C.T.}$ (cm^{-1})	$\Delta\tilde{\nu}$ (cm^{-1})	$\frac{hc}{kT}\Delta\tilde{\nu}$	$\frac{hc\,\Delta\tilde{\nu}}{2.303kT}$	K^*/K^o
benzene	9.245		33,223	3,814	18.44	8.007	1.0×10^8
ether	9.53	37,037	33,898	3,139	15.18	6.590	3.9×10^6
ethanol	10.50		34,247	2,790	13.50	5.857	7.2×10^5

a From reference (142)

b $\frac{hc}{kT} = 4.8350 \times 10^{-3}$ at 24.2°C

The known relative hydrogen-donating activity of the solvents (138) was also inconsistent with the order of the experimental rate constants (139).

Electron transfer (K^*)	PhH >	t_2O >	EtOH (137)
Hydrogen transfer (k_2)	PhH <	Et_2O <	EtOH (138)
$k_{experimental}$	PhH <	Et_2O >	EtOH (139)

This apparent anomaly disappeared if one accepted the suggestion of Porter (187) that in solution both electron transfer and hydrogen transfer may occur together. The experimental rate constants would then incorporate both the charge transfer (K^*) and the hydrogen transfer (k_2) process constants according to equation 140 where S-H represents the photolysis solvent

$$\left.\begin{array}{l} NE + h\nu \longrightarrow NE^*(\text{singlet}) \\ \qquad\qquad\quad \downarrow \\ \qquad\qquad NE^*(\text{triplet}) \end{array}\right\} + S\text{-}H \overset{K^*}{\rightleftharpoons} NE^{*-} \ldots\ldots \overset{+}{S}\text{-}H \xrightarrow{k_2} \dot{N}E\text{-}H + \dot{S} \qquad (140)$$

$$\qquad\qquad\qquad\qquad\qquad\qquad\qquad\qquad\qquad\qquad \downarrow$$

$$\qquad\qquad\qquad\qquad\qquad\qquad\qquad\qquad\qquad\qquad \text{Products}$$

The selective $n \rightarrow \pi^*$ excitation of nitrate ester groups in benzyl nitrate, and meso- and dl-hydrobenzoin dinitrates (α-phenyl substituted nitrates) permitted an estimation of the quantum yield of the photoreaction. The calculation of the required I_A^{total} values was carried out according to equation 125 as illustrated in Figure 33. The values of I_A^{total} for meso- and dl-hydrobenzoin dinitrates were essentially the same and for benzyl nitrate half of this figure was used since the change from di- to mono-substitution reduced ε by one half. Quantum yields (ϕ) were then calculated from equation 141 where $k_{\cdot} = \ell \times \sum_{\lambda} I_o \varepsilon$.

$$\phi = \frac{\text{Rate of decomposition}}{\text{Rate of excitation}} = \frac{k_{exp}[NE]}{I_A^{total}} = \frac{k_{exp}[NE]}{k_1[NE]} \qquad (141)$$

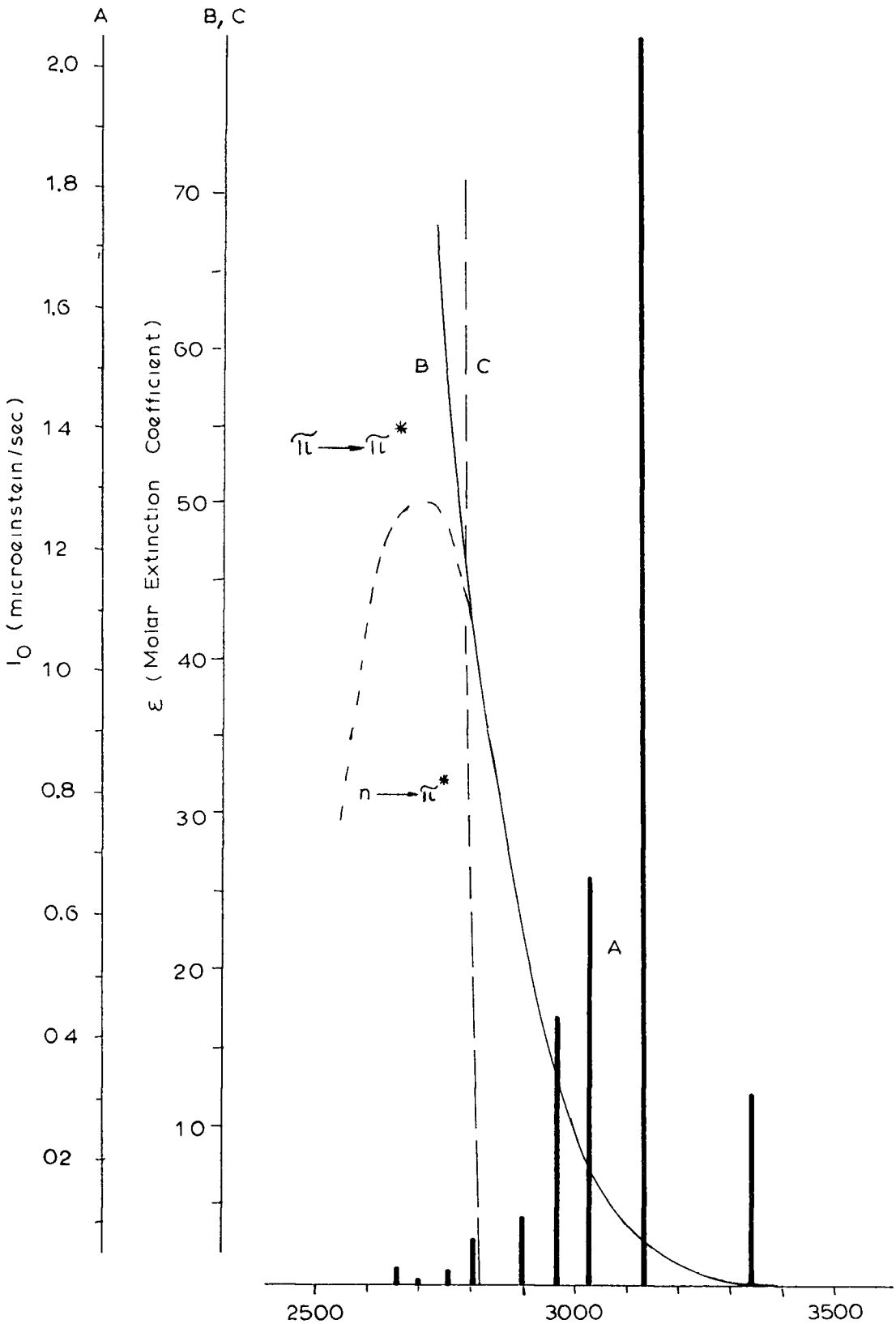

FIGURE 33. Light Energy Emitted by Source (A) and Absorbed by meso Hydrobenzoin Dinitrate (B) and Solvent Benzene (C) in the Photoreaction at 24.2°C.

The numerical values for k_1 in both benzene and non-absorbing solvents (alcohol and ether) are tabulated in Table XXIV.

Table XXIV

Calculated Values of k_1 for α -Phenyl Substituted Nitrate Esters in Benzene and in Ethanol and Ether Solutions*

λ (Å)	ε ($mole^{-1}cm^{-1}$)	$I_0 x 10^6$ (einstein $\cdot sec^{-1}$)	$I_0 x \varepsilon x 10^6$ ($sec^{-1}cm^{-1}$)	$10^6 x \sum I_0 x \varepsilon$ in benzene	$10^6 x \sum I_0 x \varepsilon$ in alcohol and ether
3341	0.4	0.301	0.120		
3130	2.8	2.033	5.692		
3025	7.0	0.670	4.690		
2967	12.0	0.441	5.292		
2894	23.0	0.110	2.530		
2804	42.0	0.072	3.024	21.35	
2753	49.0	0.020	0.980		
2700	50.0	0.014	0.520		
2652	48.0	0.030	1.440		
2571	35.0	0.002	0.070		24.36
$10^6 x \ell x \sum I_0 x \varepsilon = k_1 x 10^6 (sec^{-1})$				14.20	16.20

* See equation 125 and Figures 28 and 33.

The calculated quantum yields are listed in Table XXV. They were reasonably consistent for the three nitrate esters in one solvent and thus there was little doubt that they all reacted by the same mechanism. Furthermore in benzene solution ϕ was approximately 2 indicating that two moles of

of nitrate esters were decomposed per mole quanta (einstein) and this was in agreement with the proposed mechanism (Figure 27) which was based on the results of product analyses. It has been shown (121) that the maximum quantum yield for the gas phase photolysis of NO_2 was also 2 and since the mechanism of NO_2 photodecomposition proceeded by N-O bond cleavage (69) this lent some support to the idea that the fifth mode of scission (Figure 4) was predominant in the solution photolysis of nitrate esters rather than the homolytic fourth mode (Figure 4) as in the case in thermolysis and gas phase photolysis.

Table XXV

Calculated Quantum Yields for the Photolysis of α-Phenyl Substituted Nitrate Esters in Three Different Solvents at 24.2°.

Solvent	$k_1 x10^4$ (sec^{-1})	$k_{exp} x10^4 (sec^{-1})$			ø		
		A	B	C	A	B	C
Benzene	0.1420	0.148	0.202	0.280	2.08	1.42	1.97
Ethanol	0.1620	0.310	-	0.619	3.83	-	3.82
Diethylether	0.1620	-	-	2.42	-	-	14.9

A: benzyl nitrate

B: dl-hydrobenzoin dinitrate

C: meso-hydrobenzoin dinitrate

The fact that the quantum yields obtained in ethanol and ether were considerably higher than those in benzene pointed to a chain mechanism in the former solvents, however, further work would be required to decide whether they were really free radical chain processes or whether the mechanism simply required a larger integral number of molecules of nitrate ester per quantum than in the case of benzene solutions.

D. ESR Study of Nitrate Ester Photolysis.

The photolysis of the nitrate esters was carried out in the cavity of an electron spin resonance (ESR) spectrometer in the hope that free radical intermediates might build up a sufficiently high steady state concentration to give a detectable signal. This was found to occur and signals obtained from the vicinal dinitrates irradiated in benzene solution at room temperature are shown in Figure 34.

The spectra of the four nitrate esters were very similar, however, the distinctly greater intensity of the spectrum of the 1,2-acenaphthenediol dinitrates compared to the hydrobenzoin dinitrates indicated a higher steady state concentration of radical intermediates in agreement with the kinetic data and the previously proposed energy transfer process. A more powerful lamp (G.E.-A-H6) was used for the irradiation of the dl-hydrobenzoin dinitrate (Figure 34, D), however, the intensity of ESR spectrum was only slightly increased over that of the meso-isomer (Figure 34, C) at the same microwave power (100 m W).

The stability of these free radical species was demonstrated in an experiment (Figure 35) where the irradiated trans-1,2-acenaphthenediol dinitrate was kept in the dark at room temperature. The spectrum obtained after ten days with the same microwave power (10 m Watts) (Figure 35) was extremely weak compared to the original signal, however, a more intense microwave power (330 mW) revealed that the species responsible for the spectrum had not decayed completely. This extraordinary long lifetime suggested that the free radical present was probably some sort of relatively stable complex with an odd electron.

Recently Calvin and coworkers (188) reported ESR spectra originating from interaction of chloranil (tetrachlorobenzoquinone) and N,N,N',N',-tetra-

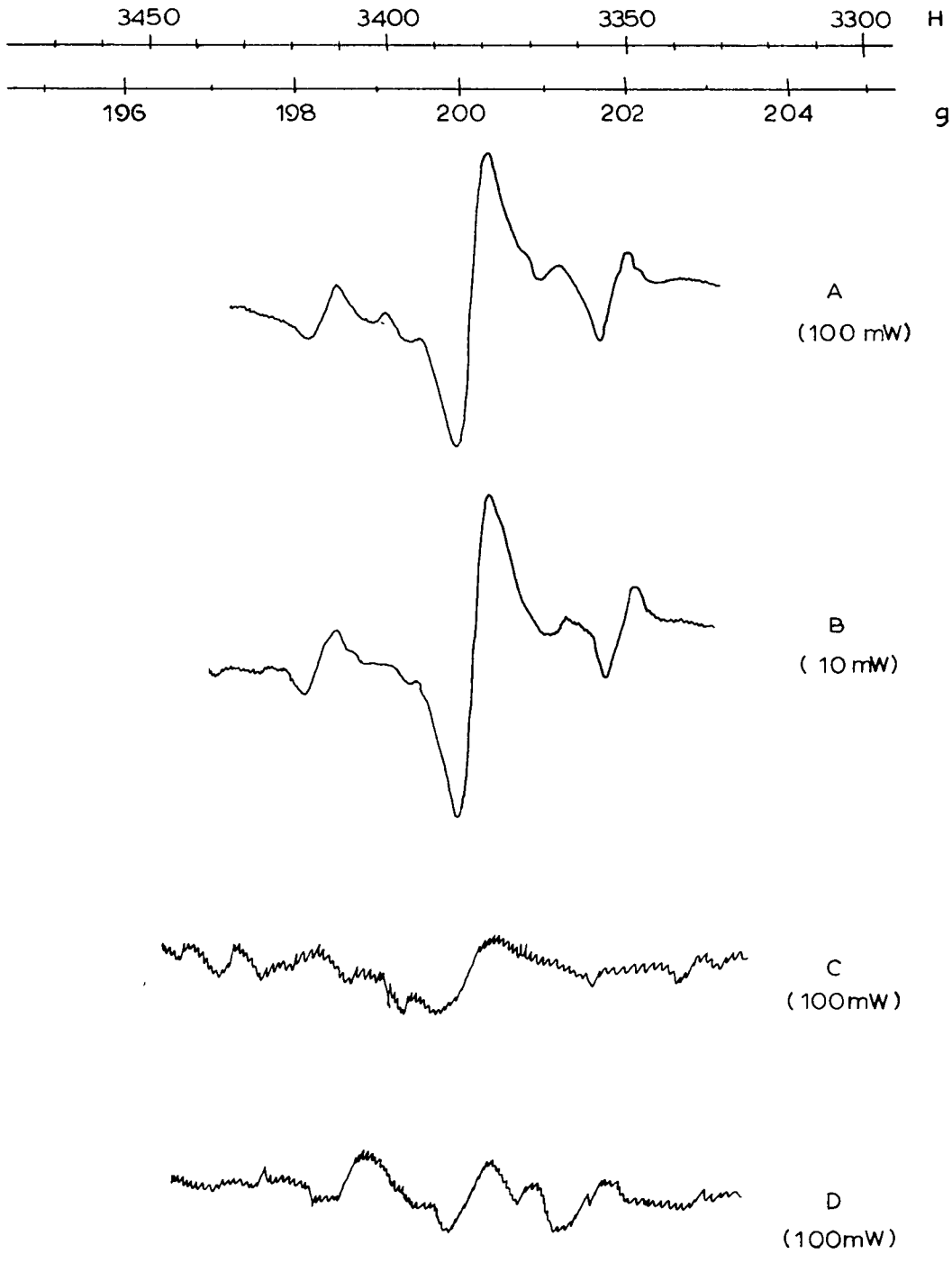

FIGURE 34 Steady State ESR Spectra of Irradiated cis-(A) and trans-(B) 1,2-Acenaphthenediol Dinitrates and meso-(C) and dl-(D) Hydrobenzoin Dinitrates in Benzene Solution at Room Temperature

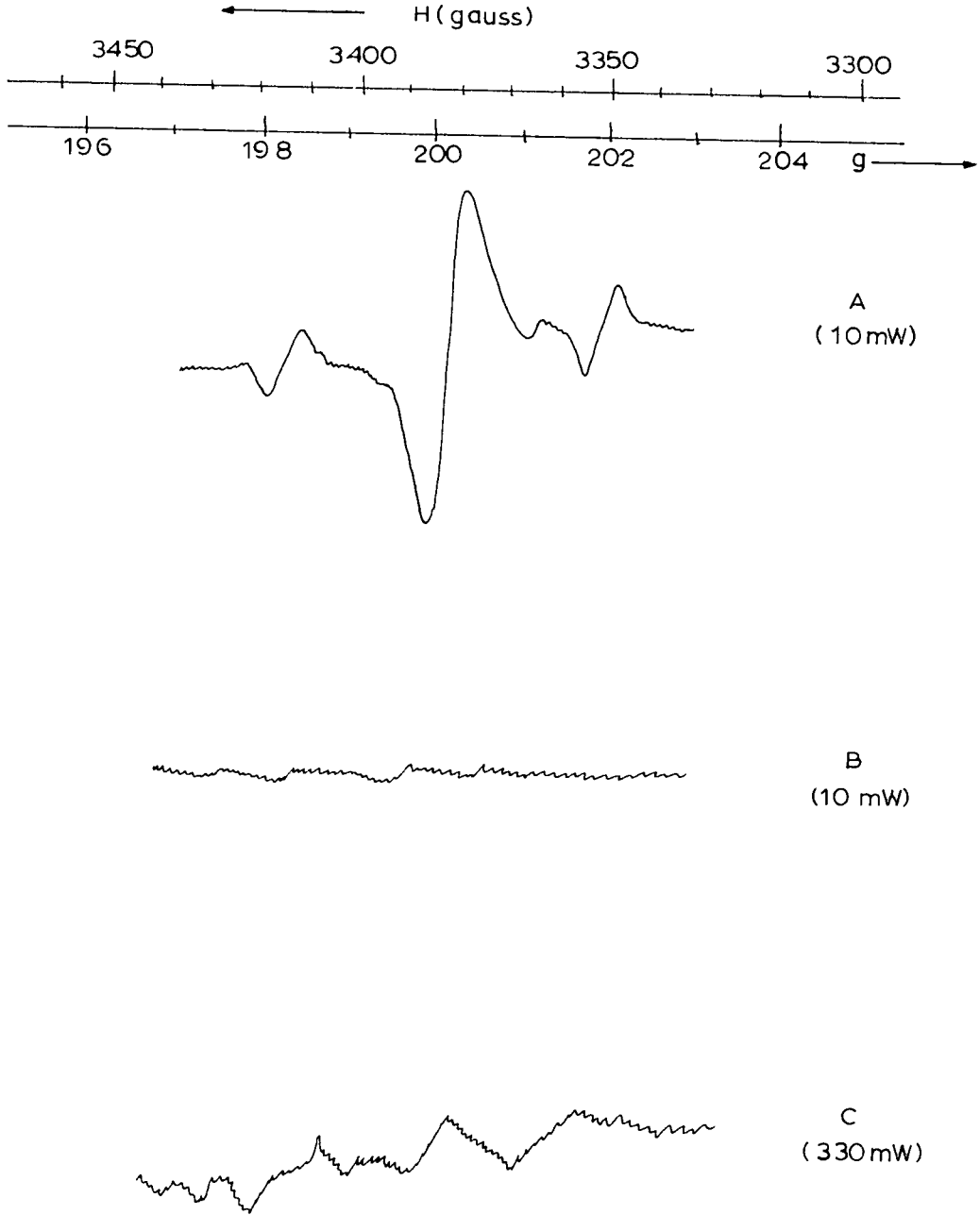

FIGURE 35 ESR Signals of Irradiated trans-1 2-Acenaphthene-diol Dinitrate Obtained Initially (A) and After Ten Days in the Dark (B and C)

methyl-p-phenylenediamine which involved charge-transfer complex and semiquinone radical. The reaction occurred in several stages but "the free radicals disappeared completely in the course of one week" (188).

No ESR signal was detected in irradiated alcohol solutions of the nitrates. This result could be rationalized in at least three different ways:

(i) The spectrum obtained in benzene solution was not due to the transforming nitrate ester but rather to the nitrophenol formation and thus it did not occur in ethanol solution. The experimental observation that signals appeared instantaneously in the benzene solution would not favour this explanation.

(ii) The spectra obtained were due to the transforming nitrate ester but the mechanisms were different in the two solvents. Although the photo-products which originated from the vicinal dinitrates were the same from benzene and alcohol solutions it was still possible, but not very likely, that there was a difference in the free radical intermediates.

(iii) The spectra were due to the transforming nitrate ester but the concentration of the species with unpaired spins was too low for detection. This third possibility agreed with the previously proposed charge-transfer complex formation (e.g. from kinetics) since K^* for alcohol was small, therefore, the complex concentration was low and a continuous fast removal of the complex from the system (large k_2) would decrease the steady state concentration further. The situation was directly opposite to this in benzene solutions and the proposed mechanism would therefore also explain the difference in ESR behaviour.

The splitting in the spectrum of NO_2 was about 50 gauss while the splitting of the three main lines in these spectra (Figure 34 and 35) was

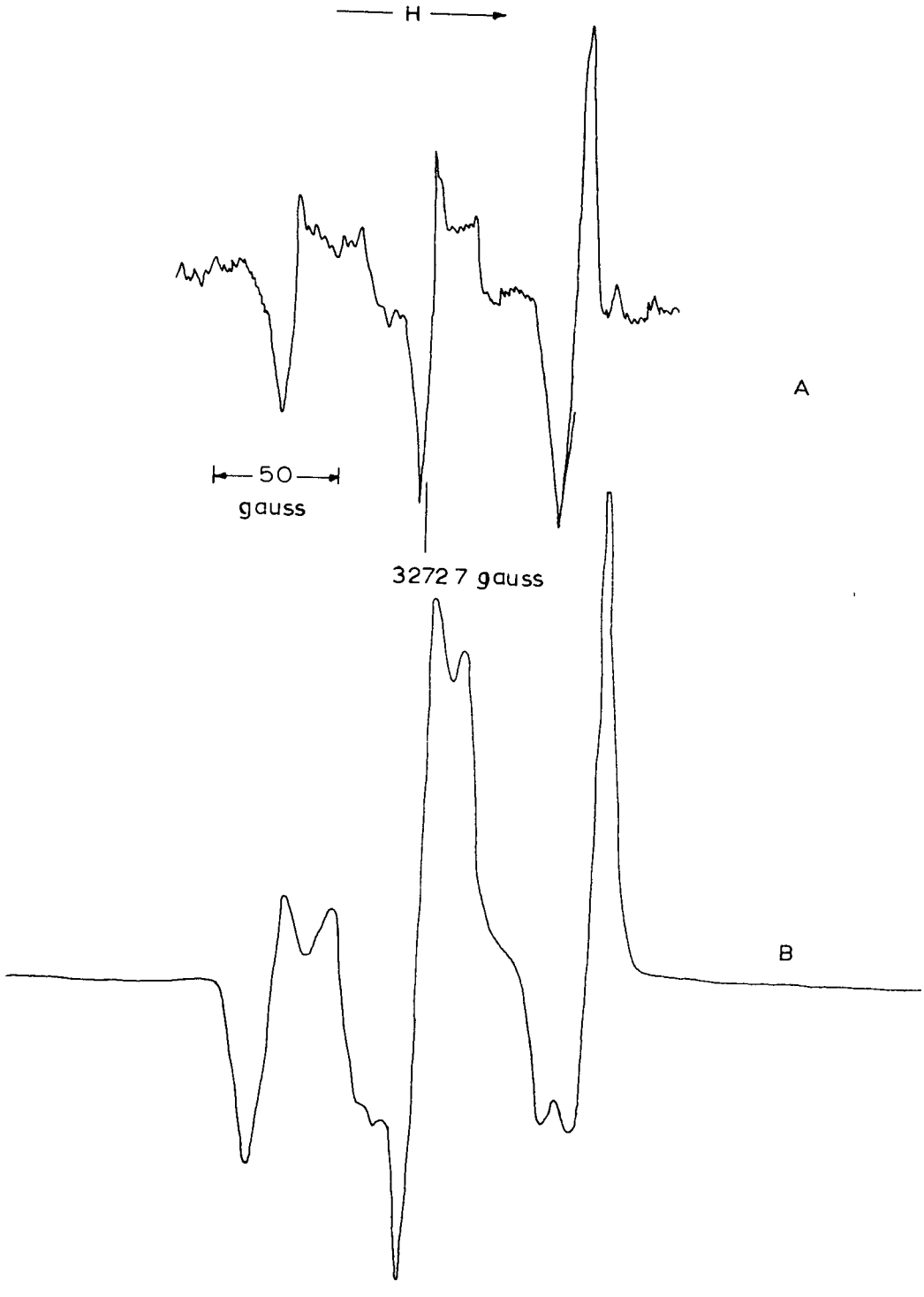

FIGURE 36 ESR Spectrum of NO_2 (A) in Solid Argon (214) and (B) Generated from trans-1,2-Acenaphthenediol Dinitrate in EPA at 77°K.

about 30 gauss and therefore the solutions did not contain appreciable amounts of NO_2. If the mechanism of the photodecomposition really involved $RO-NO_2$ scission as found in gas phase photolyses and the liberated NO_2 was responsible for the reaction with the solvent then, at the steady state concentration, NO_2 should have been detectable. Since the spectrum of NO_2 did not appear at room temperature the ESR results established the previously suggested fifth mode of scission (Figure 4) as the primary cleavage in solution photolysis of nitrate esters.

Irradiation of nitrate ester in EPA (ether-i-pentane-alcohol 8:3:5 vol/vol) glass at $77^{o}K$, however, did give rise to NO_2 as shown in Figure 36. This phenomenon could be rationalized as follows: The time required for "reactive interaction" with surrounding solvent molecules at $77^{o}K$ might be longer than the lifetime of the excited state. Thus the excited state, not making contact with reactive molecules within its' lifetime, as in gas phase, underwent decomposition at the weakest point, i.e. the $RO-NO_2$ bond.

In a control experiment NO gas was irradiated in benzene solution at the same initial nitrogen concentration (0.2 M) as used for the nitrate esters. The close similarity of the spectrum obtained to that obtained with the aromatic nitrate esters (Figure 37) pointed to a similar intermediate in the two cases. The products from these reactions were also similar as mentioned in a previous section.

In all ESR spectra obtained from photolysis of nitrate esters three lines were distinguished as major components. These were attributed to the splitting of the electron resonance by a nitrogen atom (for ^{14}N, I=1) which meant that the unpaired spin was located on a nitrogen atom.

X-Irradiation of single crystals of potassium nitrate (mounted

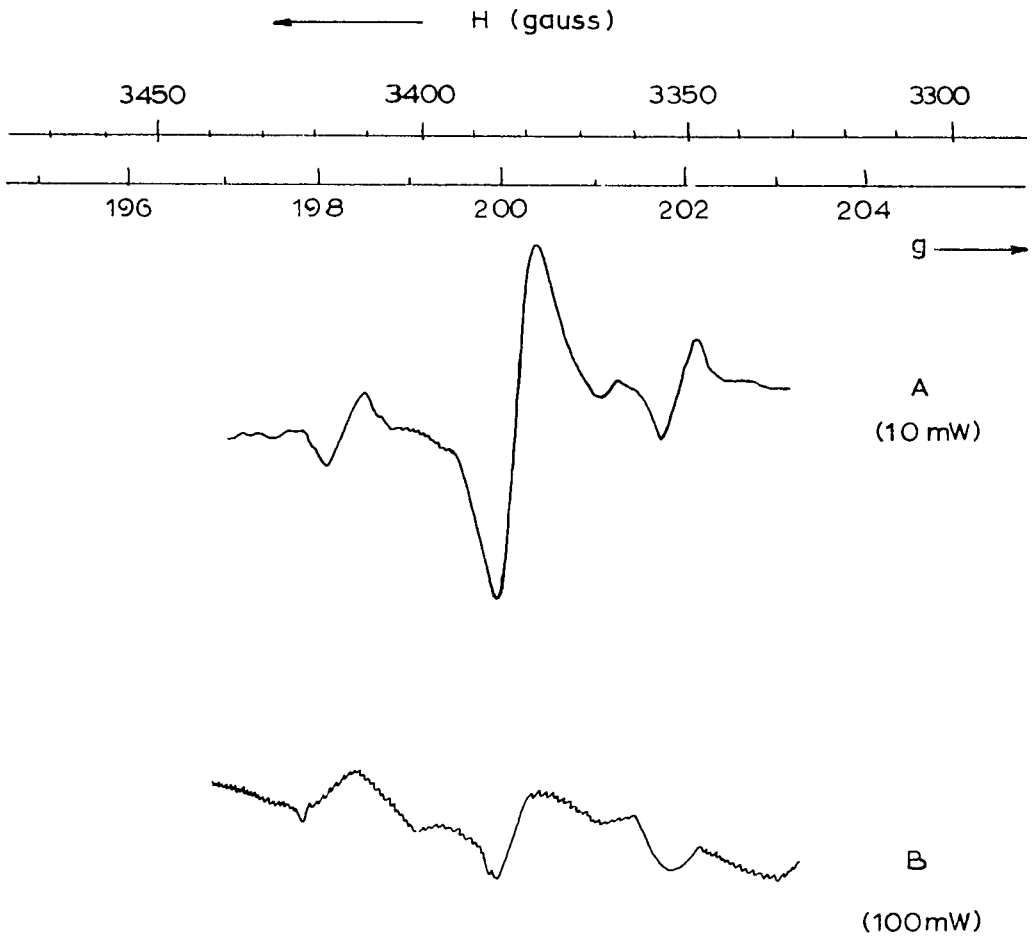

FIGURE 37 ESR Spectra of Irradiated trans-1,2-Acenaphthenediol Dinitrate (0.1 M)(A) and NO (0.2 M)(B) in Benzene Solution.

parallel or perpendicular to the major crystal axis) was reported to generate nitrate ion negative ion, $(NO_2^-)^-$ which had splittings of 62 gauss and 32 gauss measured in the parallel and perpendicular orientations respectively (189). The measured splitting between the three main lines of the spectra of nitrate esters irradiated in benzene solution (33.2 ± 1.6 gauss) was quite close to one of these values. The question was therefore raised as to whether a nitrate ester negative ion generated from a charge-transfer interaction between excited nitrate ester and benzene solvent might not be responsible for the spectrum. It was noticed from the fine structure of the spectra that the middle line was more intense than the two outside lines, indicating that the spectrum was really a resultant spectrum of more than one free radical. Since alkoxyl radicals, uncoupled by neighbouring protons, usually exhibit single peaks, a portion of the central line was tentatively assigned to an intermediate aromatic alkoxyl radical. Furthermore, additional fine structure was observed as shoulders on the central line which were clearly distinguishable at the early stage of irradiation and practically disappeared later.

In order to check the actual position of these lines a kinetic experiment was carried out in which spectra were taken at fixed time intervals rather than at steady state concentration. Figure 38 shows a typical spectrum of these series taken from photolysed trans-1,2-acenaphthenediol dinitrate after one hour. At this early stage of irradiation the satellite peaks close to the centre line became clearly observable and they were attributed to the outside pair of a second set of three lines, the middle one being hidden at the centre. The spectrum showed some asymmetry indicating that the centres of the two ~~three line~~ sets of three lines were not exactly coincident which in turn proved that the origins of two sets were two different free radical species. The measured g values for the centres of the

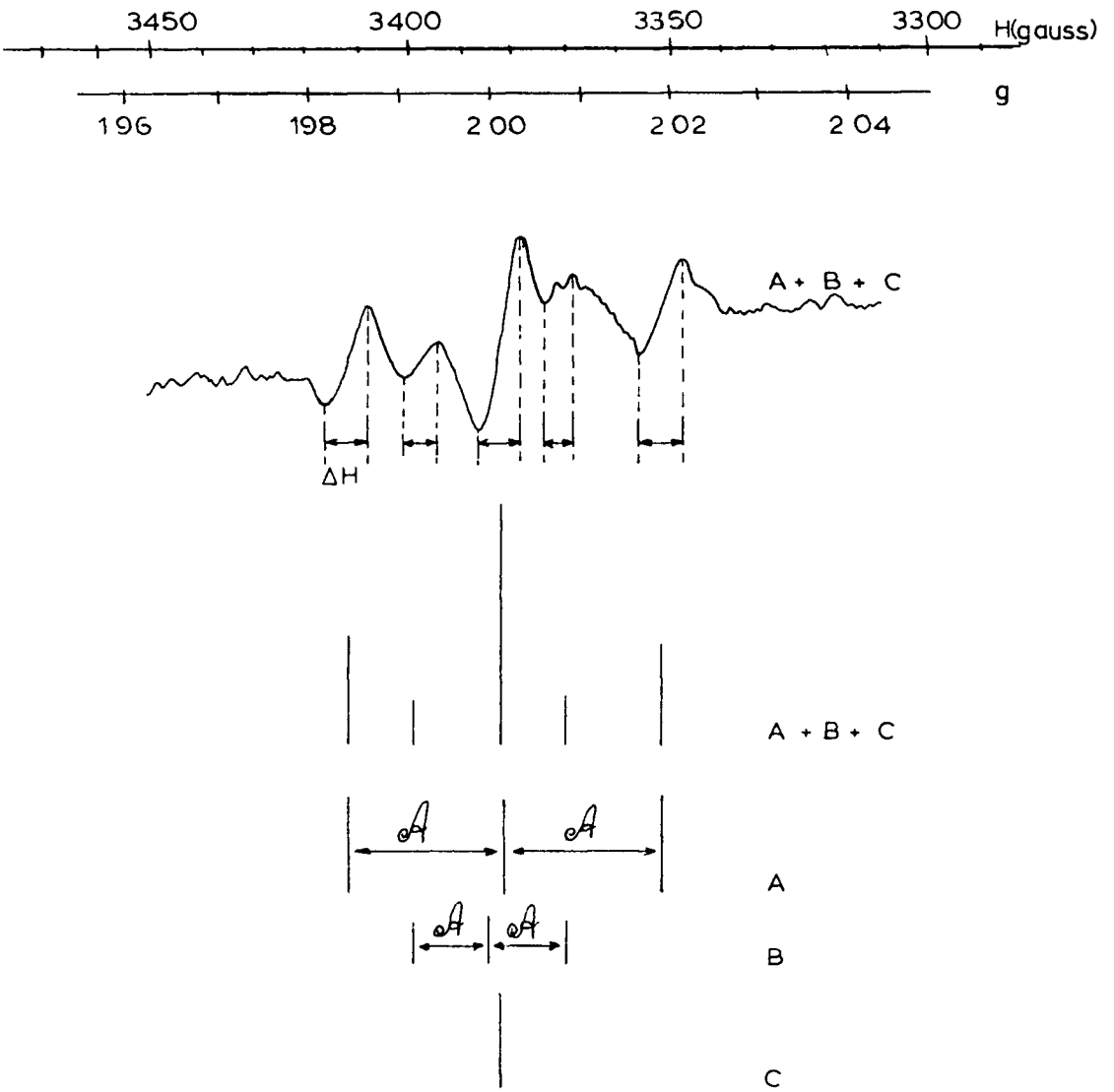

FIGURE 38 ESR Spectrum and Components of Irradiated trans-1,2-Acenaphthenediol Dinitrate

TABLE XXVI Observed Components of ESR Spectra of Irradiated Nitrate Esters

Component	Multiplicity	g value	Splitting ($\mathcal{A}$) Mc/s	Splitting ($\mathcal{A}$) gauss	Line Width (ΔH) gauss
A	triplet	2 00121	82.44	29.41	7.95
B	triplet	2 00302	36.33	12.96	5.16
C	singlet	2.00162	—	—	8 36

two sets of triplets as well as the coupling constants (ΔH in gauss) are listed in Table XXVI.

A rate plot (Figure 39) showed the generation of these components with time of irradiation and indicated that the course of the reaction was shown in equation 142.

$$A \longrightarrow B \longrightarrow C \qquad (142)$$

Species C could not be the phenoxyl radical of the forming nitrophenol since the phenoxyl radical showed a more complex spectrum (190). If, however, C represented some other intermediate alkoxyl radical, then B and A represented some form of the transforming nitrate ester. Protonated nitrate ester radical, $RO\dot{N}O_2H$, which was previously suggested as the final intermediate (140) before the nitroxy group decomposed, might have corresponded to B. However, the similarity between the spectrum of photolyzed benzene-NO mixture and photolyzed nitrate ester in benzene solution would be better explained if the spectrum of component B was assigned to a negative ion where the unpaired spin was located mostly on nitrogen. This assignment might be settled if nitrate ester negative ion were generated by some alternative means, e.g. by electrolytic reduction, in the ESR spectrometer.

If the chemical assignments of C and B were accepted as discussed above then only the nature of A remained in question. Since A must have preceded B and C (Figure 39) it was tempting to suggest that A might have been due to the nitrate ester $n \rightarrow \pi^*$ triplet state in steady state concentration.

Weissman (190) pointed out that "with randomly oriented molecules in rigid or fluid solvents ..... the direct magnetic dipolar coupling between the unpaired electrons in the triplet state" was the reason for failure to observe ESR spectra. He arrived at the conclusion that triplet states might be detectable if the "molecules containing two unpaired

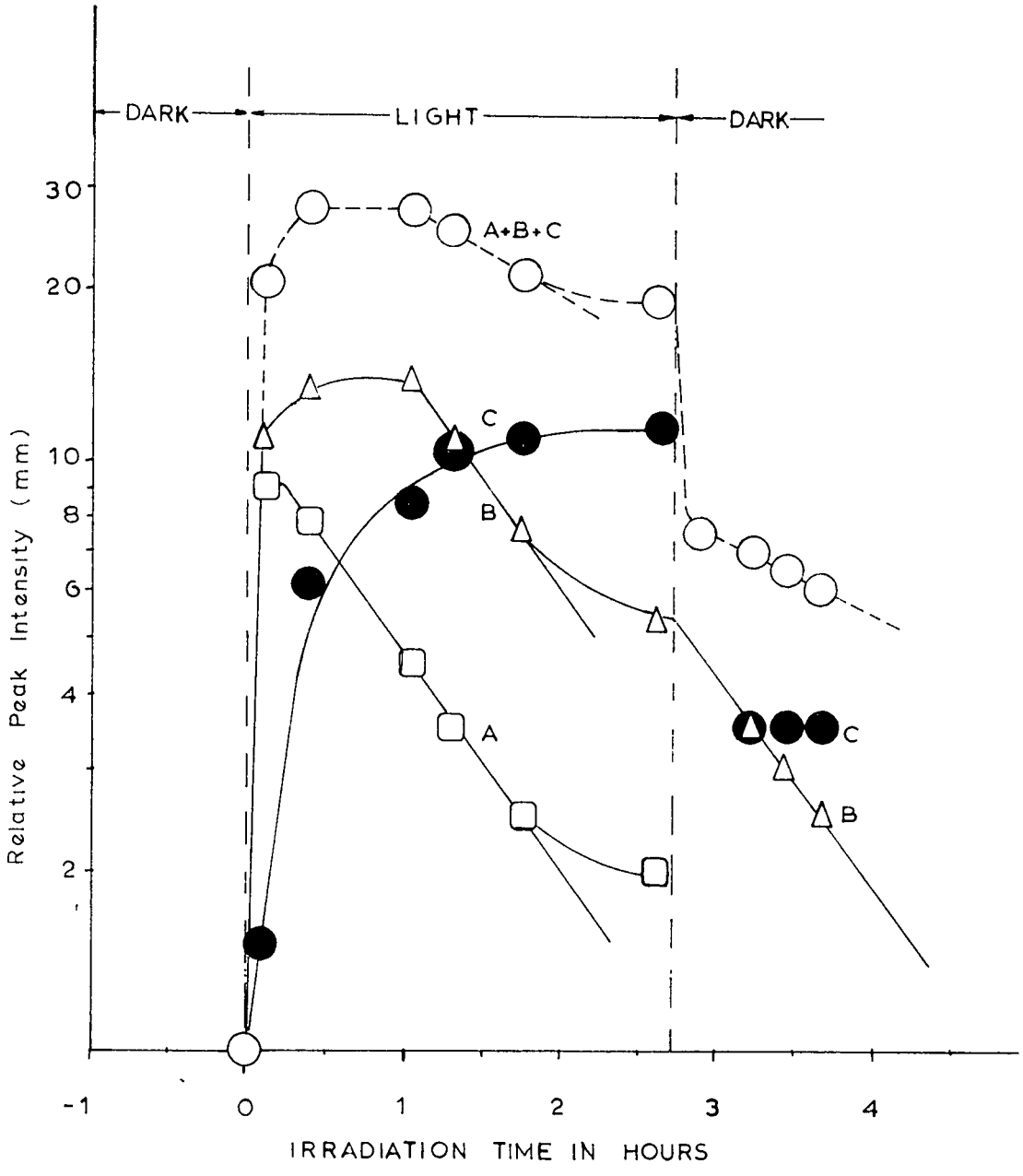

FIGURE 39 Rates of Generation of Components of ESR Spectrum of Irradiated Nitrate Ester

electrons are..... 'far apart' or if their distribution about each other is highly symmetrical" (191).

There were two speculative reasons why $n \rightarrow \pi^*$ triplet states of nitrate esters might have been more easily detectable than $\pi \rightarrow \pi^*$ triplet states. The latter have already been reported by Hutchison and Mangum (192) for oriented naphthalene molecules in durene and by Farmer, Gardner, and McDowell (182) for randomly oriented naphthalene molecules in EPA glass at $77^{o}K$.

(i) In a $\pi \rightarrow \pi^*$ triplet state one of the electrons would be located in the lowest antibonding π orbital (π^*), both of the orbitals, i.e. π and π^* would be perpendicular to the plane of the molecule. In an $n \rightarrow \pi^*$ triplet state one electron would be located in the nonbonding orbital (n) which was in the plane of the molecule while the other one would be in a molecular antibonding π -orbital perpendicular to the plane of the molecule and also to n (178).

These criteria would be valid, in general, for any $n \rightarrow \pi^*$ excited state including that of carbonyl as well as nitrate ester.

(ii) While in the $n \rightarrow \pi^*$ excited state of a carbonyl compound the two unpaired spins would be located within the neighbourhood of one carbon and one oxygen atom, in a nitroxy group they would be expected to spread over the three atom unit (NO_2) in such a way that while one electron would be in the antibonding π -orbital and might be located mostly on nitrogen, the other electron would be divided between the nonbonding p-orbitals of the two oxygen atoms (193) and this steric situation would decrease their direct interaction.

Although the ESR investigation positively proved the free radical mechanism of the nitrate ester photolysis, more work would be required to

finalize the proposed assignments.

ESR evidence was obtained for the intramolecular energy transfer process between the naphthalene moiety and nitroxy group in the acenaphthene nitrates. The $\pi \rightarrow \pi^*$ triplet state of the hydrocarbon acenaphthene was observed at 77°K in EPA glass at g ≃ 4 (Figure 40) and appeared much the same as the ESR triplet state spectrum of naphthalene (182) (194). No ESR signal of the triplet naphthalene was obtained, however, from the irradiated trans-1,2-acenaphthenediol dinitrate. The absence of the triplet state signal indicated that although the naphthalene portion became excited according to its UV-spectrum, the system did not reach its phosphorescent triplet state because of the energy transfer from the singlet excited state to the unexcited nitroxy group. With this result the energy transfer process as illustrated in Figure 30 was considered to be established.

E. Summary of Proposed Reaction Mechanism.

The proposed mechanism is summarized in Figure 41.

Irradiation of a nitrate ester in the range of the $n \rightarrow \pi^*$ band brings the nitroxy group to the first excited singlet state from which it is transferred by a radiationless process to the lowest excited triplet state. Both of these states may lose their excitational energy by physical deactivation processes or they may undergo chemical reaction. The chemical reaction that occurs may be a scission of the weakest bond ($RO-NO_2$) if no possibilities are available for combination with other molecules as in the gas phase or in a frozen glass. If, however, the excited nitrate ester comes into contact with other molecules before breaking up to fragments then other types of reaction may occur as in solution photolysis. Equation 140 (Figure 41) describes the suggested sequence of steps occurring during decomposition in solution.

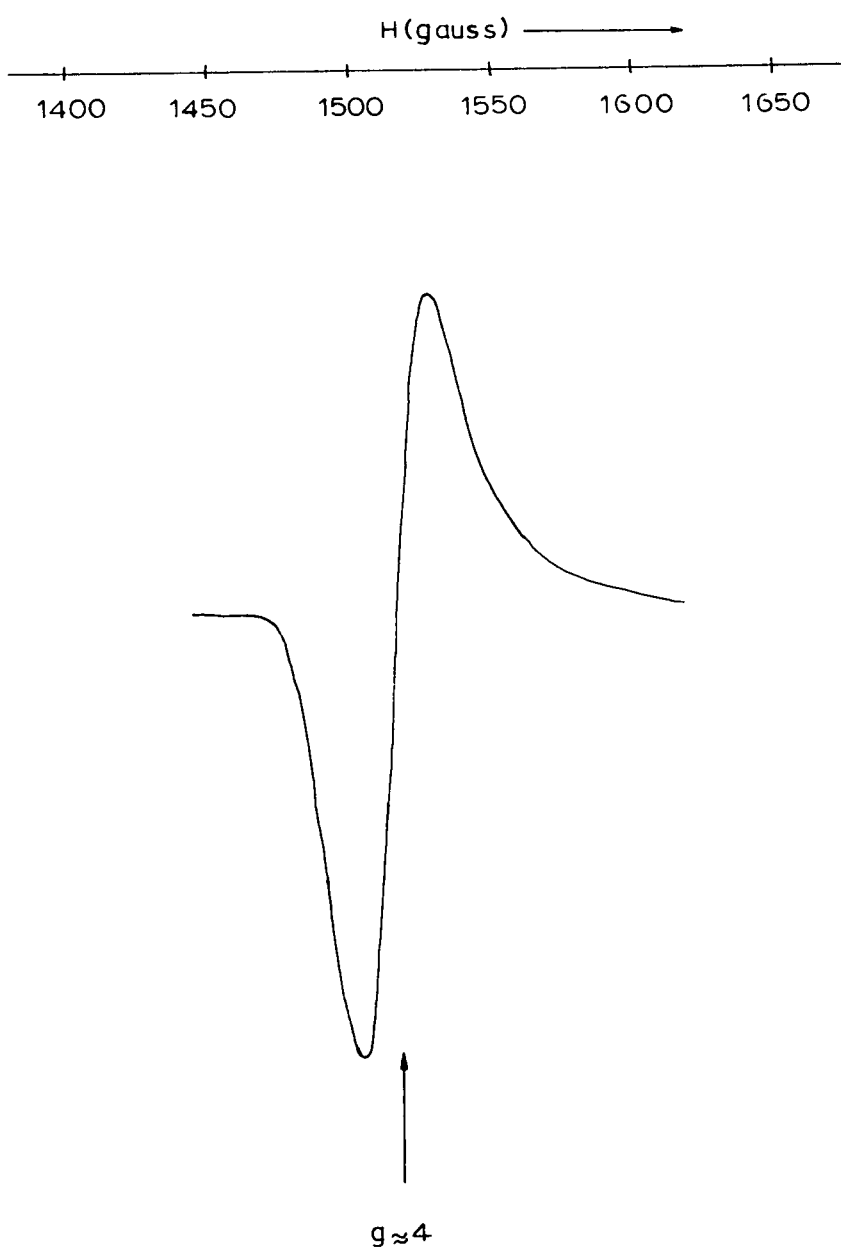

FIGURE 40 ESR Spectrum of Acenaphthene $\pi \rightarrow \pi^*$ Triplet State in EPA.

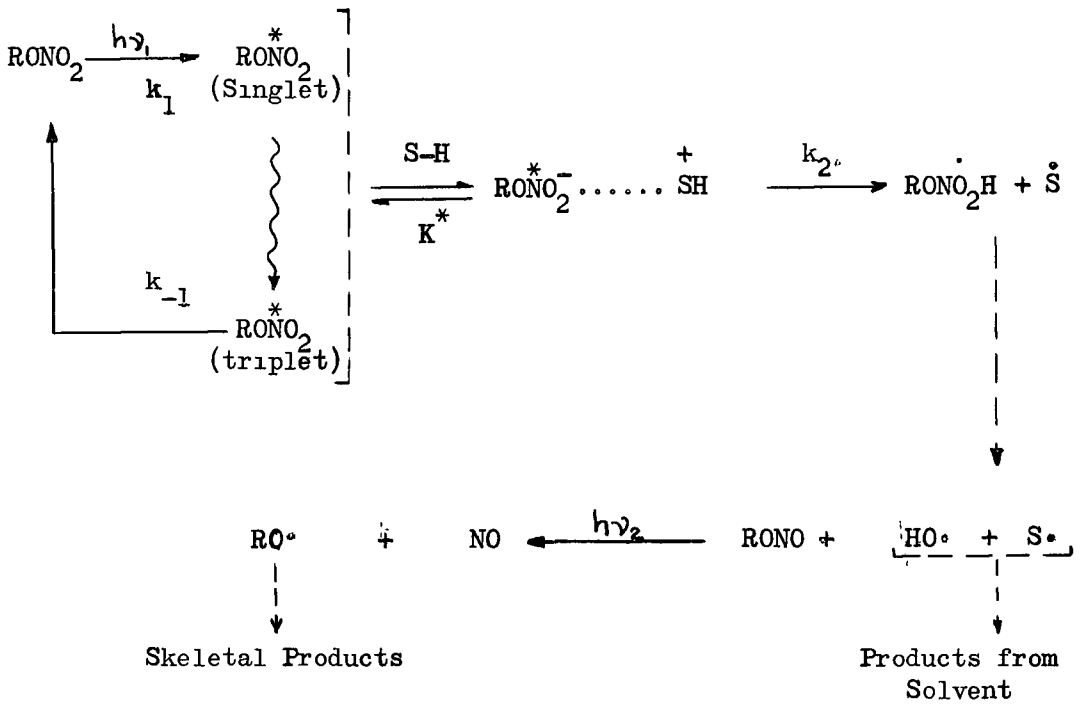

Figure 41. Proposed Mechanism of Nitrate Ester Photolysis In Solution.

The products obtained from the ester $RONO_2$, are functions of the structure of RO· and the products formed from the solvent depend on the nature of the system HO· + ·S.

The first step of excitation may take place by direct light absorption ($h\nu_1$) or by an energy transfer process. The first two steps (electronic excitations) should be the same for the photolysis in the gas phase, solution, or frozen glass, but the distinction comes at the third step when the solvent (or added active solute, like diphenylamine (105)) becomes involved in the reaction. Evidence for this charge-transfer interaction (K^*) may be gained only by physical measurements if the electron donation goes intermolecularly, however, when the charge-transfer process occurs intramolecularly chemical evidence may also confirm this step as it is reflected in the nature of the

products.

It is very likely that the significant difference in the photolytic products from benzoin nitrate, an α-keto nitrate ester, and from the other aromatic nitrates may be explained by an intramolecular process (XLVI) which would alter the course of the reaction in the former case. A recent (195) discovery that in the photolysis of 1,2; 5,6-di-O-isopropylidene -D-glucopyranose -3-nitrate in methanol solution the splitting off of the 5,6-isopropylidene group preceded the photolysis of the nitroxy group producing the corresponding 1,2-O-isopropilidene-3-O-nitro glucose also pointed toward an intramolecular charge-transfer process (XLVII).

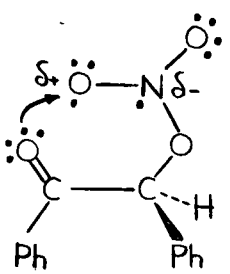

XLVI

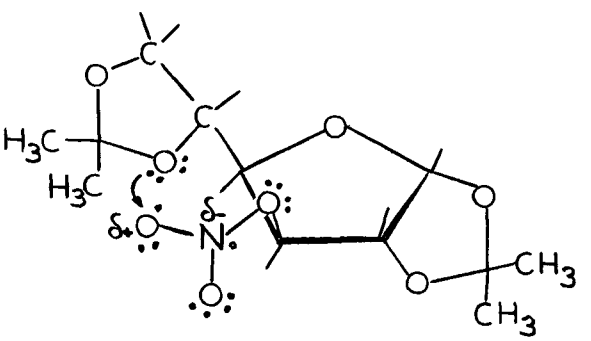

XLVII

In conclusion, this work suggested that the solution photolytic reactions be regarded, not as photodecompositions of the nitrate esters, but rather as the reactions of the excited nitrate esters with particular reagents. This obvious distinction should not be overlooked in synthetic applications of such photochemical reactions.

EXPERIMENTAL

I. Materials.

A. Solvents.

Organic solvents of reagent grade were distilled through a 22 cm. Vigreaux column before use except as follows:

Absolute Ethanol. Reagent grade absolute ethanol was dried by the ethyl phthalate method (196). The moisture content was less than 0.005% as determined by Karl-Fischer titrations.

Absolute Ether (peroxide-free). The reagent was prepared immediately before use by distilling anhydrous ether from lithium aluminum hydride.

Absolute Benzene (oxygen-free). Merck reagent grade thiophene-free benzene (No. 7216, sulfur content 0.005%) was repeatedly dried over sodium and fractionally distilled. The boiling point obtained (79.0°C/746 mm.) fitted the Cox diagram (log p versus 10^3/Tbp) for benzene. The purity of the sample was checked by vapor phase chromatography on a 1 m. "Tergitol (10% on C22 fire brick) NP 27" column at 75° under helium flow (55 ml/min) which indicated the presence of minor amounts of lower boiling impurities.

The dissolved oxygen was purged with a stream of nitrogen gas (washed with alkaline pyrogallol and dried with sulfuric acid) until the usually observable ESR signal disappeared and the benzene sample was stored in the dark under nitrogen.

Anhydrous Pyridine. A commercial reagent grade sample (Fischer Scientifics Company, No. P-368) was stored over calcium hydride for a week and distilled from fresh calcium hydride.

B. Reagents

2,4-Dinitrophenylhydrazine. A solution of the free base in methanol was acidified with sulfuric acid (196).

4-Nitrophenylhydrazine. The reagent was prepared by dissolving 1.5 g of the free base in 50 ml. of absolute ethanol acidified with 1 ml. of glacial acetic acid. From 3 to 5 ml. of the reagent was used for about 100 mg samples of the unknown aldehyde (196).

Anhydrous Nitric Acid. Reagent grade fuming nitric acid (Allied Chemical, No. 1121) containing a minimum of 90% HNO_3, (d = 1.49-1.50, 21.4 moles/liter) was vacuum distilled after mixing with an equal volume of concentrated sulfuric acid in an all glass apparatus with built in 6-plate distilling column. The colourless acid was stored at -20°C and was used within 6 months (196).

Ethylchlorofomate. Reagent grade material (Eastman Organic Chemicals) was stored over anhydrous calcium carbonate and was distilled through a 20 cm. Vigreaux column just before use, b.p. 93.5-97.5°/755 mm., reported b.p. 95°/760 mm. (197).

Palladium-Charcoal Catalyst. This was prepared according to Hartung (198) from palladium chloride (Baker Platinum of Canada Ltd.) and acid-washed "Darco-G-60" charcoal (Atlas Powder Co., New York).

C. Reference Compounds.

meso- and dl- Hydrobenzoin Diacetates. The isomeric hydrobenzoins were acetylated with acetic anhydride and pyridine (196). meso-Hydrobenzoin (1.072 g) yielded 1.10 g of diacetate which melted at 137.5-138.0°; reported

TABLE XXVII Melting Points and NMR Spectra of 2,4-Dinitrophenylhydrazones

Parent Compound	Formula	MP (°C) Reported*	MP (°C) Obtained	NMR Spectra in Trifluoroacetic Acid
—	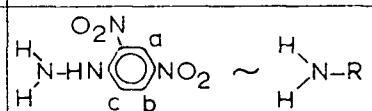	192-193	195-197	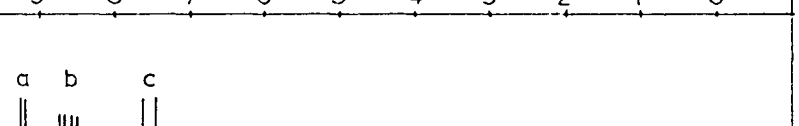
Formaldehyde	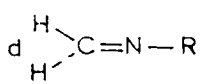	166	167-168	
Acetaldehyde	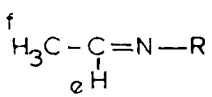	168	165.0-165.5	
Propion-aldehyde	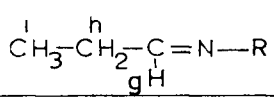	155	154-155	
Acetone	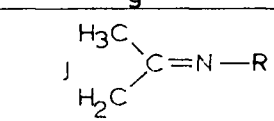	128	126-127	
Benzaldehyde	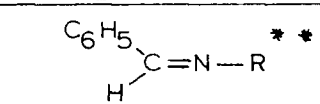 **	237	238-239	Insoluble in trifluoroacetic acid

* Reference (196)

** Calculated for $C_{13}H_{10}O_4N_4$: C, 54.55; H, 3.52, N, 19.57%. Found: C, 54.28, H, 3.69; N, 19.43%

m.p. 135° (197). dl-Hydrobenzoin monoacetate (1.025 g) yielded a total of 1.05 g of diacetate which melted at 108-109°; reported m.p. 109-110°C (197). The diacetates were chromatographically homogeneous (TLC; M-3, S-3, R-1) and the NMR spectra showed no unassigned proton signals.

2,4-Dinitrophenylhydrazones of Reference Carbonyl Compounds. The 2,4-dinitrophenylhydrazones were prepared (196) from reagent grade aldehydes and ketones with the 2,4-dinitrophenylhydrazine reagent. The products were twice recrystallized from alcohol and dried over phosphorus pentoxide and were then pure (TLC; M-4, S-2, or S-7, or S-8). The melting points and NMR spectra of these compounds are summarized in Table XXVII.

Nitrophenols.

The melting points and NMR spectra of the nitrophenols obtained and purified as described below are summarized in Table XXVIII.

2-Nitrophenol (XLVIII) (BDH) was recrystallized from benzene-petroleum ether (30-60°) mixture.

4-Nitrophenol (XLIX) (BDH) was used without further purification.

2,4-Dinitrophenol (L) (Eastman Organic Chemicals) was chromatographed on a 30x500 mm. silica gel column, eluted with solvent mixtures in the following order: petroleum ether (30-60°) -benzene, benzene, and benzene-ethyl acetate. The product thus obtained was free of the 2,6-isomer.

2,6-Dinitrophenol (Ll) (Aldrich Chemical Co.) was recrystallized from benzene-petroleum ether.

2,4,6-Trinitrophenol (picric acid) (Lll) (General Chemical and Pharmaceutical Co. Ltd., England) was recrystallized from chloroform.

Nitrated-4-Phenylphenols. To a nitrating mixture of 3.8 ml. of fuming nitric acid, 6 ml. of glacial acetic acid and 6 ml. of acetic-

TABLE XXVIII Melting Points and NMR Spectra of Nitrophenols.

COMPOUND		mp (°C) Obt	Rep	Ref	NMR Spectra in Acetone
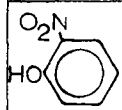	XLVIII	44 5-45 0	44 9	197	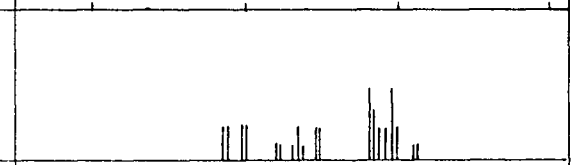
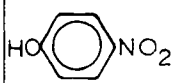	XLIX	114 5-115 5	114	197	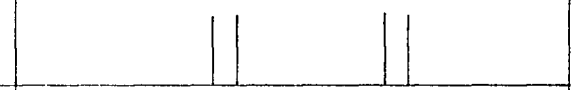
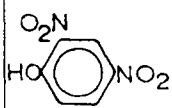	L	116.5	113	197	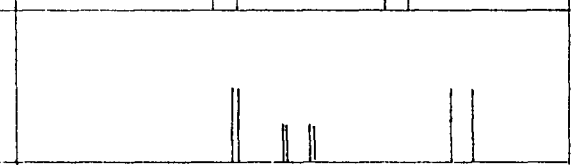
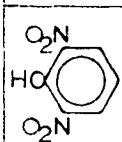	LI	63 5-64 0	63 - 64	197	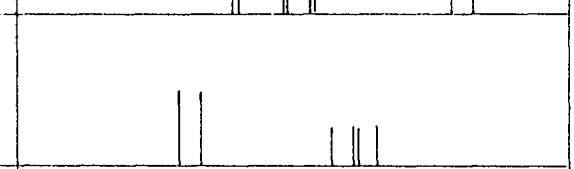
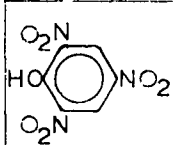	LII	123	122 5	197	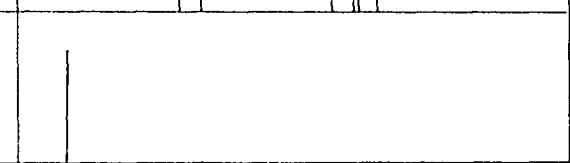
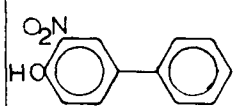	LIII	60 - 62	67	215	
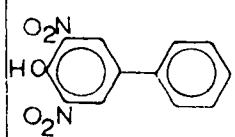	LIV	157 - 158	154 - 155	216	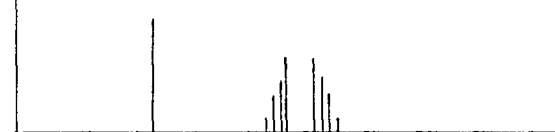
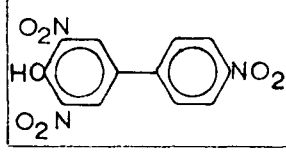	LV	208 209	201 202	216	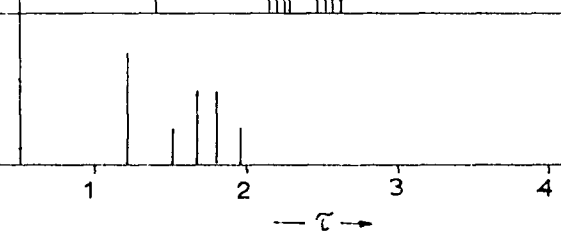

anhydride 4-phenylphenol (3.4 g, Eastman Organic Chemicals) dissolved in a mixture of acetic acid (20 ml.) and acetic anhydride (10 ml.) was added slowly with vigorous stirring. The temperature of the nitrating mixture was kept between 0° and 8° for two hours. After an additional one hour of stirring at room temperature, the mixture was transferred to ice-water and the precipitated product was collected. Thin layer chromatography (M-3, S-3) indicated the presence of several aromatic nitro compounds ranging in colour from pale yellow to dark orange-yellow and in R_f values from 0.0-0.9. Silica gel column chromatography similar to that used for 2,4-dinitrophenol provided three main fractions A,B and C in that order of elution and these were rechromatographed and recrystallized from benzene.

Fraction A (65 mg) was 2-nitro-4-phenylphenol (Llll) since both the low yield and the high R_f value on TLC pointed to monosubstitution and the melting point (Table XXVIII) was close to the reported value.

Fraction B (1.85 g) gave a single spot on TLC (M-3, S-3) and was identified as 2,6-dinitro-4-phenylphenol (LIV) from the elementary analysis and from the melting point and NMR spectrum (Table XXVIII). There were two sets of ring proton signals in the spectrum. One was typical of a monosubstituted phenyl ring as in phenol, while the other was a single peak similar to that of picric acid which would be expected from the benzene ring bearing the OH group and two ortho nitro groups. Calc. for $C_{12}H_8O_5N_2$: C, 59.51; H, 3.33; N, 11.57. Found: C, 55.33; H, 3.41; N, 10.62%.

Fraction C(760 mg) was suspected to be 2,6,4-trinitro-4-phenylphenol (LV) from its low R_f value and this was confirmed from the melting point, analysis and NMR spectrum.

The arrangement of protons in this symmetric trinitro derivative is such that the benzene ring which bears the hydroxyl group would be

analogous to picric acid while the other benzene ring nitrated on the 4-position contains four protons in an A_2B_2 systems and would be analogous to p-nitrophenol. In agreement with this the NMR spectrum consisted of a single peak at $\tau = 1.21$ (for picric acid $\tau \doteq 0.83$) and a quartet similar to that of 4-nitrophenol but at a lower τ-value.

Calc. for $C_{12}H_7O_7N_3$: C, 50.18; H, 2.46; N, 14.63.
Found: C, 47.39; H, 2.54; N, 13.70%.

D. Aromatic Nitrate Esters.

(i). Starting Materials.

cis- and trans-1,2-Acenaphthenediols.

These diols were prepared and characterized as described by the present author in an earlier thesis (68) (144).

Benzoin.

A commercial sample of benzoin (Eastman Organic Chemicals) melted correctly at 135-137° (197) and thin layer chromatography (M-3, S-3, R-1 or R-3) indicated the presence of one compound only, both before and after recrystallization from methanol.

meso- Hydrobenzoin.

Benzoin like benzil (Table XXIX) was reduced predominantly to meso- hydrobenzoin by both lithium aluminum hydride in ether and by sodium borohydride in alcohol.

Table XXIX

Reduction Products of Benzil.

Starting Material	Products	Yield		
			$LiAlH_4$ (199)	$NaBH_4$ (200)
		35°	-80°	20°
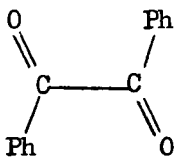	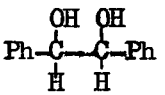 m-Hydrobenzoin m.p. 138.5° (201)	81%	90%	"predominant"
Benzil m.p. 96° (196)	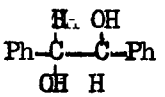 dl-Hydrobenzoin m.p. 119.5-120.5° (201)	5%	.....	.....

Reduction of benzoin with Arnd's alloy (Mg-Cu)(202) was also used, but lithium aluminum hydride gave the best results.

(a) Benzoin (83.70 g) was reduced (203) with lithium aluminum hydride (95% pure, Metal Hydrides Incorporated) (16.41 g) suspended in anhydrous ether (800 ml.) at dry ice-acetone temperature over night. The excess of lithium aluminum hydride was decomposed with ethylacetate-diethyl ether mixture (1:1), the complex formed in the reduction was destroyed with aqueous sodium hydroxide, and the aqueous solution was exhaustively extracted with diethyl ether in a continuous liquid-liquid extractor.

The residue from the ether extract (95.8% yield) was recrystallized from methanol in two fractions: A, 71.08 g, (84.1% of the theoretical) and B, 9.92 g (11.7% of the theoretical). Further recrystallization of fraction A from acetone provided pure material (53.80 g, 63.7%) which melted at

137.5-140.5°. Reported m.p. 138.5° (201). This product gave only one spot detectable by TLC (M-3; S-3; R-1 or R-3). The ultraviolet, infrared and proton magnetic resonance spectra were recorded.

(b) Benzoin (21.1998 g) was added to an ice-cold methanolic solution of sodium borohydride (7.9984 g). After three hours of vigorous stirring the ice bath was removed and the mixture was left over night at room temperature. The excess borohydride was destroyed with acetic acid and the sodium ions were precipitated with concentrate hydrochloric acid (pH adjusted to 6). The filtrate was evaporated to dryness and the boric acid formed was removed by repeated distillations with methanol.

The crude product (18.842 g, 88.0% yield) was recrystallized from 270 ml. of methanol. Three main fractions were obtained:
A, 6.680 g, (31.2%) m.p. 140°C; B, 1.691 g, (7.9%) m.p. 136-140°C; and C, 6.118 g, (28.6%) m.p. 117-137°C. Reported m.p. for meso-Hydrobenzoin 138.5°; for dl-Hydrobenzoin, 119.5-120.5°C (201). Recrystallization of the two main fractions A and C from methanol provided samples which melted at 139.0-139.5°C and 137.0-139.5°C respectively. The infrared spectra also indicated that both were pure meso-isomer.

(c) Benzoin (1.0377 g,) was dissolved in methanol (75 ml.) and the solution was diluted with distilled water (70 ml.) and 5ml. of an aqueous solution of magnesium chloride (200 g, per liter)(204). About 5 grams of finely powdered Arnd's alloy (40% Mg, 60% Cu) *(205)(206) was added with vigorous stirring, and the mixture was refluxed for 4 hours. The silver white alloy turned copper-red and some magnesium hydroxide precipitated out. The hot suspension was filtered with suction and the filtrate was concentrated in vacuo. Three crops of crystals were isolated: A, 341.3 mg (32.5%) melted at 138.5-140.0°; B, 143.7 mg (13.7%) melted at 136-140° and

---

* Kindly supplied by Dominion Magnesium Limited (Domal) Haley, Ontario.

C, 216.6 mg (20.7%) melted over a wide range below 110°. TLC (M-3, S-3, R-1 or R-3) indicated that A and B were benzoin-free and judging from their melting points** were pure meso-hydrobenzoin, fraction C, however, was about a 1:1 mixture of unreacted benzoin and reduction product.

dl-Hydrobenzoin.

Racemic or dl-hydrobenzoin was prepared by a series of three steps according to Fieser (200).

In the first step meso-stilbene dibromide was prepared from 100 grams of commercial trans-stilbene (Eastman Organic Chemicals) in 83% yield (157 g). The product decomposed during melting at 251.0-252.5°; reported m.p. 238°(200).

In the second step meso-stilbene dibromide was transformed via a Walden inversion to dl-hydrobenzoin monoacetate. This reaction was carried out with various amounts (2-50 gram) of dibromide yielding about 53% of pure crystalline dl-hydrobenzoin monoacetate which melted at 87-89°; reported m.p. 87° (200).

In the third step the acetate group was hydrolysed and the dl-hydrobenzoin produced was recrystallized from a diethyl ether-petroleum ether (b.p. 30-60°) mixture yielding long white needles (58%), which melted at 122.5-124.5°; reported m.p. 119.5-120.5° (200).

Benzoin Ethylcarbonate

Benzoin (4.3 millimole; 906.0 mg) was dissolved in anhydrous pyridine (10 ml.) and 1.0 ml. (10.5 millimoles, about 150% excess) of ethyl chloroformate was added to the solution. The mixture was left at room temperature for 24 hours and was heated to 100° for an additional 15 minutes. Pyridinium

---

** TLC did not distinguish between meso- and dl- hydrobenzoins.

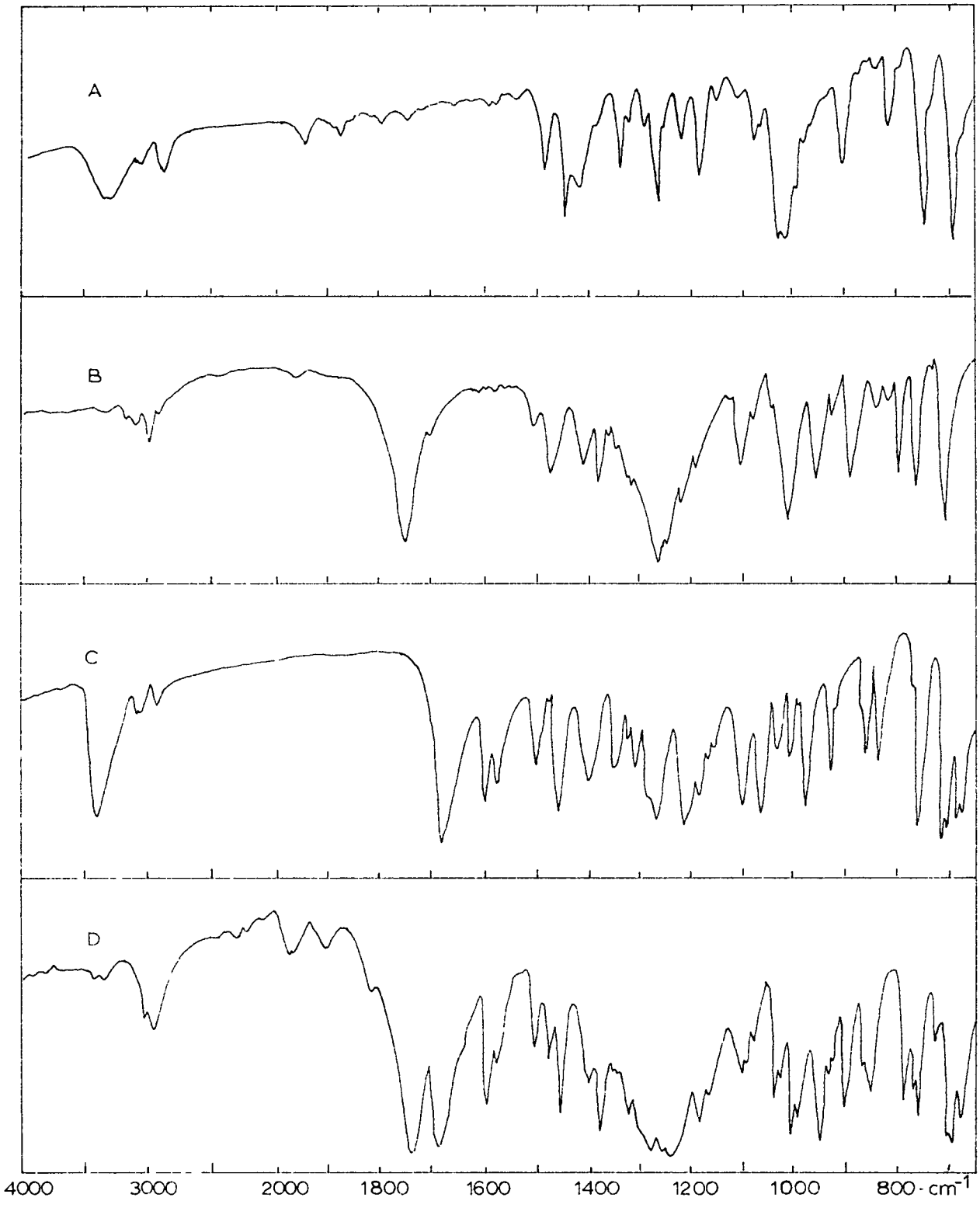

FIGURE 42 Infrared Spectra of Ethylcarbonates of 1,2-Diphenyl-ethane Derivatives A. meso-Hydrobenzoin; B meso-Hydrobenzoin Di-(Ethylcarbonate); C: Benzoin; D: Benzoin Ethylcarbonate

chloride separated in crystalline form during the reaction. The excess pyridine was removed in vacuo and the solid residue was extraced with three 30 ml. portions of boiling diethyl ether. The residue from the ether extract was recrystallized from benzene, yielding a colourless crystalline product (118.0 mg, 9.72%) which melted at 74.0-76.0°. Calculated for $C_{17}H_{16}O_4$: C, 71.81; H, 5.32. Found: C, 71.71; H, 5.96%.

The infrared spectrum showed two distinct absorption bands in the region of carbonyl stretching frequencies one for the keto carbonyl (1682 cm^{-1}) (in benzoin itself $_{C=O}$ = 1675 cm^{-1}) and one for the carbonate carbonyl (1740 cm^{-1}) in equal intensity. The NMR spectrum of the compound was also recorded.

meso-Hydrobenzoin Di-(ethylcarbonate)

meso-Hydrobenzoin (2.15 millimole, 458.0 mg) in anhydrous pyridine (5 ml.) was treated with 1.08 ml. (10.5 millimoles, about 150% excess) of ethyl chloroformate in the same way as in the case of benzoin. The product obtained from the ether extract was recrystallized from methanol and yielded 125.8 mg. (16.4%) of meso-hydrobenzoin-1,2-diethylcarbonate which melted at 113.5-115.5°. Calc. for $C_{20}H_{22}O_6$: C, 67.02; H, 6.19.
Found: C, 67.28; H, 6.45%.

The infrared spectrum showed only one carbonyl stretching frequency corresponding to the ethylcarbonate absorption at 1740 cm^{-1}. The NMR spectrum of the sample was also recorded.

(ii) Aromatic Nitrate Esters via Direct Esterification.

cis- and trans-1,2-Acenaphthenediol Dinitrates.

The cis and trans-1,2-acenaphthenediols were nitrated as previously reported (68) (144) with 100% nitric acid-acetic acid - acetic anhydride in

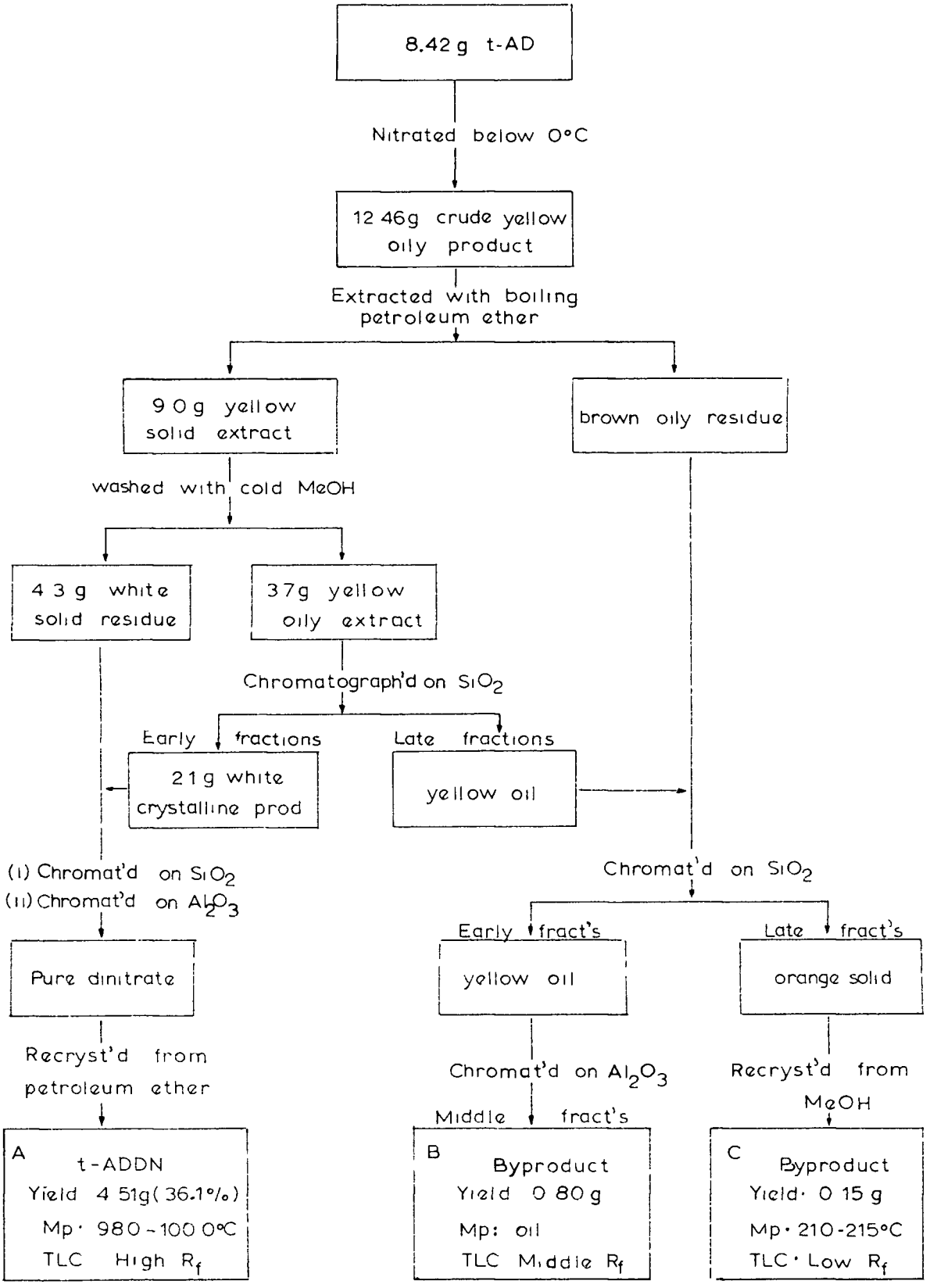

FIGURE 43 Flow Sheet of Separation of Nitration Products from trans-1,2-Acenaphthenediol (t-AD)

molar proportions 4.0:3.3:20 per mole diol at -15° to -5°. The only modification of the original procedure was in the working-up process. Both silicic acid and alumina columns were used in the purification of the dinitrates; in the case of silicic acid a 1:1 (vol./vol.) benzene-petroleum ether (b.p. $30-60^{\circ}$) mixture and in the case of alumina, anhydrous diethyl ether were used as eluting solvents. For the products from 8.4 g, of diol, columns 20 x 750 mm. or 30 x 500 mm., corresponding 300 or 400 ml of adsorbent respectively were used. The separation procedure was equally satisfactory for the two isomers and is illustrated for the trans-1,2-acenaphthenediol dinitrate (t-ADDN) in the form of a flow sheet in Figure 43.

Benzoin Nitrate

To a mixture of acetic acid (5.6 ml) nitric acid (5.0 ml) and acetic anhydride (11.0 ml) which was kept at -10° with an ice-salt bath a solution of benzoin (12.32 g) in acetic anhydride (25 ml.) was added dropwise with vigorous stirring. A further 20 ml. portion of acetic anhydride was added and the mixture, after 20 minutes total reaction time, was poured into ice-water which precipitated a crude product (13.59 g, 91.0%). The colourless solid was twice recrystallized from a benzene-petroleum ether ($30-60^{\circ}$) mixture. The final product (5.30 g, 35.5%) melted at $77-78^{\circ}$.
Calc. for $C_{14}H_{11}O_4N$: N, 5.45. Found: N, 5.47%.

Thin-layer chromatography (M-3, S-1, R-2) indicated that the mother liquors from the recrystallization contained some ring-nitrated product, while the crystalline nitrate ester gave only one spot which indicated the absence of by-products. The solid state infrared spectrum showed a broad triplet absorption at 1643, 1672 and 1695 cm^{-1} and indicated that the most intense band at 1672 cm^{-1} probably represented the

carbonyl absorption (benzoin absorbed at 1675 cm^{-1}). The NMR spectrum of the sample was also recorded.

meso-Hydrobenzoin Dinitrate

meso-Hydrobenzoin (21.0 g) was nitrated as described above for 30 minutes and the temperature was maintained between -12 and +2°C. The mixture was transferred to ice-water and left overnight. The crude product (32.28 g, 112%) was separated by filtration and was recrystallized from benzene-petroleum ether. The nearly colourless crystalline product was chromatographed on a 30 x 500 mm. alumina column, eluted with a 1:1 mixture of benzene-petroleum ether (30-60°) and was finally recrystallized from the same solvent. The yield was 17.20 g, (57.7%); m.p. 148.5-149.5°. The solid state infrared spectrum showed characteristic nitrate absorptions. Calc. for $C_{14}H_{12}O_6N_2$: C, 55.26; H, 3.98; N, 9.21. Found: C, 55.46; H, 3.91; N, 9.11%.

Hydrogenolysis of 47.2 mg. of the dinitrate in 25 ml. of absolute ethanol with 48.6 mg. of palladium-charcoal catalyst at 60 psi of hydrogen for 3.5 hours produced the parent meso-hydrobenzoin which was identified by its melting point (137-140°), TLC (M-3, S-3, R-1), and infrared spectrum.

dl-Hydrobenzoin Dinitrate.

dl-Hydrobenzoin (21.0 g) was nitrated as for the meso- isomer. The crude product (25.5 g, 85.6%) was recrystallized from benzene-petroleum ether (30-60°) mixture and chromatographed on alumina. Further recrystallized from benzene-petroleum ether yielded 9.07 grams (30.4%) of pure product which melted at 105.5-107.0°. The infrared spectrum showed characteristic nitrate absorptions. Calc. for $C_{14}H_{12}O_6N_2$: N, 9.21. Found: 9.17%.

Hydrogenolysis of 47.7 mg of the dinitrate as above produced the parent dl-hydrobenzoin which melted at 99-105°. Thin layer chromatography

and the infrared spectrum indicated the presence of only traces of impurities.

(iii) Aromatic Nitrate Esters *via* Exchange Reactions.

Benzyl Nitrate

Benzyl nitrate was prepared from freshly distilled reagent grade benzyl chloride according to Ferris and co-workers (35). The crude product was distilled in vacuum from solid silver nitrate. The early fraction contained a trace amount of benzyl-chloride but the bulk of the material distilled at 59-62°/0.37mm. and gave the correct infrared and NMR spectra for pure benzyl nitrate. The reported boiling point was 45°/0.5 mm. (43).

meso-Hydrobenzoin Dinitrate

According to Fishbein (36) *meso*-2,3-dibromobutane gave *dl*-2,3-dinitroxy-butane with silver nitrate *via* Walden inversion. The effect of silver nitrate on *meso*-dibromo stilbene in acetic acid solution was studied by von Walter and Wetzlich (207) in 1900 who claimed it produced hydrobenzoin dinitrate which melted at 132°. Since no sterochemical assignment was provided by von Walter and Wetzlich and the dinitrates synthesized by direct esterification in this work melted at different temperatures, we repeated their synthesis in both acetic acid (a) and acetonitrile (b) solvents.

(a) *meso*-Dibromostilbene (3.400 g, m.p. 251.0-252.5°) was suspended in acetic acid (100 ml.) at the boiling point. Silver nitrate (4.100 g, 50% excess) was dissolved in distilled water (5 ml.) and after dilution with acetic acid (5 ml.) was added dropwise to the hot bromide suspension with vigorous stirring. The colourless suspension gradually changed to the pale yellow colour of silver bromide. After 15 minutes the mixture was filtered on a sintered glass funnel and the cloudy filtrate was poured

into distilled water (500 ml.) and the aqueous solution was placed in the refrigerator. The precipitate which formed after 10 hours was collected (1.609 g, 52.6%) and recrystallized from 50 ml. of petroleum ether (30-60°). The crystals (695.8 mg, 22.8%) melted at 139.5-142.0° and since TLC (M-3, S-1, R-1) indicated the presence of a number of lower-running impurities they were further purified by thick-layer chromatography (M-5, S-1). The final product obtained melted at 146-148° and was shown to be identical to authentic meso-hydrobenzoin dinitrate by infrared spectroscopy and TLC (M-3, S-1, R-1).

(b) meso-Dibromostilbene (3.402 g) was suspended in acetonitrile (50 ml.) at the boiling point. Silver nitrate (4.100 g, 50% excess) was dissolved in acetonitrile (5 ml.) and added to the suspension. After 15 minutes the mixture was filtered and the filtrate was evaporated in vacuo. The brown, crude product (4.94 g) was extracted with 4 x 60 ml. of hot petroleum ether (65-110°) and then with two portions of 60 ml. of hot methanol. The residue from the methanol extract was re-extracted with hot petroleum ether and the petroleum ether extracts were combined and evaporated to give 1.602 g, (52.6%) of solid product which was recrystallized from 80 ml. of petroleum ether (30-60°) and melted at 140-146°. Further purification by thick-layer chromatography yielded meso-hydrobenzoin dinitrate which melted at 145-147° and had the correct infrared spectrum and R_f values (TLC, M-3, S-1, R-1).

The parent alcohol, meso-hydrobenzoin, was recovered by hydrogenolysis of the dinitrate and was identified by its melting point (137.0-139.5°, reported m.p. 138.5°) (201) and infrared spectrum.

TABLE XXX Attempted Syntheses of Aromatic Nitrate Esters from Cyclic and Ethylcarbonates

Carbonates	Sample (mg)	Solvent* (ml)	$AgNO_3$ (mg)	Reaction Condition**		M P (°C)		
				Temp. (°C)	Time (hrs)	Starting Material	Expected Nitrate Ester	Product Obtained
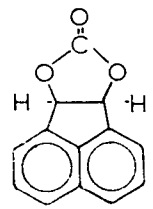 <u>cis</u>-1,2-Acenaphthenediol Carbonate (LVI)	5.4	5.0	14.4	60	20	231	128-130	228-234
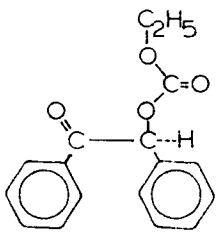 Benzoin Ethylcarbonate (LVII)	43.0	5 0	179	Bp	3	74-76	77-78	76-78
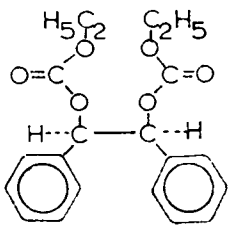 <u>meso</u>-Hydrobenzoin Di (Ethylcarbonate) (LVIII)	50 7	5 0	142	Bp	3	113 5-115.5	148 5-149.5	116.5-118.5

* Acetonitrile

** Procedure according to Boschan (37)

Attempts to Exchange Carbonate Groups for Nitroxy Groups

The cyclic carbonate of cis-1,2-acenaphthenediol (LVI) and the ethyl carbonate derivatives of benzoin (LVII) and meso-hydrobenzoin (LVIII) were treated with silver nitrate in acetonitrile solutions as described by Boschan (37) for the replacement of the o-chloroformate group by the o-nitro group. The details of these experiments are shown in Table XXX. The melting points and R_f values (TLC, M-3, S-1, R-1) of the products indicated the recovery of the unreacted carbonates.

II. Analyses.

A. Melting Point Determinations.

Melting points were observed ($\pm 0.5^{\circ}$) with a hot stage polarizing microscope (Wetzlar, No. 48114, Ernst Leitz, Germany).

B. Elementary Analyses.

Carbon, hydrogen, and Dumas nitrogen analyses were made by Mrs. A. E. Aldridge, Microanalytical Laboratory, Department of Chemistry, University of British Columbia.

III. Spectra

A. Ultraviolet Spectra (UV)

All ultraviolet spectra were taken on Cary recording spectrophotometers (Model 14 or Model 11) in 1 cm. quartz cells in one of the following solvents:

Methyl alcohol	Absolute
Ethyl alcohol	95% Reagent
Diethyl ether	Anhydrous, peroxide free
Benzene	Absolute, oxygen free
Hexane	Spectra grade

Some of the measurements were made by Mrs. M. Zell, Spectroscopic Laboratory, Department of Chemistry, University of British Columbia.

B. Infrared Spectra (IR)

All infrared spectra were recorded on a Perkin Elmer No. 21 spectrometer in potassium bromide ~~windows~~ pellets or in solvent-compensated cyclohexane solutions by Mrs. M. Zell, Spectroscopic Laboratory, Department of Chemistry, University of British Columbia.

C. Electron Spin Resonance Spectra (ESR)

Electron spin resonance spectra were recorded on a Varian V-4500 spectrometer, equipped with a ~~10~~ 12 inch magnet and a 100 Kc field modulator. The cavity used contained slots for entry of ultraviolet light which permitted simultaneous irradiation with ESR measurements. Most of the spectra were taken at room temperature ($\sim 300^{\circ}K$) but for some experiments an 11 mm. o.d. quartz Dewar vessel was inserted in the cavity for studies at liquid nitrogen temperature ($77^{\circ}K$). UV sources were either a G.E.-H85-A3 medium pressure mercury arc lamp or a more powerful G.E.-A-H6 high pressure mercury arc lamp. The unfiltered light was focused in the cavity by means of a quartz lens system and the final position of the lamp for maximum light intensity was determined with the aid of a photocell inserted in place of the sample to be irradiated.

D. Nuclear Magnetic Resonance Spectra (NMR)

The proton resonance spectra were taken on a Varian A-60 analytic 60 Mc. high resolution spectrometer in deutero-chloroform, acetone or trifluoroacetic acid as solubility permitted with tetramethyl silane as internal or external reference. The spectra were recorded by Mrs. E. M. Brion,

Spectroscopic Laboratory, Department of Chemistry, University of British Columbia.

IV. Chromatography.

Conventional wet-packed column chromatography was used in preparative procedures on a macro scale while thick-layer chromatography (0.5 to 8.0 mm.) was used in the isolation of semi-micro amounts of pure compounds. Thin-layer chromatography (TLC, 0.25-0.5 mm.) was used for qualitative analysis and the isolation of micro quantities of reaction products. Colourless compounds were detected on chromatograms by the use of specific spray reagents or by examination under ultraviolet light (Chromato-Vue, Ultraviolet Products Inc., San Gabriel, California) before and after the application of spray reagents.

The adsorbing media (M), solvents (S) and spray reagents (R) are described in Tables XXXI, XXXII, XXXIII respectively.

Table XXXI

Adsorbents and Supporting Materials for Chromatography

No.	Adsorbent	Used as	Ref.
M-1	Silica gel (BDH "for chromatography" No. 311270)	Column	——
M-2	Alumina (E. Merck "Aluminum Oxide" No. 71707)	Column	(62)
M-3	Silica Gel G. (E. Merck and Co., Darmstadt.)	TLC	——
M-4	Aluminum Oxide-G. (E. Merck and Co., Darmstadt.)	TLC	——
M-5	Silicic acid (Mallinckrodt, 100 mesh)-Plaster of Paris*-Water (4:1:8)	TLC and Thick-layer	(105) (208)

*Gypsum, Lime and Alabastine Company Limited, Vancouver, B.C.

Table XXXII

Solvents for Chromatography

No.	Solvents	Ratio of Volumes	Ref.
S-1	Benzene-petroleum ether*	1:1	—
S-2	Benzene-petroleum ether**	3:1	(209)
S-3	Benzene-diethylether	4:1	—
S-4	Benzene-ethylacetate	1:1	—
S-5	Benzene-acetic acid	49:1	—
S-6	Benzene	—	—
S-7	Petroleum ether—diethyl ether**	9:1	(210)
S-8	Petroleum ether**-chloroform	1:1	—
S-9	Chloroform	—	—
S-10	Methylene chloride	—	—

* b.p. range 30-60°C.

** b.p. range 60-80°C.

Table XXXIII

Spray Reagents for Chromatography

No.	Reagent		Ref.
R-1	5% (vol/vol)	Fuming nitric acid in conc. sulfuric acid	(105)
R-2	1% (wt/vol)	Diphenylamine in 95% ethanol	(211)
R-3	1% (wt/vol)	Potassium permanganate in	(212)
	2% (wt/vol)	aqueous sodium carbonate	

V. Photolyses

A. Light Sources and Apparatus

Three lamps were used as light sources throughout these experiments.

G.E. - H85-A3, a medium pressure mercury arc lamp, was used for the preliminary experiments and for some of the ESR measurements. The lamp was surrounded with a copper cooling coil and housed in a sheet steel box (100 x 100 x 150 mm.) tinned on the inner surfaces with a 10 x 25 mm. window for the light beam. The factory report of energy distribution for the lamp together with the observed relative intensities are shown in Figure 44.

G.E.-A -H6, a high pressure mercury arc lamp, was used for some of the ESR measurements since it had a greater output in the absorption region (2600-3000 Å) of the nitroxy group. The factory report for power output is plotted against wavelength in Figure 45.

Hanovia - 8A36 - 00066, a high pressure mercury arc lamp was used for all the reaction kinetic measurements and preparative irradiation experiments. The lamp was placed inside of a test tube-shaped Corex filter (Hanovia, No. 513-27-114) and this in turn was placed inside a quartz, water-jacketed well, thus the light was filtered throughout all experiments by successive layers of Corex glass, quartz, distilled water, and quartz.

The quantitative data on the lamp output are summarized in Figure 46. Figure 46c. shows the spectral distribution as observed on a Beckman DU spectrophotometer, while Figure 46b. shows the power output in units of watts and calories/sec. These calibrations, according to the factory report, were taken through a quartz water cell with an Ag-Bi thermopile, calibrated against a standard lamp (National Bureau of Standards). The measurement was performed on several lamps and thus represents a good average for this lamp. No doubt the actual output values varied from lamp to lamp but are probably

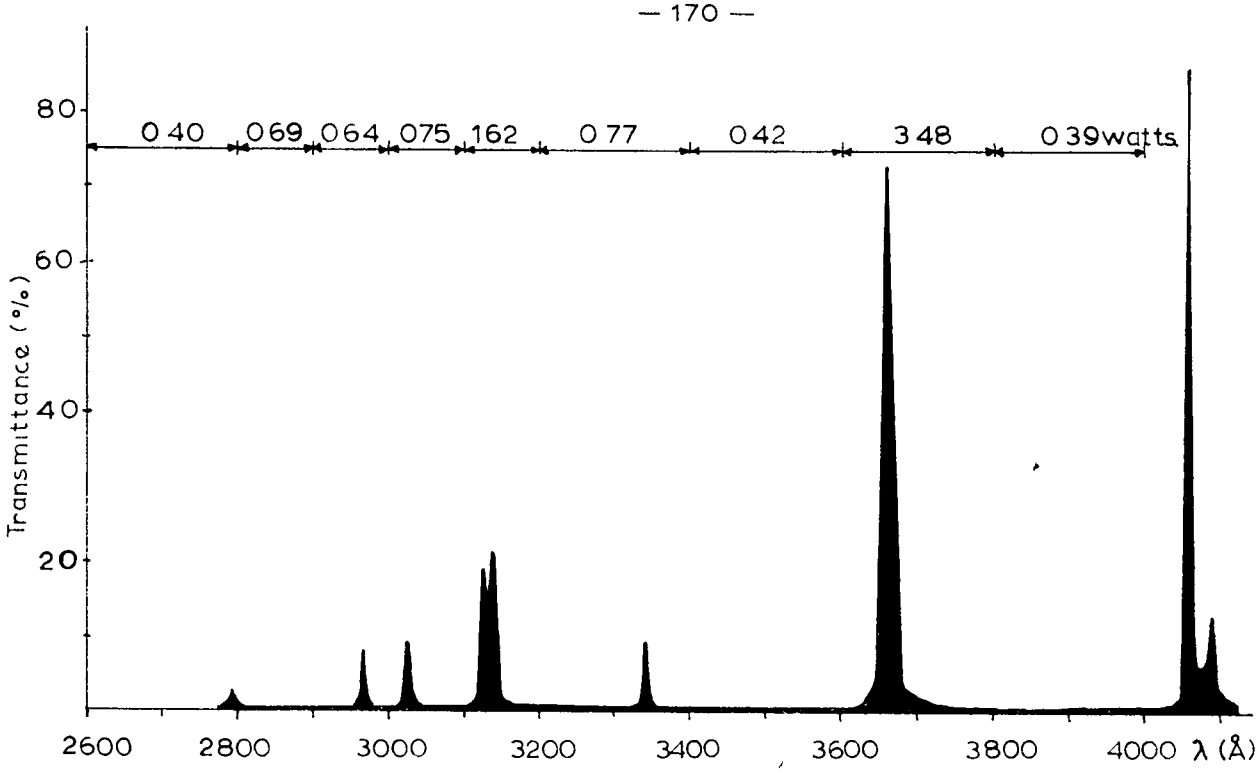

FIGURE 44 Reported Power Output and Observed Spectral Distribution for GE-H85-A3 Medium Pressure Mercury-Arc Lamp

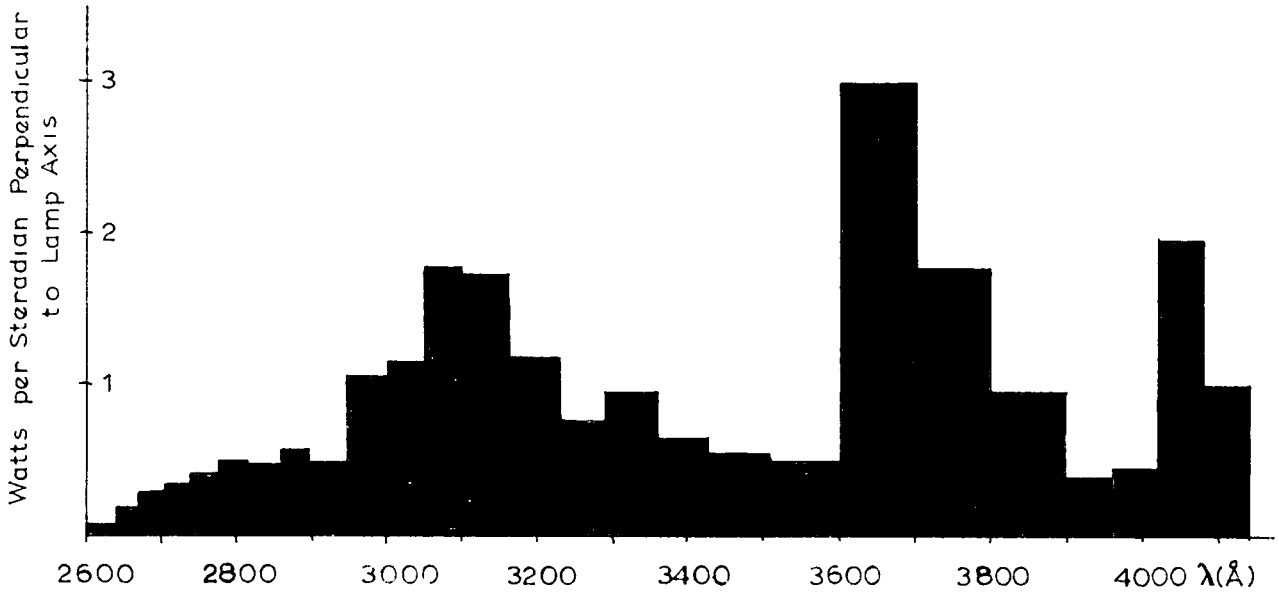

FIGURE 45 Reported Power Output for GE-A-H6 High Pressure Mercury-Arc Lamp

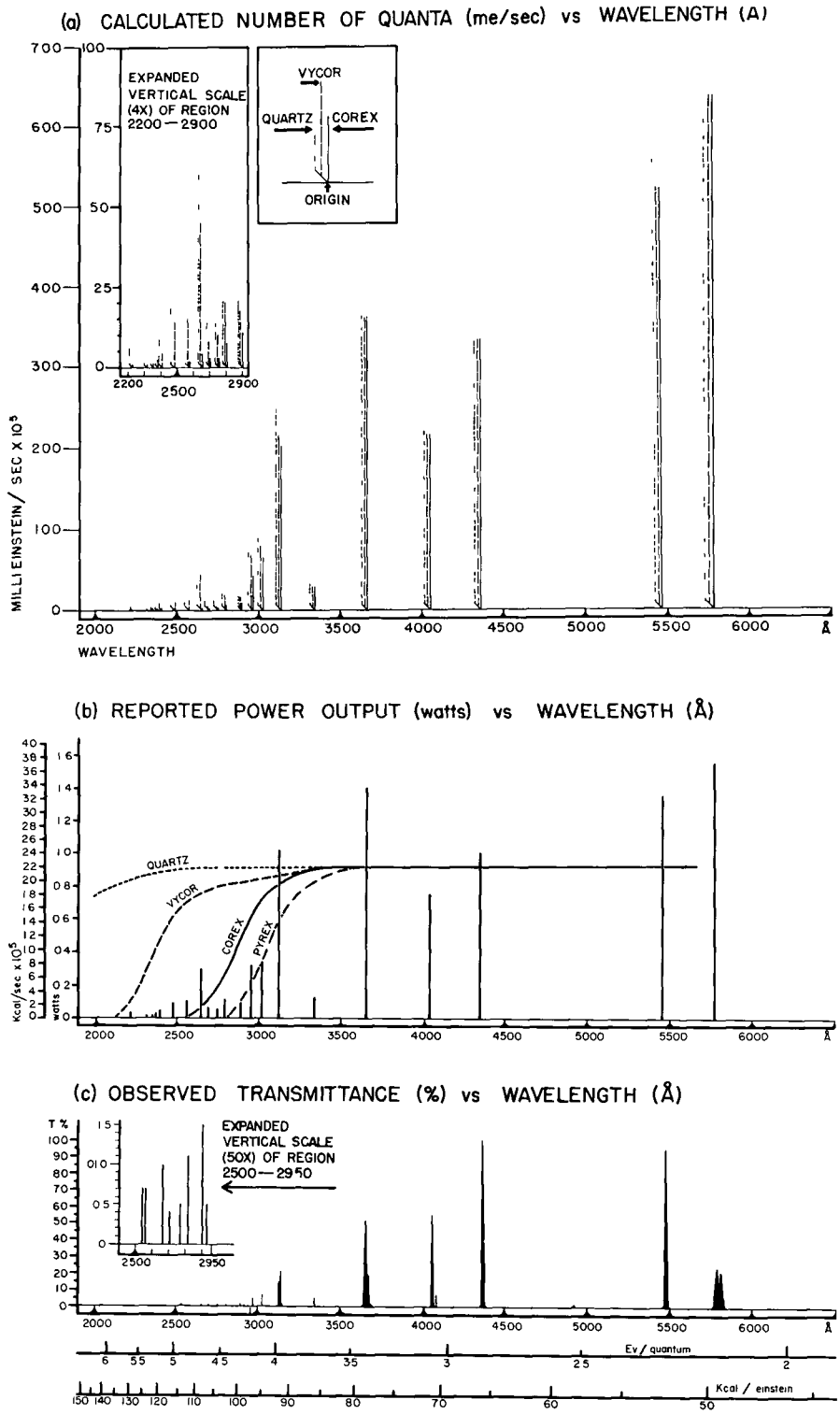

Fig 46 LIGHT ENERGY EMITTED

BY HANOVIA 100 WATT HIGH PRESSURE MERCURY ARC LAMP

reliable within $\pm 10\%$.

Figure 46a. shows the output in number of quanta per second versus wavelength. The figures plotted were calculated from the factory report on the following basis:

(i) Given the total energy output (e, cal/sec) for each wavelength.

(ii) The energy (ε) of one individual photon is

$\varepsilon = h\nu = \frac{hc}{\lambda}$ (ergs/particle) and the energy of an Avogadro number of photons (einstein) is given by

$$E = N\frac{hc}{\lambda(\text{cm})} \text{ (ergs/mole)} = \frac{2.87\text{x}10^8}{\lambda(\text{Å})} \text{ (cal/mole)}$$

(iii) The ratio of values thus obtained in (i) and (ii) gave the number of molequanta/sec

$$\frac{e}{E}\left(\frac{\text{cal}}{\text{sec}} \Big/ \frac{\text{cal}}{\text{moles}}\right) = \frac{e}{E}\left(\frac{\text{mole}}{\text{sec}} \equiv \frac{\text{einstein}}{\text{sec}}\right)$$

<u>Photoreactor</u>. The apparatus was constructed ~~by~~ of Pyrex glass surrounding an Hanovia quartz immersion well as indicated in Figure 47. The thickness of the solution which surrounded the lamp was 0.665 cm. A Teflon-coated magnet bar stirrer and helium gas stream provided efficient circulation of the irradiated solution. The inert gas stream was passed successively through alkaline pyrogallol and sulfuric acid wash bottles, then a U-shaped silica gel column and finally it was saturated with the vapours of the solvents used for the photolyses. The saturation was necessary in order to prevent appreciable solvent loss during prolonged irradiations. A hard polyethylene tubing was used for the connection between the solvent wash bottle and the photoreactor since Tygon tubing was attacked by benzene vapour which dissolved some oily material (plasticizer?) from the tubing. The gas flow was started one-half hour prior to the photolysis in order to purge

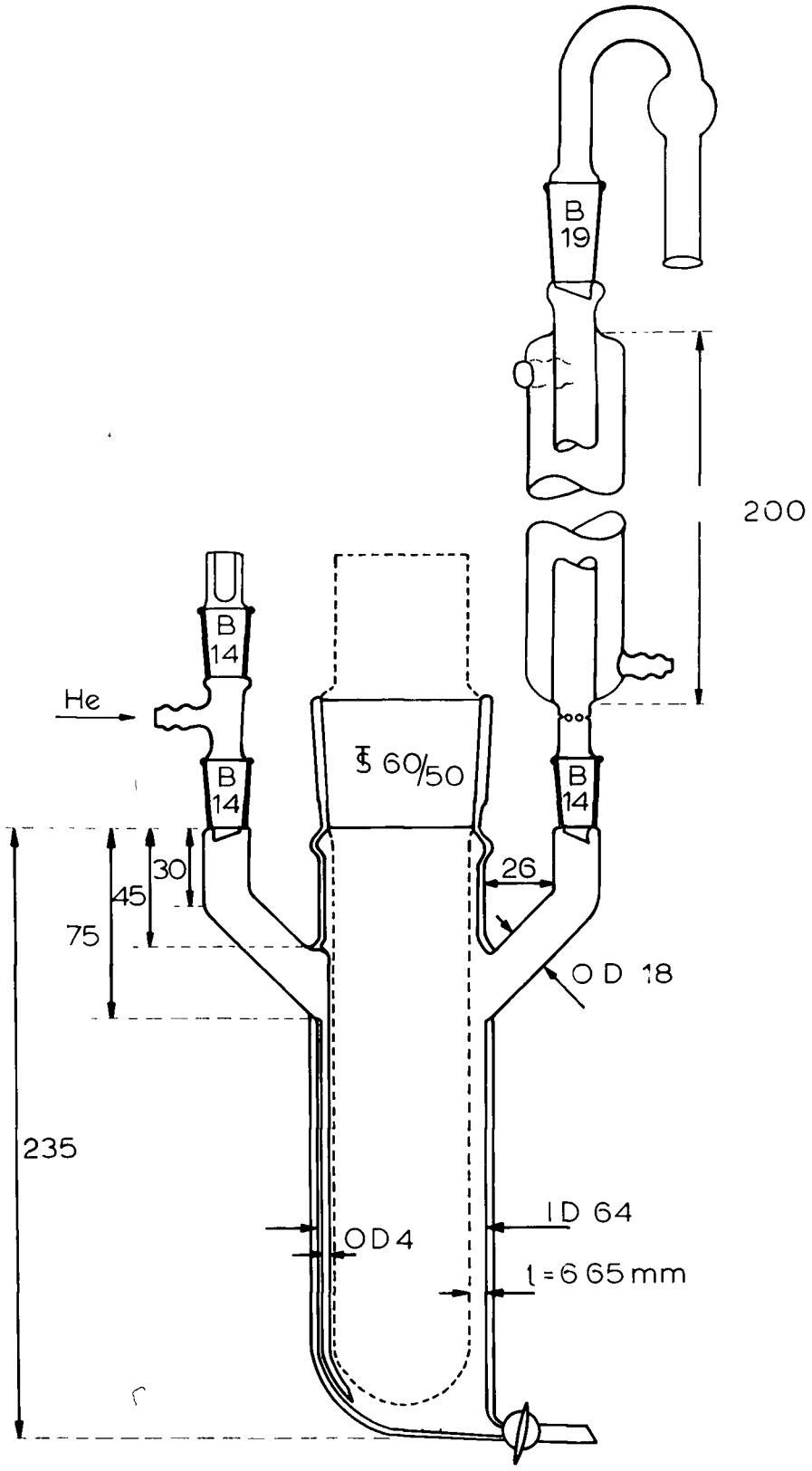

Fig 47 PHOTOREACTOR

dissolved oxygen and was maintained continuously during the irradiation.

Constant temperature ($\pm$ 0.05°) was maintained in the reactor by circulating cooling water from an external bath through the water jacket of the immersion well. The inlet temperature was 23.70° and the outlet temperature was 24.70° so that the average of the two, 24.20°, was taken as the reaction temperature and this was also checked from time to time by measuring the solution temperature with the same thermometer. To ensure thermal equilibration, the cooling water circulation was started 30 minutes before an irradiation experiment.

For certain experiments the calcium chloride tube (Figure 47) was replaced by a set of traps cooled at various temperatures to separate and retain gaseous reaction products.

B. Preliminary Experiments.

Experiment No. 1 A 0.1 M solution of trans-1,2-acenaphthenediol dinitrate in benzene (20.9g. in 0.75 ml.) in a stoppered quartz test tube was purged with nitrogen and placed in a Beckman DU spectrometer. The sample was irradiated for successive 2 hour periods with the 3660, 3140, and 3030 Å bands of a GE -H85 -A3 UV lamp. No colour formation was observed in the solution at the above wavelengths either because they were too long or because the intensity of the light after passing through the monochromator was too low. An additional 2 hour irradiation with the total output of the lamp at 20 cm. distance produced a yellow solution indicating photodecomposition.

The solution was analysed by TLC (M-5, S-1, R-1) and the pattern of spots confirmed that the nitrate ester had been photolysed. (Figure 48). The blue fluorescent spot "C" was removed from a thick-layer chromatogram and deposited as a film on a sodium chloride plate and the IR spectrum was

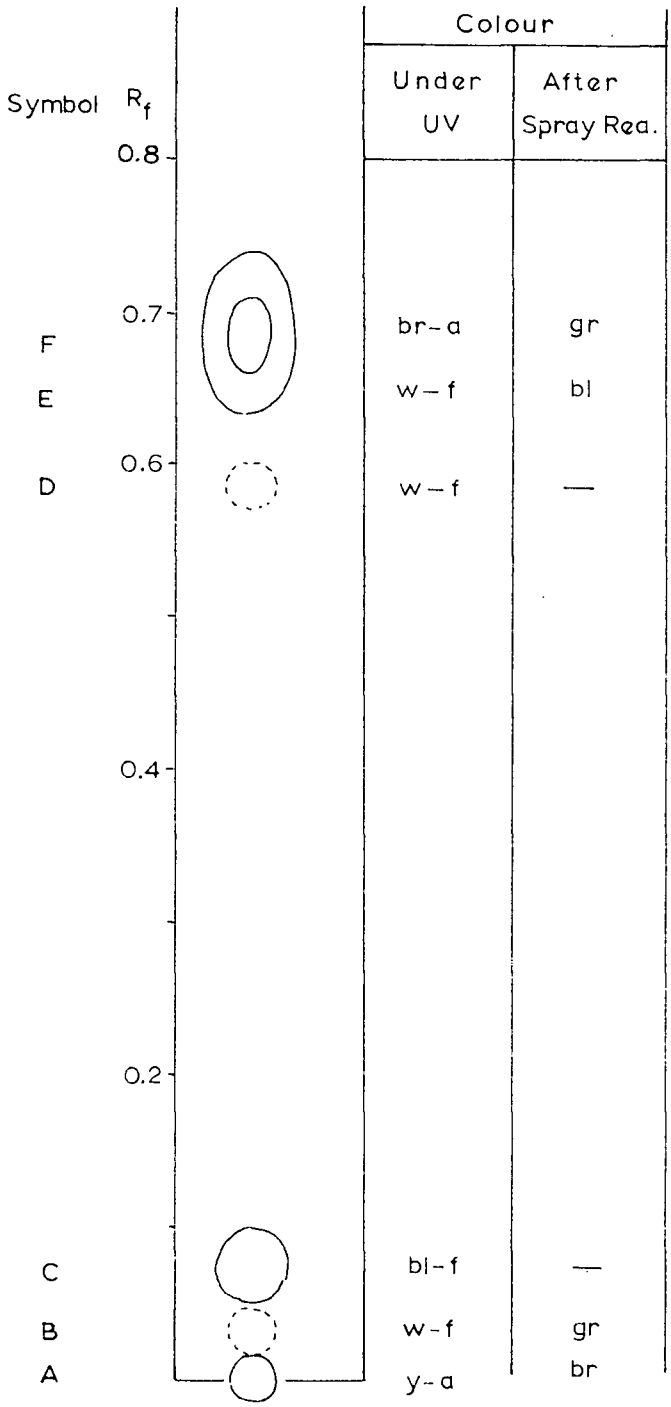

FIGURE 48. TLC (M-5, S-1, R-1) of <u>trans</u>-1, 2-Acenaphthenediol Dinitrate Photolysed in Benzene Solution.

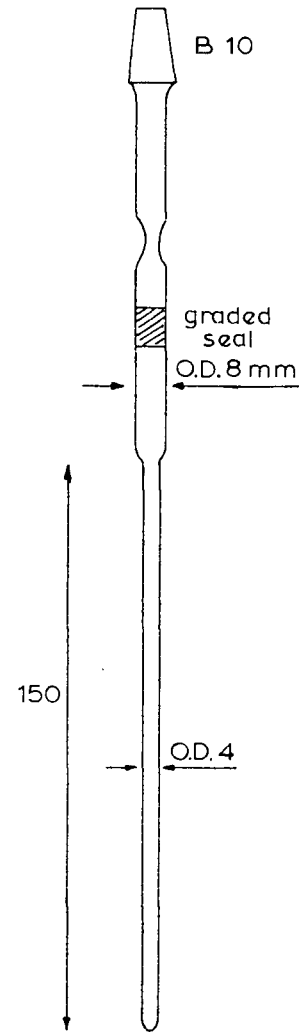

FIGURE 49. ESR Tube. Scale 2:1

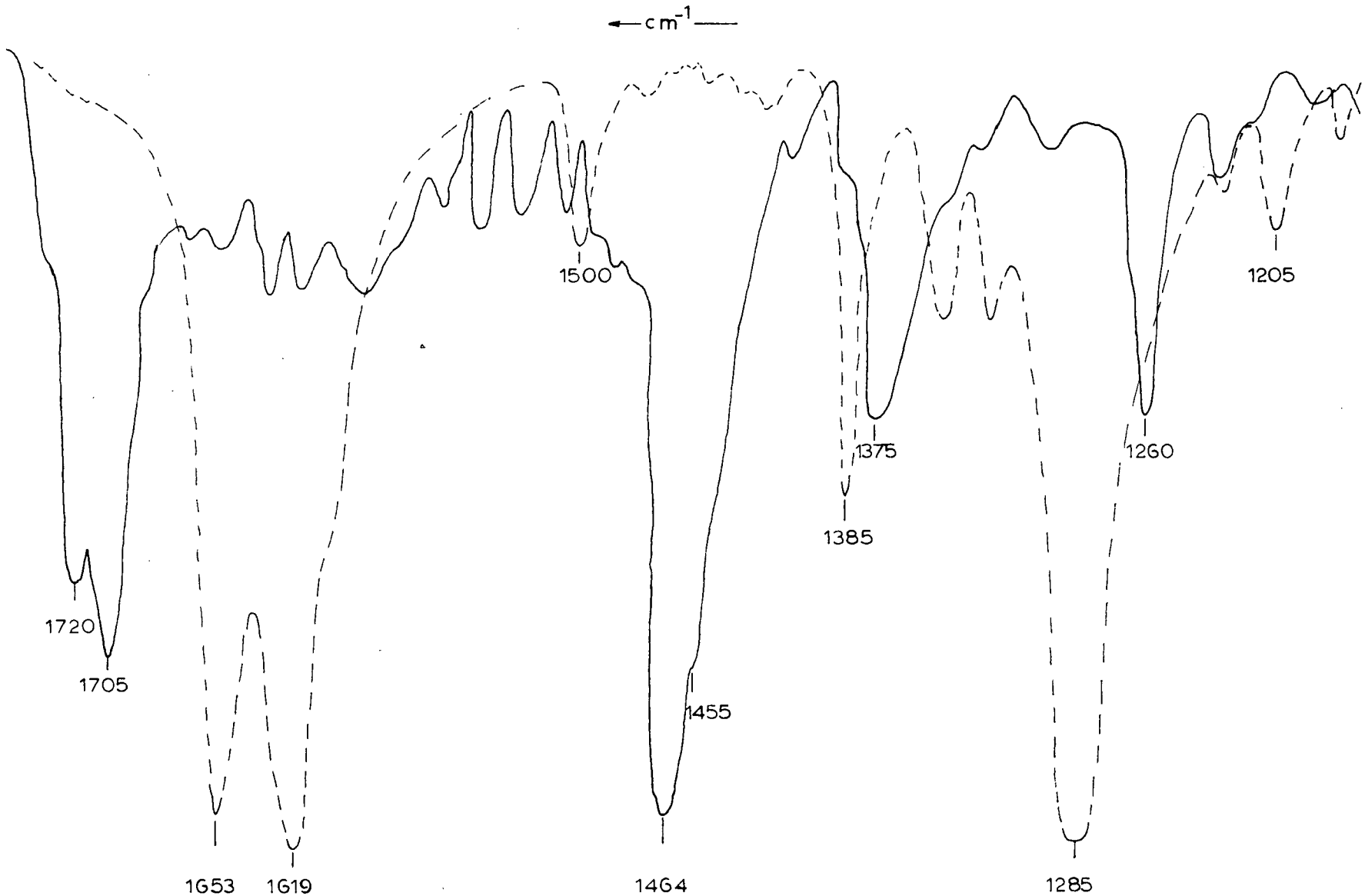

FIGURE 50. Solid State Infrared Spectra of trans-1,2-Acenaphthenediol Dinitrate and One of Its Photolysis Products. (- - - - - - - t-ADDN; ——— fluorescent photolysis Product (C)).

recorded (Figure 50). The sample was free of the original nitrate ester according to the spectrum.

Experiment No. 2 Two oxygen-free samples (0.01 M) of trans-1,2-acenaphthenediol dinitrate in benzene were irradiated simultaneously with the GE - H85 -A3 lamp in 1cm. quartz and Corex cells at a distance of about 20 cm. for a period of 12 hours. A similar 0.1 M solution was irradiated with the same lamp for the same time in the ESR spectrometer in a degassed and sealed tube (Figure 49). Figure 51 shows the chromatographic analysis of the three samples.

Experiment Nos. 3 and 4 Solutions (1.0 ml., 0.01 M) of six nitrate esters (Table XX) in benzene in small quartz test tubes were purged with nitrogen and irradiated in close contact with the water cooled Hanovia - 8A36 - 00066 lamp for a total of 9 hours. Aliquots were taken of the solutions at 0, 0.5, 1.5, 4.0, and 9.0 hours and examined by TLC (M-3, S-6, and S-10) (Figures 18 and 19 and Table XX). Similar experiments were carried out in degassed, sealed ESR tubes (0.1 ml., 0.1 M.) for 22 hours, on opening, the colourless gas in the tubes became yellow-brown (Table XX).

C. Kinetic Experiments.

Irradiations for measured time intervals were carried out in the photoreactor on solutions containing 0.02 moles of nitroxy group per liter. The solvent was removed from the photolysed solution under reduced pressure, the residues were taken up in acetone, a few grams of silica gel was added and the acetone was evaporated. The photolytic products adsorbed on the silica gel were transferred to 20 x 500 mm. columns packed with silica gel and the chromatograms were developed with one liter of a mixture of petroleum ether (30-60°) and benzene (3:1) which removed the unreacted nitrate esters and these were recovered on evaporation of the eluate fractions and

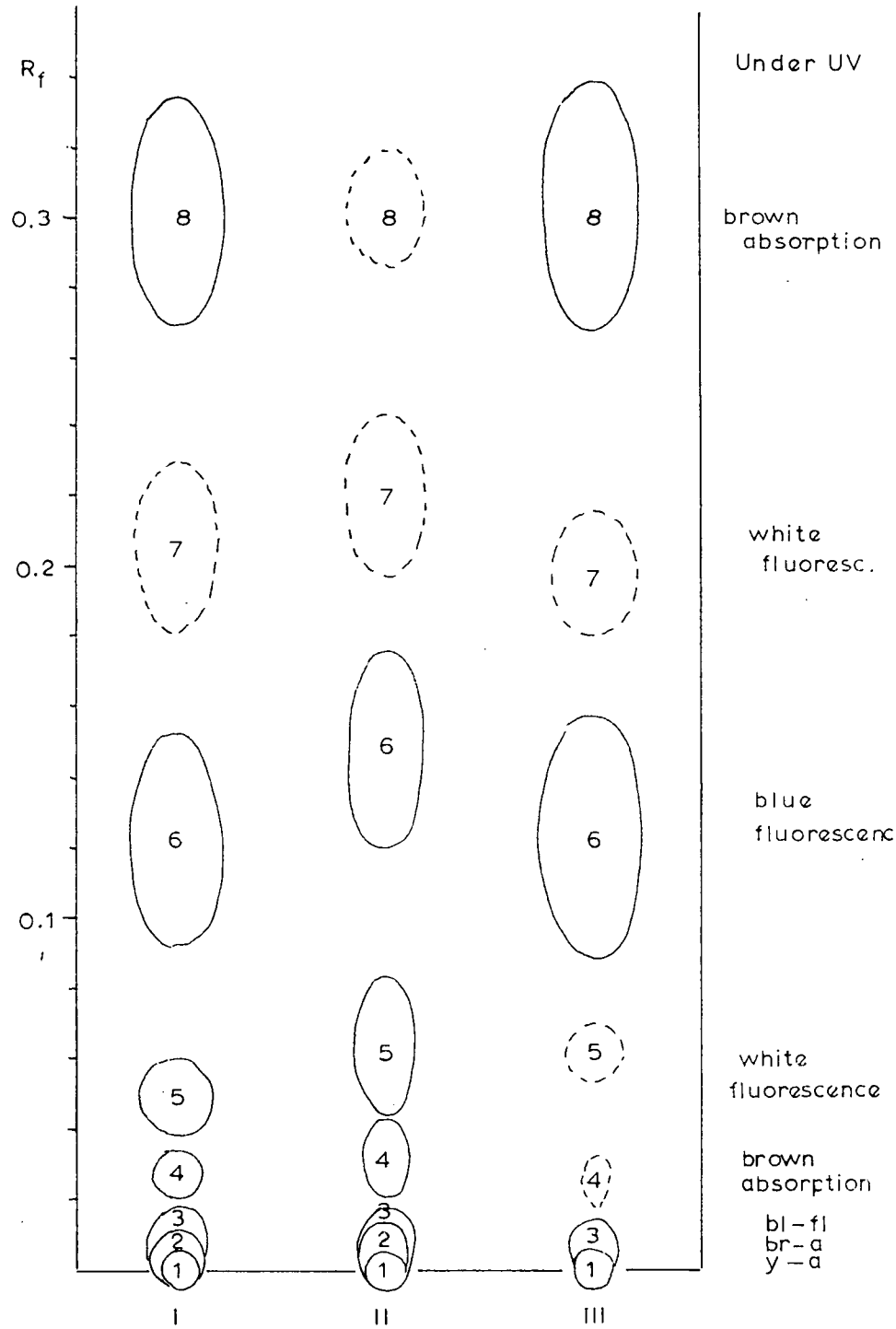

FIGURE 51. TLC (M-5, S-6) of trans 1 2 Acenaphthenediol Dinitrate after Photolysis in Benzene Solution.
I. in Quartz Cell (0.01 M) II. Quartz ESR Tube (0.1 M)
III. in Corex Cell (0.01 M)

weighed.

The columns were then eluted with methanol to remove the photoproducts which were recovered in a similar manner. In the case of the 1,2-acenaphthenediol dinitrates the order of eluting solvents was the following: (i) petroleum ether-benzene (3:1), (ii) benzene, (iii) chloroform, (iv) methanol. The unreacted nitrate esters were removed by the first solvent and solvents (ii) to (iv) removed other photolysis products. After the irradiations of meso-hydrobenzoin dinitrate and benzyl nitrate in ethanol solution the evaporated alcohol was collected and volatile aldehydes were isolated from it as the corresponding 2,4-dinitrophenylhydrazones.

D. Isolation and Identification of Photoreaction Products.

(a) Products from 1,2-Acenaphthenediol Dinitrates Irradiated in Benzene Solution.

The fractions obtained from the kinetic irradiation experiments by elution of the columns with benzene and chloroform were combined (TLC showed similar patterns) and evaporated at reduced pressure. The acetone soluble material was filtered, evaporated under nitrogen and dried *in vacuo* for a week to remove traces of acetone and then treated with the p-nitrophenylhydrazine reagent. Two crops of the dark red crystals were isolated which were similar in appearance but the first crop isolated from the *trans*-isomer melted at 225-227°, close to the reported melting point of the bis-p-nitrophenylhydrazone of 1,8-naphthalene dialdehyde (227°) (213) while the corresponding first crop from the *cis*-dinitrate melted over the range 140-190° indicating a mixture. The second crops originating from the two isomers melted at 174-180° and 174-181° respectively indicating that they might be the same compound.

The methanol eluate from the columns were evaporated and the residues after standing open to the air for several weeks did not redissolve completely in methanol. The methanol-soluble portions contained nitrophenols (TLC) while the insoluble portions contained fluorescent material. The methanol-insoluble, yellow solids were extracted with boiling saturated aqueous sodium bicarbonate solution and the alkaline extracts after cooling were acidified with sulfuric acid to pH 1. The colourless crystalline products which precipitated were 1,8-naphthalic acid (TLC, M-3, S-5, yellow-white fluorescence of under UV) which melted at 271-272° for the sample which originated from the cis-dinitrate and at 257-272° for the sample which originated from the trans-isomer. The melting point of a recrystallized commercial sample of the acid was 271-272°, while the reported value was 270° (213). The infrared spectra confirmed the identity.

The sodium bicarbonate-insoluble portions of the residues were dissolved in ethyl acetate and treated with charcoal. The colourless solutions obtained showed the same two yellow-white and blue fluorescent spots (TLC) in about equal intensity. One of these spots (yellow-white) had the R_f value of 1,8-naphthalic acid while the identity of the other, blue fluorescent, lower-R_f spot remained unknown.

(b) Products from meso-Hydrobenzoin Dinitrate Irradiated in Benzene Solution.

A solution of meso-hydrobenzoin dinitrate (608.3 mg) in benzene (200 ml.) was photolysed for 12 hours at 24.5^{o}. The benzene solution was evaporated *in vacuo* yielding a partially crystalline product (569.5 mg) which contained unreacted nitrate ester and photolysis products. The volatile compounds were distilled from a boiling water bath at 10^{-2} mm.

pressure in a microdistillation apparatus into a receiver cooled in dry ice-acetone. The yellow distillate had a very intense odor of benzlaldehyde and TLC indicated the presence of o-nitrophenol as well.

To one portion of the distillate 2,4-dinitrophenylhydrazine reagent was added and caused an immediate precipitation of a solid product which was filtered off, washed with methanol and recrystallized twice from ethanol. The compound melted at 237.5-238.5°C; the reported m.p. for benzaldehyde 2,4-dinitrophenylhydrazone was 237°C. Calc. for $C_{13}H_{10}O_4N_4$: C, 54.5; H, 3.52; N, 19.57. Found: C, 54.23; H, 3.79; N, 19.23%.

Another portion of the distillate was exposed to a stream of oxygen gas in order to oxidize the benzaldehyde in the mixture to benzoic acid. The product was then treated with distilled water (100 ml.) acidified with sulfuric acid and the o-nitrophenol was steam distilled into 25 ml. of 2N sodium hydroxide solution. The yellow distillate was acidified with sulfuric acid and extracted with ether. The dried (sodium sulfate) ether solution yielded a small amount of yellow oily solid which contained o-nitrophenol and benzoic acid (TLC). Calc. for $C_6H_5O_2N$: N, 10.07%. Found: N, 4.57%.

The residue from the steam distillation was extracted with ether and the solid residue recovered was recrystallized from water. The pale yellow crystals melted at 117 - 120°. The reported m.p. for benzoic acid was 121° (197). The NMR spectrum (in deuterochloroform) was identical with that of an authentic sample. Calc. for $C_7H_6O_2$: C, 68.84; H, 4.95. Found: C, 67.87; H, 5.67%.

The products from several other photodecomposition experiments on meso-hydrobenzoin dinitrate in benzene solution were worked up as described above by column and thick- and thin-layer chromatography in attempts to isolate and identify other compounds originating from the benzene solvent.

Although several pure fractions were obtained, the quantities of the several compounds involved were so small as to preclude positive identification. In general these products appeared to be nitrophenols similar to those listed in Table XXVIII as judged from their behaviour on chromatograms, colour, sensitivities toward oxidizing reagents (R-3) and infrared spectra (Figure 24).

(c) Products from meso-Hydrobenzoin Dinitrate Irradiated in Ethanol Solution.

A 0.02 M solution of the dinitrate was photolysed for a period of 10 hours at 24.2°C. The alcohol was distilled off under reduced pressure in a rotary evaporator which was equipped with a solvent trap followed by a water condenser and receiver kept at dry ice-acetone temperature. The solvent trap, which was at room temperature, retained the high boiling benzaldehyde identified as the 2,4-dinitrohenylhydrazone. The sample melted at 238-239° (cf. Table XXVII).

The UV spectrum of the alcohol solution trapped at ca.-80° showed the characteristic band for acetaldehyde. (Figure 52). 2,4-Dinitrophenylhydrazine reagent was added and the yellow precipitate obtained after long standing at room temperature was twice recrystallized from methanol. The product was the 2,4-dinitrophenylhydrazone of acetaldehyde; m.p. 164.5-165.5° (cf. Table XXVII).

(d) Products from Benzyl Nitrate Irradiated in Ethanol Solution.

Three solutions each containing 30.6 mg. of benzyl nitrate in 200 ml. of absolute ethanol were irradiated for 4, 7, and 10 hours respectively and worked up as described above. From the ethanol distillates after combination, acetaldehyde was isolated as the 2,4-dinitrophenylhydrazone.

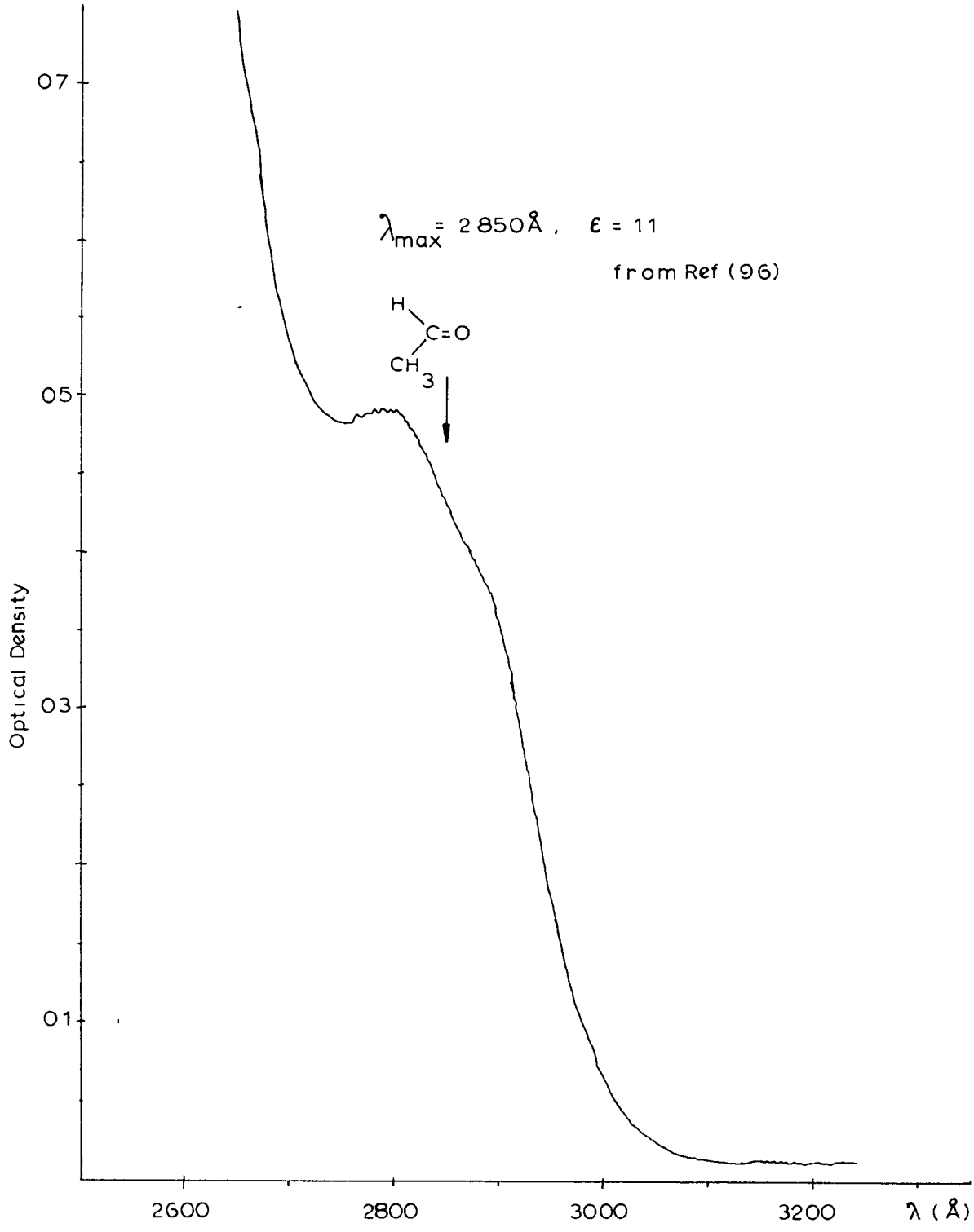

FIGURE 52 UV Spectrum of Acetaldehyde from the Photolysis of <u>meso</u>-Hydrobenzoin Dinitrate in Ethanol

The sample melted at 164.5-165.5°. The NMR spectrum taken in trifluoracetic acid matched that of an authentic sample (Table I). Calc. for $C_8H_8O_4N_4$: C, 42.86; H, 3.60; N, 24.99. Found: C, 42.47; H, 3.93; N, 24.33%.

After chromatographic separation (cf. kinetic experiments) of the unreacted nitrate ester the methanol eluates from the three solutions were combined and evaporated to a viscous oil which did not resemble benzaldehyde, because it smelled like burned sugar. However, the 2,4-dinitrophenylhydrazone isolated melted at 238-245°; the reported m.p. for benzaldehyde 2,4-dinitrophenylhydrazone was 237°. An authentic sample melted at 240-241° and the mixed melting point was found to be 241-243°.

REFERENCES

1. A. Schönberg. Preparative Organische Photochemie. Springer-Verlag, Berlin. 1958.

2. C. Reid. Excited States in Chemistry and Biology. Butterworths Scientific Publications, London. 1957.

3. M. Calvin and J. A. Basham. The Photosynthesis of Carbon Compounds. W.A. Benjamin Inc. Publisher, New York. 1962.

4. G. Ferrari and R. Cultrera. Gazz. chim. ital. 90, 1712 (1960).

5. R. Cultrera and G. Ferrari. Agrochimica 5, 108 (1961).

6. L. Pauling. The Nature of the Chemical Bond. Cornell University Press. 2nd Edn. 1960, p.98.

7. J. Hinze and H. H. Jaffe. J. Am. Chem. Soc. 84, 540 (1962).

8. Y. Tanaka and A. S. Jursa. J. Chem. Phys. 36, 2493 (1962).

9. D. C. Frost, D. Mak and C.A. McDowell. Can. J. Chem. 40, 1064 (1962).

10. T. Nakayama, M. Y. Kitamura and K. Watanabe. J. Chem. Phys. 30, 1180 (1959).

11. M. Green and J. W. Linnet. Trans. Farad. Soc. 57, 1 (1961).

12. K. L. McEwen. J. Chem. Phys. 32, 1813 (1960).

13. R. Daudel, R. Lefebvre and C. Moser. Quantum Chemistry, Methods and Applications. Interscience Publisher 1959, p. 74-75.

14. H. Gilman and F. Schulze. J. Am. Chem. Soc. 49, 2904 (1927).

15. R. E. Dessy. J. Am. Chem. Soc. 82, 1580 (1960).

16. L. H. Long and D. Dollimore. J. Chem. Soc. 3902, 3906 (1953).

17. R. B. Booth and C. Kraus. J. Am. Chem. Soc. 74, 1415 (1952).

18. J. C. Lockhart. J. Chem. Soc. 1197 (1962).

19. A. Chaney and M. L. Wolfrom. J. Org. Chem. 26, 2998 (1961).

20. R. E. Banks and R. N. Haszeldine. Perfluoroalkyl Derivatives in Adv. Inorg. Chem. and Radiochem. (Edited by H.J. Emelius and A. G. Sharpe) 3, 363-364 (1961).

21. J. A. Young, S. N. Tsoukalas and R. D. Dresdner. J. Am. Chem. Soc. 80, 3604 (1958).

22. F. E. Ray and G. J. Szasz. J. Org. Chem. 8, 121 (1943).

23. M. Schmidt and H. Schmidbaur. Angew. Chem. 71, 220 (1959).

24. J. Honeyman and J. W. W. Morgan. Adv. Carb. Chem. 12, 117 (1957).

25. M. A. Cook. The Science of High Explosives. Reinhold Publ. Co. (1958).

26. C. R. Marshall. J. Pharmacol. Exptl. Therap. 83, 106 (1948).

27. P. Gray and L. D. Hayward. The Chemistry of Nitrate Esters. In preparation.

28. L. Pauling and L. O. Brockway. J. Am. Chem. Soc. 59, 13 (1937).

29. A. D. Booth and F. J. Llewellyn. J. Chem. Soc. 847 (1947).

30. W. B. Dixon and E. B. Wilson, Jr. J. Chem. Phys. 35, 191 (1961).

31. F. Rogowski. Ber. 75, 244 (1942).

32. H. E. Weaver, B. M. Tolbert and R. C. LaForce. J. Chem. Phys. 23, 1956 (1955).

33. A. Streitwieser, Jr., Molecular Orbital Theory for Organic Chemists. John Wiley & Sons Inc. (1961) p.43.

34. J. Chedin. J. Phys. Radium (Series 7) 10, 445 (1939). Chem. Abstr. 34 1250 (1940).

35. A. F. Ferris, K. W. McLean, I. G. Marks and W. D. Emmons. J. Am. Chem. Soc. 75, 4078 (1953).

36. L. Fishbein. J. Am. Chem. Soc. 79, 2959 (1957).

37. R. Boschan. J. Am. Chem. Soc. 81, 3341 (1959).

38. G. A. Mortimer. J. Org. Chem. 27, 1876 (1962).

39. E. D. Hughes, C. K. Ingold and R. B. Pearson. J. Chem. Soc. 4357 (1958).

40. S. Israelashvili. Nature 165, 686 (1950).

41. E. L. Blackall, E. D. Hughes, C. K. Ingold and R. B. Pearson. J. Chem. Soc. 4366 (1958).

42. R. Boschan, R. T. Merrow and R. W. vanDolah. Chem. Rev. 55, 485 (1955).

43. E. Buncel and A. N. Bourns. Can. J. Chem. 38, 2457 (1960).

44. L. D. Hayward. Abstract of Papers. C.I.C. Organic Symposium, Edmonton, September 6-7 (1960); Chemistry in Canada 12, 77 (Oct. 1960).

45. H. R. Wright and W. J. Donaldson. U. S. Pat. 2,416,974. Chem. Abstr. 41, 3485 (1947).

46. A. V. Topchiev. Nitration of Hydrocarbons and other Organic Compounds. Pergamon Press, New York. 1959. p.289.

47. E. Bodker. Bull. soc. chim. France [4] 3, 726 (1908).

48. H. Moissan and P. Lebeau. Compt. rend. 140, 1621 (1905).

49. H. Moissan and P. Lebeau. Compt. rend. 140, 1573 (1905).

50. G. Hetherington and P. L. Robinson. J. Chem. Soc. 3512 (1954).

51. G. Hetherington and P. L. Robinson. Recent Aspects of the Inorganic Chemistry of Nitrogen. The Chemical Society (London). Special Publication 10, 23 (1957).

52. C. C. Price and C. A. Sears. J. Am. Chem. Soc. 75, 3276 (1953).

53. R. J. Gillespie and D. J. Millen. Quart. Rev. 2, 278 (1948).

54. G. W. H. Cheeseman. J. Chem. Soc. 115 (1957).

55. J. W. Baker and D. M. Easty. J. Chem. Soc. 1193 (1952).

56. J. W. Baker and D. M. Easty. J. Chem. Soc. 1208 (1952).

57. M. Anbar, F. Dostrovsky, D. Samuel and A. D. Yoffe. J. Chem. Soc. 3603 (1954).

58. L. D. Hayward. J. Am. Chem. Soc. 73, 1974 (1951).

59. G. G. McKeown and L. D. Hayward. Can. J. Chem. 33, 1392 (1955).

60. G. H. Segall and C. B. Purves. Can. J. Chem. 30, 860 (1952).

61. L. D. Hayward and C. B. Purves. Can. J. Chem. 32, 19 (1954).

62. M. Jackson and L. D. Hayward. Can. J. Chem. 38, 496 (1960).

63. A. Zane, M.Sc. Thesis, University of British Columbia (1958).

64. J. Hine. "Physical Organic Chemistry". McGraw Hill (1956) Chapt. 7. p.168.

65. J. W. Baker and D. M. Easty. J. Chem. Soc. 1193 (1952).

66. J. W. Baker and T. G. Heggs. J. Chem. Soc. 616 (1955).

67. G. W. H. Cheeseman. J. Chem. Soc. 448 (1959).

68. I. G. Csizmadia, M.Sc. Thesis, University of British Columbia (1959).

69. E. Buncel and A. N. Bourns. Can. J. Chem. 38, 2457 (1960).

70. P. Gray and A. Williams. Chem. Rev. 59, 239 (1959).

~~71. M. A. Cook. "The Science of High Explosives". Reinhold Publishing Co. (1958).~~

72. J. Powling and W. A. W. Smith. Combustion and Flame. 1, 308 (1957).

73. P. Gray and A. D. Yoffe. Proc. Roy. Soc. A200, 114 (1949).

74. J. Powling and W. A. W. Smith. Combustion and Flame 2, 157 (1958).

75. H. A. Bent and B. Crawford, Jr. J. Phys. Chem. 63, 941 (1959).

76. F. Shafizadeh, M. L. Wolfrom and P. McWain. J. Am. Chem. Soc. 81, 1221 (1959).

77. M. L. Wolfrom, A. Chaney and K. S. Ennor. J. Am. Chem. Soc. 81, 3469 (1959).

78. M. L. Wolfrom and G. P. Arsenault. J. Am. Chem. Soc. 82, 2819 (1960).

79. W. Will. Z. Angew. Chem. 14, 774 (1901).

80. R. Steinberg, C. A. Orlick and V. P. Schaaf. J. Am. Chem. Soc. 77, 4748 (1955).

81. J. B. Levy. J. Am. Chem. Soc. 76, 3790 (1954).

82. L. Phillips, Thesis, University of London, 1949.

83. L. Phillips, Nature 160, 753 (1947).

84. A. I. Serbinov. Zh. fiz. Khim 33, 559 (1959).

85. R. W. Phillips, C. A. Orlick, R. Steinberg, J. Phys. Chem. 59, 1034 (1955).

86. M. A. Millett, R. M. Seborg, L. L. Zoch and F. J. Masuelli. Tappi 44, 636 (1961).

87. L. F. R. Cafferata, J. E. Sicre and H. J. Schumacker. Z. für Phys. Chem. (Frankfurt) 29, 188 (1961).

88. W. E. Skiens and G. H. Cady. J. Am. Chem. Soc. 80, 5640 (1958).

89. D. H. R. Barton, J. M. Beaton, L. G. Geller and M. M. Pecket. J. Am. Chem. Soc. 82, 2640 (1960).

90. L. H. Piette and W. C. Landgraf. J. Chem. Phys. 32, 1107 (1960).

91. A. L. Nussbaum and C. H. Robinson. Tetrahedron 17, 35 (1962).

92. H. W. Thomson and C. H. Purkis. Trans. Farad. Soc. 32, 674 (1936).

93. S. F. Mason. Quart. Rev. 15, 287 (1961).

94. J. A. Gray and D. W. G. Style. Trans. Farad. Soc. 48, 1137 (1952).

95. H. E. Ungnade and R. A. Smiley. J. Org. Chem. 21, 993 (1956).

96. C. N. R. Rao. Ultra-Violet and Visible Spectroscopy. Butterworths, London, (1961).

97. J. W. Sidman. J. Am. Chem. Soc. 79, 2669 (1957).

98. S. Nagakura. Mol. Phys. 3, 152 (1960).

99. J. A. Gray and D. W. G. Style. Trans Farad. Soc. 49, 52 (1953).

100. P. A. Leighton. Photochemistry of air pollution. Academic Press, New York, 1961.

101. H. Watanabe and Y. Toyoda. Japan Pat. 3393 ('60) April 9. Chem. Abstr. 55, 5035 ab (1961).

102. J. A. Hicks. Trans. Farad. Soc. 52, 1526 (1956).

103. S. Claesson and G. Wettermark. Arkiv for Kemi 17, 355 (1961).

104. S. Claesson, G. Palm and G. Wettermark. Arkiv for Kemi 17, 579 (1961).

105. L. D. Hayward, R. A. Kitchen and D. J. Livingstone. Can. J. Chem. 40, 434 (1962).

106. G. Ciamician and P. Silber. Ber. 34, 2040 (1901).

107. P. de Mayo and S. T. Reid. Quart. Rev. 15, 393 (1961).

108. J. K. Fawcett. B.Sc. Thesis. University of British Columbia (1962).

109. V. M. Csizmadia and L. D. Hayward. Personal communication.

110. M. Davis and N. Jonathan. Trans. Farad. Soc. 54, 469 (1958).

111. P. Coppens. J. Chem. Phys. 36, 2523 (1962).

112. O. P. Strausz and H. E. Gunning. Can. J. Chem. 39, 2549 (1961).

113. W. Kemula and A. Grabowska. Bulletin de l'Academie Polonaise des Sciences 8, 517 (1960).

114. J. P. Simons. Quart. Rev. 13, 3 (1959).

115. C. Reid. Quart. Rev. 12, 205 (1958).

116. M. Kasha. Chem. Rev. 41, 401 (1947).

117. W. Kemula and A. Grabowska. Bulletin de l'Academie Polonaise des Sciences 6, 747 (1958).

118. W. Kemula and A. Grabowska. Bulletin de l'Academie Polonaise des Sciences 9, 525 (1960).

119. R. G. W. Norrish. J. Chem. Soc. 50, 774 (1928).

120. R. G. W. Norrish. J. Chem. Soc. 51, 1604 (1929).

121. R. G. W. Norrish. The Adv. of Sci. (BAAS) No.74, 1 (1961 November).

122. H. Ford. Progress Report No. 20-393. Jet Propulsion Laboratory (Calif. Inst. of Techn. Pasadena. Calif) (1960).

123. J. L. Riebsomer. Chem. Rev. 36, 157 (1945).

124. P. Gray and A. D. Yoffe. Chem. Rev. 55, 1069 (1955).

125. M. Berthelot. Compt. rend. 127, 83 (1898).

126. W. C. Reynolds and W. H. Taylor. J. Chem. Soc. 101, 131 (1912).

127. H. A. Mahlman. J. Chem. Phys. 35, 936 (1961).

128. B. B. Coldwell and S. R. McLean. Can. J. Chem. 36, 652 (1958).

129. B. B. Coldwell and S. R. McLean. Can. J. Chem. 37, 1637 (1959).

130. H. M. Brown and G. C. Pimental. J. Chem. Phys. 29, 883 (1958).

131. T. Kubota and M. Yamakawa. Bull. Chem. Soc. Japan. 35, 555 (1962).

132. N. Hata. Bull. Chem. Soc. Japan. 34, 1440 (1961).

133. Table of Interatomic Distances and Configuration in Molecules and Ions, The Chemical Society, (London), Special Publication No. 11, Burlington House, W.1., (1958).

134. V. Gold, E. D. Hughes and C. K. Ingold. J. Chem. Soc. 2476 (1950).

135. H. Burton and P. F. G. Praill. J. Chem. Soc. 729 (1955).

136. J. Chedin and S. Feneant. Comp. rend. 229, 115 (1949).

137. R. A. Marcus and J. M. Fresco. J. Chem. Phys. 27, 564 (1957)

138. M. A. Paul. J. Am. Chem. Soc. 80, 5329 (1958).

139. A. Fischer, J. Packer, J. Vaughan and G. J. Wright. Proc. Chem. Soc. 369 (1961).

140. R. D. Brown, J. Chem. Soc. 2224 (1959).

141. E. D. Hughes. Kekule Symposium. Butterworths Scientific Publications, London. (1958) p.209.

142. K. Watanabe. J. Chem. Phys. 26, 542 (1957).

143. D. A. Hahan and H. E. Holmes. Ind. Eng. Chem. 13, 822 (1921).

144. I. G. Csizmadia and L. D. Hayward. Tetrahedron in press.

145. L. Robert. Compt. rend. 234, 2066 (1952).

146. W. A. Schroeder. J. Am. Chem. Soc. 73, 1122 (1951).

147. R. K. Iller. The Colloid Chemistry of Silica and Silicates, Cornell University Press, Ithaca, N. Y. (1955) p.238.

148. R. P. Eischens and W. A. Pliskin. Advances in Catalysis, Academic Press, New York. 10, 1-56 (1958).

149. R. S. McDonald. J. Phys. Chem. 62, 1168 (1958).

150. M. Folman and D. J. C. Yates. Proc. Roy. Soc. (London). 246 A, 32 (1958).

151. M. Folman and D. J. C. Yates. J. Phys. Chem. 63, 183 (1959).

152. M. R. Basila. J. Chem. Phys. 35, 1151 (1961).

153. A. H. Sporer and K. N. Trueblood. J. Chromat. 2, 499 (1959).

154. E. Lederer and M. Lederer. Chromatography. 2nd ed. Elsevier Publishing Co. Amsterdam. (1957).

155. I. G. Csizmadia, D. J. Livingstone and L. D. Hayward, unpublished results.

156. G. R. Duncan. J. Chromat. 8, 37 (1962).

157. G. R. Ritter and G. M. Meyer. Nature 193, 941 (1962).

158. W. E. Elias and L. D. Hayward. Tappi. 41, 246 (1958).

159. J. Noguchi. Sci. Papers Osaka Univ. No. 221 (1951).

160. D. J. Livingstone. Personal communication.

161. P. R. Hammond. J. Chem. Soc. 1370 (1962).

162. B. P. Dailey and J. N. Schoolery. J. Am. Chem. Soc. 77, 3977 (1955).

163. J. A. Pople, W. G. Schneider and H. J. Bernstein. High -Resolution Nuclear Magnetic Resonance. McGraw Hill Book Co., New York, (1959).

164. I. G. Csizmadia and L. D. Hayward. Abstract of Papers C.I.C. 45th Conference, Edmonton. May 27-30, (1962). Chemistry in Canada 14 (No. 4) 29 (1962).

165. V. M. Csizmadia and L. D. Hayward. To be published.

166. R. D. Guthrie and H. Spedding. J. Chem. Soc. 953 (1960).

167. D. N. W. Anderson, G. O. Aspinall, J. L. Duncan and J. F. Smith, Spectrochim. Acta. 17, 1001 (1961).

168. F. Pristera, M. Halik, A. Castelli and W. Fredericks. Anal. Chem. 32, 495 (1960).

169. R. A. E. Carrington, Spectrochim. Acta 16, 1279 (1960).

170. H. von Halban and J. Eisenbrand. Z. Phys. Chem. 132, 401 (1928).

171. M. Ito and N. Hata. Bull. Chem. Soc. Japan 28, 260 (1955).

172. M. Ito, K. Inuzuka and S. Imanshi. J. Chem. Phys. 31, 1694 (1959).

173. M. Ito, K. Inuzuka and S. Imanishi. J. Am. Chem. Soc. 82, 1317 (1960).

174. H. E. Ungnade, E. D. Longhran and L. W. Kissinger. J. Phys. Chem. 64, 1410 (1960).

175. C. C. Price and R. J. Convery. J. Am. Chem. Soc. 79, 2941 (1957).

176. P. Gray. Tetrahedron 18, 879 (1962).

177. P. Kabasakalian, E. R. Townley and M. D. Yudis. J. Am. Chem. Soc. 84, 2716 (1962).

178. R. M. Hochstrasser and G. B. Porter. Quart. Rev. 14, 146 (1960).

179. A. Terenin and Vl. Ermaldov. Trans. Farad. Soc. 52, 1042 (1956).

180. G. Porter and F. Wilkinson. Trans. Farad. Soc. 57, 1686 (1961).

181. W. M. Moore and M. Ketchum. J. Am. Chem. Soc. 84, 1368 (1962).

182. J. B. Farmer, C. L. Gardner and C. A. McDowell. J. Chem. Phys. 34, 1058 (1961).

183. W. West and W. E. Miller. J. Chem. Phys. 8, 849 (1940).

184. O. Schnepp and M. Levy. J. Am. Chem. Soc. 84, 172 (1962).

185. A. Weller. Fast Reactions of Excited Molecules. In Progress in Reaction Kinetics (Edited by G. Porter) Pergamon Press. New York, 1961. Vol. 1. p.187.

186. W. Bartok, D. J. Lucchesi and N. S. Snider. J. Am. Chem. Soc. 84, 1842 (1962).

187. G. Porter. Mechanism of Photosensitization in Solution. In Photochemistry in Liquid and Solid State (Edited by L.S. Heidt, R. S. Livingstone, E. Rabinowith, and F. Daniels.) John Wiley, New York 1960. p.35.

188. J. W. Eastman, G. Engelsma and M. Calvin. J. Am. Chem. Soc. 84, 339 (1962).

189. J. Cunningham. J. Phys. Chem. 66, 779 (1962).

190. T. J. Stone and W. A. Waters. Proc. Chem. Soc. 253 (1962).

191. S. I. Weissman, J. Chem. Phys. 29, 1189 (1958).

192. C. A. Hutchison, Jr., and B. W. Mangum. J. Chem. Phys. 29, 952 (1958).

193. S. Nagakura. Molec. Phys. 3, 152 (1960).

194. C. L. Gardner. Personal communication.

195. L. D. Hayward and D. J. Livingstone. Unpublished results.

196. A. I. Vogel. Practical Organic Chemistry. Longmans London. 3rd. Edn. 1959.

197. Sir.I. Heilbron and H. M. Bunbury. Dictionary of Organic Compounds. Eyre and Spottiswoode, London, 1946.

198. W. H. Hartung. J. Am. Chem. Soc. 50, 3372 (1928).

199. L. W. Trevoy and W. G. Brown. J. Am. Chem. Soc. 71, 1676 (1949).

200. L. F. Fieser. Experiments in Organic Chemistry. D. C. Heath Co., 3rd Edn. 1957.

201. H. Merween and R. Schmidt. Ann. 444, 234 (1925).

202. G. Faust. J. Pract. Chem. 6 (No.1), 14 (1958).

203. D. J. Cram, N. L. Allinger and H. Steinberg. J. Am. Chem. Soc. 76, 6132 (1954).

204. L. Erdey. Introduction to Chemical Analysis Vol. 2. Volumetric Analysis. 2nd Ed. Academia Publisher, Budapest, (1951).

205. T. Arnd. Angew. Chem. 30, 169 (1917)

206. G. Grime and W. M. Jones. Phil. Mag. 7, 1113 (1929).

207. R. von Walther and A. Wetzlich. J. Pract. Chem. (2) 61, 169 (1900).

208. V. M. Csizmadia, M.Sc. Thesis. University of British Columbia (1961).

209. L. B. Rockland and M. S. Duran. Science 109, 539 (1949).

210. J. H. Dhout and C. de Roy. Analyst 86, 74 (1961).

211. M. Jackson and L. D. Hayward. J. Chromat. 5, 166 (1961).

212. R. U. Lemaeux and H. F. Bauer. Anal. Chem. 27, 920 (1959).

213. R. H. Callighan, M. F. Tarker, Jr., and M. H. Wilt. J. Org. Chem. 26, 1379 (1961).

214. F. J. Adrian. J. Chem. Phys. 36, 1692 (1962)

215 L.C Raiaford and Colbert J Am Chem Soc 47, 1454 (1925)

216 A G Banus and J Guteras An Soc españ 21, 127 (1923).